A Preliminary Investigation of Modelling the Atlantis Aquifer

Jasper L. Muller and Joseph F. Botha

WRC Report No. 113/1/87

A Preliminary Investigation of Modelling the Atlantis Aquifer

by

Jasper L. Müller
Joseph F. Botha

Research done by the Institute for Ground-water Studies
in conjunction with the Department of Water Affairs
under contract for the Water Research Commission

November, 1986

113/1/87

ACKNOWLEDGEMENTS

A number of people and institutions have contributed significantly towards finishing this report. The authors take this opportunity to list these contributors and to thank them.

The personnel of the Institute for Ground-water Studies for their assistance during the course of this investigation. In particular, Mrs. C. le Roux for the draughting of the figures and Mrs. M.J. Botha for the excellent word processing of this report.

The following institutions for information supplied:

The Division Geohydrology of the Department of Environment Affairs.
The Geological Survey (Bellville Office).
The Divisional Council of the Cape.
The Engineering Firm, Liebenberg and Stander.

The financial assistance by the Water Research Commission and the Department of Environment Affairs are hereby gratefully acknowledged.

CONTENTS

CONTENTS (CONT.)

PAGE

LIST OF FIGURES

LIST OF FIGURES (CONT.)

LIST OF FIGURES (CONT.)

PAGE

LIST OF FIGURES (CONT.)

LIST OF FIGURES (CONT.)

PAGE

LIST OF TABLES

EXECUTIVE SUMMARY

1 INTRODUCTION (PAGE 1)

The main purpose of the present study was the development of a preliminary mathematical-physical model, describing ground-water flow in the Atlantis aquifer. The main objective in developing the model was to:

(i) simulate the physical conditions prevailing in the aquifer.

(ii) delimit areas where additional information should be generated in order to be able to construct a model suitable for management purposes.

(iii) determine the period for which the existing ground-water supply will last, given a certain demand.

(iv) optimize the future development of the production fields, and

(v) study the phenomenon of sea-water intrusion in the Atlantis aquifer.

2 PHYSIOGRAPHY (PAGE 7)

The main physiographical feature which influences the flow of ground water in the area is a coastal flat running parallel to the coast with a width of approximately 5 kilometres. The inland part of the aquifer, in the vicinity of Atlantis and Wesfleur, is separated from the coastal flat by a sudden rise in bed-rock topography, also manifested in the present topography.

Another important physiographical feature is the existence of drift sand dunes on the farms Buffels River, Duynefontein and Kleine Springfontein. These features may play a significant role in natural recharge of the aquifer due to rainfall and requires further attention.

The climate of the Atlantis area is Mediterranean with a mean annual rainfall varying between 369 mm and 416 mm. The variability of the rainfall, both on monthly and annual basis, is relatively large.

3 GEOLOGY (PAGE 12)

The geological features of the area is of importance only in so far as they form the physical flow medium and the boundaries of the aquifer. For this reason it will suffice to say that the aquifer is bounded from below by weathered material of the Malmesbury formation, consisting of a relative uniform clay layer, assumed to be impervious to ground-water movement.

The lateral boundaries are defined by the coast-line in the west, and by the pinching out of the water-bearing sand formations in the north, east and south.

The water-bearing strata of the Atlantis aquifer consists of Cenozoic sand deposits of both marine and aeolian origin. Depending on lithology and areal distribution, the sand can be divided into a number of stratigraphic units and sub-units. For the purpose of modelling the aquifer, however, the water-bearing strata is taken as the Cenozoic sand. All differences in lithology and hydraulic character was incorporated in the model by utilizing the flexibility of the finite element method used to construct the model.

4 GEOHYDROLOGY (PAGE 18)

In modelling an aquifer, the need for an accurate physical and hydraulic description of the aquifer cannot be over-emphasized. The accuracy attainable by any model can never exceed the accuracy of the data used in the construction thereof.

Some of the more important properties to be considered in the physical and hydraulic description of the aquifer are:

(i) the geometry of the aquifer with specific reference to the boundary conditions.

(ii) the water-level distribution,

(iii) the aquifer parameters, hydraulic conductivity and storativity,

(iv) the total discharge from the aquifer, and

(v) the total recharge to the aquifer.

4.1 GEOMETRY

A detailed geometrical description of the aquifer entails the determination of the three-dimensional distribution of the geological formations prevailing in the area. To accomplish this, the spatial distribution of both the underlying Malmesbury rocks and the Cenozoic sand deposits have to be known.

In previous studies several geophysical techniques were utilized to determine the elevation of the bed-rock topography and the thickness of the overlying sand deposits. None of these techniques, however, provided conclusive answers and therefore the geological logs of 128 boreholes drilled in the region, together with the existing geological map of the area, were used in establishing the geometry of the aquifer.

Contour maps depicting the bed-rock elevation and the sand thickness were consequently drawn by utilizing advanced computer techniques. Before discussing these maps, it should be stressed, however, that due to a lack of information in certain areas, especially in the vicinity of the aquifer boundaries, one should be careful not to absolutize the results.

The most outstanding features of the bed-rock elevation contour map are:

(i) The sharp decline in bed-rock elevation parallel to the coast at a distance of approximately 6 kilometres from the coast. This feature will most certainly influence the ground-water flow in this region significantly.

(ii) In the Silwerstroom area the elevation of the bed-rock is below sea-level, thus facilitating the possible intrusion of sea-water.

In studying the sand thickness contour map the following is noteworthy:

(i) The continuation below sea-level of the sand deposits in the Silwerstroom area.

(ii) The thick sand deposits between Silwerstroom and Atlantis which appear to be contradictive to the existence of the steep gradients in the bed-rock topography in the same region. This feature may, however, be attributed to the existence of the drift sand dunes in this area.

(iii) The closed contour lines in the south near Melkbosstrand. No significance should be attached to this, because it is known that thick sand deposits continue right down to Melkbosstrand. The closed contours were caused by a lack of quantitative data.

(iv) The non-uniformity of the sand thickness could affect the modelling of the aquifer adversely, if significant lowering of the water-table was to occur.

4.2 WATER-LEVELS

Perhaps, the most important quantity in the study of any aquifer is the prevailing water-levels. Both the physical and hydraulic characteristics of an aquifer are manifested in its water-level distribution.

During the present investigation considerable difficulty was experienced in obtaining representative water-level contour maps for the Atlantis aquifer for prolonged periods of time. This was mainly due to two factors:

(i) Observation boreholes are clustered around the production fields and very little information along the boundaries are available.

(ii) The observation network varied considerably with time. This presented a serious problem in the standardization of the maps drawn by computer.

The problems experienced, hampered the accurate estimation of the volume of water present in the aquifer, as well as the accurate calibration of the numerical model. In spite of this, quite a few interesting deductions could, nevertheless, be made:

(i) The sharp gradient parallel to the coast, formed by the bed-rock, is clearly manifested in the water-levels.

(ii) Regions where water may leak out of the system (along the coast-line, in the north near Mamre, in the south-eastern part of the aquifer, and in the extreme south near Melkbosstrand) could be identified.

(iii) The positive ground-water gradient along the coast-line will counteract possible sea-water intrusion.

(iv) The aquifer is, in principle, an unconfined aquifer.

4.3 HYDRAULIC PARAMETERS

From a modelling point of view, the quantitative knowledge of the hydraulic parameters is of the utmost importance. Usually these values are quantified by means of conducting pumping tests. Values for 16 locations were obtained in this way and values for 22 more locations were obtained by utilization of Hazen's formula applied to the granulometric properties of sand obtained from additional boreholes. The degree of these values being representative of the entire aquifer, was studied by utilization of an advanced geostatistical method known as kriging. The advantages of using this method are:

(i) Areas where additional data should be generated, can be delimited.

(ii) During the calibration of the numerical model, the method can be used to ensure that the hydraulic parameters used in the model, are realistic in that they do not contradict physical acceptable values.

Using this method, it could be shown that there exist large areas in the eastern part and along the boundaries of the aquifer, where the uncertainty in the present data is disturbingly large. Another interesting feature evident from the data is the existence of a steep conductivity gradient between the Atlantis-Wesfleur and the Silwerstroom-Witzand areas. This transition zone once again corresponds with the zone of steep gradients evident in both the bed-rock and water-level contour maps. Furthermore, the storativity in the Silwerstroom and Witzand areas is fairly constant, suggesting that the water-bearing strata is relatively homogeneous. The range of storativity values in the Atlantis aquifer further strengthens the belief that it is, in fact, a water-table (unconfined) aquifer.

4.4 VOLUME OF WATER IN THE AQUIFER

Determination of the volume of water in the aquifer was based on the information discussed so far. Because of the uncertainties in the water-level and storativity values especially, it was decided to base the calculation for volume on a mean storativity value of 10 per cent; the mean value for the determined storativity values being in excess of 17 per cent, thus compensating largely for the uncertainties. Hence a volume of 413 x 10^6 m^3 for January, 1979, was obtained.

4.5 PRODUCTION RATES

At present water is supplied to Atlantis from 13 production boreholes and the Silwerstroom spring. Of these boreholes five are situated in the Silwerstroom production field, six in the Witzand production field and two in the Atlantis-Wesfleur area. In 1981 the volume of water withdrawn totalled 1,783 693 x 10^6 m^3. As the demand will certainly increase in the foreseeable future, more attention should be directed to the understanding and development of the aquifer. Expansion of the existing production fields is already being planned.

4.6 RECHARGE OF THE AQUIFER

Although recharge of the Atlantis aquifer is a very important aspect, almost no information is available on this subject. The present study could, therefore, only touch this important aspect. The estimation of recharge was based only on the change in storage observed for the period January, 1979, till January, 1980.

Once again, due to uncertainties in information regarding water-levels, sand thickness and storativity values, the estimated value cannot be taken as conclusive.

A value for effective recharge as manifested by rising water-levels, amounts to 4, 603 x 10^6 m^3 for the period January, 1979 - January, 1980. This figure was arrived at by taking artificial withdrawal into account, but neglecting factors such as seaward seepage and evapotranspiration. The above value accounts for 6.52 per cent of the annual rainfall for the same period. When seaward seepage (approximately 2,169 x 10^6 m^3 annually) is also taken into consideration, a total recharge of 9.59 per cent of the annual rainfall is obtained.

4.7 GROUND-WATER QUALITY

Once again very little information was available, thus restricting the present investigation to the construction of a chloride contour map. This map indicates that there is a possibility of interaction between water from the Malmesbury formation and water from the Cenozoic sand deposits. No evidence could be found of sea-water intrusion along the coast-line at present.

5 CONSTRUCTION AND CALIBRATION OF THE NUMERICAL MODEL (PAGE 60)

The model proposed is based on the finite element method whereby the two-dimensional flow of ground water as described by the well-known diffusion equation, is solved in a piecewise continuous fashion, subject to the specification of suitable initial and boundary conditions. Unfortunately, the boundaries of natural aquifers are very rarely, if ever, regular and simple. The flexibility of the finite element method in handling curved boundary conditions, is one of the main reasons for it being such a powerful tool in modelling ground-water systems.

The basis for the construction of a model of this kind is the construction of a finite element mesh. The mesh used in this vestigation consisted of isoparametric quadrilateral elements. The following factors have to be considered when drawing up the finite element mesh:

(i) Topography.

(ii) Bed-rock.

(iii) Ground-water levels.

(iv) Geology.

(v) Natural boundaries of the aquifer.

(vi) Locality of boreholes and springs.

In retrospect, it can be said that the present mesh needs a few refinements before it can be used to construct a management model. These include: the incorporation of proposed production boreholes at nodes in the mesh, and a refinement of the mesh (smaller elements) in the vicinity of the steep ground-water gradients. Although the latter was implemented in the present mesh, a management model would require even smaller elements.

With the mesh constructed, the next step in the development of the model, is the generation of the necessary data. The relevant information required, consists of initial heads, bottom of the flow domain, hydraulic parameters, rates of withdrawal and boundary conditions. In the present model constant head boundary conditions were used and the January, 1979, water-levels were utilized as initial heads.

5.1 CALIBRATION OF THE NUMERICAL MODEL

The basic procedure for the calibration of the model is rather straightforward. The computer is supplied with the necessary information. It then calculates head values for the different time steps. These calculated values are then compared with the heads observed at these times. If they agree, the model can be assumed as being calibrated. If not, the numerical solution must be considered in error and corrective measures taken. These measures comprise the manipulation of the physical data. It must, however, be kept in mind that the observed values are the only physical information available for the system, and hence when adjusting these parameters, care should be taken to keep within physical acceptable limits.

During the calibration of the present model, several deficiencies were identified while the existence of others were confirmed. Among these were:

(i) Insufficent incorporation of production facilities.

(ii) Too large elements in regions of steep ground-water gradients.

(iii) Insufficient knowledge regarding recharge.

(iv) Deficiencies in data regarding initial heads and hydraulic parameters.

The initial calibration over the one year period January, 1979, till January, 1980, was verified with a three year simulation for the period January, 1979, till January, 1982. Once again the existing deficiencies in the available data were confirmed. The model not only confirmed the leakage from the system in the regions indicated in section 4.2, but also requires an influx of water from the area north of Silwerstroom.

6 APPLICATION OF THE NUMERICAL MODEL (PAGE 110)

Although not quite fit for management purposes, the present model can nevertheless be used advantageously in studying the general behaviour of the system in a qualitative fashion. One such application called for at this stage is the evaluation of the proposed additional production boreholes in the Witzand and Silwerstroom production fields, where the future need is estimated at 11.82×10^6 m^3 per annum.

The only problem experienced during this exercise was that the exact positions of the proposed production boreholes were not fully determined and could, therefore, not be incorporated in the finite element mesh. To simulate their effect, an assumed production rate for each borehole was distributed among the nodes in their immediate proposed vicinity.

Apart from the effect of the proposed additional increased withdrawal rates, the effect of recharge on the system was also simulated.

The results obtained from these simulations can briefly be summarized as follows:

(i) The proposed rate of withdrawal of 11,82 x 10^6 m^3 per annum. causes extensive cones of dewatering to develop around the production fields and will dewater the coastal plain the the long run.

(ii) A recharge rate of 9.59 per cent of the annual rainfall had almost no effect on the cones of dewatering. It was only when a recharge rate of 30 per cent of the annual rainfall was specified that the interference of the two production fields could be minimized. In this connection it may be interesting to note that the Silwerstroom and Witzand production fields start to interfere with each other after a period of 36 months. with a recharge rate of 9.59 per cent.

(iii) If the ground-water gradient towards the sea is reversed, sea-water intrusion will be inevitable.

7 MODELLING SEA-WATER INTRUSION (PAGE 136)

There are two methods that can be utilized to study the phenomenon of sea-water intrusion:

(i) The analytical method.

(ii) The numerical method.

To derive an analytical solution, a number of simplifying assumptions have to be made. As these assumptions exclude some of the most important physical features of the real system, it was decided to opt for the numerical approach.

In view of the complexity of the phenomenon and the lack of suitable data. it was decided to restrict the present investigation to a two-dimensional vertical model. based on the alternating direction collocation approximation of the equation of mass conservation.

All the relevant information regarding physical and hydraulic parameters as well as initial and boundary conditions were obtained from the horizontal flow model. Deficiencies in existing information include:

(i) Physical dimensions of the permeable zone connecting the aquifer with the sea.

(ii) Representative values for hydraulic parameters.

(iii) Present position and dimensions of the salt/fresh interface.

7.1 RESULTS OF THE SIMULATIONS

Three simulations were carried out during which the critical boundary conditions were varied in order to obtain a complete image regarding the possibility of sea-water intrusion into the Atlantis aquifer. The results can be summarized as follows:

(i) Given the present prevailing physical and hydraulic conditions, a positive ground-water gradient towards the sea can be maintained and no sea-water intrusion will take place.

(ii) The large-scale withdrawal of water from the Silwerstroom production field can result in a serious sea-water intrusion problem. This intrusion can be prevented by recharging the aquifer artificially on the seaward side of the field.

Seen in the light of the above results, a detailed study regarding the physical and hydraulic characteristics of the region, bordering the coast-line, is recommended.

CHAPTER 1

INTRODUCTION

1.1 SCOPE OF THE INVESTIGATION

The main purpose of the present study was the development of a preliminary mathematical-physical model, based on existing data and to evaluate the sufficiency of the data for such a model. The questions arising from such a study are numerous and cannot all be answered in a preliminary study. It was, therefore, necessary to restrict this investigation to the following more important aspects:

(i) The construction of a suitable numerical model that describes the physical conditions according to existing information.

(ii) The delimitation of uncertainties in the model and areas where further information should be generated, in order to construct a management model.

(iii) The period for which the existing ground-water supply will last, given a certain demand.

(iv) The future development of production fields to ensure the optimum use of the ground-water supply.

(v) The possible contamination of the aquifer by sea-water intrusion.

1.2 LOCATION AND EXTENT OF THE STUDY AREA

The Atlantis aquifer is situated on the west coast of the Cape Province, approximately 50 kilometres north of Cape Town and covers an area of approximately 250 square kilometres. A locality map of the aquifer is shown in Figure 1.1. The Atlantis development area, which was declared a national growth point by Parliament, is situated in the centre of the study area and has an approximate population of 30 000 (Van der Merwe, 1980). No less than 45 factories were in production by the end of 1981. The new Koeberg nuclear power station, situated on the farm Duynefontyn, lies in the southernmost part of the study area.

1.3 PREVIOUS WORK

1.3.1 GEOLOGICAL INVESTIGATIONS

The area was first mapped by S.H. Haughton (1933), who reviewed earlier work on scattered deposits of phoscrete. The area has subsequently been remapped under supervision of H.N. Visser and J.N. Theron, but unfortunately the revised map is still in preparation and could, therefore, not be included in this report. Adjoining sheets 3118C, Doringbaai, and 3218A, Lambertsbaai, were mapped by Visser and Toerien (1971) and sheets 3317B and 3318A, Saldanhabaai, by Visser and Schoch (1973). A detailed description regarding the composition and lithostratigraphy of the Cenozoic sediments in the area, was undertaken by Rogers (1980). The interpretation of geophysical data concerning Cenozoic sediment thickness and pre-Mesozoic bed-rock topography, was initially undertaken by Noble (1975/1976), but has since been re-interpreted by Botha and Bekker (1977).

1.3.2 GEOHYDROLOGICAL INVESTIGATIONS

The first geohydrological investigation in the area was initiated in 1972 by the Geological Survey on behalf of the Cape Divisional Council. The first of 182 boreholes drilled in the area, was sunk by the then Department of Water Affairs in 1974.

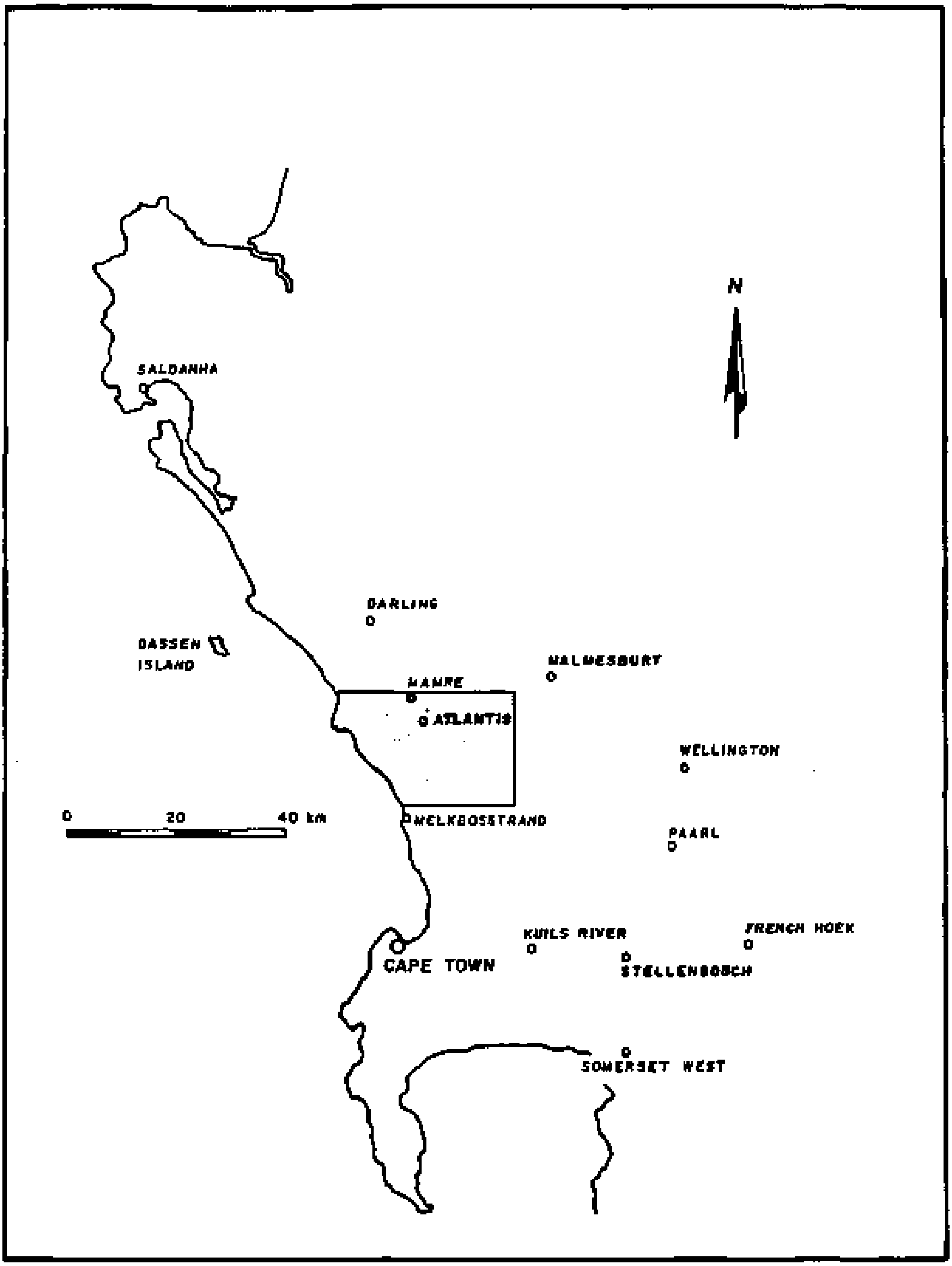

Figure 1.1. Locality map of the study area.

The initial investigation into the ground-water potential of the area was carried out by Noble (1976), while Smit (1976) investigated the drainage patterns and general ground-water levels in his study on sewage disposal. Other reports pertaining to the ground water are those by Vegter *et al* (1976) and Kok (1977).

The first comprehensive report on the ground water of the area was compiled by Van der Merwe (1980). This was followed in quick succession by the reports of Vandoolaeghe and Bertram (1982) and Bredenkamp and Vandoolaeghe (1982). The main objectives of these studies can be summarized as follows:

(i) The behaviour of the ground-water system under artificial stress.

(ii) Re-estimation of the available volume of water in the aquifer.

(iii) Suggestions for the optimal use of the aquifer.

The results obtained during these investigations will be discussed in more detail when the need arises.

1.4 OUTLINE OF THE PRESENT INVESTIGATION

As stated earlier, the main objective of this study is the construction of a numerical model based on available information. Although not directly a part of such a model, the physiographic features of the Atlantis area do play a role in the construction of such a model. For this reason factors such as topography and drainage, paleotopography and climate and vegetation are discussed in Chapter 2 of this report.

Inherent to the construction of any ground-water model, is a sound knowledge of the geology of the area. Of particular importance are ;

(i) the formations forming the bed-rock of the aquifer and

(ii) the Cenozoic sediments that actually form the water-bearing units of the aquifer. A discussion of these formations can be found in Chapter 3.

The most basic information needed in the construction of a numerical model describing a ground-water system, is its geometry and hydraulic properties. Chapter 4, therefore, starts with a discussion of the geometry of the bed-rock formation and delineation of the aquifer boundaries. This is followed by a discussion of the observed water-levels for the period 1978-1983 in section 3 and the hydraulic parameters in section 4.

The volume of water in the aquifer, determined by numerical integration, is estimated in section 5, while section 6 describes the behaviour of the system under stress.

Although a detailed study of recharge and losses from the aquifer do not fully lie within the scope of the present investigation, a short discussion regarding it is given in sections 7 and 8. The Chapter concludes with a summary of the ground-water quality in section 9.

The construction of the numerical model is discussed in Chapter 5. The first section gives an introduction to the mathematical statement of the problem of ground-water flow and its two-dimensional representation by the heat equation. In section 2 the solution of this equation is discussed with special reference to the boundary and initial conditions.

The finite element approximation of the ground-water flow equation is discussed in section 3, with emphasis on the Galerkin formulation and time and space discretization, as well as the construction of a suitable finite element mesh. The calibration of the numerical model is detailed in sections 4 and 5.

Chapter 6 is concerned with the application of the model. Particular attention was paid to the behaviour of the system when subjected to external influences, e.g. large-scale abstraction of water and natural recharge. Section 2 contains a short discussion of the proposed expansion of the production fields and its effect on the water-levels, while recharge is investigated in section 3.

The final Chapter is devoted to a discussion of a numerical model that can be utilized to study the problem of sea-water intrustion into the aquifer. The model itself is described in section 3 and the results obtained with it in section 4.

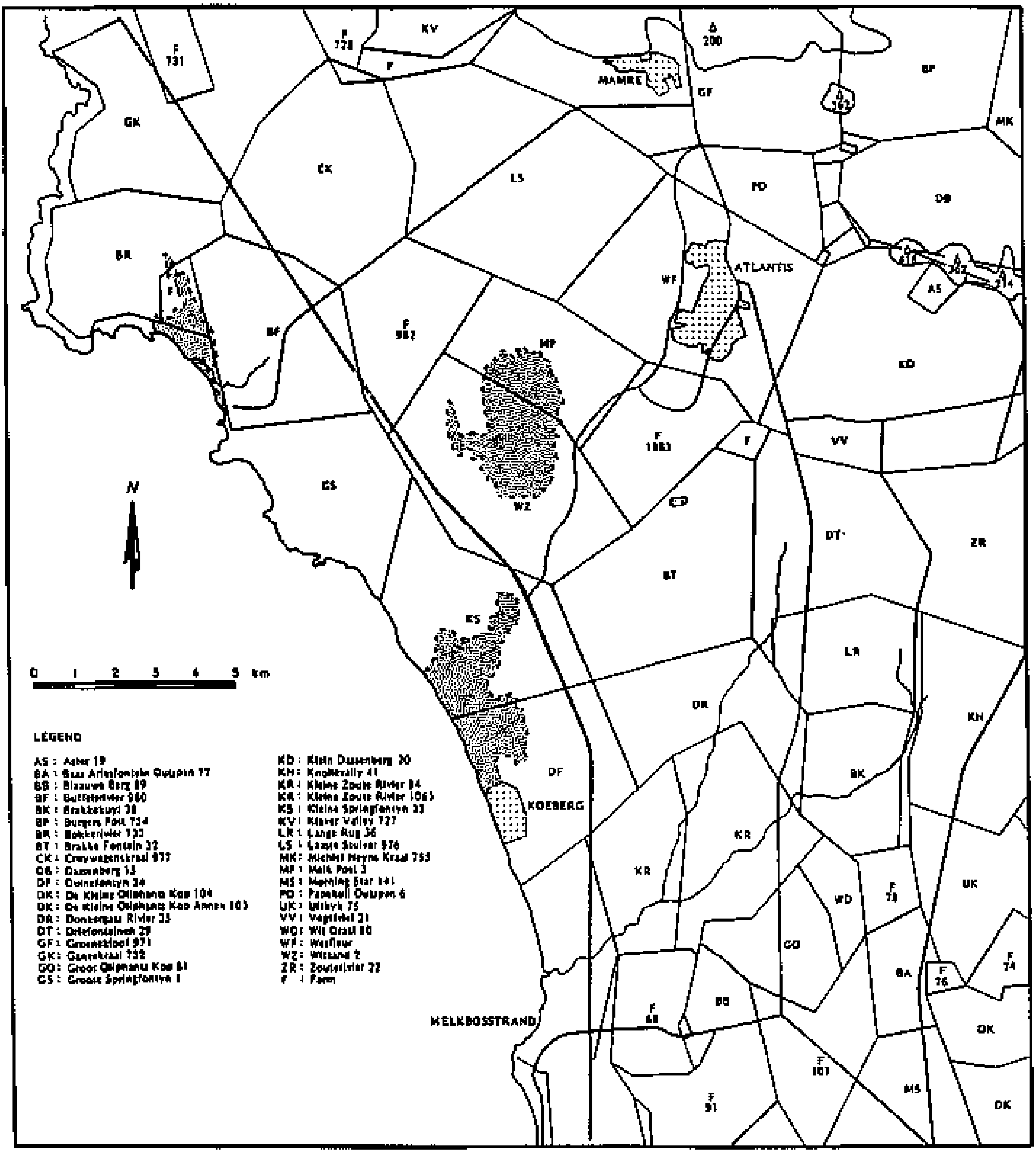

Figure 2.1. Main physiographical features of the Atlantis area.

CHAPTER 2

PHYSIOGRAPHY

2.1 TOPOGRAPHY AND DRAINAGE

The main topographical features of the study area can briefly be summarized as follows. The western part, adjacent to the Atlantic Ocean, consists of featureless coastal plains with an elevation that varies between 20 metres and 60 metres above mean sea-level. Further to the east there is a sudden rise in the topography to form a high-lying area of approximately 100 - 150 metres above sea-level in the south-eastern corner. In the vicinity of Atlantis and Mamre the topography varies between 160 metres and 200 metres above sea-level. It continues to rise in a north-easterly direction to reach a height of 418 metres in the granite kopjes of Dassenberg, Kanonkop and Mamre-Darling. Along the eastern boundary of the study area, a significant drop in the topography, due to the eroding effect of the Diep River, can be observed.

A very distinctive feature of the area is the drift sand dunes. These dunes are present north of the Silwerstroom beach on the farm Buffels River, and southwards adjacent to the coast on the farms Duynefontyn and Kleine Springfontyn. It also occurs to the north-east on the farms Witzand and Melk Post (see Figure 2.1).

The main arteries for surface drainage in the area are the Buffels River in the north-west, the Green River and Diep River in the east and the Sout River in the south.

2.3 CLIMATE

The climate of the Atlantis area is Mediterranean, with a mean maximum temperature of 23,2°C and a mean minimum temperature of 11,8°C as measured at Darling.

The main rainy season is in the winter months. The mean annual rainfall varies from 416 mm, as measured at Melkbosstrand, to 369 mm measured at Mamre. The variability of the rainfall, both on monthly and annual basis, is relatively large as can be seen in Figure 2.3.

Another form of precipitation frequently observed, is condensation from fog. Nothing is, however, known about the contribution of the condensation to the total precipitation. It will consequently be neglected in the discussion to follow.

2.4 VEGETATION

According to Acocks (1975), the vegetation in the Atlantis area, commonly known as Fynbos, is of the Macchia type. It is a very complex vegetation, consisting of a great number of indigenous species. Some foreign species, for example the Rooikrans (*Acacia cyclops*), are abundant in the area and easily supplant the indigenous vegetation. The Fynbos is particularly associated with sandstone and poor, white, sandy soil and requires at least 250 mm of winter rain per annum.

This form of vegetation tends to develop a deep root system and may, therefore, contribute significantly to the evapotranspiration rate of the area, especially during the warm and generally dry summer months. As evapotranspiration can play a significant role in both replenishing and depletion of the ground-water reserves, it will be necessary for the future development of the aquifer to pay more attention to it. For the present it will, however, be neglected.

2.2 PALEOTOPOGRAPHY

Of particular importance for the movement of ground water is the paleotopography of the area. The available information indicates that this consists mainly of rocks of the Malmesbury Formation, weathered over a large area. Not much is known about the hydraulic characteristics of the Malmesbury Formation, except that it tends to form an impervious clay in the weathered state. For the present it will, therefore, be assumed that the Atlantis aquifer is bounded from below by this clay layer. A three-dimensional representation of the paleotopography, derived from available borehole logs (Rogers, 1980) and geophysical soundings (Van der Merwe, 1983), is given in Figure 2.2. It is interesting to note that the surface topography more or less follows the paleotopography.

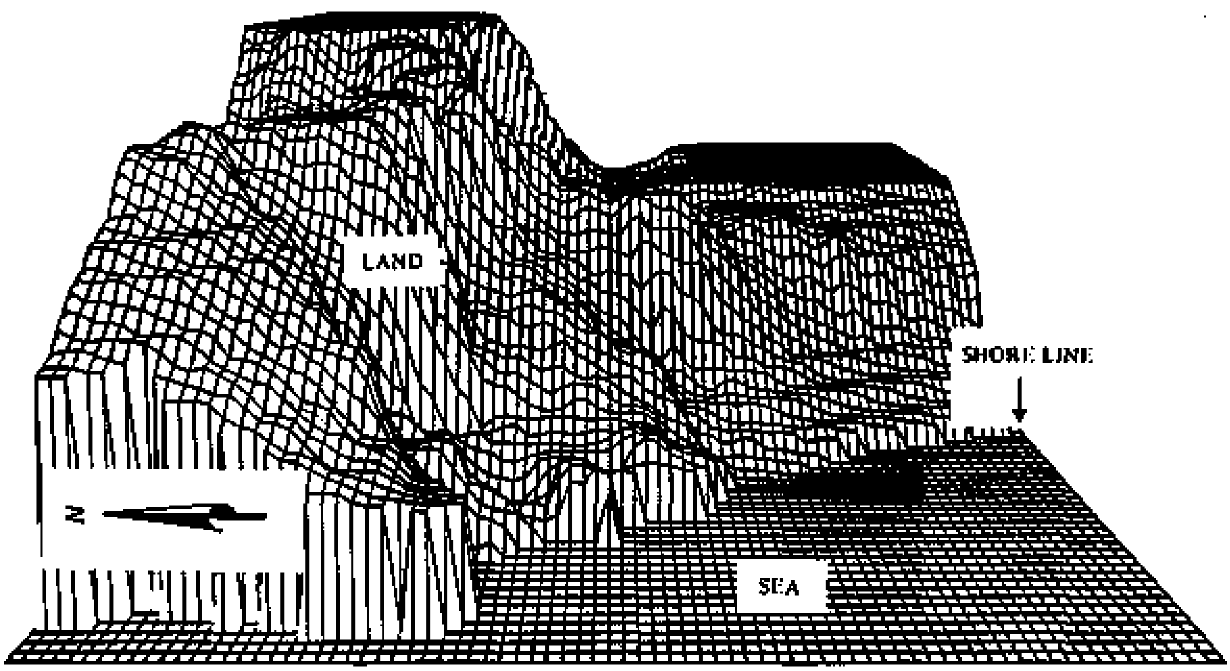

Figure 2.2. Three-dimensional representation of the paleotopography.

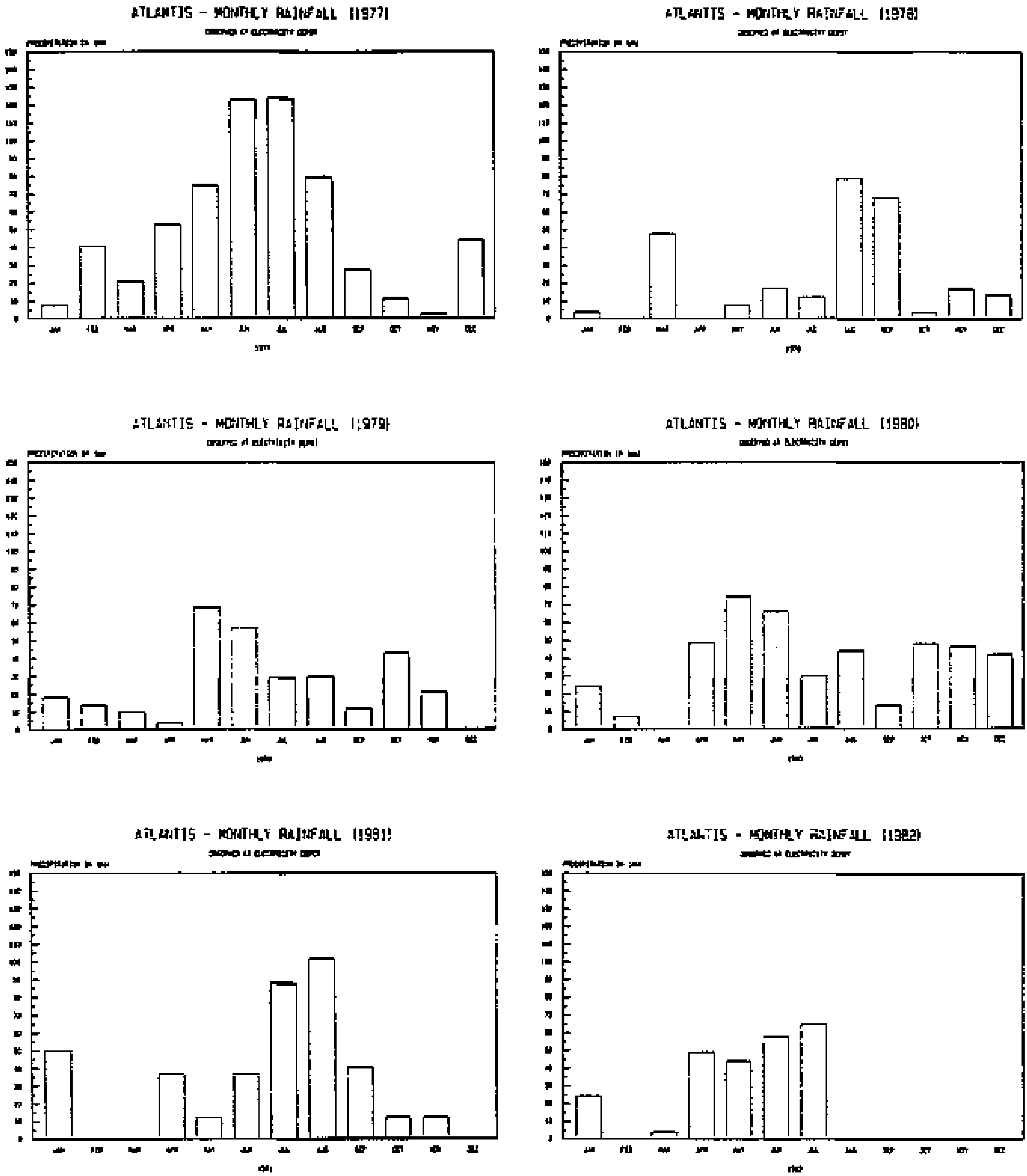

Figure 2.3. *Bar charts showing the monthly rainfall at Atlantis for the period January 1977 till July 1982.*

CHAPTER 3

GEOLOGY

3.1 INTRODUCTION

A detailed description of the geology of the area does not fall within the scope of the present discussion. However, since the physical conditions prevailing in the aquifer are largely dependent on the geology, it cannot be completely neglected. A geological map, given in Figure 3.1, was thus compiled from data received from the Department of Environment Affairs (Van der Merwe, 1983) and the Geological Survey (Bellville Office). This map may not be accurate to the last detail, but is the best available. (A more detailed one may be published in the near future by the Geological Survey).

The geology in the Atlantis area can be divided chronologically into three main units.

(i) The Malmesbury Group.

(ii) Intrusive granite of the Darling Pluton.

(iii) Cenozoic sediments.

Although the Cenozoic sediments are considered to be the main water-bearing unit, the other geological units form an integral part of the aquifer, at least to the extent that they form the physical boundaries of the flow domain.

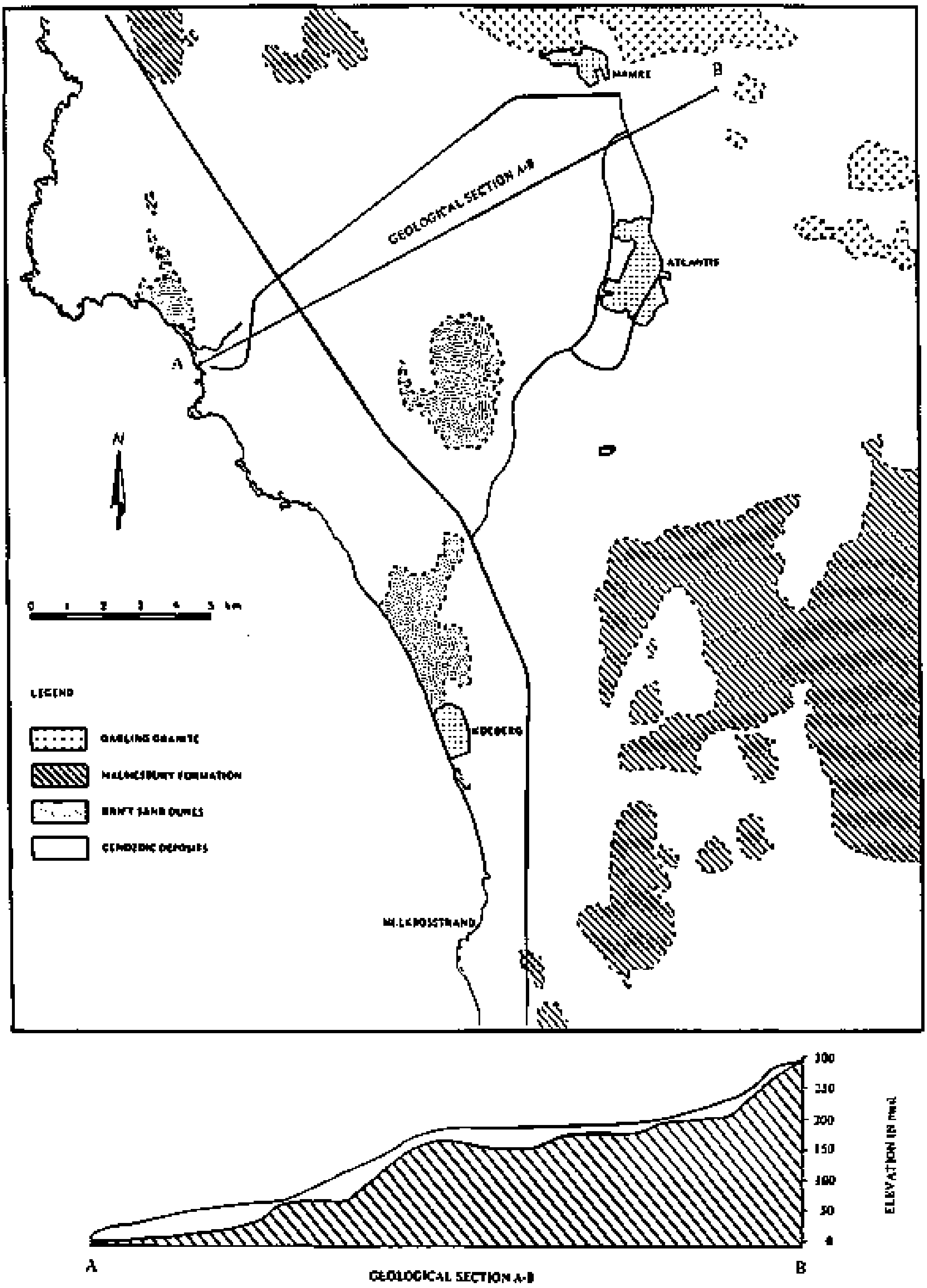

Figure 3.1. *Geological map of the Atlantis area.*

3.2 THE MALMESBURY GROUP

The Malmesbury Formation underlies the younger sediments over the entire area and, as noted in section 2.2, forms the impervious bottom of the flow domain. It is important to note that the upper contact of the Malmesbury rocks is seldomly observed below sea-level (Rogers, 1980). In fact, it frequently rises above sea-level along the coast, where it can be observed as rocky shoals such as Robbesteen. Inland the bed-rock rises relatively steeply and is very close to the surface in the transition zone between the coastal plain and the plateau.

According to Visser and Schoch (1973), the Malmesbury Formation consists predominantly of greywacke that ranges from a massive medium-grained type to a fine-grained, more phyllitic variety. Subordinate phyllitic shale occurs as partings and bands of varying width in alternation with greywacke. Small quartz veins are very common in the Malmesbury rocks and are most abundant in the shale.

Bedding can clearly be distinguished, but in the massive greywacke the cleavage and bedding can easily be confused. Generally, the cleavage has a steeper inclination than the bedding.

Numerous boreholes in the area indicate that the Malmesbury rocks are deeply weathered beneath the Cenozoic sediments. The weathered zone consists of a clay layer of varying thickness. According to Vandoolaeghe (personal communication), this clay layer can easily be confused with layers consisting of sedimentary clay. The elevation of the bed-rock, as given in the borehole logs, may, therefore, be under suspicion in certain cases. Exploratory drilling has also revealed that along the coastal region, from Matroosbaai to Melkbosstrand, the clay layer may often be absent, and that the Malmesbury rocks in this region tend to be more sandy.

Very little is at present known about the water-bearing characteristics of the Malmesbury rocks. What is known, however, is that when water is encountered in the Malmesbury rocks, the quality tends to be relatively poor.

3.3 INTRUSIVE GRANITE OF THE DARLING PLUTON

The importance of the granite in the area is to be found in that it presumably forms an impervious lateral boundary of the sand aquifer. Several varieties of granites, whose mutual relationships are highly complex, are present. Numerous xenoliths of Malmesbury rocks are found in the intrusive Darling granites. As is the case with the Malmesbury rocks, very little is known regarding the water-bearing characteristics of the granite.

3.4 CENOZOIC SEDIMENTS

The sedimentary Cenozoic deposits form the main water-bearing unit of the Atlantis aquifer. These marine and aeolian deposits reach thicknesses of up to 60 metres in the central and eastern parts, while a thickness of 80 metres has been observed in the south-western part of the area.

Because of the variation in lithology, both vertically and horizontally, the sand cannot be regarded as being homogeneous. Rogers (1980) consequently divided the sand into a number of stratigraphic units and sub-units.

3.4.1 VARSWATER FORMATION (MARINE ORIGIN)

This Formation, which is of marine origin, is divided by Rogers into two members: Silwerstroom and Duynefontyn members.

3.4.1.1 Silwerstroom member

This member comprises gravel, sand and mud. The gravel consists of shell fragments and rounded pebbles of weathered Malmesbury metasediments (Rogers, 1980). The sand fraction is poorly sorted and contains quartz and shell fragments, with its most distinctive component being phosphatized shell fragments. The Silwerstroom member never occurs above sea-level (Rogers, 1980).

3.4.1.2 Duynefontyn member

The Duynefontyn member overlies either the Silwerstroom member or where the latter has pinched out, Malmesbury metasediments. In the Duynefontyn area it is found below sea-level, but in other parts of the area it occurs as high as 42 metres above sea-level. The Duynefontyn member comprises fine sand that is well-sorted. It is composed of polished quartz and minor quantities of black phosphatized shell fragments.

3.4.2 BREDASDORP FORMATION (AEOLIAN ORIGIN)

Although the sediments of the Bredasdorp Formation are considered to be of aeolian origin, the Gastropod bed of the Springfontyn member is interpreted as being a regressive, exposed-beach horizon (Rogers, 1980).

3.4.2.1 Springfontyn member

According to Rogers (1980), a distinctive characteristic of the Springfontyn member is a basal Gastropod bed. Internal casts of gastropods are distributed along subhorizontal laminae in laminated, well-sorted, fine and coarse sand.

The rest of the Springfontyn member is a clean, well-sorted fine to coarse quartz sand. No shell fragments are found in the Springfontyn member. This member seems to be the main water-bearing unit in the area.

3.4.2.2 Mamre member

The Mamre member is considered to be the inland equivalent of the Springfontyn member. The main difference is the high peat and silt content of the Mamre member. According to Bredenkamp and Vandoolaeghe (1982), this characteristic is very prominent in the deposits south of Mamre, in the Witzand area and in the boundary zone of the Silwerstroom area. The high silt content of this member can clearly influence the hydraulic conductivity of the aquifer adversely.

3.4.2.3 Witzand member

According to Rogers (1980), the Witzand member consists mainly of semi-consolidated, shelly, calcareous, aeolian sands. Since the Witzand member usually occurs above the water-table, it does not play a significant role in ground-water movement as such (Bredenkamp and Vandoolaeghe, 1982). It could, however, play a very significant role in the recharge of the aquifer, a factor which has to receive more attention in future research.

CHAPTER 4

GEOHYDROLOGY

4.1 GENERAL

The main objective of this investigation, as stated earlier, is to construct a numerical model that describes the physical conditions according to existing information. At this stage, it should be pointed out that the accuracy attainable by any model can never exceed the accuracy of the data used in constructing the model. An accurate model for a given system can thus only be constructed if sufficient information on the system is available.

Some of the more important properties, as far as ground-water modelling is concerned, are (i) the geometry of the aquifer with specific reference to the boundary conditions, (ii) water-level distribution, (iii) the aquifer parameters, hydraulic conductivity and storativity, (iv) discharge rates, i.e. abstraction and evaporation rates and (v) recharge rates including natural infiltration.

In the present chapter the available data for the Atlantis aquifer will be analysed with the view of obtaining as much information as possible on these properties.

4.2 GEOMETRY OF THE ATLANTIS AQUIFER

4.2.1 INTRODUCTION

The important role played by the boundary conditions in any mathematical model requires a knowledge of the physical boundaries of the system that is as accurate as possible. After careful consideration of all available information (Van der Merwe, 1983; Bredenkamp and Vandoolaeghe, 1982), it was decided to restrict the extent of the Atlantis aquifer to the sand deposits in the area. Although there are indications of some interaction between the sand aquifer and water in the Malmesbury Formation (Van der Merwe, 1983), this had to be neglected in the present investigation due to insufficient information.

4.2.2 BED-ROCK ELEVATION AND SAND THICKNESS

The sand deposits in the Atlantis area are bounded in the west by the sea and inland by outcrops of Darling granite and the Malmesbury Formation (see Figure 3.1). The extent of the area, covered by sand, can thus in principle be obtained from the geological map of the area. The thickness of the sand cover and its spatial variation can, however, only be obtained from geophysical soundings and borehole logs.

The main sources containing the geophysical soundings of Atlantis are the gravity and seismic surveys, conducted by the Geological Survey of South Africa (Botha and Bekker, 1977; Botha and Thompson, 1977). However, the difficulties experienced in distinguishing between the assumed clay layer that underlies the sand and the sand itself, cannot always be explained from these profiles alone. In fact, cases are known where the interpreted profile does not correspond with the known geology of the area. A case in point is the interpreted gravity profile, AL, located as shown in Figure 4.1. While the profile line is bisected by an outcrop of Malmesbury rocks, the interpreted profile (Figure 4.2) shows a constant thickness of sand across the geological contact. This is in agreement with an observation by Van der Merwe (1983) that neither the gravity nor the seismic surveys give conclusive results regarding the elevation of the weathered Malmesbury Formation. He, in fact, states categorically that where no borehole data is available, the elevation of the bed-rock cannot be established beyond all doubt, using the geophysical results alone.

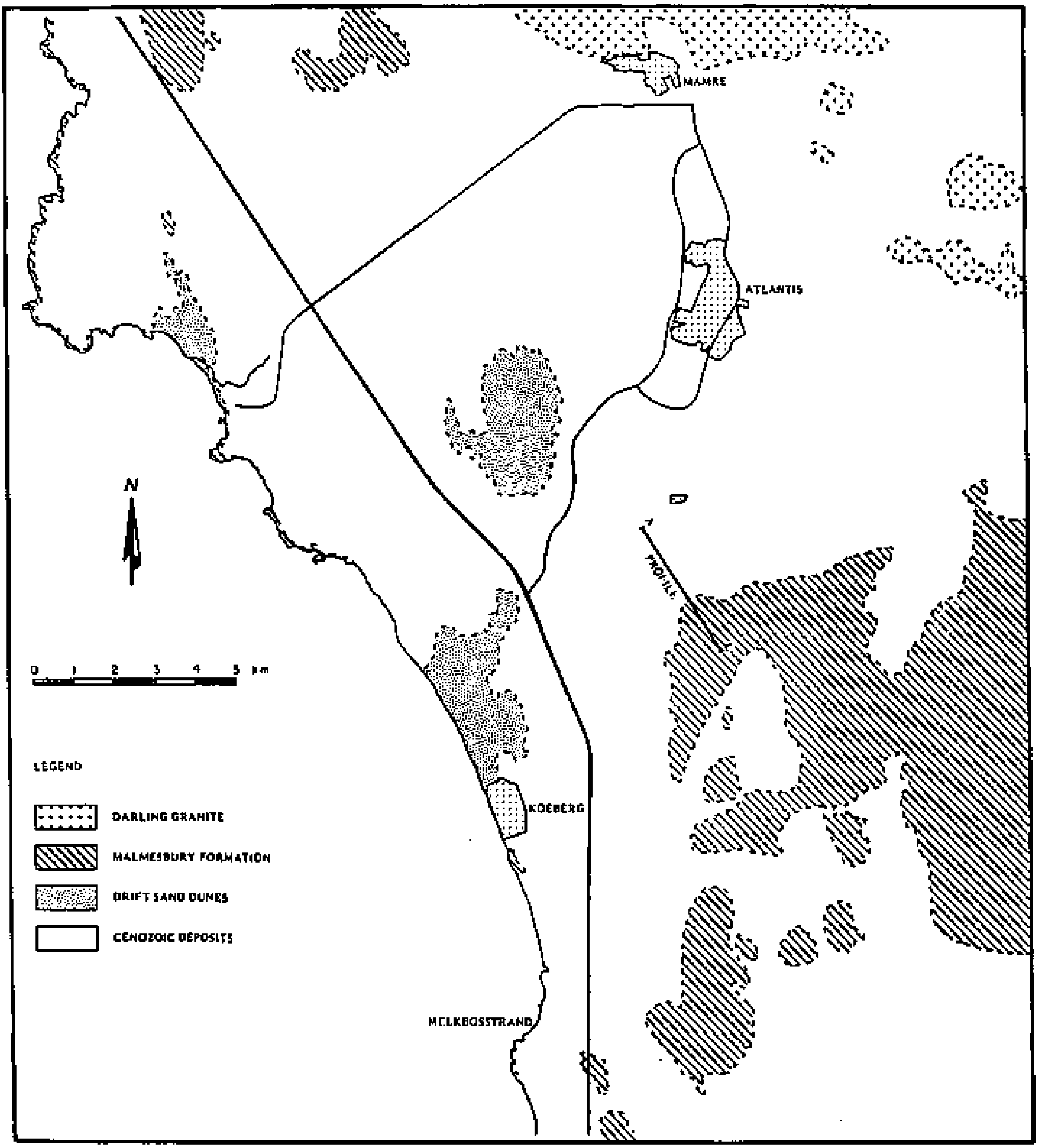

Figure 4.1. Map showing the locality of the gravity profile line AL.

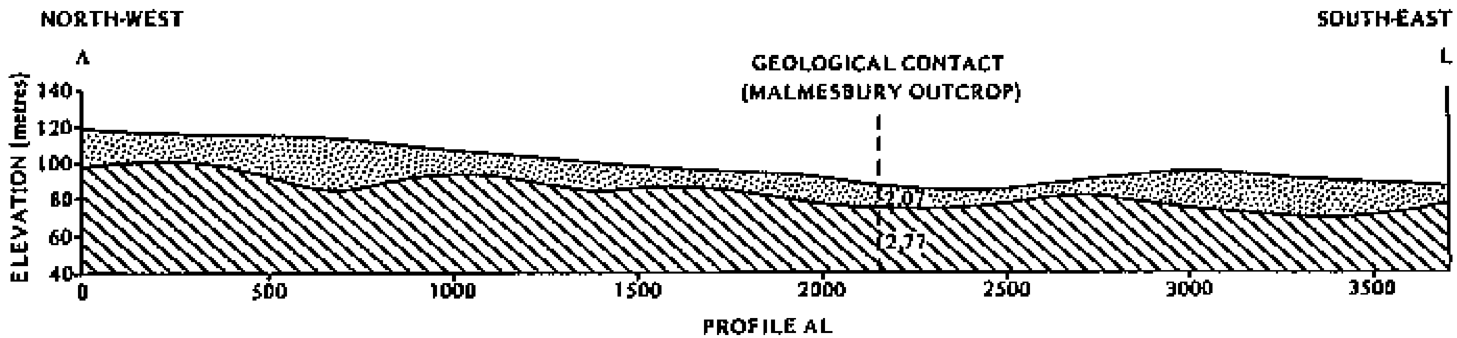

Figure 4.2. *Interpreted gravity profile line AL, showing a constant sand thickness across a geological contact mapped in the field.*

Because of this uncertainty in the geophysical profiles, it was decided to base the bed-rock elevation, used in this investigation, solely on the geological logs of 128 boreholes in the area (Rogers, 1980) and the geological map in Figure 3.1.

A contour map of the bed-rock elevation, determined in this way, is given in Figure 4.3. In view of the limited number of data points used in its construction, this map may not be very accurate, but it is the best that can be constructed from the available data.

The most outstanding feature of the contour map in Figure 4.3 is perhaps the sharp decline in the bed-rock elevation, parallel to the coast and at a distance of + 9 km from the coast. This phenomenon will surely influence the ground-water flow in the aquifer significantly. It is also interesting to note that only in the Silwerstroom area does the bed-rock actually lie below sea-level. This could be of great importance when the case of sea-water intrusion is to be considered.

It is a simple exercise to determine the sand thickness once the bed-rock elevation has been determined. For this purpose use was again made of the geological records of the 128 boreholes, and Figure 3.1, supplemented by data taken from the published topographical map of the area. A contour map of the sand thickness, determined in this way, is shown in Figure 4.4. This map may, for the same reasons stated earlier, again not be very accurate. In particular the position of the 1 metre sand isopach may be in doubt. This is so, because only a small number of boreholes are situated near the boundaries of the system and therefore the position of this contour line had to be based mainly on data obtained from the geological map in Figure 3.1.

No significance should be attached to the closed contour lines in the area south of Duynefontyn. It is, in fact, known that relative thick sand deposits continue right down to Melkbosstrand, but no quantitative data is available at present.

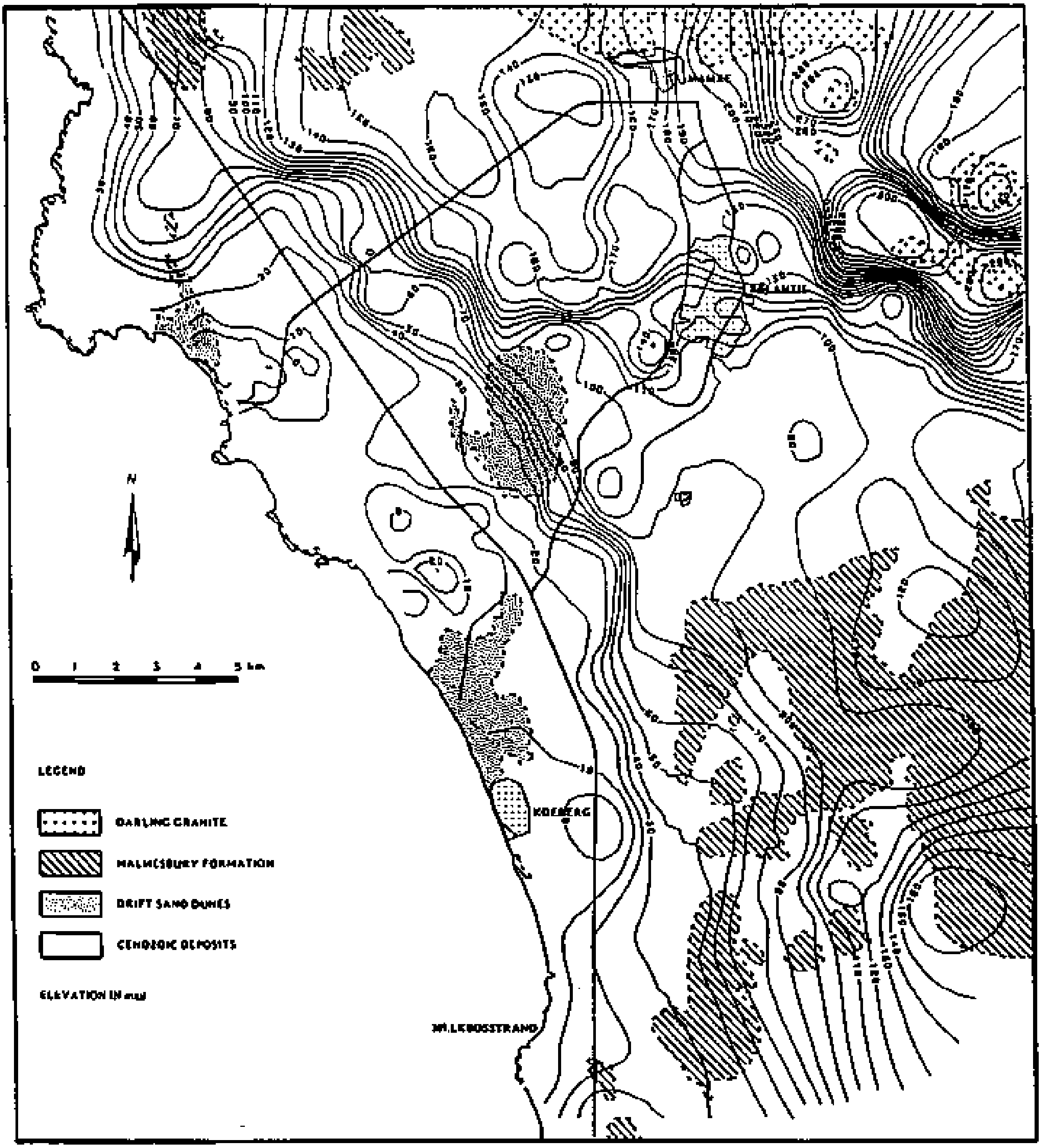

Figure 4.3. Bed-rock elevation contour map.

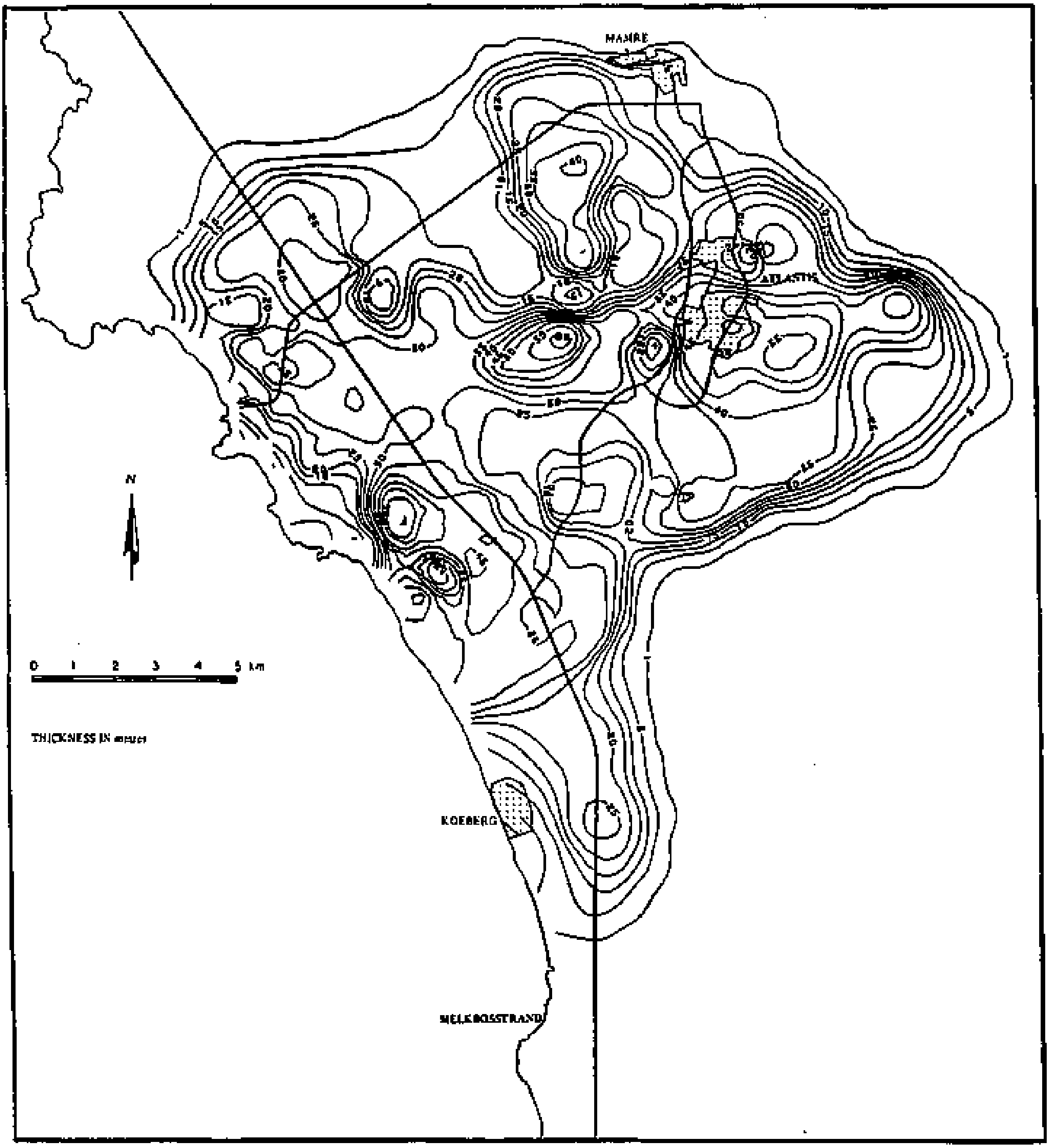

Figure 4.4. Sand thickness contour map.

Another interesting phenomenon that can be observed in Figure 4.4 is the non-uniformity of the sand thickness. This could affect the modelling of the aquifer, as well as its potential, adversely if significant lowering of the water-levels were to occur.

4.2.3 LATERAL BOUNDARY

The restriction of the aquifer to the sand deposits immediately provides an upper bound for its lateral boundaries. However, as indicated by the water-levels in the few boreholes close to these boundaries, the present water-table covers a much smaller area. It was therefore decided to select the sea and the 1 metre sand thickness contour in Figure 4.4 as aquifer boundaries. This choice has the advantage that it makes ample provision in case the water-table rises considerably in the aquifer.

4.3 WATER-LEVELS IN THE ATLANTIS AQUIFER

The single, most important, quantity in the study of any aquifer is perhaps the water-levels. To construct water-level contour maps, use was made of the water-levels supplied by the Division of Geohydrology of the Department of Environment Affairs. Unfortunately, the number of boreholes used to observe these water-levels vary considerably over the years for which observations are available. Furthermore, the boreholes form a few large clusters instead of being spread more evenly across the aquifer. The result is that the accuracy of contour maps is not always the same. This is, for example, shown in the contour maps of the January water-levels for each year from 1978 up to 1983, given in Figures 4.5 - 4.10. The + signs on these maps indicate the position of the observation boreholes, the water-levels of which have been used in the construction of the maps.

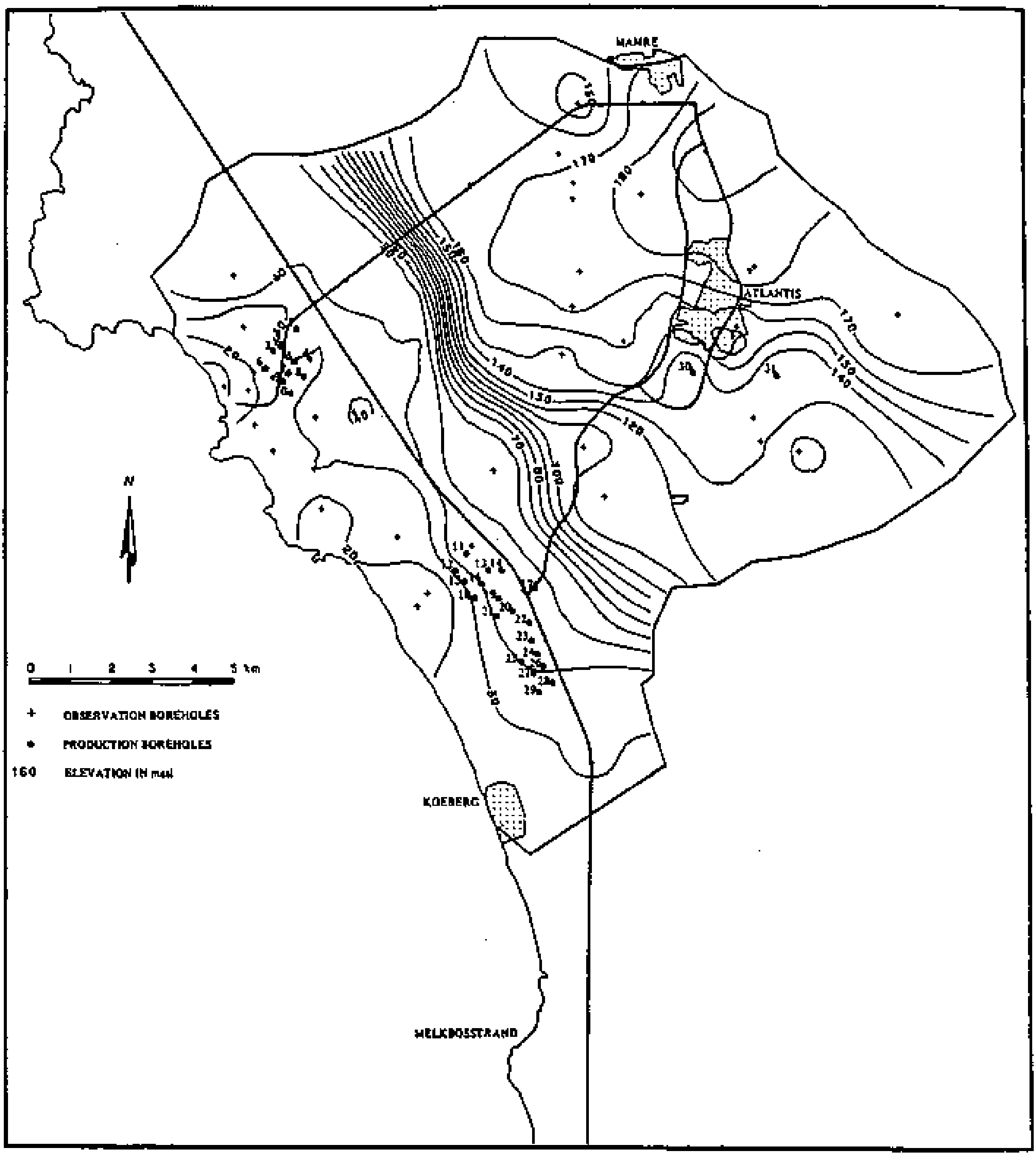

Figure 4.5. Water-level elevation - January 1978.

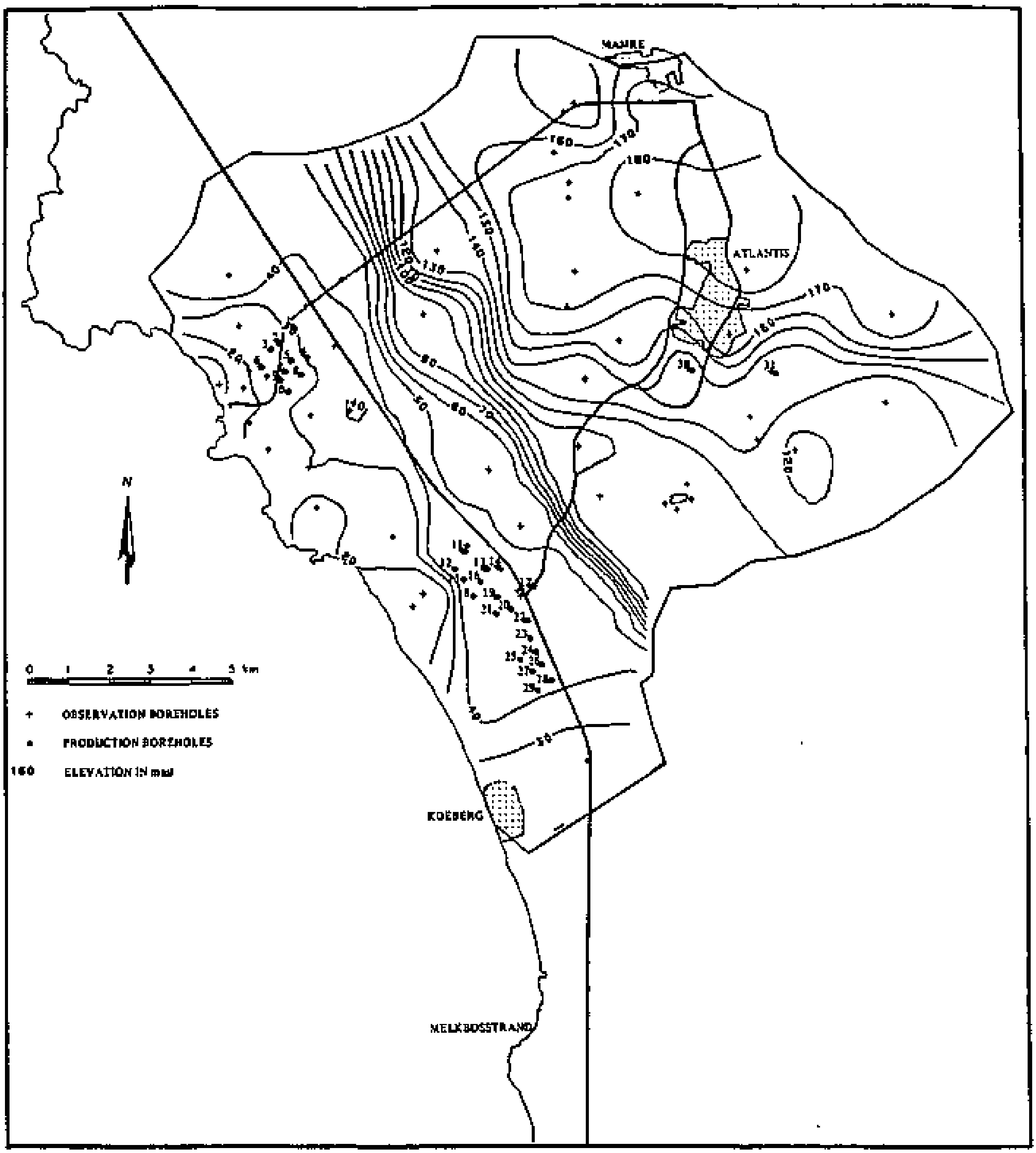

Figure 4.6. Water-level elevation - January 1979.

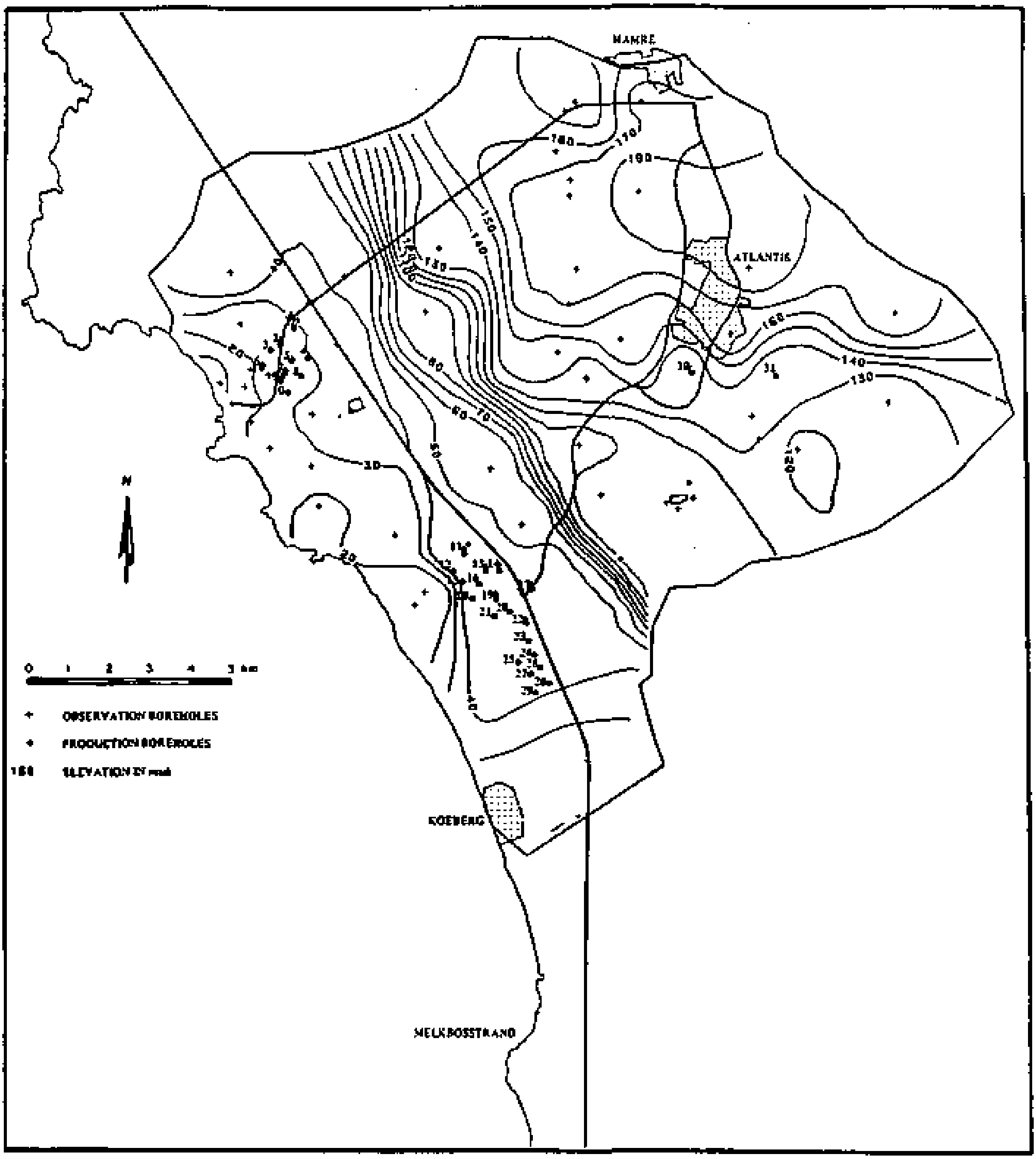

Figure 4.7. Water-level elevation - January 1980.

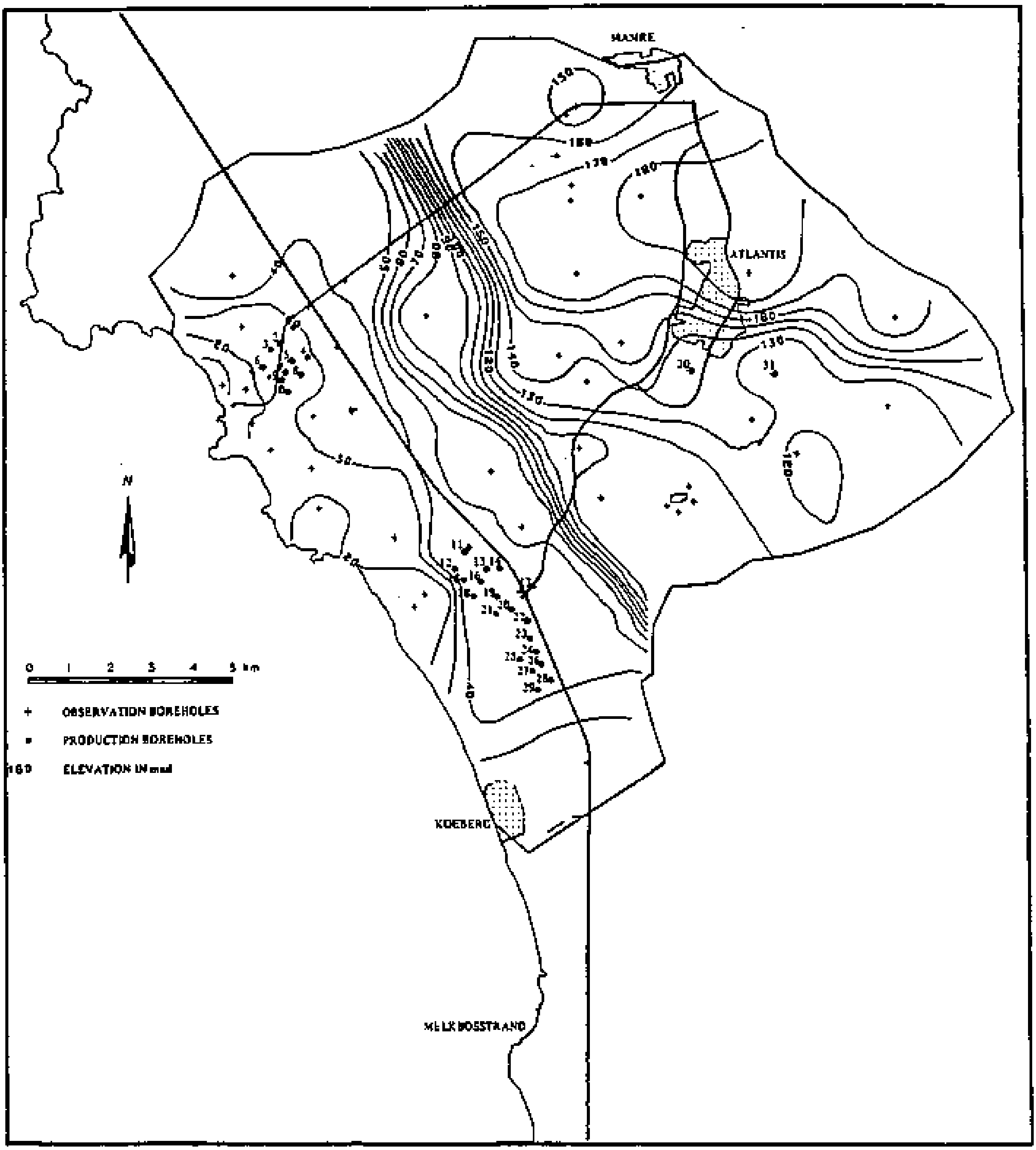

Figure 4.8. Water-level elevation - January 1981.

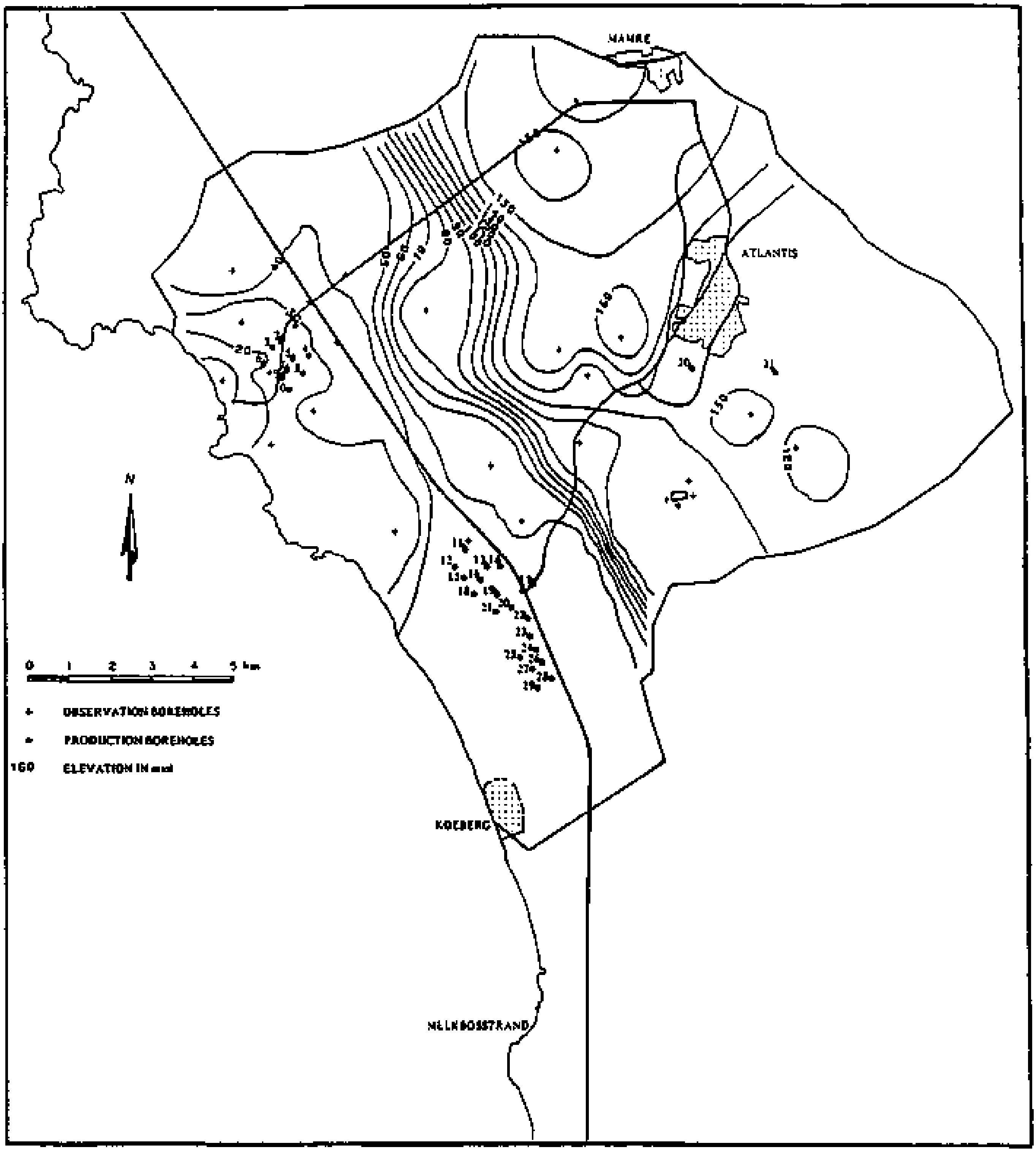

Figure 4.9. Water-level elevation - January 1982.

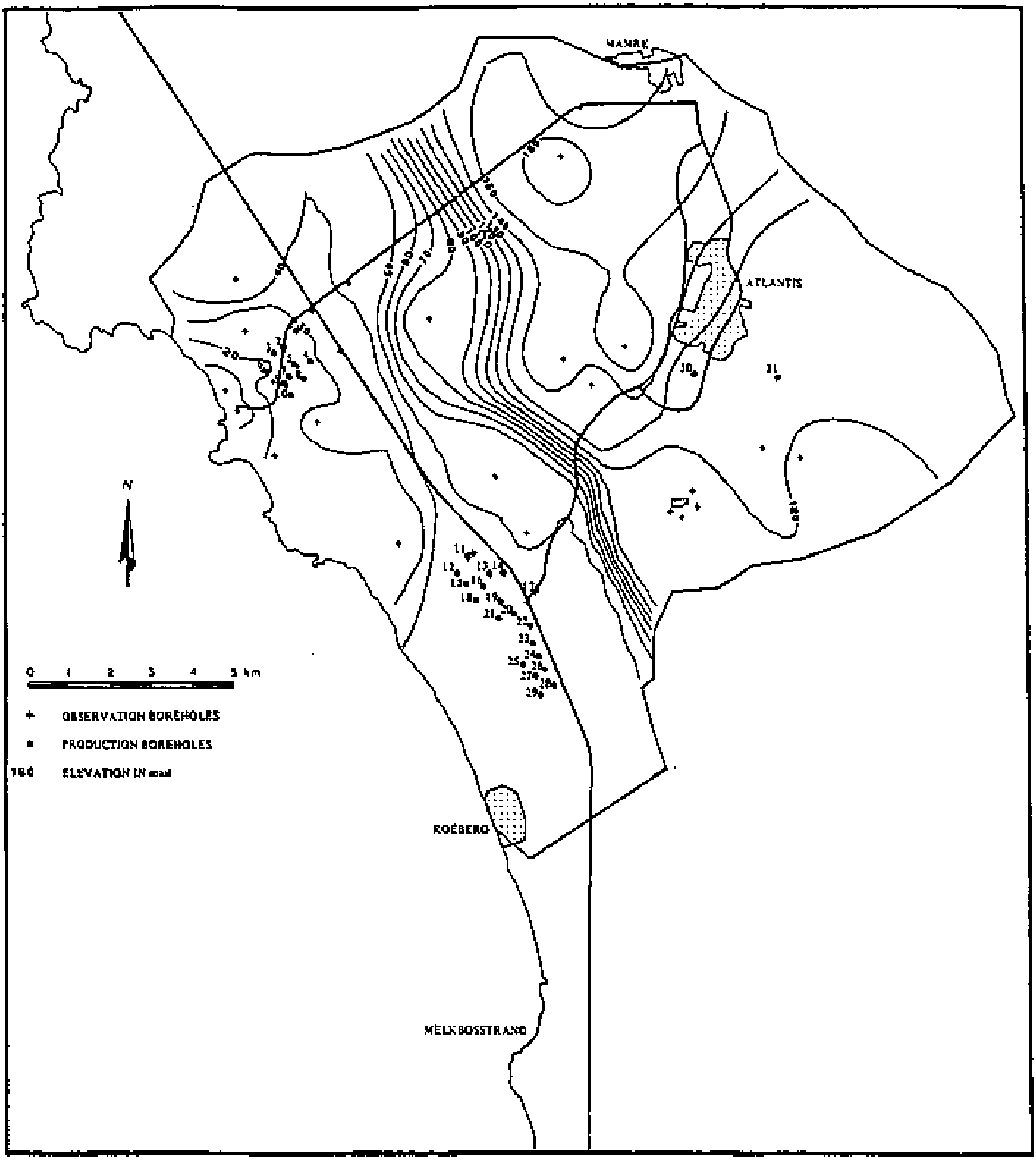

Figure 4.10. Water-level elevation - January 1983.

It is rather unfortunate that the number of observation boreholes in the Atlantis aquifer decreased over the years. This does not only make it more difficult to estimate fundamental quantities such as the volume of the aquifer, but will certainly also hamper the calibration of any model set up for the aquifer. It is, therefore, suggested that, depending on the planned future development of the aquifer, the number of observation holes in the aquifer be increased or at least better spaced than the existing ones. In the discussion that follows, only the three maps for the period January 1979 - January 1981 will, therefore, be considered.

A comparison of the water-level contours, with the bed-rock contours, in Figure 4.3 indicates that the water-levels follow, in general, the bed-rock. Just as in the case of the bed-rock, there is a fairly steep ground-water gradient running parallel to the coast, which separates the Silwerstroom and Witzand production fields from the Atlantis-Wesfleur production area. This implies that the gradient of the ground water is always positive towards the sea; a very important situation as far as the possible intrusion of sea-water is concerned.

According to the ground-water contours, there are four regions where water may leak out of the system:

(i) Along the coast-line.

(ii) In the north near Mamre.

(iii) In the south-eastern part of the aquifer.

(iv) In the extreme south near Melkbosstrand.

One region where the aquifer may be recharged from outside is the region just north of the Silwerstroom area. Whether water actually leaves or enters the system at these regions, cannot be decided on from the available data. However, although the abstraction of ground water in the Silwerstroom area has almost doubled during the period January 1979 till January 1981, no significant lowering of the ground-water levels for this region can be observed in the contour maps. This fact must surely indicate that some form of recharge must exist in this area. If the aquifer is going to be used more intensively in future, these regions should be investigated in more detail. Another interesting observation that follows from the contour maps, is the relative high elevation of the ground water along the coast-line in the vicinity of Grootte Springfontyn. This could be an indication of the low permeability of the Malmesbury rocks.

The fact that the water-level contour lines seem to continue across the boundaries, does not necessarily mean that the actual water-levels in the sand aquifer continue across the boundaries into the surrounding rocks. Although it may well be the case, it can at present also be ascribed to a lack of water-level data along the boundaries of the aquifer.

When taken together, the present evidence indicates that the system is basically a non-homogeneous water-table aquifer. This will, therefore, form the basis of the model to be developed for the system.

4.4 HYDRAULIC PARAMETERS OF THE ATLANTIS AQUIFER

From a modelling point of view and more specifically for the purpose of constructing a management model, knowledge of the hydraulic parameters of a ground-water system is of the utmost importance. It is therefore necessary to obtain as much accurate data concerning these parameters as possible. Normally values for hydraulic conductivity and storativity are obtained by means of pump tests. Unfortunately such tests were only carried out at the 16 production boreholes. Bredenkamp and Vandoolaeghe (1981) supplemented these pump test data with results obtained from Hazen's formula, applied to the granulometric properties of the sand obtained by sampling of the sand during the drilling of the boreholes. In this way they succeeded in estimating these values at the 38 locations shown in Table 4.1.

TABLE 4.1. HYDRAULIC PARAMETERS OF THE ATLANTIS AQUIFER

LOCATION	CONDUCTIVITY (m/day)	STORATIVITY
Spring	100,8	0,18
G29749	3,2	0,10
G29757	9,1	0,21
G29773	9,8	0,18
G29775	7,0	0,18
G29781	1,7	0,05
G29782	1,3	0,05
G29786	6,0	0,18
G29793	9,7	0,18
G29794	13,2	0,22
G29800	1,6	0,05
G30835	0,8	0,15
G30849	1,4	0,15
G30850	6,9	0,18
G30851	0,0	0,18
G30865	8,2	0,21
G30926	1,2	0,15
G30927	17,3	0,18
G30928	8,9	0,18
G30929	3,9	0,18
G30932	10,0	0,18
G30935	11,2	0,18
G30936	8,2	0,21
G30938	8,3	0,18
G30939	7,5	0,18
G30940	4,9	0,18
G30943	6,3	0,18
G30944	9,3	0,18
G30946	8,6	0,18
G30948	8,3	0,20
G30965	9,6	0,27
G30966	7,5	0,14
G30969	9,9	0,19
G30971	14,9	0,25
G30972	7,9	0,19
G30981	12,3	0,26
G30991	11,7	0,21
G30999	14,1	0,16

The way in which these values have been derived, casts some doubt on their accuracy. Fortunately there exists a good objective method to investigate this; the method of kriging. This method is particularly useful when applied to hydraulic parameters (Van Tonder, 1982). Contours of these parameters and the associated 95 per cent confidence levels were consequently calculated for both parameters. The contour maps are shown in Figures 4.11 and 4.12, while the 95 per cent confidence maps are shown in Figures 4.13 and 4.14 for the hydraulic conductivity and storativity respectively.

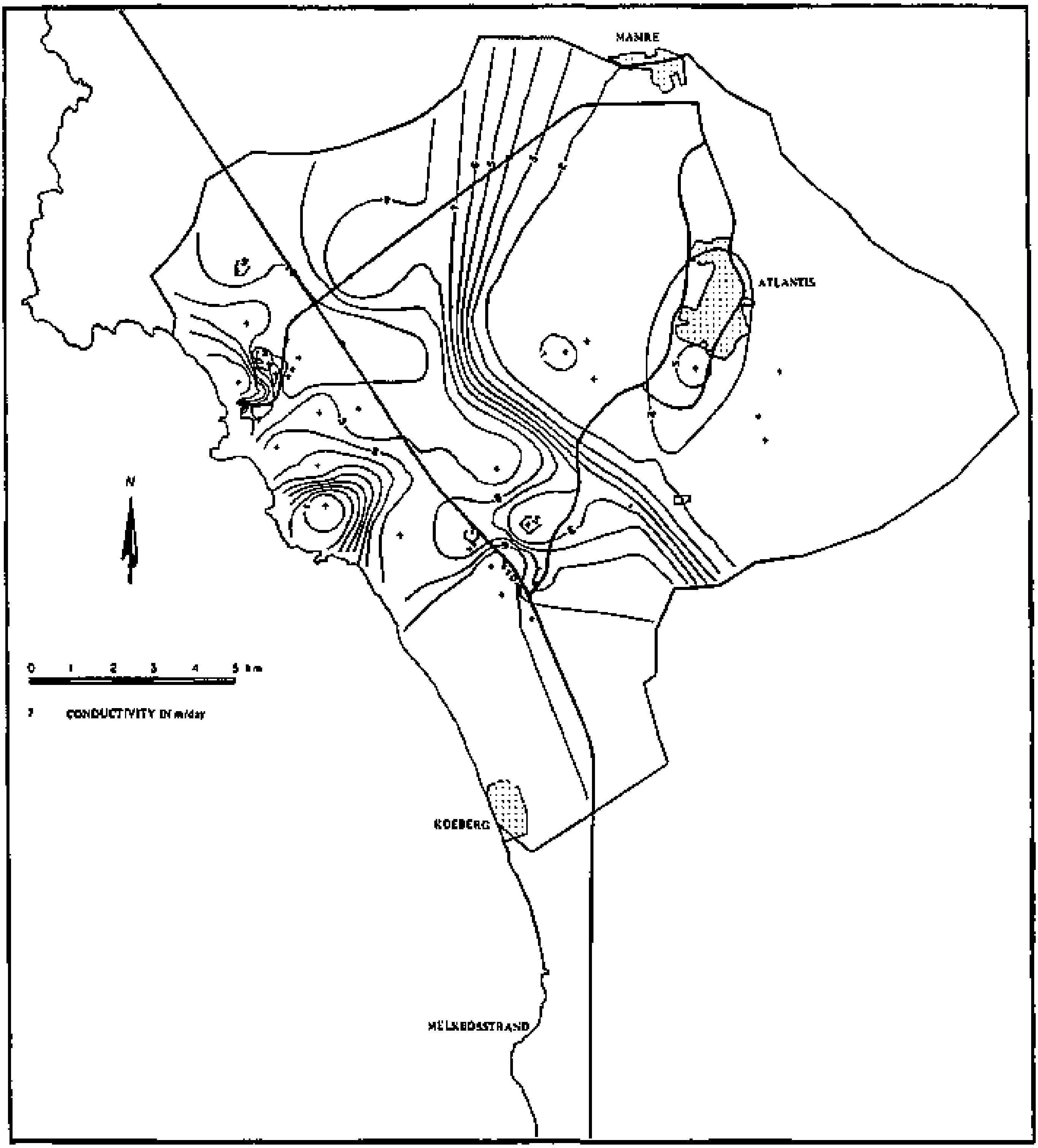

Figure 4.11. Hydraulic conductivity contour map.

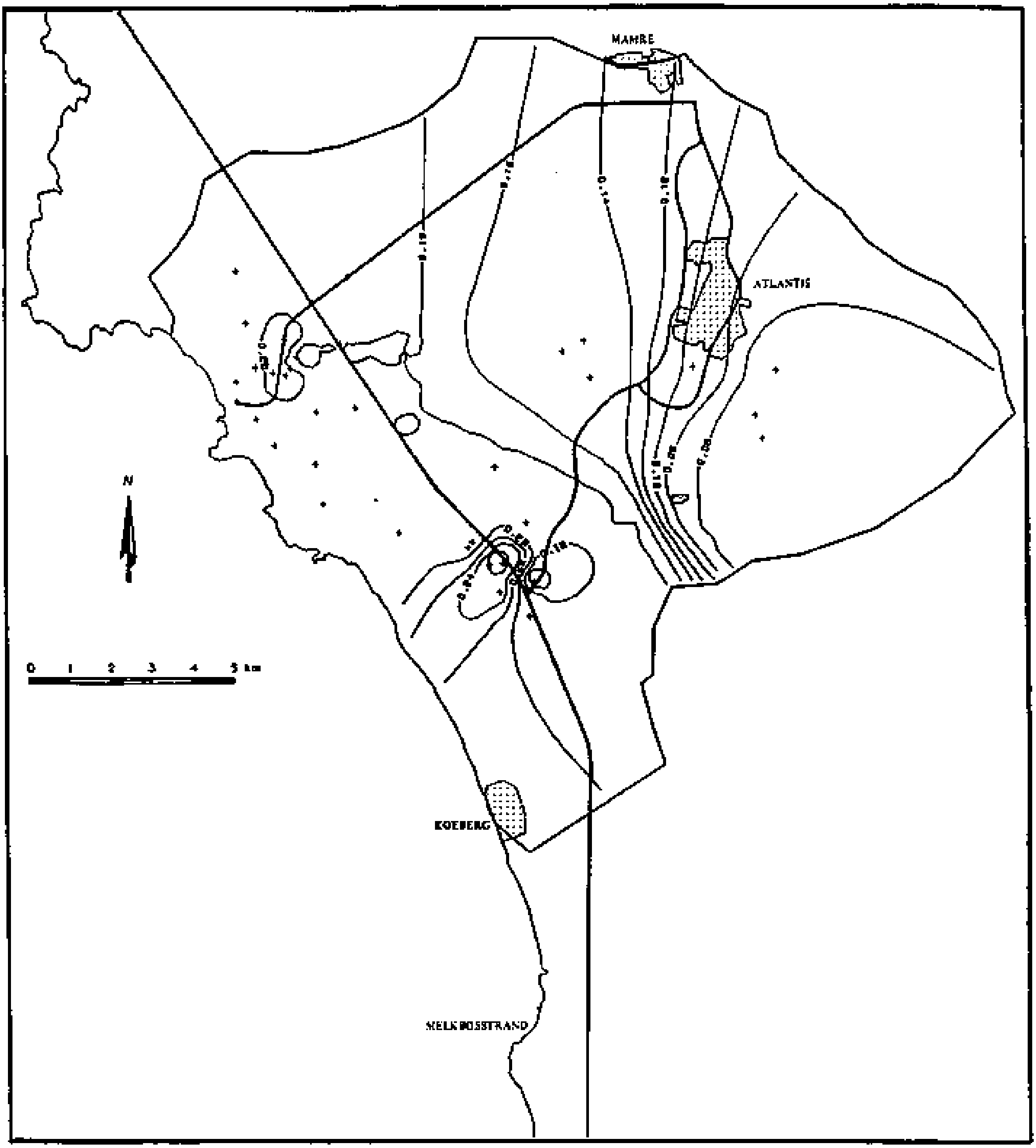

Figure 4.12. Storativity contour map.

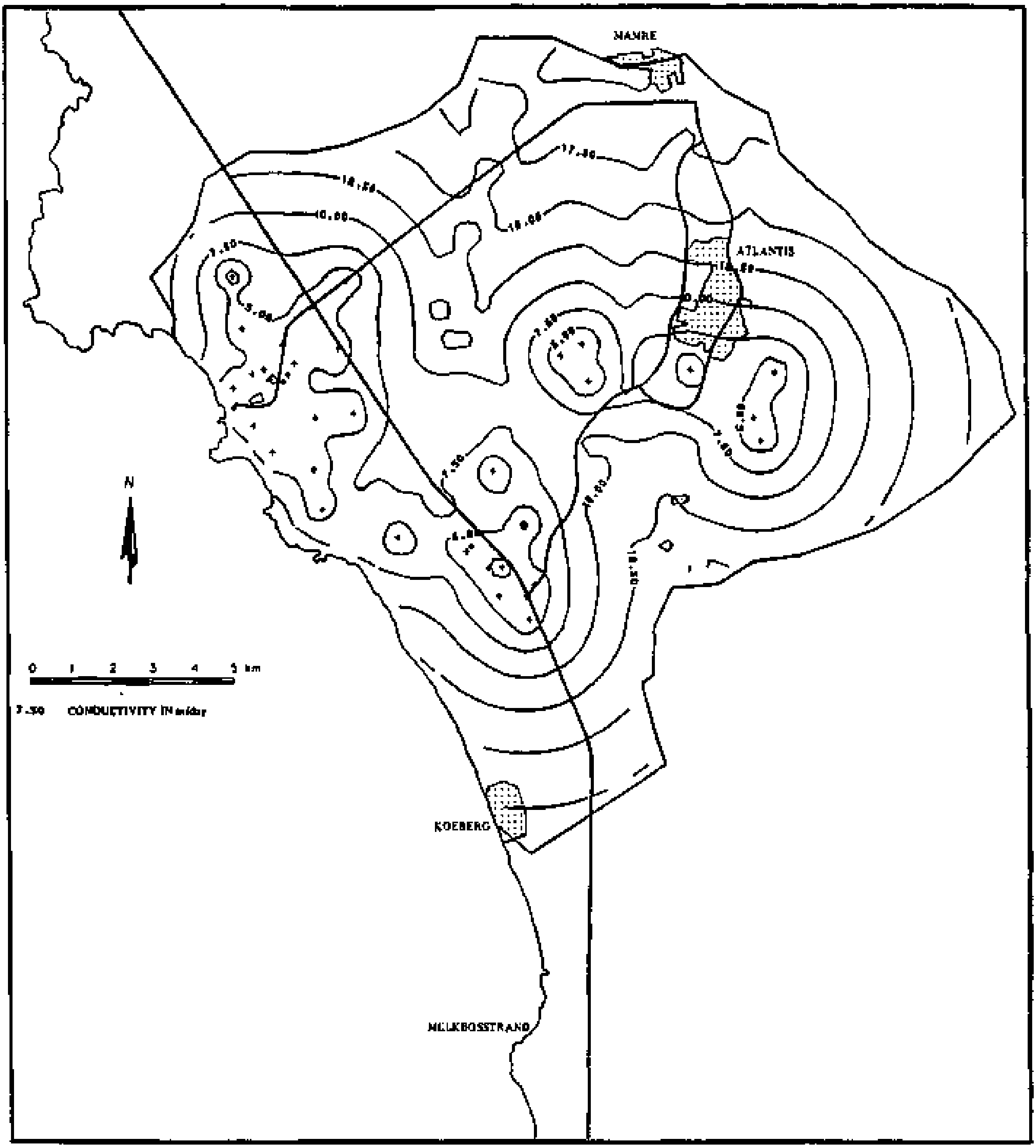

Figure 4.13. Kriging standard deviation confidence map for the hydraulic conductivity contours shown in Figure 4.11.

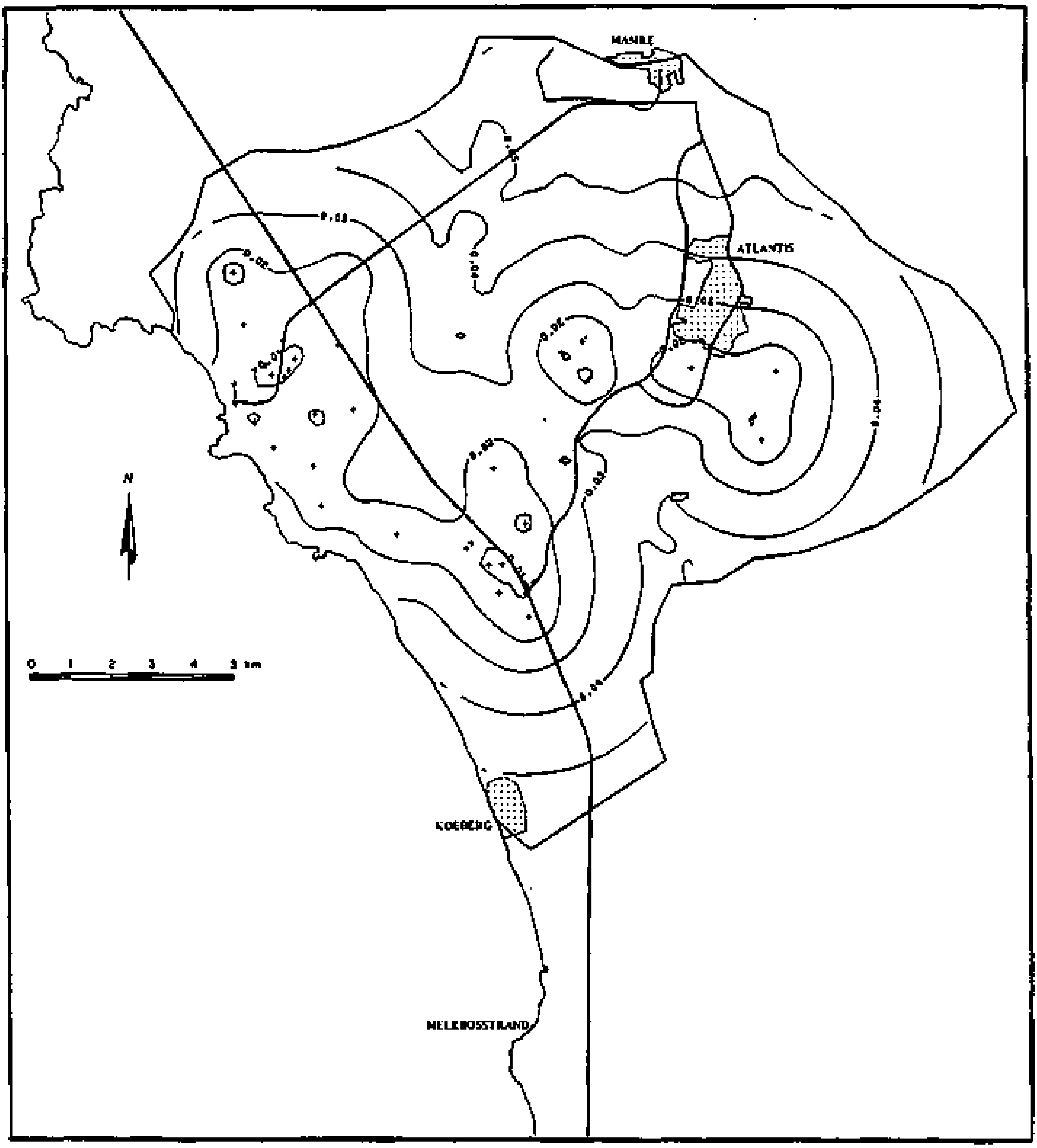

Figure 4.14. Kriging standard deviation confidence map for the storativity contours shown in Figure 4.12.

It is important to remember when discussing these maps that the contour lines on the 95 per cent confidence maps represent the standard deviation from the field data. These maps should, therefore, always be studied in context with the conductivity and storativity contour maps (Figures 4.11 and 4.12). There are various advantages in using this approach of which the most important are:

(a) The delimitation of areas where additional data should be generated. (This is particularly useful when considering the development of a management model).

(b) During the calibration of the numerical model, these maps can be used to ensure that the hydraulic parameters used in the model, are realistic in the sense that they do not contradict physical acceptable values for sand deposits.

The most important deduction that can be made from these maps is that there exist large areas, particularly in the eastern part and along the boundaries of the aquifer, where the uncertainty in the present data is disturbingly large. For example, the standard deviation of the hydraulic conductivity in the Mamre area may be as much as eight times larger than the hydraulic conductivity itself. In view of the planned future development of the system, particular attention should be given to the problem of determining more accurate hydraulic parameters for the aquifer as a whole.

In view of the inaccuracies in the present data, no general conclusion can really be drawn from them. Nevertheless, the data does indicate that there exists a steep conductivity gradient that forms a transition zone between the lower conductivities of the Atlantis-Wesfleur area and the higher conductivities of the Silwerstroom and Witzand areas. It is also interesting to note that this transition zone more or less coincides with a zone of steep ground-water gradients. Another interesting fact is that the storativity in the Silwerstroom area is fairly constant. This suggests that the sand is fairly homogeneous in this area. The range of the storativity values in the Atlantis aquifer is also typical of a water-table aquifer.

4.5 VOLUME OF THE AQUIFER

4.5.1 VOLUME OF THE SATURATED SAND

Of prime importance in the evaluation of any aquifer, is the volume of saturated materials it contains. This can easily be calculated once the bed-rock elevation and water-levels have been determined. In view of the remarks in section 4.3 on the quality of the water-level data, it was decided to base this calculation for Atlantis on the January 1979 water-levels.

There are a number of ways in which the volume of an irregular body, such as an aquifer, can be calculated. The simplest method is perhaps through the numerical integration of the saturated sand thickness of the aquifer. An isopach map of the saturated sand thickness was therefore constructed (see Figure 4.15). Three straight lines X_1 X_2, X_3 X_4 and X_5 X_6 were then imposed on the map (see Figure 4.16). The line X_1 X_2 is perpendicular to the coast-line and more or less bisects the aquifer, while the lines X_3 X_4 and X_5 X_6 are used to approximate the northern and southern boundaries of the aquifer respectively. The isopach map was then divided into a series of elements by profile lines on regular intervals (500 metres), perpendicular to line X_1 X_2. The length of each profile line, which is bisected by line X_1 X_2, is determined by taking the bigger distance along the profile line between line X_1 X_2 and either line X_3 X_4 or line X_5 X_6. This procedure ensures that every profile line will always be of sufficient length to reach the boundaries of the aquifer. Each of these profile lines was again divided into regular intervals, 500 metres apart. The complete network of these profile lines, covering the entire aquifer, can be seen in Figure 4.17.

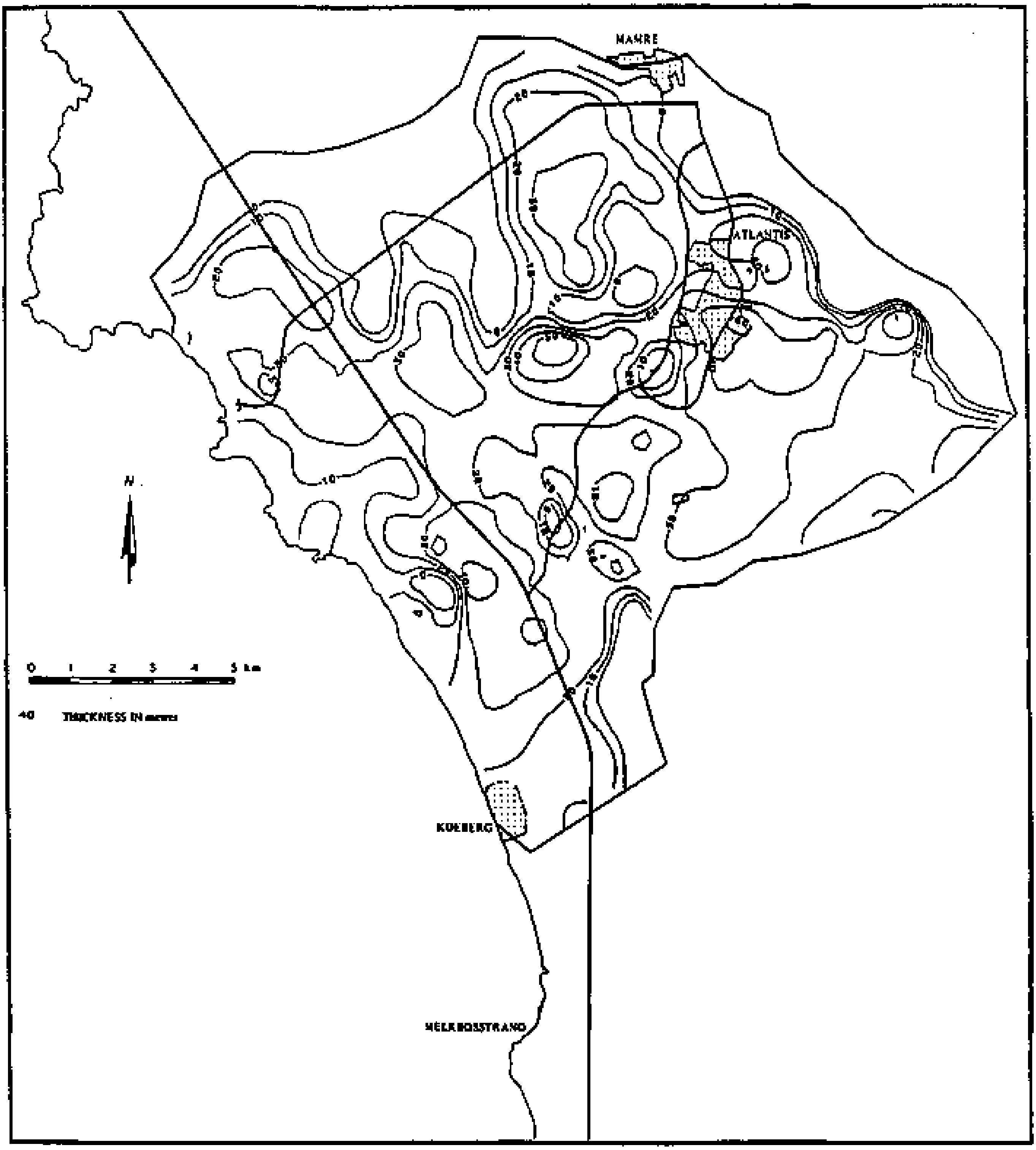

Figure 4.15. Saturated sand thickness - January 1979.

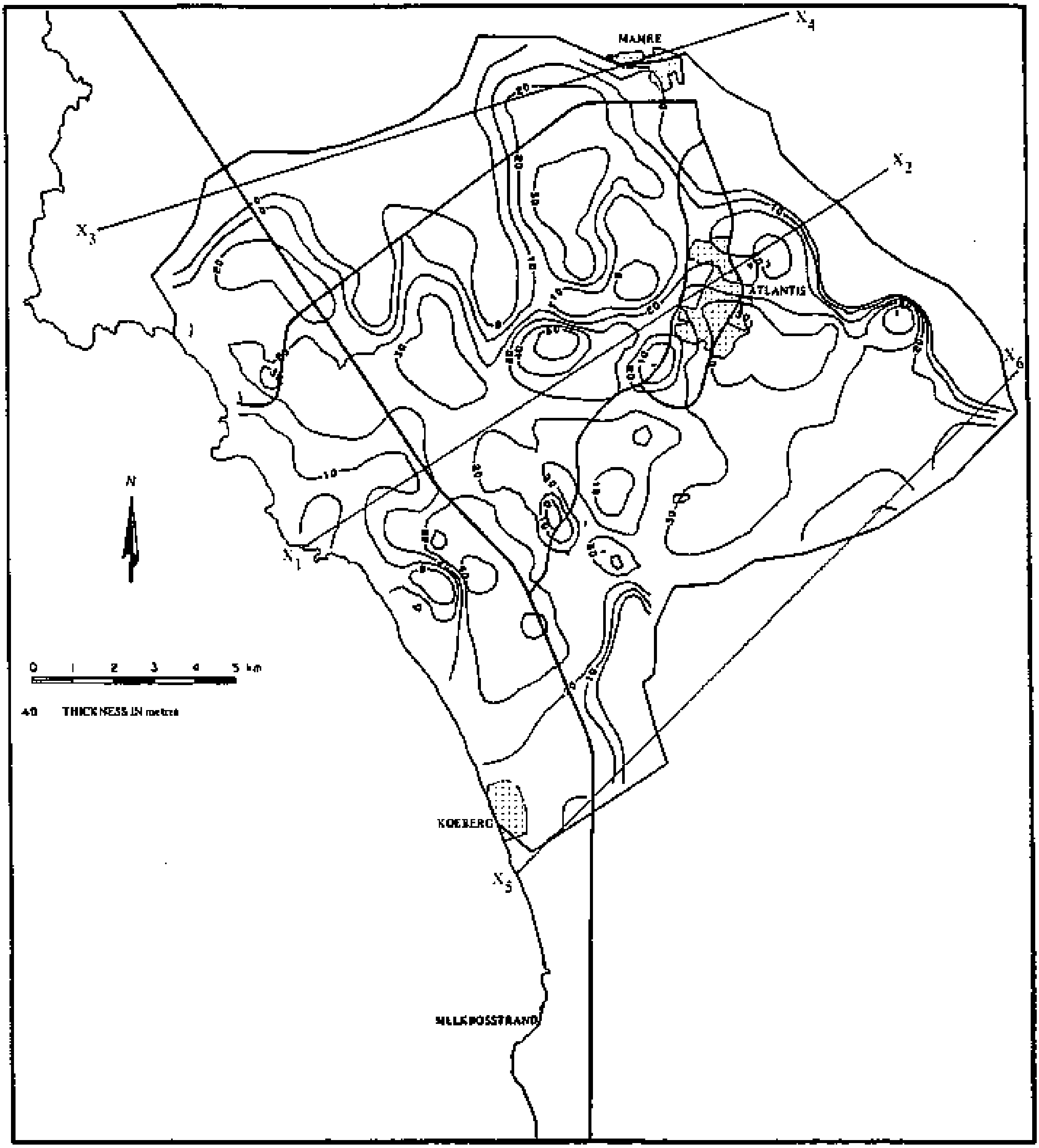

Figure 4.16. Map showing the locality of the lines X_1 X_2, X_3 X_4 and X_5 X_6 constructed to facilitate the construction of the profile lines by means of a digital computer.

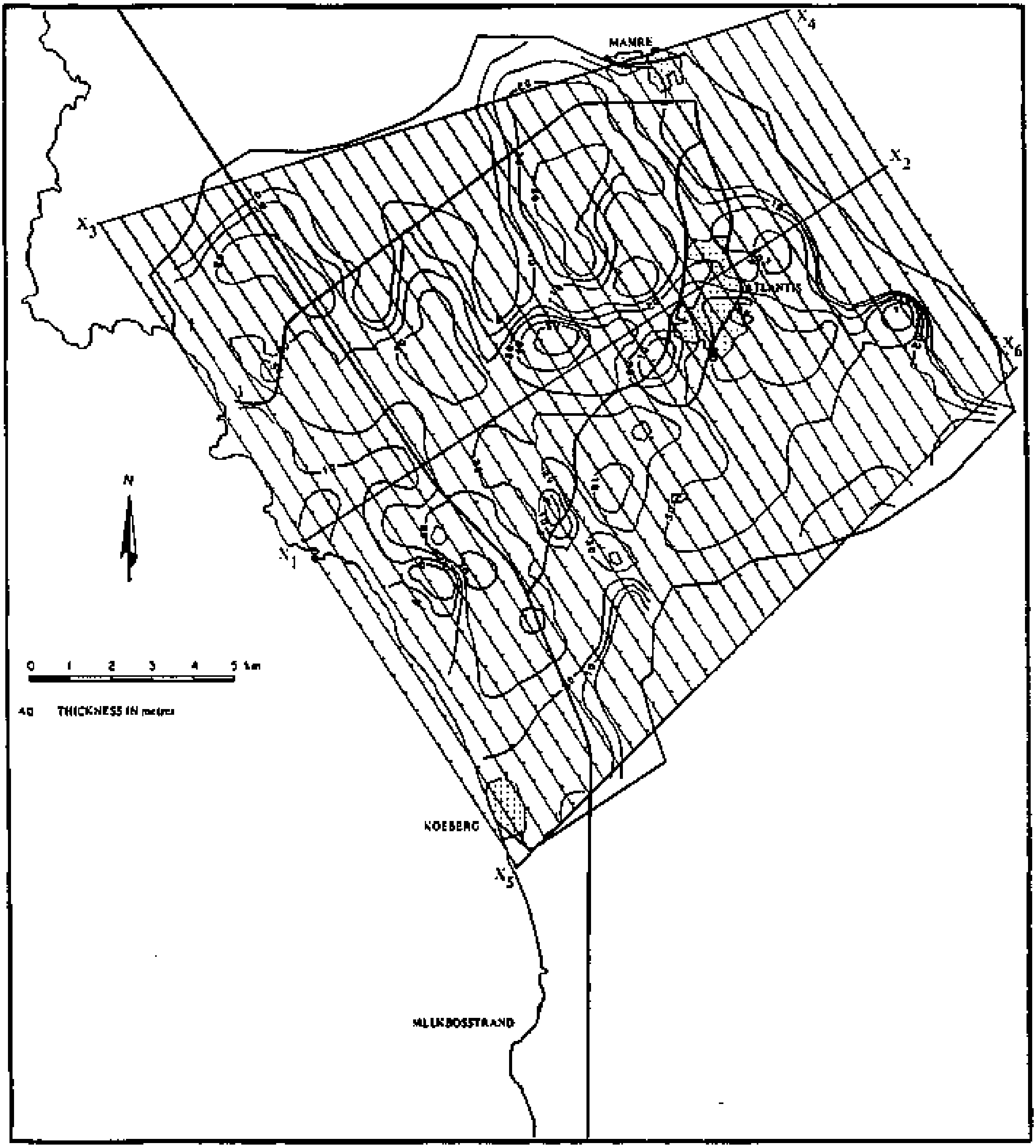

Figure 4.17. Network of profile lines used for the numerical integration of saturated thickness values to obtain the saturated volume of the aquifer.

To calculate the volume of the aquifer, one has to interpolate saturated thickness values to each and every one of the interval marks on all the profile lines. This was effected by using the kriging method of interpolation (Van Tonder, 1982). Application of Simpson's rule to the interpolated sand thicknesses yields cross-sectional areas whose mid-points lay on line X_1 X_2 at 500 metre intervals. Subsequent integration along line X_1 X_2 will yield the saturated volume of the aquifer.

Although the procedure, described above, may seem to be complicated, it can easily be implemented on a computer. Following this procedure, the total volume of saturated sand in the Atlantis aquifer for January 1979 was calculated as

$$4136,05 \times 10^6 \ m^3$$

4.5.2 VOLUME OF WATER IN THE AQUIFER

An accurate estimate of the volume of the water in the aquifer can easily be established once the storativity throughout the aquifer is available. However, as indicated in section 4.4, this is not the case. It was therefore decided to base all calculations on the conservative value of 10 per cent, the mean of the values in Table 4.1 being 17,53 per cent. With this value, the estimated volume of water in the Atlantis aquifer for January 1979 amounts to

$$413,605 \times 10^6 \ m^3$$

4.6 ABSTRACTION FROM THE ATLANTIS AQUIFER

Artificial abstraction of ground water from the Atlantis aquifer commenced in September 1976, with 16 730 m^3 water pumped from the Silwerstroom spring. Since then several production boreholes have been drilled and by December 1982, 13 of these were utilized to withdraw ground water from the aquifer. In the Silwerstroom area 5 production holes were in use by December 1982. They are boreholes G 29757, G 29794, G 30865, G 30991 and G 30999. In addition to water being pumped from these boreholes, water from the Silwerstroom spring is also used. In the Witzand area 6 boreholes are in use. They are G 30965, G 30966, G 30969, G 30972, G 30974 and G 30981. The other production boreholes in use at present, are situated in the Wesfleur area. They are boreholes G 29749 and G 29800. The locations of all the production boreholes can be seen in Figure 4.18.

The actual volume of water abstracted from the Atlantis aquifer has escalated from a humble 0,103 x 10^6 m^3 during the last four months of 1976 to a formidable 8,896 x 10^6 m^3 by the end of April 1983. Bar charts showing the monthly abstraction of ground water for the period September 1976 up to April 1983, are given in Figure 4.19. As can be expected from a winter rainfall area, the demand for water during the winter months is much lower than during the summer period.

4.7 RECHARGE OF THE AQUIFER

A detailed study of the recharge of the Atlantis aquifer falls outside the scope of the present investigation. However, some information on the recharge of the system will be needed in the model to be developed later. In view of the limited knowledge regarding factors such as subsurface seepage into and out of the aquifer, as well as evapotranspiration, it was decided to use a simplified version of the classic ground-water balance equation to obtain an estimate for the effective recharge due to precipitation. Such an estimate can be based on the equation

$$A = P \pm \Delta s \qquad (4.1)$$

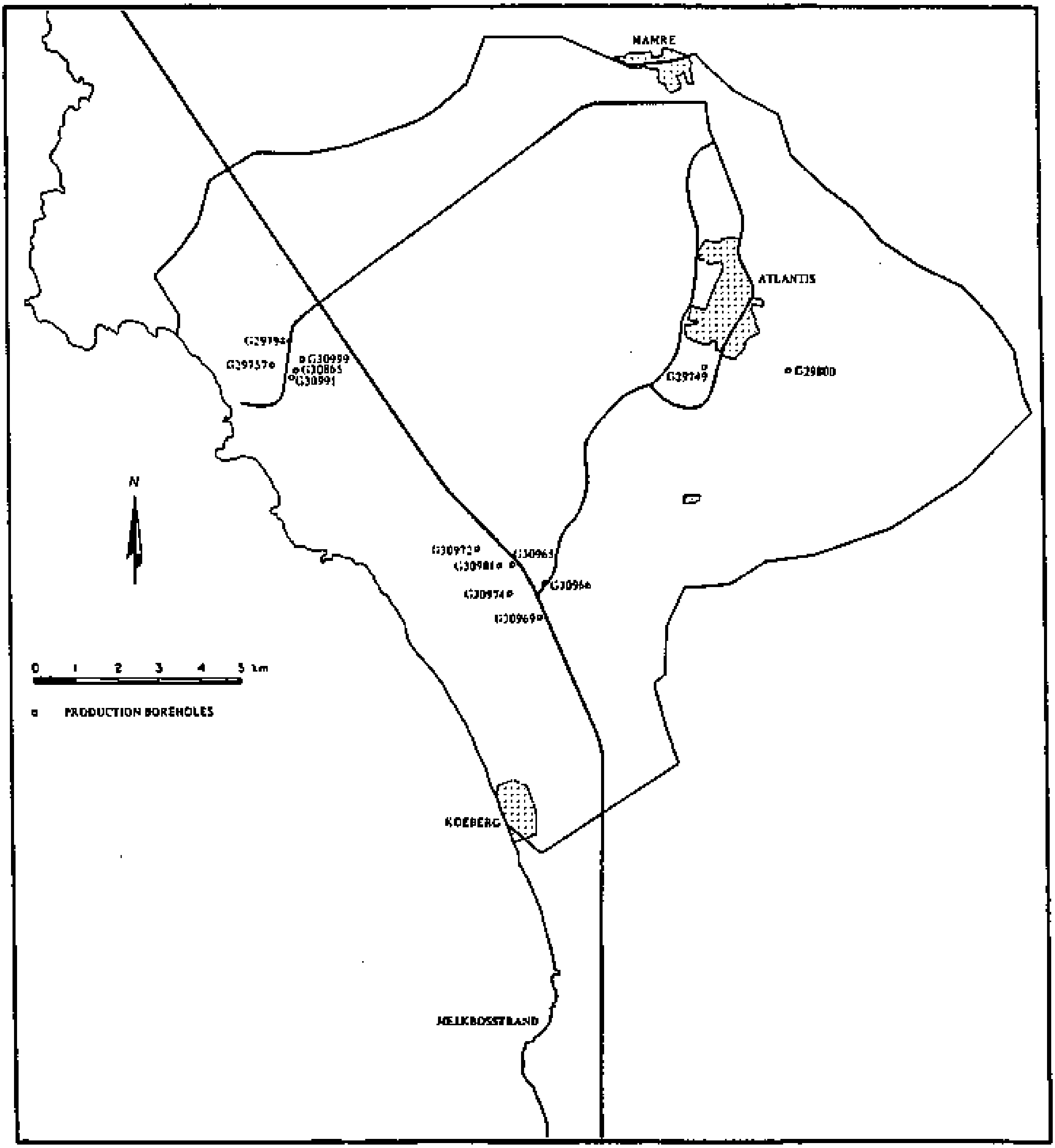

Figure 4.18. Location of the production boreholes in the Atlantis aquifer.

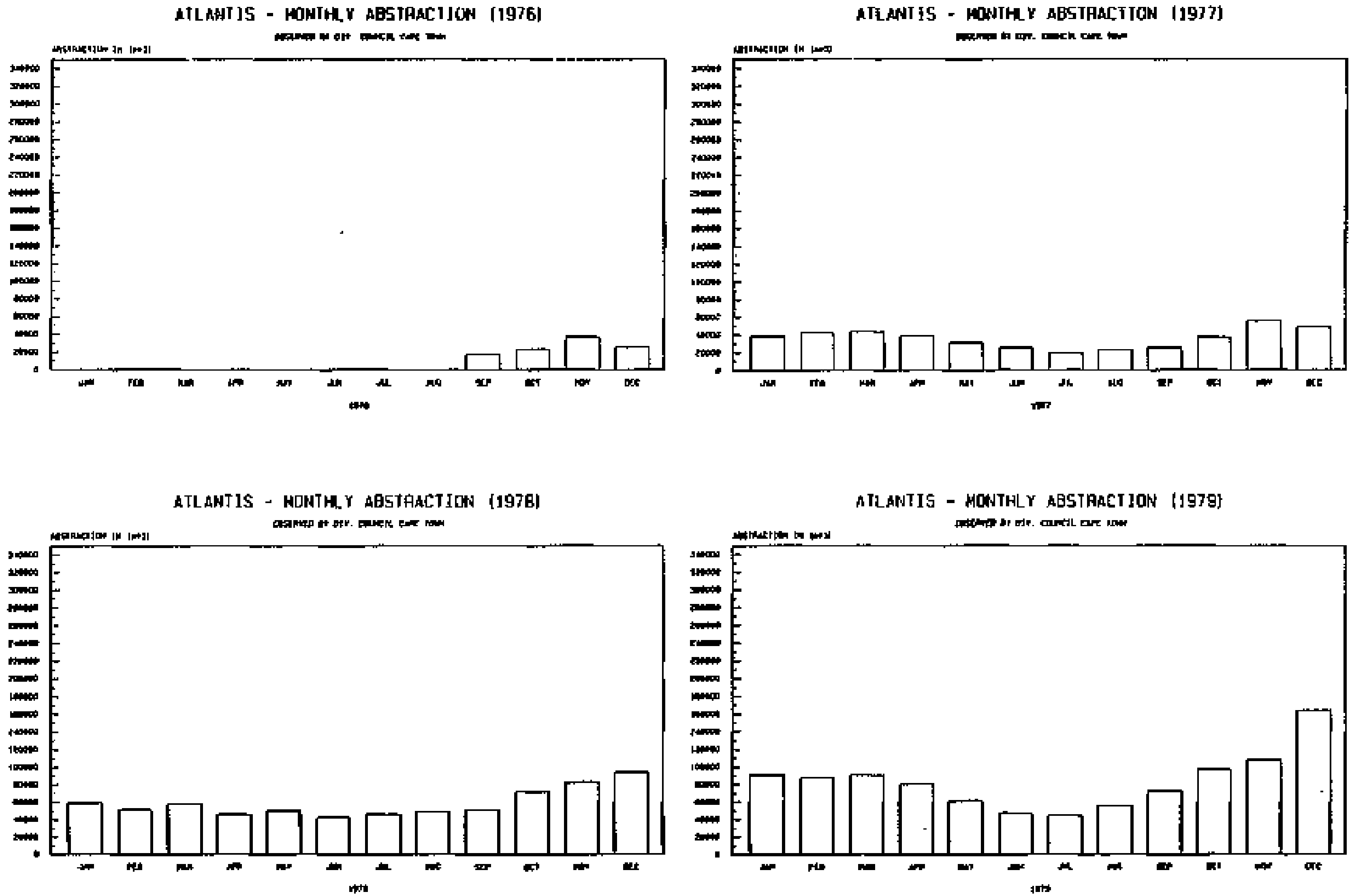

Figure 4.19. Bar charts showing the monthly abstraction from the Atlantis aquifer for the period September 1976 - April 1983.

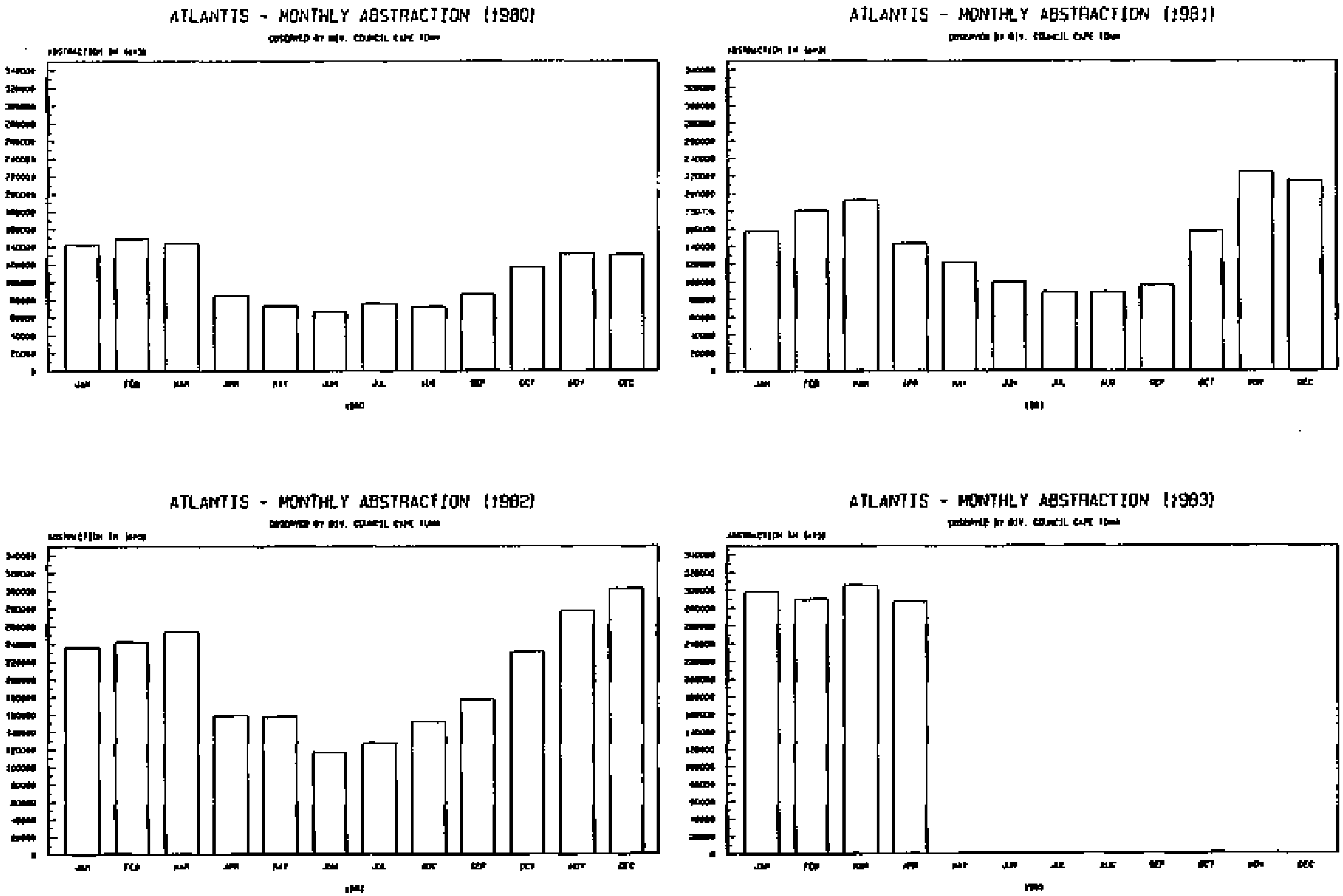

Figure 4.19. (Continued).

where

A	=	recharge
P	=	abstraction from the system
Δs	=	change in ground-water storage

The only unknown quantity that appears on the right-hand side of equation (4.1) is Δs. Hence, if this term can be estimated or calculated, one would have an estimate for the recharge. In section 4.5.2 the volume of water in the aquifer, as at January 1979, was calculated to be

$413{,}605 \times 10^6 \; m^3$

Subsequent calculations for January 1980 and January 1981 yielded the following results:

Volume of water (January 1980) = $417{,}365 \times 10^6 \; m^3$
Volume of water (January 1981) = $398{,}202 \times 10^6 \; m^3$

The change in storage is therefore as follows:

Period (January 1979 - January 1980) = (+) $3{,}597 \times 10^6 \; m^3$
Period (January 1980 - January 1981) = (-) $19{,}163 \times 10^6 \; m^3$

[(+) increase in storage; (-) decrease in storage].

The value for the period January 1979 - January 1980 being positive, coincides with an increase in observed water-level elevations. The substantial negative value for the period January 1980 - January 1981, however, does not coincide with a corresponding drop in water-levels. The only possible explanation for this big decrease in storage is the fact that water-levels in only 81 boreholes were available for the calculation of the January 1981 volume, whilst 92 and 93 boreholes were used for the January 1979 and

January 1980 calculations respectively. The importance of having the largest possible observation network or perhaps a more suitable observation network available in the area, can therefore not be over-emphasized. Based upon this evidence, it was therefore decided to restrict calculations concerning the storage of the aquifer to the period January 1979 - January 1980.

According to the data supplied by the Department of Environment Affairs, the total volume water abstracted during the period January 1979 - January 1980 amounts to

$$1{,}006 \times 10^6\ m^3$$

This figure includes the natural flow of the Silwerstroom spring as far as it can be represented by the pumping rates measured at the reservoir. Substitution of these calculated values in equation (4.1) yields

$$\begin{aligned} A &= 3{,}597 \times 10^6\ m^3 + 1{,}006 \times 10^6\ m^3 \\ &= 4{,}603 \times 10^6\ m^3 \end{aligned}$$

as effective recharge for the period January 1979 - January 1980. This figure amounts to 6,52 per cent of the annual rainfall for the same period.

It should be stressed once more that the figure derived above, does not include either subsurface leakage or evapotranspiration. Nevertheless, the way in which Δs was calculated, will partially correct for this.

4.8 SEAWARD SEEPAGE OF FRESH WATER

Another quantity that plays an important part in coastal aquifers is the loss of fresh water to the sea. This can be calculated if one knows the area of the leakage face and the gradient of the water-levels. This information is unfortunately not available for Atlantis. In what follows, it will be assumed that the Malmesbury rocks are impervious to ground-water flow. With this assumption there are, according to Figure 4.20, two areas where water can possibly leak towards the sea. These are accentuated in Figure 4.20.

Profile lines were constructed along the coast-line for both areas and sand thickness values were interpolated to points on the profile line. In the case of area II (see Figure 4.20), it was found that the sand deposits do not continue below sea-level and therefore no subsurface leakage can take place in this region. The cross section obtained for area I along the profile line A-B (see Figure 4.20) is shown in Figure 4.21. The total area of the cross section for area I amounts to

9212,5 m^2

Once the cross-sectional area of a region exposed to the sea is known, one can easily calculate the flux of water to the sea from Darcy's law:

$$Q = KADh(x) \tag{4.2}$$

where

Q	=	ground-water flux [m^3/day]
K	=	hydraulic conductivity [m/day]
A	=	cross-sectional area [m^2]
Dh(x)	=	gradient of the water-table at the coast

As in the case of the sand thicknesses, values for the hydraulic conductivity were also interpolated to points on the profile line A-B. In view of the inaccuracy of the hydraulic conductivity values throughout the aquifer (section 4.4), it was decided that the mean value obtained from the 11 interpolated hydraulic conductivity values, will be taken as being representative of the hydraulic conductivity for the entire cross section. The mean of the 11 interpolated values is

32,25 m/day

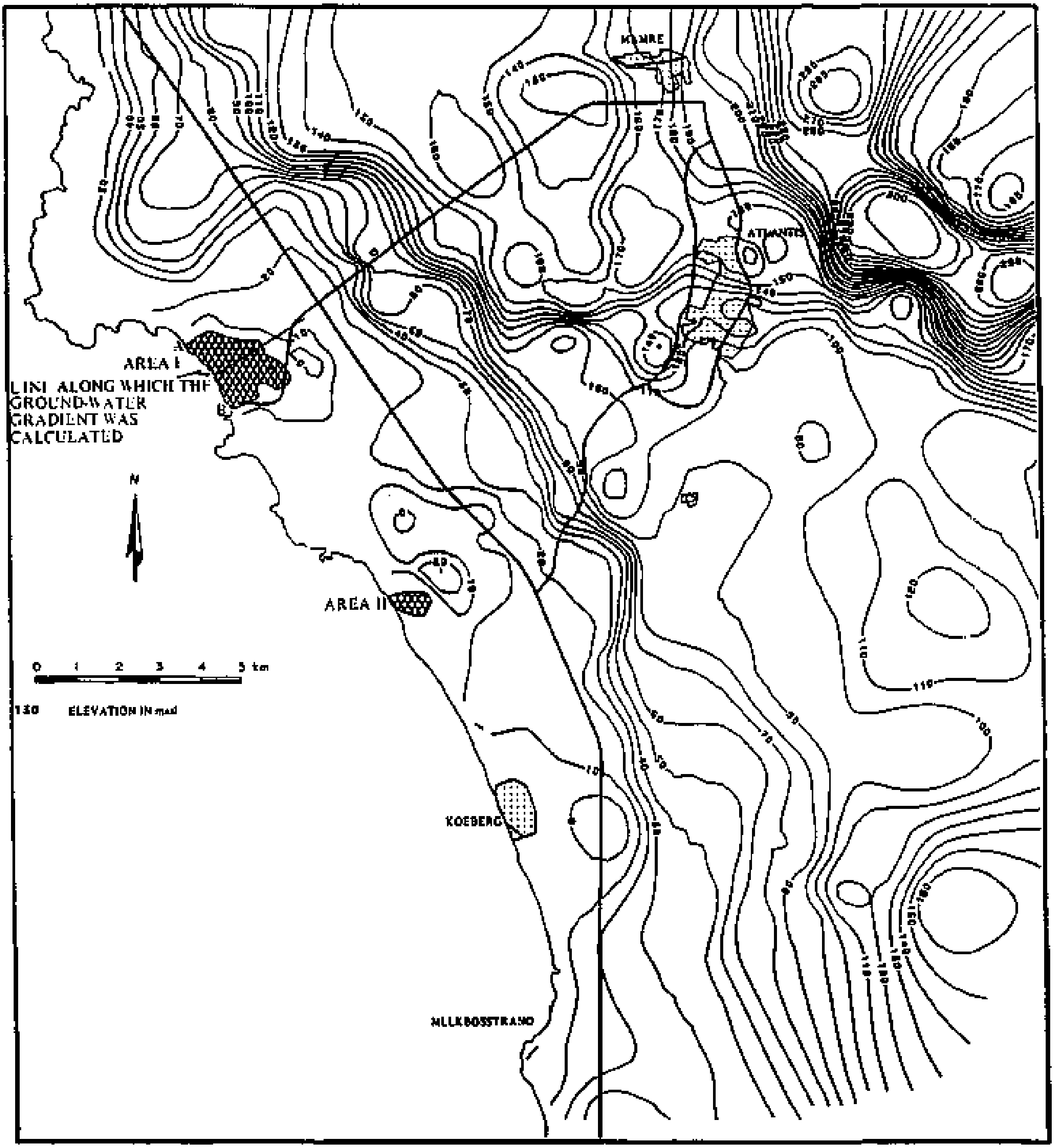

Figure 4.20. Location of the two areas in the Atlantis aquifer where the sand deposits continue below sea-level.

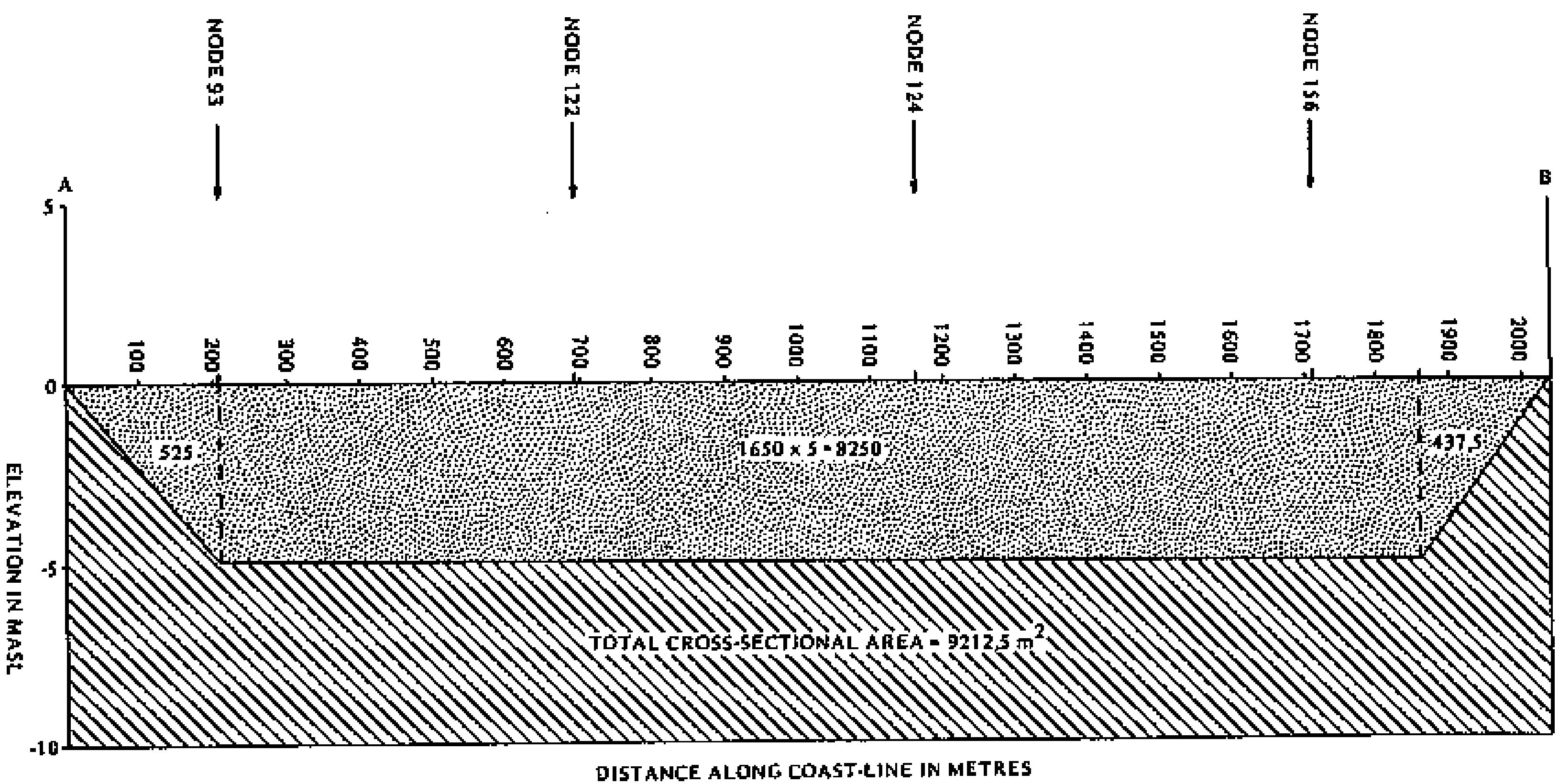

Figure 4.21. Cross section A-B, showing the thickness of the saturated sand lying below sea-level in Area I.

The only unknown quantity remaining is the gradient of the water-table at the coast. The gradient used, was calculated over a distance of 1 000 metres from the coast inland, along the line shown in Figure 4.20. The January 1979 water-level elevations were used in this calculation. A value for Dh(x) of 0,02 is obtained. Substitution of the above-calculated values in equation (4.2) yields a flux of fresh water towards the sea of

$2,169 \times 10^6 \ m^3/year$

This figure represents 3,07 per cent of the annual rainfall for 1979.

To summarize, it is interesting to note that 6,52 per cent of the annual rainfall can be taken as effective recharge to the aquifer, whilst a further 3,07 per cent of the annual rainfall is lost from the system due to subsurface leakage along the coast-line. This implicates a recharge of 9,59 per cent of the annual rainfall for 1979.

4.9 GROUND-WATER QUALITY

According to Van der Merwe (1983) and Bredenkamp and Vandoolaeghe (1982), the general quality of the ground water in the Atlantis aquifer is satisfactory. The only problem at this stage is the hardness of the water pumped from the Witzand boreholes. This problem can be overcome by mixing this water with water from the Silwerstroom production field (Bredenkamp and Vandoolaeghe, 1982).

A factor that must be considered is the possible contamination of the aquifer from external sources. Two such possible sources are:

(i) Contamination of the aquifer by seepage of low quality ground water from the Malmesbury Formation, due to the abstraction of large quantities of ground water.

(ii) Sea-water intrusion along the coast-line.

To distinguish between the two sources is almost impossible with the available data. In the first place very little information is available. Secondly, water from the Malmesburg Formation is characterized by a relatively high Na^+ and Cl^- content (Van der Merwe, 1983). It would thus be difficult to distinguish between pollution from the Malmesbury Formation and sea-water.

A list of the boreholes for which data is available, is given in Table 4.2, together with representative values of their Cl^- content. These values were used to construct the contour map in Figure 4.22.

TABLE 4.2. CHLORIDE CONCENTRATION OF ATLANTIS GROUND WATER

BOREHOLE	YEAR SAMPLED	CONCENTRATION (mg/l)
G27031	1975	196,0
G29749	1978	425,0
G29772	1975	168,0
G29773	1975	95,0
G29778	1975	60,5
G29779	1976	73,0
G29781	1975	280,0
G29782	1975	130,0
G29784	1975	204,0
G29786	1975	183,0
G29790	1975	200,0
G29792	1975	138,0
G29793	1975	79,0
G29794	1975	128,0
G29800	1977	192,3
G30835	1978	72,0
G30850	1978	340,9
G30864	1976	44,9
G30865	1976	90,0
G30882	1977	59,7
G30883	1976	385,5
G30902	1977	945,8
G30903	1977	125,9
G30904	1977	3832,0
G30913	1977	67,5
G30914	1977	131,8
G30923	1977	96,1
G30926	1977	71,4
G30928	1978	240,5
G30929	1978	113,8
G30932	1978	450,5
G30935	1978	127,3
G30940	1978	70,4
G30944	1978	67,3
G30947	1978	89,6
G30965	1978	75,0
G30966	1979	160,0
G30969	1979	145,0
G30971	1980	105,0
G30972	1979	80,0
G30991	1979	75,0
G30999	1979	95,0

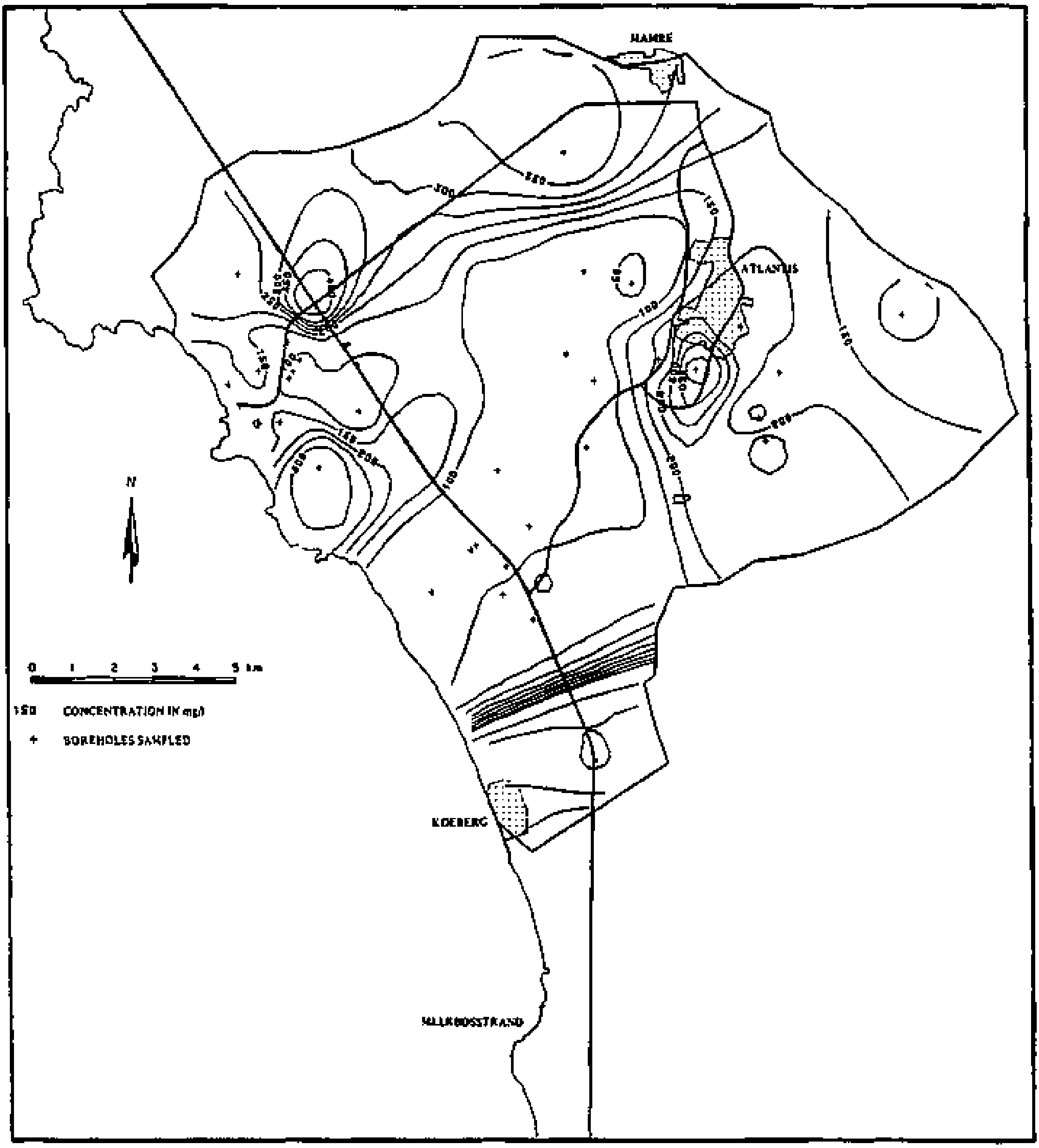

Figure 4.22. Contour map showing the chloride concentration distribution of Atlantis ground water.

As shown by the map, the general chloride concentration is within the 500 ppm limit, however, in the vicinity of the production fields, it ranges between 100 ppm and 350 ppm. Only two boreholes, namely G 30902 and G 30904, which lie in the extreme south of the aquifer, yield values in excess of 500 ppm. According to Van der Merwe (1983), this can be ascribed to contamination from the Malmesbury Formation.

As noted in section 4.8, there are two areas where sea-water intrusion may be of importance; one in the Silwerstroom area and the other one further south. The latter has since been ruled out as a possibility. Nevertheless, the only region on the coast where a relatively high chloride concentration can be observed in Figure 4.22, lies between the Silwerstroom and Witzand production areas and does not correspond to either area I or II in Figure 4.20. As it can be correlated with an area where the Malmesbury Formation lies close to the surface (see Figure 4.4), the high chloride concentration in this region can thus probably again be ascribed to the Malmesbury Formation. Sea-water intrusion thus does not seem to be a problem, at least not at present.

Most of the areas where a high concentration of chloride is present in Figure 4.22, can be associated with the Malmesbury Formation. It would be interesting to see if the chloride concentration has increased in the vicinity of the production boreholes, due to the artificial abstraction of substantial quantities of ground water. For this purpose, graphs were compiled of the chloride concentration over a period of 31 months for 5 production boreholes and the spring in the Silwerstroom production field. The graphs are shown in Figure 4.23.

As can be seen from these graphs, the chloride concentration does vary from month to month, but never exceeds the 250 ppm level. Moreover, with the exception of borehole G 29794, the variations tend to oscillate around the mean concentration throughout the 31 month period. It may, therefore, be concluded that no substantial quantities of water have been drawn from

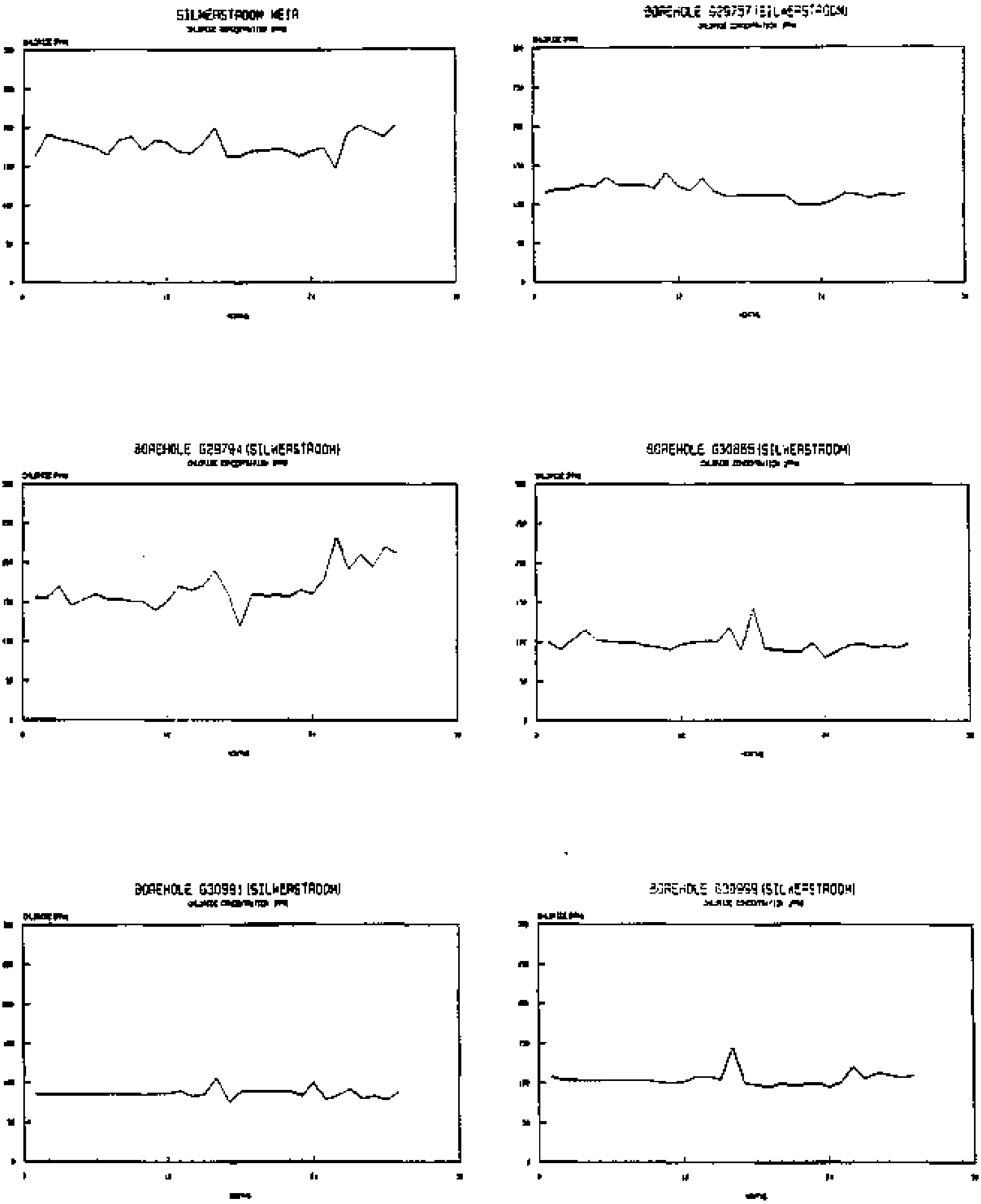

Figure 4.23. Graphs showing the chloride concentration for several boreholes as well as the Silwerstroom spring, for the period January 1980 - July 1982.

the Malmesbury Formation. The only possible exception being borehole G 29794, whose behaviour can be explained by an influx of water of a lower quality, present immediately north of the Silwerstroom production field.

Another interesting feature occurring on all, but one, of the graphs, is the increased chloride concentration for April 1981. Initially it was thought that the increase could be explained in terms of rainfall or abstraction, but no conclusive evidence could be found.

In conclusion, it can be said that the quality of the ground water in the area is satisfactory. There are indications (Fig. 4.23. borehole G29794) that water of lower quality, associated with the Malmesbury Formation, is drawn towards the Silwerstroom production field. In view of the possible construction of a management model, the general quality and quantity of data available, leaves much to be desired. An effort should, therefore, be made to conduct a more detailed investigation of the chemical composition of the ground water in the aquifer as a whole. Aspects that may receive particular attention include a better chemical description of water in the Malmesbury Formation and industrial pollution of the aquifer. With the future development of the area, the latter problem may become increasingly important.

CHAPTER 5

CONSTRUCTION AND CALIBRATION OF THE NUMERICAL MODEL

5.1 INTRODUCTION

In the previous chapters an attempt was made to analyse and describe the physical properties of the Atlantis aquifer as accurately as possible. Having completed this, the construction of a suitable numerical model that will describe the physical system, can now commence.

Modelling of ground-water systems by means of numerical techniques is of recent origin. In fact, a literature survey indicated that the first model of this kind was constructed only in 1968 (Pinder and Bredehoeft, 1968), to be followed by Prickett and Lonnquist (1971). These first numerical models utilized the finite difference method to obtain a solution for the partial differential equations, governing the flow of ground water. It was only six years later in 1974, that Pinder introduced the finite element technique into ground-water modelling. Since then the finite element method has proved itself to be a very powerful tool in analysing the behaviour of ground-water systems.

The reasons for this can briefly be summarized as follows:

Geological and hydrogeological data such as that discussed in the previous chapters, provides in general a broad picture about the properties of an aquifer. However, it is difficult to derive any detailed information on the future behaviour of the aquifer from this information. At present the only method by which this can be achieved, is by the construction of a suitable numerical model.

The two-dimensional flow of ground water can adequately be described by the diffusion equation

$$SD_t h = D_x(T_{xx}D_x h) + D_y(T_{yy}D_y h) - Q - K/\ell' (h - h_w) - C(h - h^i) \qquad (5.1)$$

where

$C = C(x,y)$	=	transient leakage coefficient $[T^{-1}]$
T_{xx}, T_{yy}	=	main components of transmissivity $\underline{T}(x,y)[L^2T^{-1}]$
$S(x,y)$	=	storage coefficient
$Q(x,y,t)$	=	strength of a source (+) or sink (-) function $[L^3T^{-1}]$
$K(x,y)$	=	vertical hydraulic conductivity of a confining layer $[LT^{-1}]$
$\ell'(x,y)$	=	thickness of the confining layer $[L]$
$h_w(x,y,t)$	=	hydraulic head in the adjacent aquifer $[L]$
$h^i(x,y,t)$	=	initial hydraulic head in the aquifer $[L]$
x,y	=	orthogonal coordinates
t	=	time $[T]$

subject to suitable initial and boundary conditions (Bear, 1979)..

Equation (5.1) is, neglecting unsaturated flow, a linear parabolic partial differential equation, for which a solution always exists, provided that suitable boundary and initial conditions are prescribed. Unfortunately, the boundaries of natural aquifers are very rarely, if ever, regular and simple. Hence, it is almost impossible to obtain an analytical solution and one, therefore, has to resolve to numerical methods. The flexibility of the finite element method in handling curved boundary conditions, is one of the main reasons for it being such a powerful tool in modelling ground-water systems.

5.2 SOLUTION OF THE GROUND-WATER FLOW EQUATION

5.2.1 BOUNDARY CONDITIONS

The boundary conditions most frequently encountered in aquifers, are generally of two types:

(i) prescribed head or 'Dirichlet' boundary conditions, and

(ii) prescribed flux or 'Neumann' boundary conditions.

Neumann boundary conditions entail the specification of a prescribed flux across the boundary of the region of interest and are most commonly encountered where a river cuts across an aquifer. It can also be used when the physical boundaries of the aquifer is not well-defined, but one has some knowledge regarding the flow of water in the aquifer.

Prescribed head (Dirichlet) boundary conditions mean (as the name implies) that water-levels along the boundaries of the aquifer are kept at the prescribed level. In the case of Atlantis, the available information indicates that the water-levels near the boundaries of the aquifer vary very little. This can clearly be seen in the water-level contour maps, drawn up for the periods January 1979, January 1980 and January 1981 (Figures 4.6 - 4.8). Hence, it would seem to be appropriate to use constant Dirichlet boundaries here.

5.2.2 INITIAL HEAD SPECIFICATION

The reaction of a ground-water system can only be judged from its observed water-level distribution. When modelling such an aquifer as Atlantis, particular attention should thus be given to obtain as a reliable set of initial hydraulic heads (h^1) as possible, otherwise it would be impossible to obtain accurate and realistic answers. After a careful examination of the Atlantis data, it was decided to use the water-level distribution for January 1979, shown in Figure 5.1, as initial heads. Several factors played a role in this decision. The most extensive monitoring of water-levels started in January 1979 and continued on a monthly basis for the whole of 1979. This data not only represents the most accurate information on water-levels, but the period for which it is available, simplifies the calibration of the model. Another contributing factor to this decision was that no extensive artificial abstraction occurred at that time.

5.2.3 ABSTRACTION FROM THE SYSTEM

The parameter Q in equation (5.1) represents, in general, recharge to or discharge from the system. In the case where water is abstracted, mostly through boreholes situated at (x_i,y_i) and pumped at specific rates of say $Q_w(x_i,y_i t)$, this discharge can be expressed mathematically as

$$Q(x,y,t) = \sum_{i=1}^{n} Q_w(x_i,y_i,t) \; \delta\,(x - x_i)(y - y_i) \qquad (5.2)$$

where the Dirac delta function (δ) has the property that when integrated over x and y, the function Q will equal Q_w at (x_i,y_i). This enables one to treat a well or borehole as a point source or sink.

Although $Q_w(x_i,y_i,t)$ varies over short intervals, it would be difficult and time-consuming to account for all these variations in a numerical model. Hence, in the model developed for the Atlantis aquifer, only monthly abstraction rates are used.

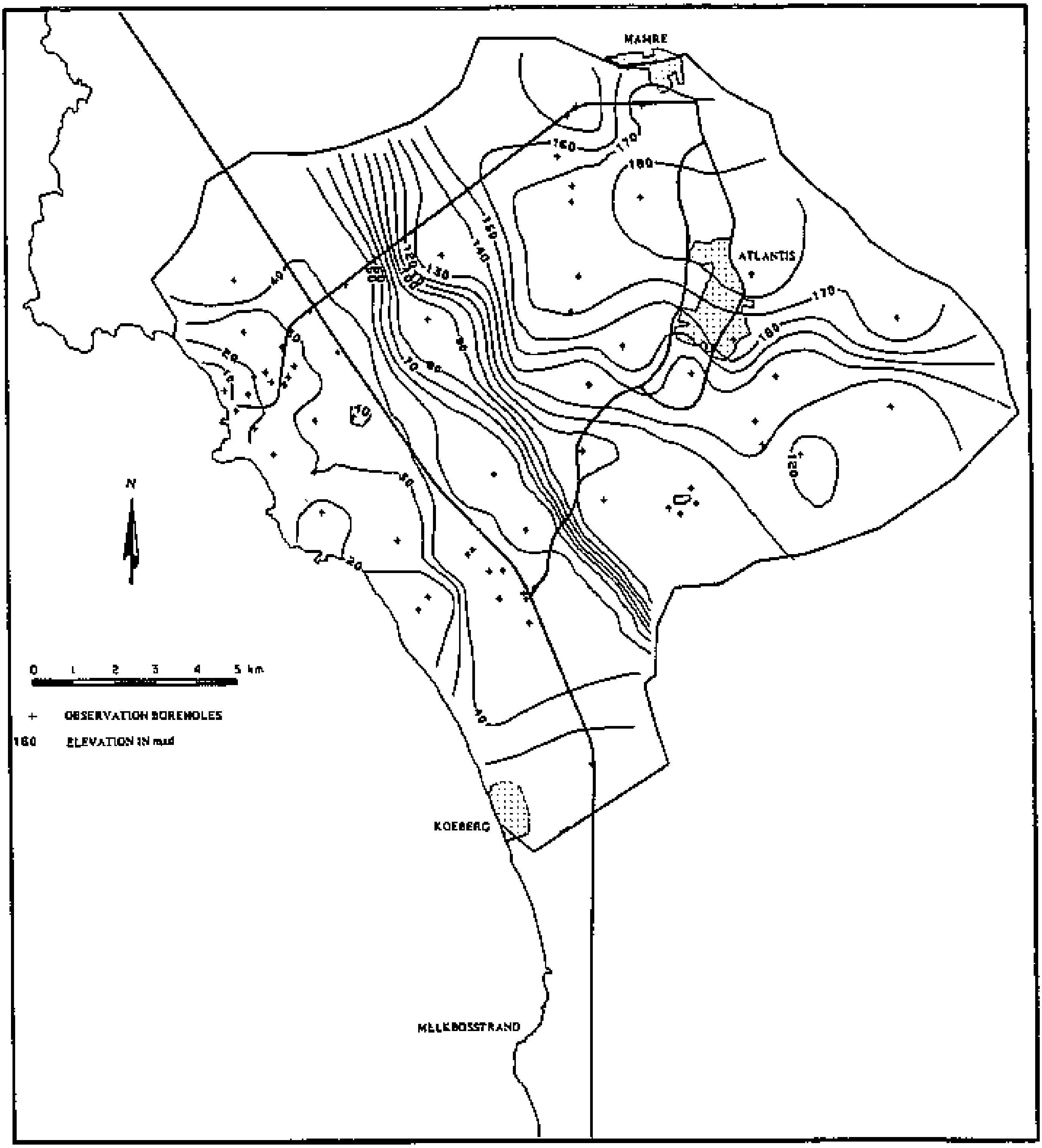

Figure 5.1. Water-level contour map for January 1979, used as initial heads in the present simulation.

5.2.4 HYDRAULIC CONDUCTIVITY AND STORATIVITY

Also very important in the construction of a numerical model, is the availability of values for hydraulic conductivity and storativity. Not only do these parameters control the flow and amount of water present in a groundwater system, but they are, besides the initial heads, the only parameters that can be used to manipulate the numerical model so that it describes the physical system. A detailed discussion regarding the hydraulic aquifer parameters, is given in section 4.4 of this thesis. At this stage it will suffice to show the contour maps depicting the hydraulic conductivity and storativity used in the construction of the numerical model. These maps are shown in Figures 5.2 and 5.3 respectively.

5.3 FINITE ELEMENT IMPLEMENTATION

5.3.1 THE GALERKIN FORMULATION

The implementation of the finite element method in simulating the flow of ground water has frequently been described in literature (Pinder and Gray, 1977). In the discussion to follow, attention will thus be restricted to only the most pertinent aspects of the method and new developments that have been incorporated in the model for Atlantis.

Equation (5.1) can conveniently be expressed in operator form as

$$SD_t h = Lh + f \tag{5.3}$$

defined over a domain Ω. The basic idea behind the finite element method is now to select a set of piecewise continuous polynomials, $\{\psi_i\}_{i=1}$, defined over Ω. The solution of (5.1) can now be approximated in terms of this ψ_i as

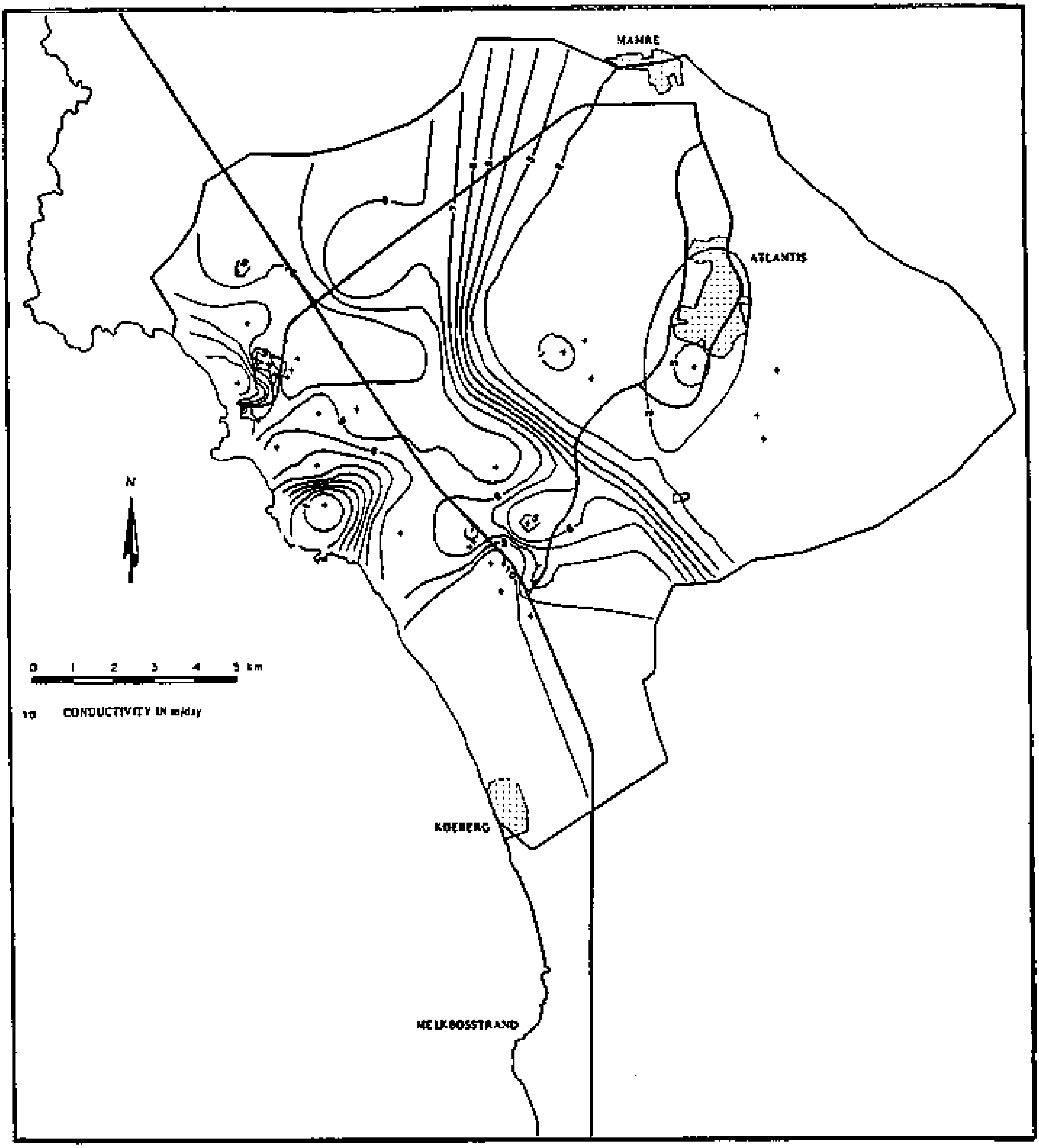

Figure 5.2. Contour map of hydraulic conductivity values used for the construction of the model. The + signs indicate the positions of the data points.

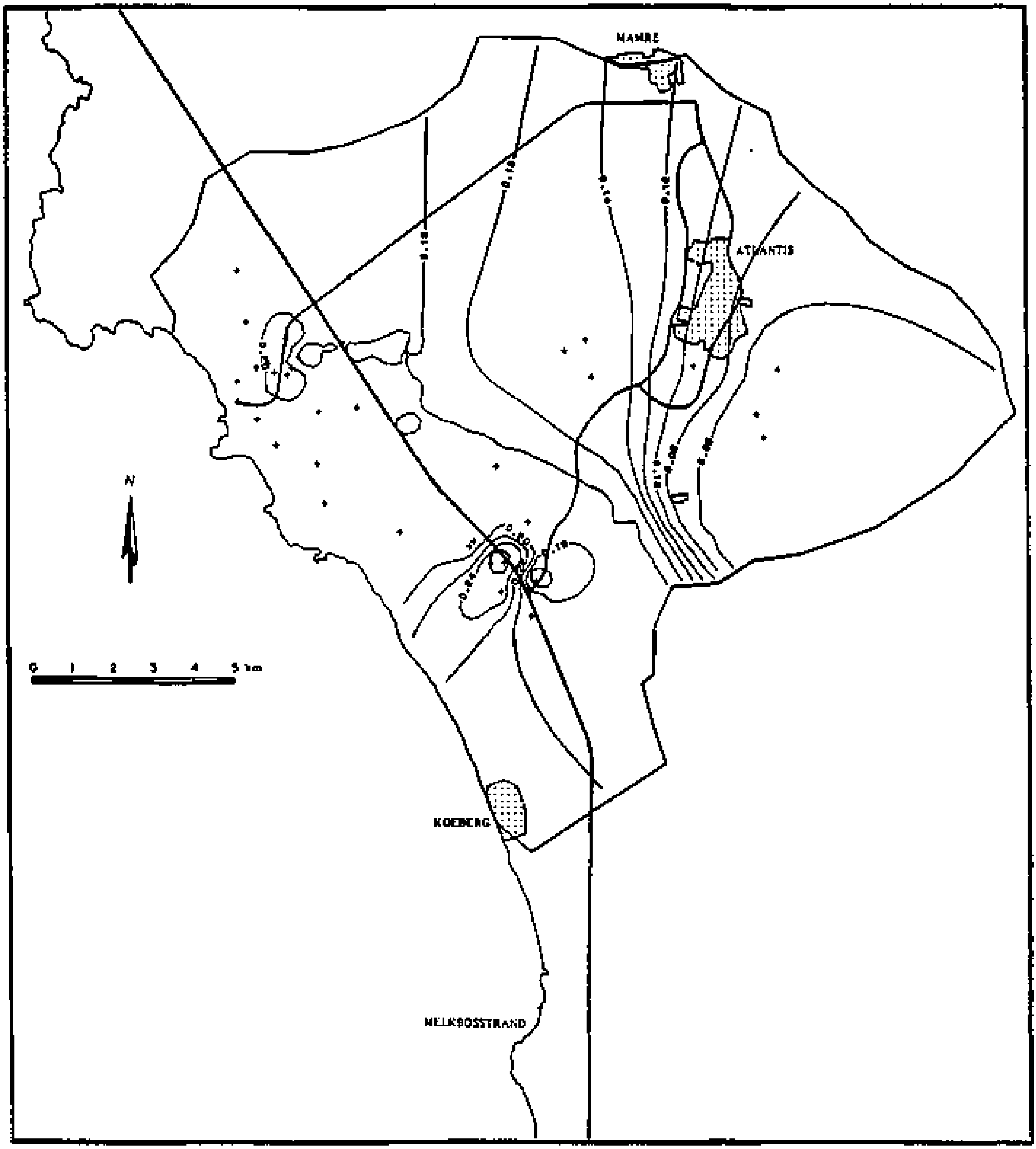

Figure 5.3. Contour map of the storativity values used for the construction of the model.

$$h(x,y,t) \simeq \hat{h}(x,y,t) = \sum_{i=1}^{n} h_i(t)\psi_i(x,y) \tag{5.4}$$

with h_i the unsolved coefficient.

In the Galerkin approach (used here) the h in (5.1) is replaced by this approximation and the resulting equation multiplied by one of the basis functions and integrated to obtain

$$\int_{\Omega} [T_{xx}\left(\sum_{j=1}^{n} h_j D_x \psi_j\right) D_x \psi_i + T_{yy}\left(\sum_{j=1}^{n} h_j D_y \psi_j\right) D_y \psi_i + S D_t \sum_{j=1}^{n} h_j \psi_j \psi_i$$

$$+ Q\psi_i + (K/\ell' + C)\sum_{j=1}^{n} h_j \psi_j \psi_i - (K/\ell' \, h_w + (h')\psi_i] \, d\Omega$$

$$- \oint_{\partial\Omega} [\underline{T}\nabla\hat{\underline{h}}\cdot\underline{n}]\psi_i \, dS = 0 \qquad i = 1,\ldots,n \tag{5.5}$$

where ∇ is the gradient operator and $\underline{n}$ is the unit normal vector on the boundary $\partial\Omega$ of Ω.

Equation (5.5) can conveniently be expressed in matrix form as

$$\underline{M}D_t\underline{h}(t) = \underline{K}\underline{h}(t) + \underline{F} \tag{5.6}$$

with typical elements

$$M_{ij} = - \iint [T_{xx}(D_x \psi_i D_x \psi_j) + T_{yy}(D_y \psi_i D_y \psi_j) + (K/\ell' + C)\psi_i \psi_j] dxdy \tag{5.6a}$$

$$K_{ij} = \iint S \psi_i \psi_j \, dxdy \tag{5.6b}$$

$$F_{ij} = \iint \psi_i (K/\ell' \; h_w - Q + (h'))dxdy - \int \psi_i [\underline{T}\nabla\psi_j \cdot \underline{n}] \, dS \tag{5.6c}$$

If Neumann boundary conditions are prescribed, all the quantities in the line integral appearing in (5.6) are known. However, if Dirichlet boundary conditions are prescribed, a different approach has to be used. The easiest is to force the approximation (5.4) to satisfy these conditions and then require that the $\psi_i(x,y)$ not connected to the boundary, vanish on the boundary. In both situations (5.6) reduces to a set of linear ordinary differential equations in time, which have to be solved for the vector of unknowns, $h_i(t)$.

5.3.2 TIME DISCRETIZATION

Although (5.6) can be solved by any method suitable for a system of first order ordinary differential equations, the large number of equations and their structure merit the use of special methods. A very efficient method that can be used for this purpose is the optimal Θ-method, developed by Botha *et al* (1981), based on earlier work done by Laurie (1975). As with all numerical methods available for solving ordinary differential equations, this method also discretizes (5.6) in time. Its main advantage is, however, that it allows one to choose the time step optimally. This is achieved by specifying an upper bound, ε, for the local truncation error in time and then solve (5.6), first with a time step $2\Delta t_n$ and then twice with the time step Δt_n. The next step to be taken can then be expressed in the form

$$\Delta t_{n+1} = \alpha(\Delta t_n) \tag{5.7}$$

where

$$\alpha = (1/s) \sqrt{\varepsilon u/e_n} \tag{5.7a}$$

$s \simeq (1,1)$ is a safety factor implemented to ensure the optimization of the time increments

e_n is a measure of the local truncation error at the present time step

u is a measure of the magnitude of $h_i(t)$ also at the present time.

If the solution of (5.6) obtained with the two consecutive time steps Δt, is denoted by $h_i\,(2\Delta t)$ and that with the single time step $2\Delta t$, by $\hat{h}_i\,(2\Delta t)$, suitable expressions for u and e_n would be (Botha *et al*, 1981)

$$e_n = \sqrt{\sum_i [h_i(2\Delta t) - \hat{h}_i(2\Delta t)]^2} \tag{5.7b}$$

$$u = \sqrt{\sum_i [h_i\,(2\Delta t)]^2} \tag{5.7c}$$

By using the optimal Θ-method, (5.6) can also be expressed in the form

$$[\underline{M} - \Theta\Delta t K]\,h^{n+1} = [M + (1 - \Theta)\Delta t K]\underline{h}^n + \underline{F} \tag{5.8}$$

which can be solved for the $\underline{h}^{n+1}$.

5.3.3 DISCRETIZATION OF THE DOMAIN

Piecewise continuous polynomials are defined over very small regular domains or elements. Application of the finite element method to (5.1) would thus require that Ω be divided into a number of rectangular elements. Since Ω is, as already noted, usually irregular, this can be a problem. However, this can be avoided by using isoparametric quadrilateral elements (Pinder and Gray, 1977). In this case one uses irregular elements defined in (x,y) space (global coordinates) and transforms them into a local (ξ, η) coordinate system. A typical element in (x,y) space and its transformed equivalent in (ξ, η) space, is shown in Figure 5.4.

This introduces some rather complex terms into the integrals appearing in (5.8), with the result that gaussian quadrature has to be used for their evaluation, but fortunately this does not complicate matters very much.

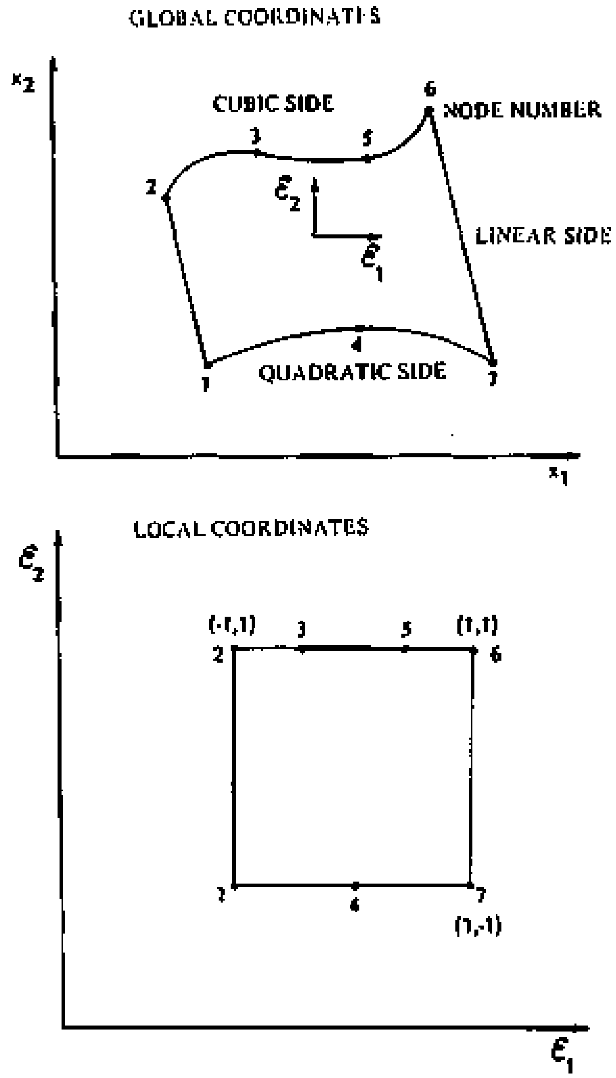

Figure 5.4. Deformed isoparametric quadrilateral element in global (x,y) and local (ξ, η) coordinates.

The construction of a suitable mesh for a given domain can be quite time-consuming. Hence, it is always worthwhile to take into account all possible factors that may influence the final mesh during its construction. The most important of these are:

(i) Topography.
(ii) Paleotopography.
(iii) Ground-water levels.
(iv) Geology.
(v) Natural boundaries of the aquifer.
(vi) Locality of boreholes and springs.

Locality of production boreholes, in particular, presents a problem, because such boreholes must always be located on a mesh point or when using the boundary flux method (Bakkes and Botha, 1981), a special element must be constructed. Thus it is always wise to incorporate not only existing boreholes into the mesh, but future ones as well. It is for this reason that Table 5.1, which contains the monthly pumping rates at various production holes in the Atlantis aquifer for 1979, also includes a number of production holes that actually came into use much later.

Another important aspect is the size of the various elements. This will in the first place be determined by the general nature of the aquifer. However, it also has a direct bearing on the accuracy of the solution (Oden and Reddy, 1976). It must thus be constructed in a way so as to ensure that its influence on the accuracy of the solution can be neglected. In the case of the Atlantis aquifer with its steep gradients in topography, paleotopography and water-levels (see Figures 4.3 and 4.5 - 4.10), this can be a serious problem. After a limited number of experiments, it was decided to use the mesh shown in Figure 5.5. Regarding the boundaries of the mesh, they were dictated by the coast-line of the Atlantic Ocean in the western part of the area, while the rest of the mesh boundaries coincided with the 1 metre sand thickness contour line (see section 4.2.3).

With the mesh constructed, the next step is to number the nodes (Pinder and Gray, 1976). This is not as trivial as one might think, because this will

TABLE 5.1. MONTHLY PUMPING RATES FOR EXISTING PRODUCTION BOREHOLES IN THE ATLANTIS AQUIFER FOR THE PERIOD JANUARY 1979 - DECEMBER 1979

BOREHOLE		SPRING	G29794	G30999	G29757	G30865	G30991	G30972	G30971	G30981	G30965	G30966	G30969	G30926	G29749	G29782	G29800
NODE		119	86	87	88	116	151	302	329	327	326	351	354	200	230	287	260
1979	J	2662.0	122.0	.0	92.0	184.0	.0	.0	.0	.0	.0	.0	.0	.0	.0	.0	.0
	F	2232.0	13.0	.0	335.0	380.0	.0	.0	.0	.0	.0	.0	.0	.0	.0	.0	.0
	M	2483.0	308.0	.0	.0	261.0	.0	.0	.0	.0	.0	.0	.0	.0	.0	.0	.0
	A	2362.0	113.0	.0	59.0	126.0	.0	.0	.0	.0	.0	.0	.0	.0	.0	.0	.0
	M	2068.0	.0	.0	.0	.0	.0	.0	.0	.0	.0	.0	.0	.0	.0	.0	.0
	J	1530.0	16.0	.0	5.0	15.0	.0	.0	.0	.0	.0	.0	.0	.0	.0	.0	.0
	J	1443.0	24.0	.0	9.0	7.0	.0	.0	.0	.0	.0	.0	.0	.0	.0	.0	.0
	A	729.0	415.0	.0	280.0	465.0	.0	.0	.0	.0	.0	.0	.0	.0	.0	.0	.0
	S	1460.0	398.0	.0	417.0	146.0	.0	.0	.0	.0	.0	.0	.0	.0	.0	.0	.0
	O	907.0	787.0	.0	517.0	794.0	.0	.0	.0	.0	.0	.0	.0	.0	.0	.0	.0
	N	1757.0	860.0	.0	385.0	614.0	.0	.0	.0	.0	.0	.0	.0	.0	.0	.0	.0
	D	2271.0	792.0	.0	631.0	869.0	.0	.0	.0	.0	.0	.0	.0	.0	178.0	.0	728.0

PUMPING RATES ARE GIVEN IN m^3/day FOR A 30 DAY MONTH

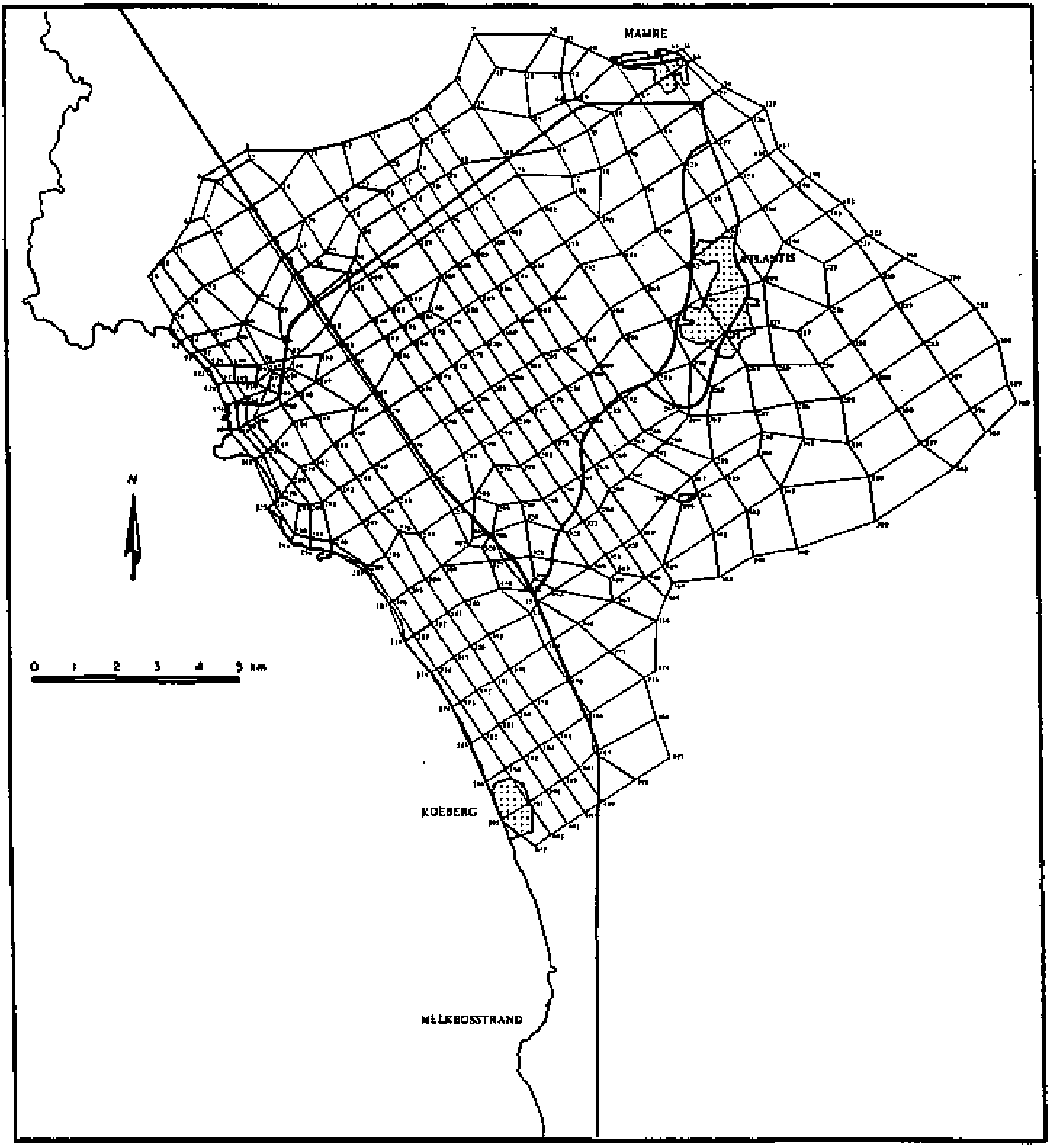

Figure 5.5. The finite element mesh used in the present simulation of the Atlantis aquifer. The mesh consists of 365 isoparametric quadrilateral elements and 403 nodes.

ultimately determine the computer memory space and time required during the simulation (Pinder and Gray, 1976). To keep these quantities within bounds, it is imperative that the maximum difference between two node numbers in any element be kept as small as possible. It is for this reason that the node numbers in Figure 5.5 do not follow a regular pattern.

5.4 CALIBRATION OF THE NUMERICAL MODEL

The finite element program used in this study is a modified version of the ISOQUAD program originally developed by Pinder and Gray. The modifications pertain in particular to the inclusion of the optimal Θ-method (Botha *et al*, 1981) and the boundary flux method (Bakkes and Botha, 1981), as well as numerous changes to the input and output statements. The program was implemented on a Univac 1100 series computer at the University of the Orange Free State. For further information regarding the program documentation, see Lynch (1982). It is, however, important to note at this stage that in this program all information, except the storativity values, must be supplied nodewise. The storativity has to be specified element-wise. A further fact to be noted is that the program facilitates the modelling of confined, leaky or water-table conditions. Since all available data indicates that the Atlantis aquifer is a water-table aquifer (see Chapter 4), the latter option was used in the present simulation.

The basic procedure for the calibration of the model is rather straightforward. The computer is supplied with the necessary information required to solve (5.8), which comprises boundary and initial values and the various hydraulic parameters. It will then calculate values for $\underline{h}^n$ at various time steps $n = 1,2,...$. These calculated values are then compared to the heads observed at these times. If they do not differ more than 2 metres to either side, the model can be assumed as being calibrated. If not, the numerical solution must be considered in error and corrective measures taken.

The first source of error is that the mesh used, is not fine enough. This situation can be avoided by using meshes of various refinements and to keep refining it until the change in the solution is sufficiently small. (For another approach using the optimal Θ-method, see Lynch, 1982). The mesh given in Figure 5.5, was actually determined in this way, so in the present model this should not be a problem. (Note that this convergence proof can be carried out with hypothetical hydraulic parameters).

A second and usually the most serious source of errors in modelling groundwater flow, is insufficient knowledge of the hydraulic parameters. This can be corrected for either physically (drilling more holes and conducting pump tests on them) or mathematically. The mathematical approach (used here) consists of kriging the available data and then using the resulting kriging error maps to adjust the hydraulic parameters accordingly (Van Tonder, 1982). This will usually lead to acceptable solutions. If not, it is possible that the boundaries of the aquifer are incorrect; a situation that calls for a complete new field investigation.

The three hydraulic parameters available for manipulation in the mathematical correction of errors are the initial head, hydraulic conductivity and storativity. The final adjusted values for the three parameters obtained in the calibration of the Atlantis aquifer, using the available data (described in Chapter 4), are shown as contour maps in Figures 5.6 to 5.8.

When using the mathematical approach, it must be kept in mind that the observed values are the only physical information available for the system. Hence, when adjusting these parameters, the observed values should not be changed unless there exists supplementary information to the contrary.

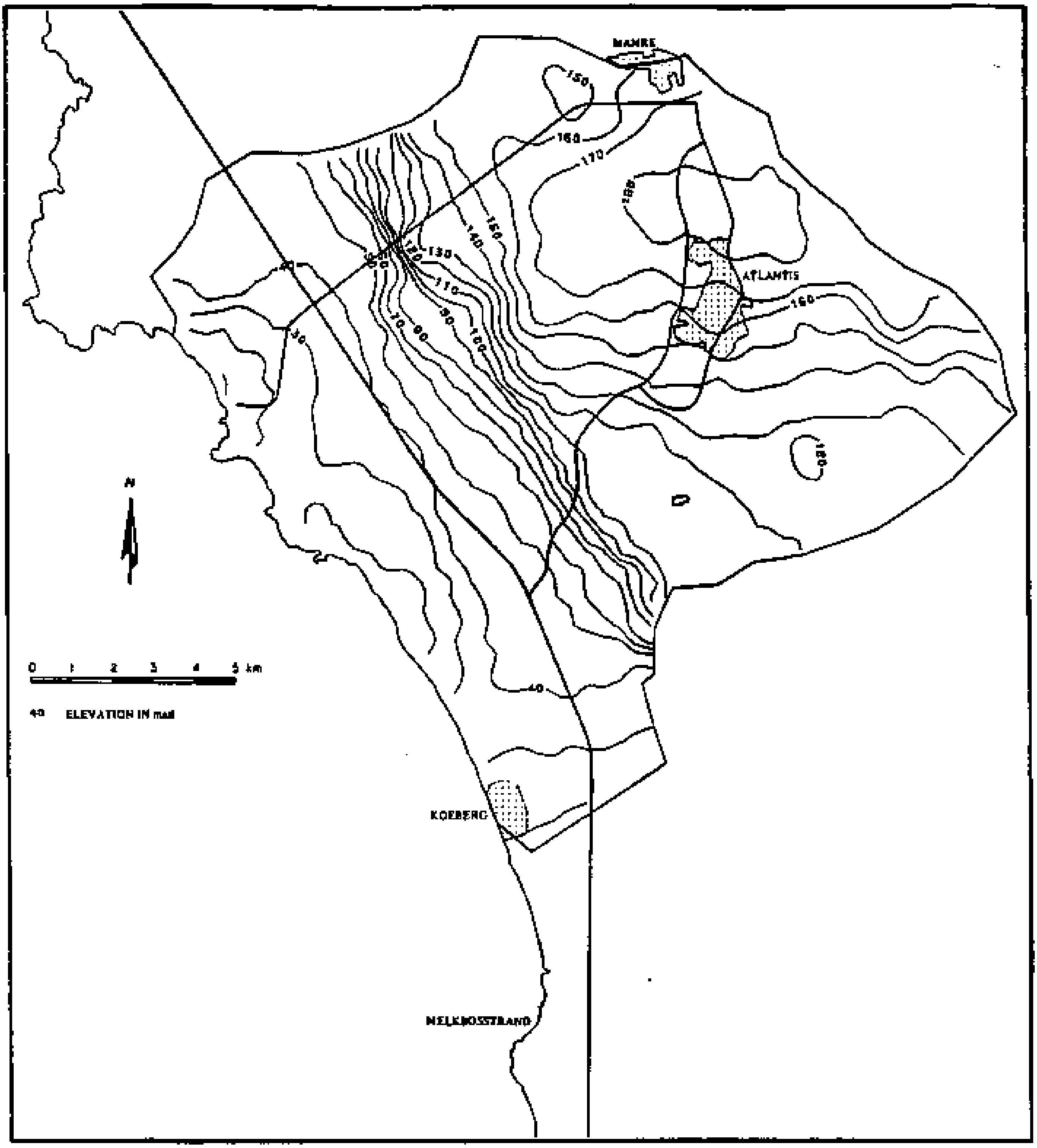

Figure 5.6. The calibrated initial head distribution in the Atlantis aquifer for January 1979.

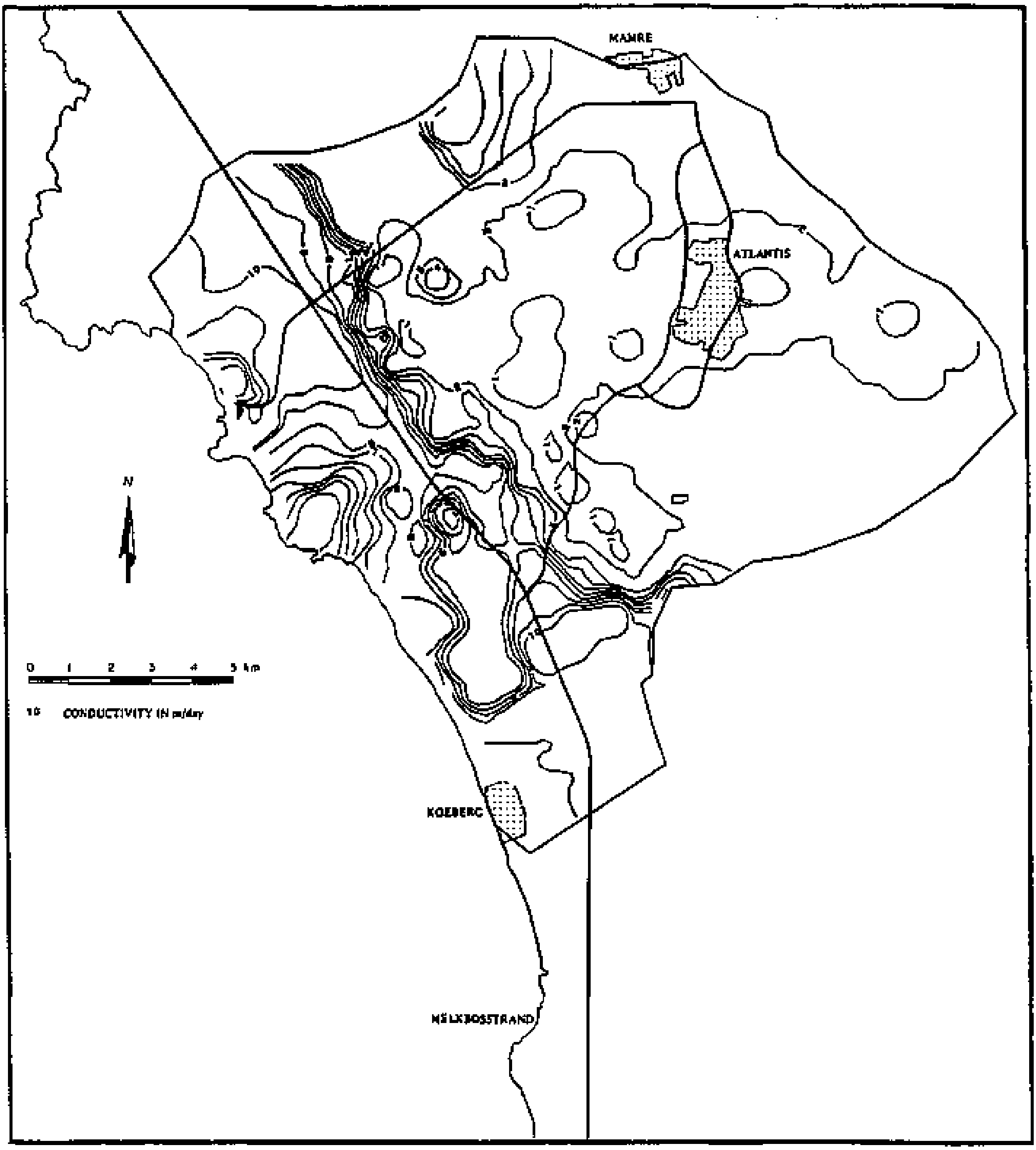

Figure 5.7. Contour map of the calibrated hydraulic conductivity distribution for the Atlantis aquifer.

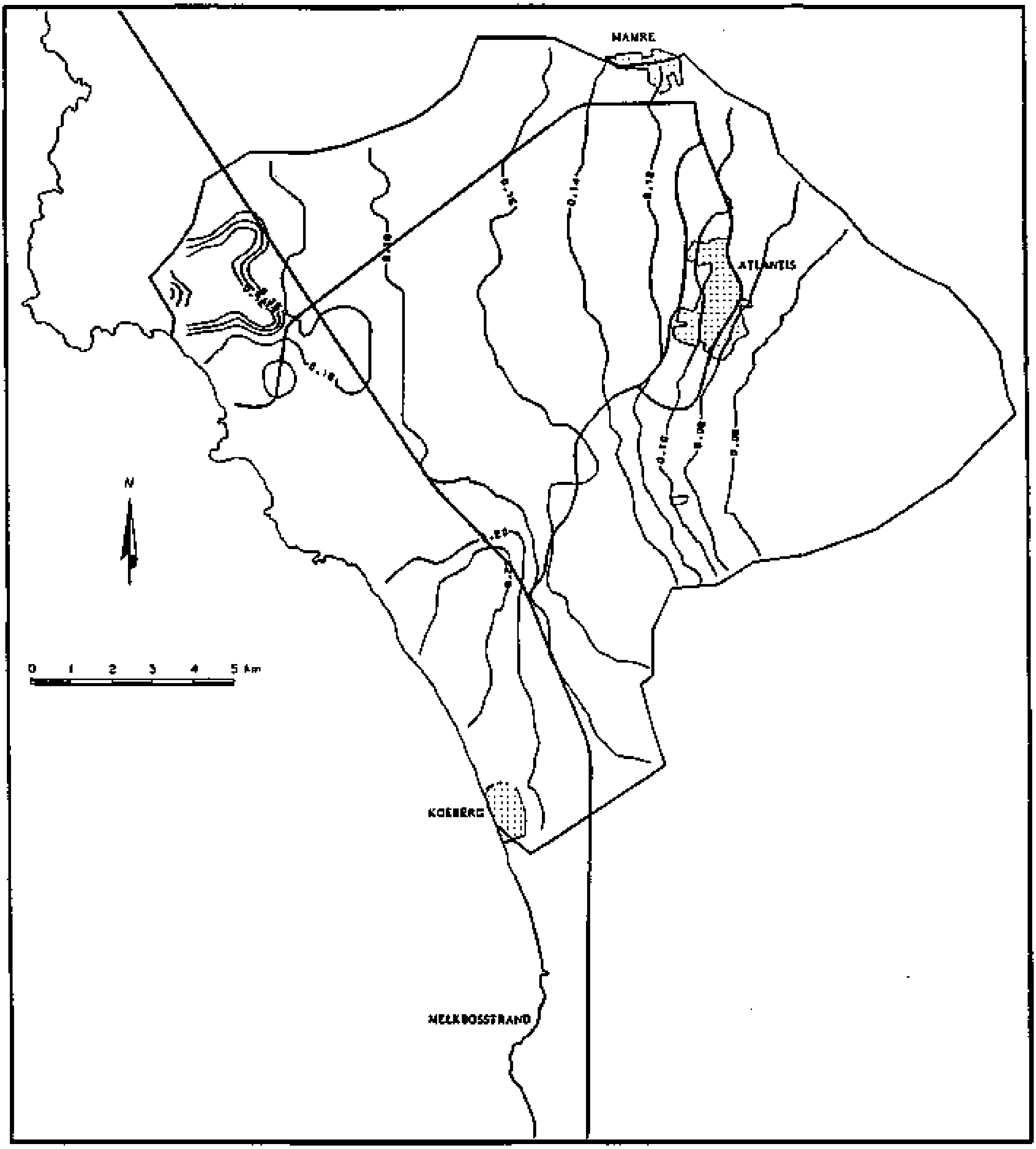

Figure 5.8. Contour map of the calibrated storativity distribution for the Atlantis aquifer.

5.5 SIMULATION OF THE ATLANTIS AQUIFER

5.5.1 GENERAL

The effectiveness of the calibration can best be judged by visual comparison of the observed water-level contour map at a specific time with the simulated one at the same time. Since the number of observation holes are usually many times smaller than the number of nodes used in the simulation, the interpolation procedure applied in the construction of these maps may distort the picture completely. Take, for example, the water-level contour map of January 1980 in Figure 4.7, constructed from the available 93 observed water-levels. The water-levels at the 403 nodes used in the finite element simulation of the aquifer were extracted from this map and contoured again, with results as shown in Figure 5.9. There are clearly large differences between the maps. However, the map in Figure 5.9 compares favourably with the one simulated for January 1980, shown in Figure 5.10. This shows that when comparing contour maps obtained during simulations with those obtained from actual observations, care should be exercised to ensure that both are constructed from the same set of points. For comparison purposes the ideal would be to use only observed and simulated values at the established observation points in the aquifer. Fitting these two sets of values is precisely the objective of the simulation exercise. Such a comparison would, therefore, yield no new information regarding the behaviour of the ground-water system at localities other than the observation boreholes. In the discussion to follow, all contour maps used will thus be based on values at the nodes of the finite element network shown in Figure 5.5, obtained from either the model or by interpolation from the observed data. Note that the finite element method is basically also an interpolation procedure, so that such a procedure is mathematically well justified.

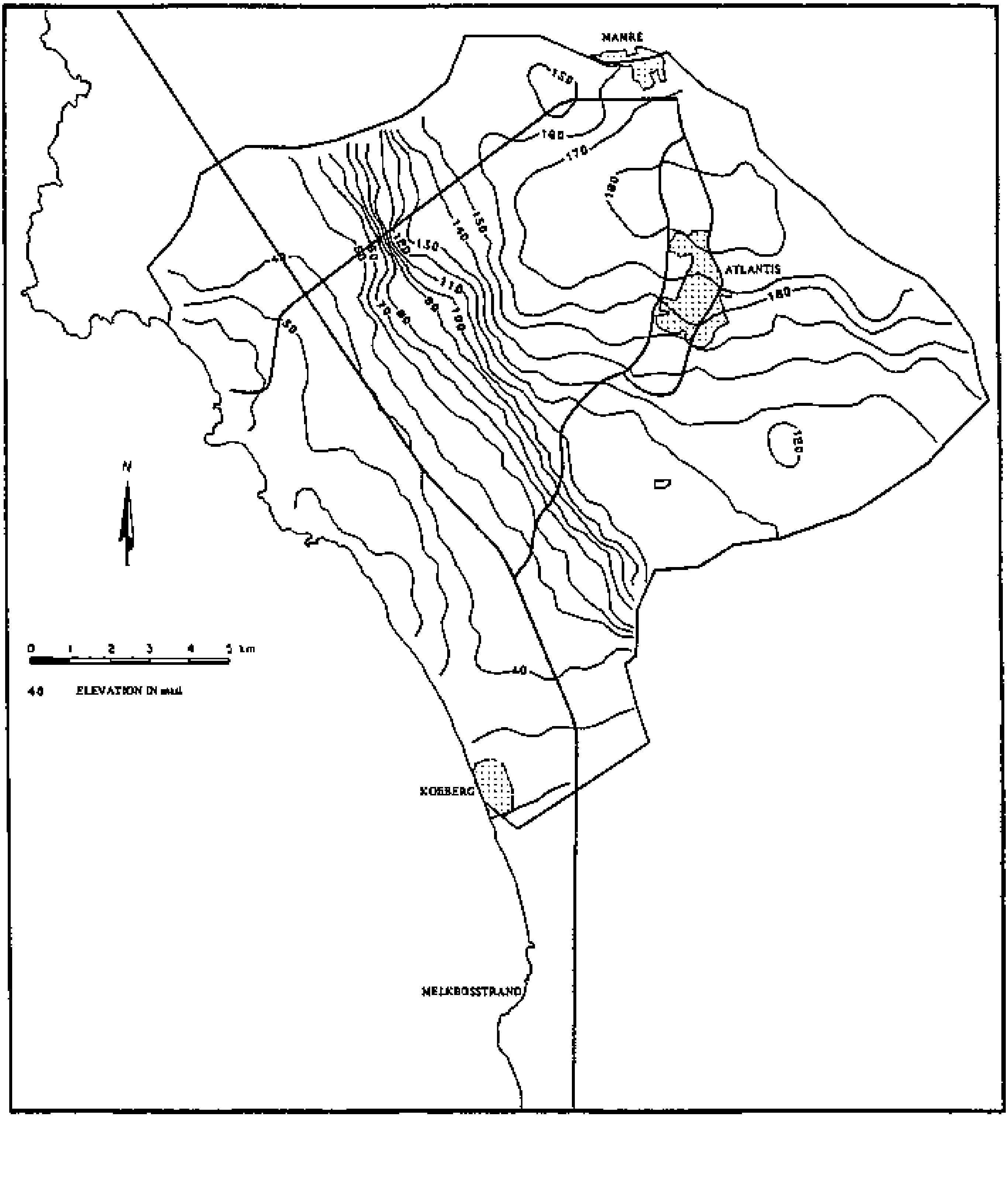

Figure 5.9. Water-level contour map for January 1980 used for comparison with simulated water-levels during the calibration stage.

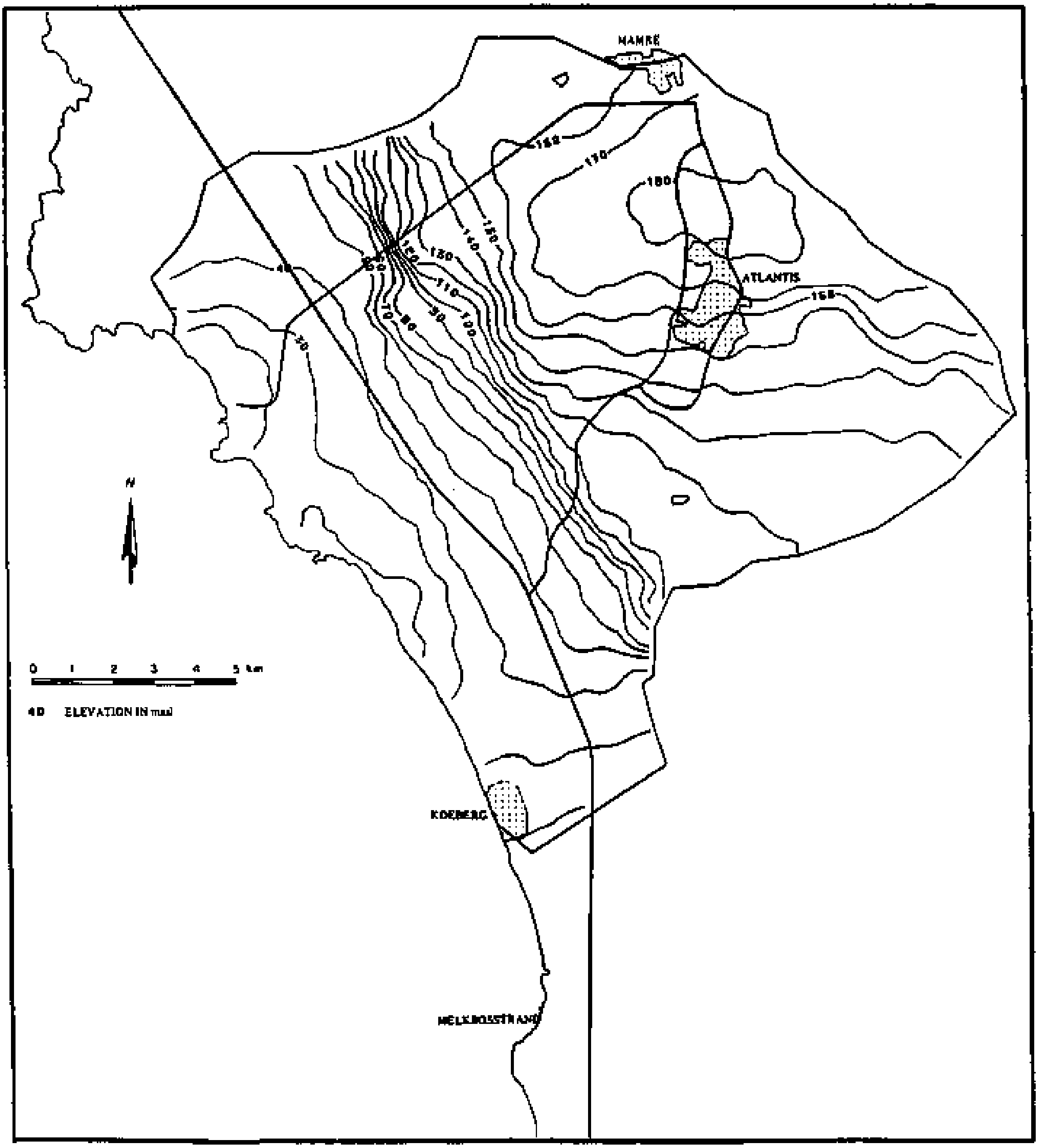

Figure 5.10. Simulated water-level distribution for the Atlantis aquifer - January 1980.

5.5.2 THE PERIOD JANUARY 1979 - JANUARY 1980

Comparison of the initial head contour map (Figure 5.6) and the water-level contour map for January 1980 (Figure 5.9) indicates that there was almost no change in water-levels during the period January 1979 - January 1980. It is well-known in calibrating a model that it is much easier to simulate large drawdowns than small ones. Hence, the data for Atlantis provides one with an extreme test of the model. On comparing Figures 5.9 and 5.10, it is evident that the present model is quite successful. This applies in particular to the production fields. The fact that the model also succeeded in simulating the observed system satisfactorily in areas where the ground-water gradient is steep, can be taken as clear indication of its overall validity.

There are, however, a few places where the simulated heads differ from the observed water-levels. The most important of these being the area to the immediate north of the Silwerstroom production field, where differences of up to 10 metres are found. To correct for this, would require values of the hydraulic parameters outside those allowed for by their kriging error maps. The only feasible explanation at this stage would thus be that the model does not interpret the physical system correctly. Since very little data is available in the area, the reason for this behaviour can only be explained after a more detailed field investigation in the area.

A more detailed view of the behaviour of the model can be obtained by comparing the observed and simulated heads for particular boreholes over the calibration period and beyond, if possible. Graphs of these results are given in Figures 5.11 to 5.16.

The first group of graphs in Figure 5.11 represents the observation boreholes for which the simulated water-levels closely resemble the observed water-levels. In the second group of graphs (Figure 5.12), a very interesting behaviour of the numerical model can be observed. During the first 30 days of

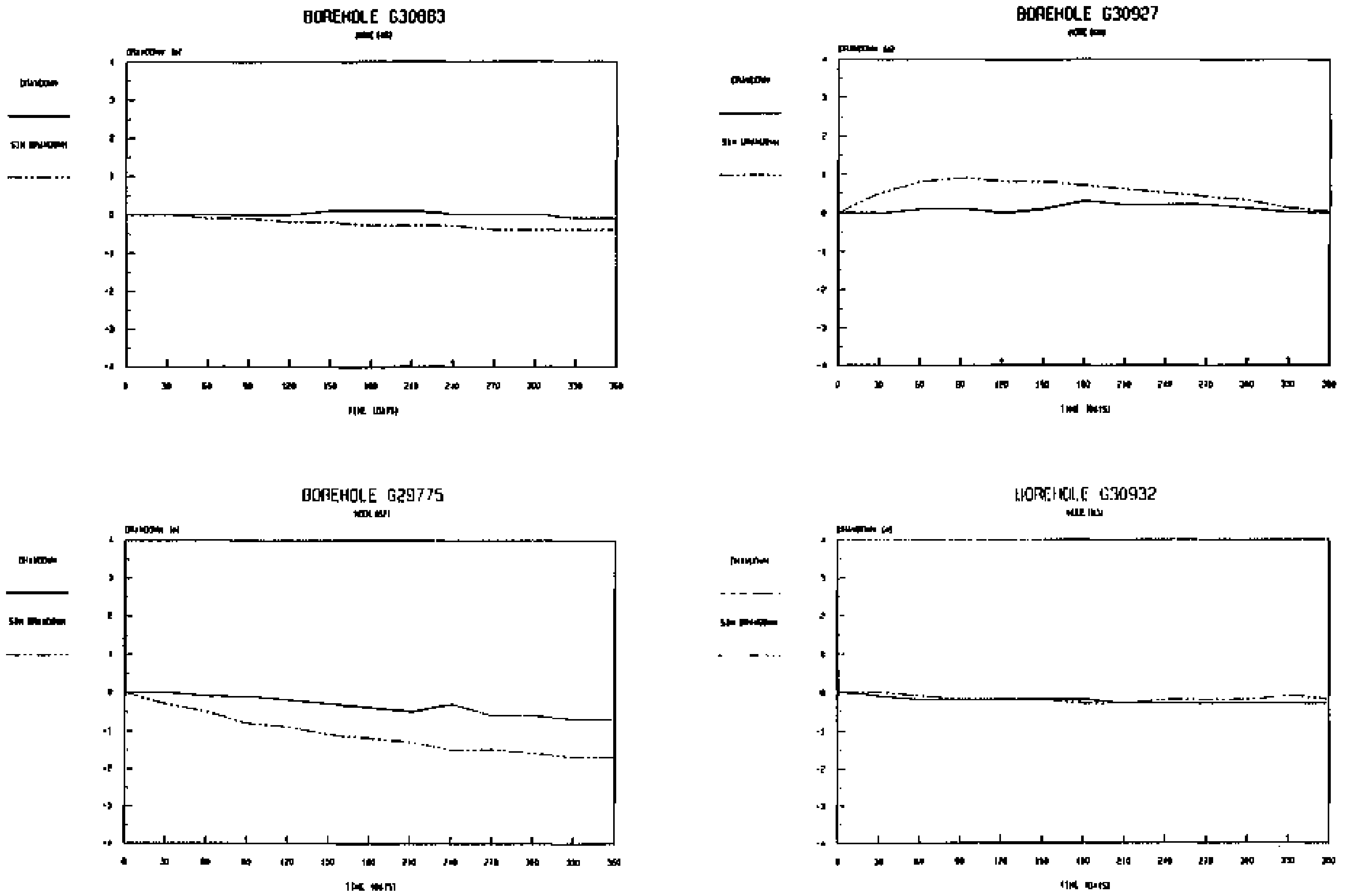

Figure 5.11. Reaction of the model compared to the observed reaction of the ground-water system at selected observation boreholes (Group 1).

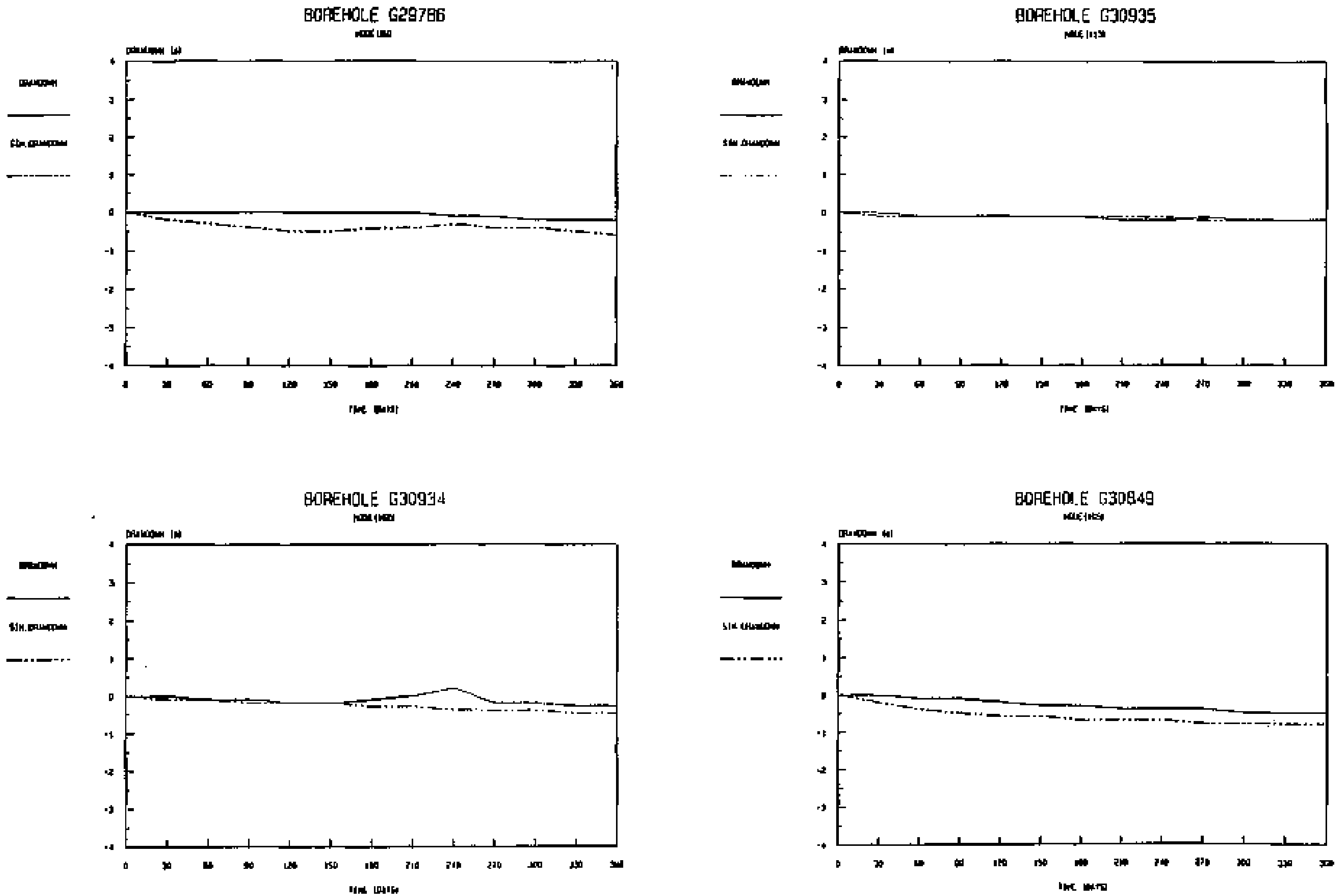

Figure 5.11. (Continued).

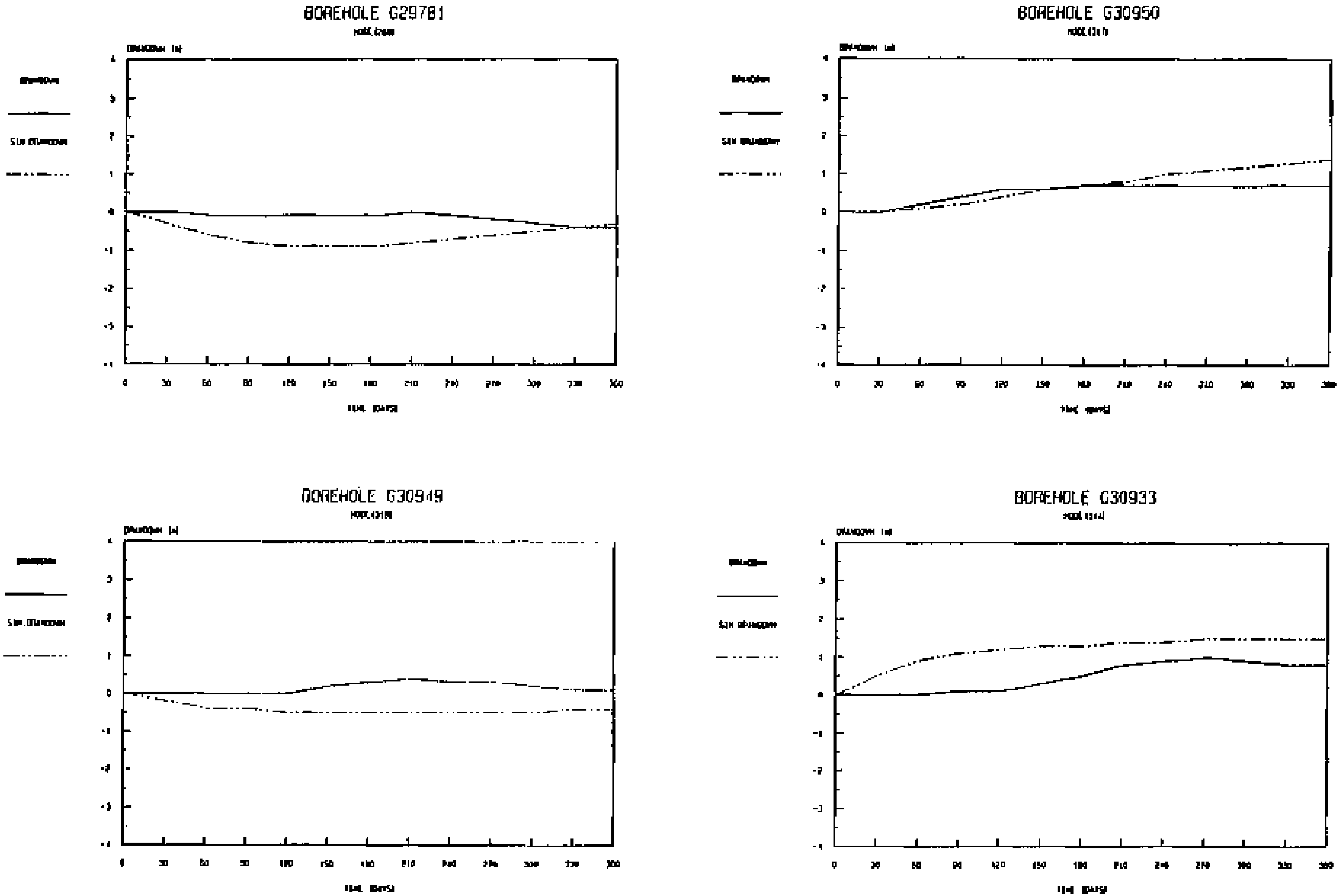

Figure 5.11. (Continued).

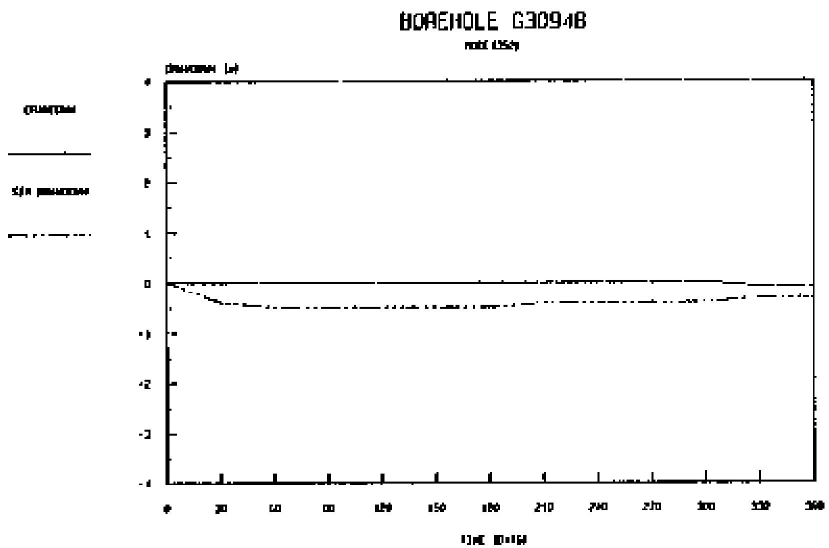

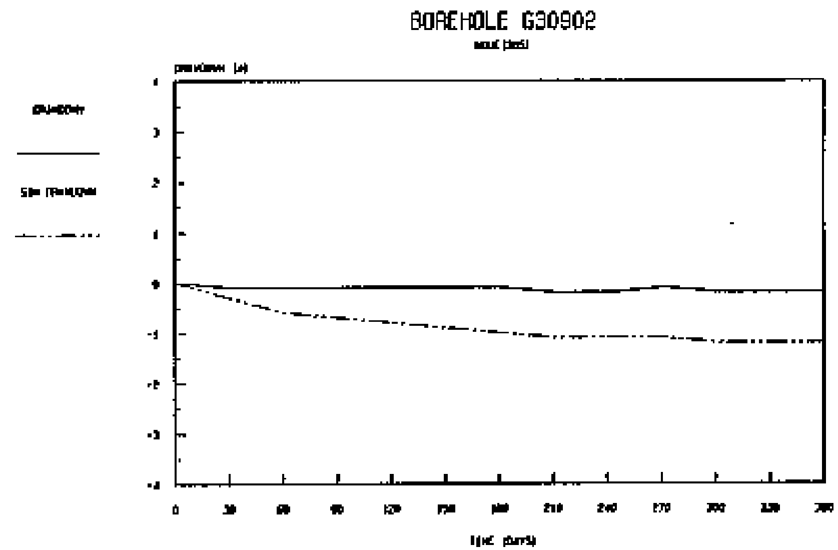

Figure 5.11. (Continued).

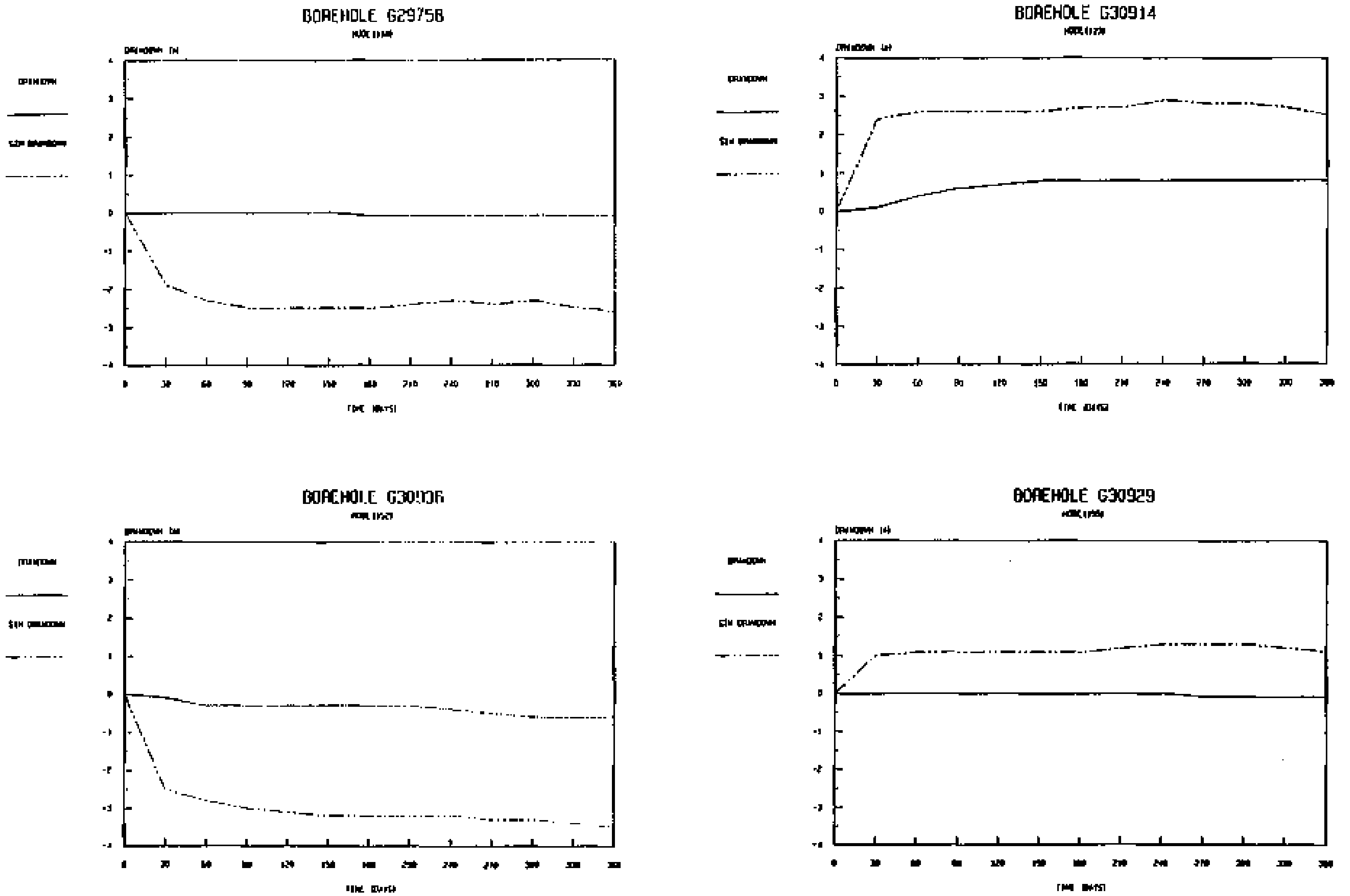

Figure 5.12. Reaction of the model compared to the observed reaction of the ground-water system at selected observation boreholes (Group 2).

simulation time, the water-levels rise or decline rather markedly, after which they stabilize and closely resemble the observed behaviour of the physical system for the rest of the period. Such a behaviour can usually be ascribed to erroneous initial head values, but this would imply that the observed water-level elevations for these boreholes are erroneous. Even so, it was decided to change the initial heads at nodes 118, 123, 152 and 155, according to the decline or rise in simulated heads over the first 30 days of simulation time. The old and new initial head values at the four nodes can be seen in Table 5.2.

TABLE 5.2. OLD AND NEW INITIAL HEAD VALUES AT NODES 118, 123, 152 AND 155

Borehole No.	*Node No.*	*Old Head (MASL)*	*New Head (MASL)*
G29758	118	17,9	15,4
G30914	123	9,0	11,5
G30936	152	24,0	21,5
G30929	155	12,4	13,4

After implementation of the changed initial heads, the model was once again run for the 12 month period, January 1979 - January 1980. The results of this simulation run, at the four nodes in question, are shown in Figure 5.13.

From the graphs in Figure 5.13, it can clearly be seen that the strange behaviour of the simulated heads over the first 30 days has been eliminated by the changing of the initial head values. In the case of node 152, it may be necessary to lower the initial head by another 0,5 m to obtain a perfect fit.

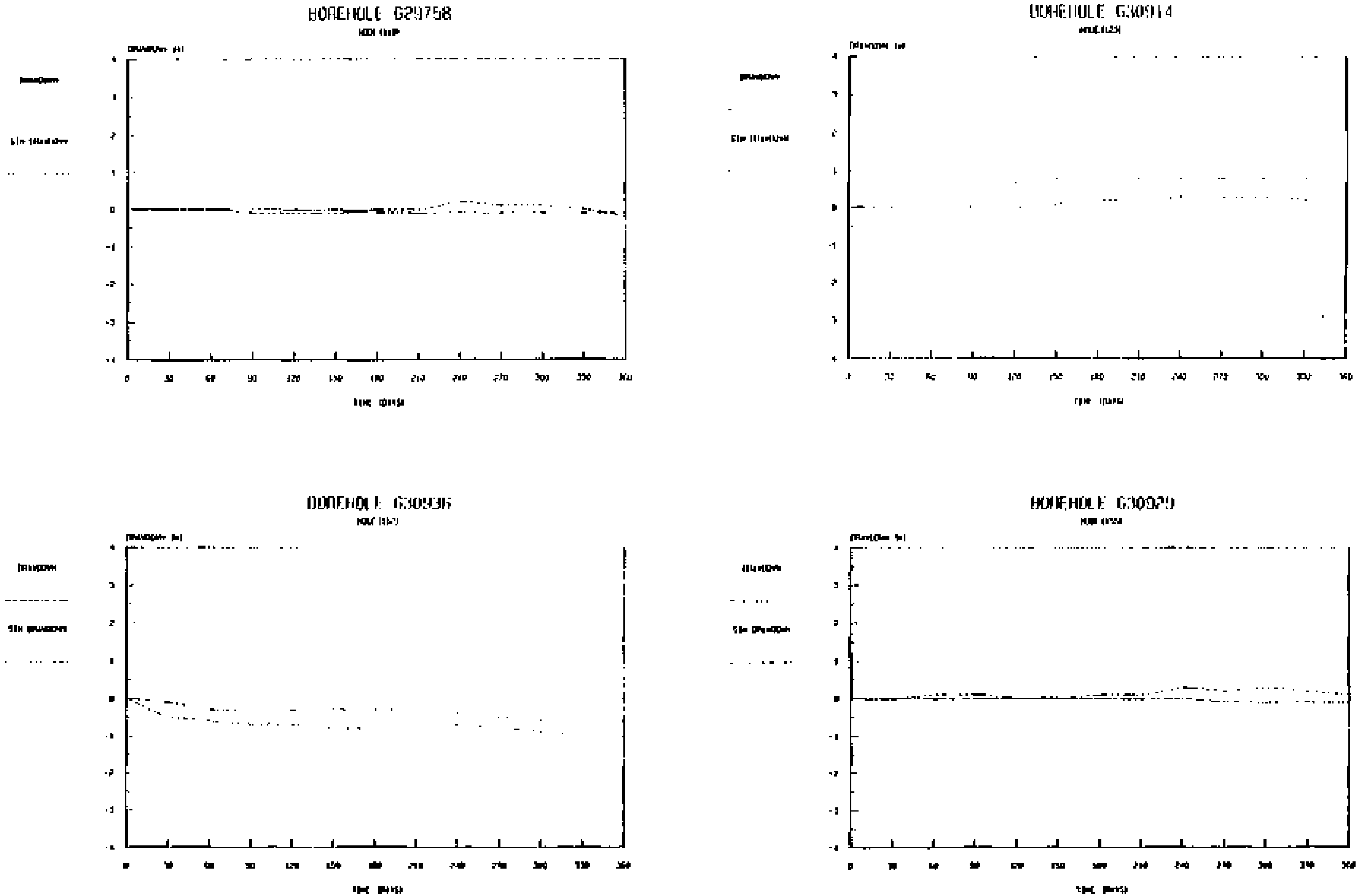

Figure 5.13. Reaction of the model compared to the observed reaction of the ground-water system at selected observation boreholes (Group 2).

Although we have now proved that the strange behaviour of the model at nodes 118, 123, 152 and 155 can be corrected by changing the initial head values, we must keep in mind that if the observed values at the four observation boreholes situated at these nodes, prove to be accurate, another explanation as to the strange behaviour of the model, would have to be given. One explanation that came to mind, arose from the fact that all four observation boreholes showing this strange behaviour, lie in the Silwerstroom area (see Figure 5.17). Here one has the situation of an observed hydraulic conductivity of 100 m/day at the Silwerstroom spring, while the observed values for the boreholes in its vicinity are mostly of the order of 10 - 15 m/day (Bredenkamp and Vandoolaeghe, 1982). The behaviour of the simulated water-levels may thus also be ascribed to inaccurate K and S values obtained from the kriging procedure. This hypothesis is strengthened by the simulated behaviour of other boreholes in the vicinity, which can be seen in the third group of graphs shown in Figure 5.14. Only a more detailed investigation of the hydraulic parameters in this area can prove if this hypothesis is correct.

The fourth group of graphs (Figure 5.15) shows the simulated water-levels in a number of boreholes situated in the vicinity of the steep gradient in the water-table (see Figure 5.17). It is interesting to note that boreholes for which the simulated water-level elevations are lower than the observed ones, invariably lie at the top of a zone where steep ground-water gradients occur and vice versa (see Figure 5.17). This can be corrected for by using a mesh with finer elements in these regions, so as to control the flux of ground water more effectively.

The fifth and last group of graphs (Figure 5.16) represents the only observation boreholes for which a satisfactory solution could not be obtained by adjusting the numerical model. These boreholes are all situated near the assumed boundary of the aquifer (see Figure 5.17). What they seem to indicate, is that the Dirichlet or prescribed head boundary values used in the

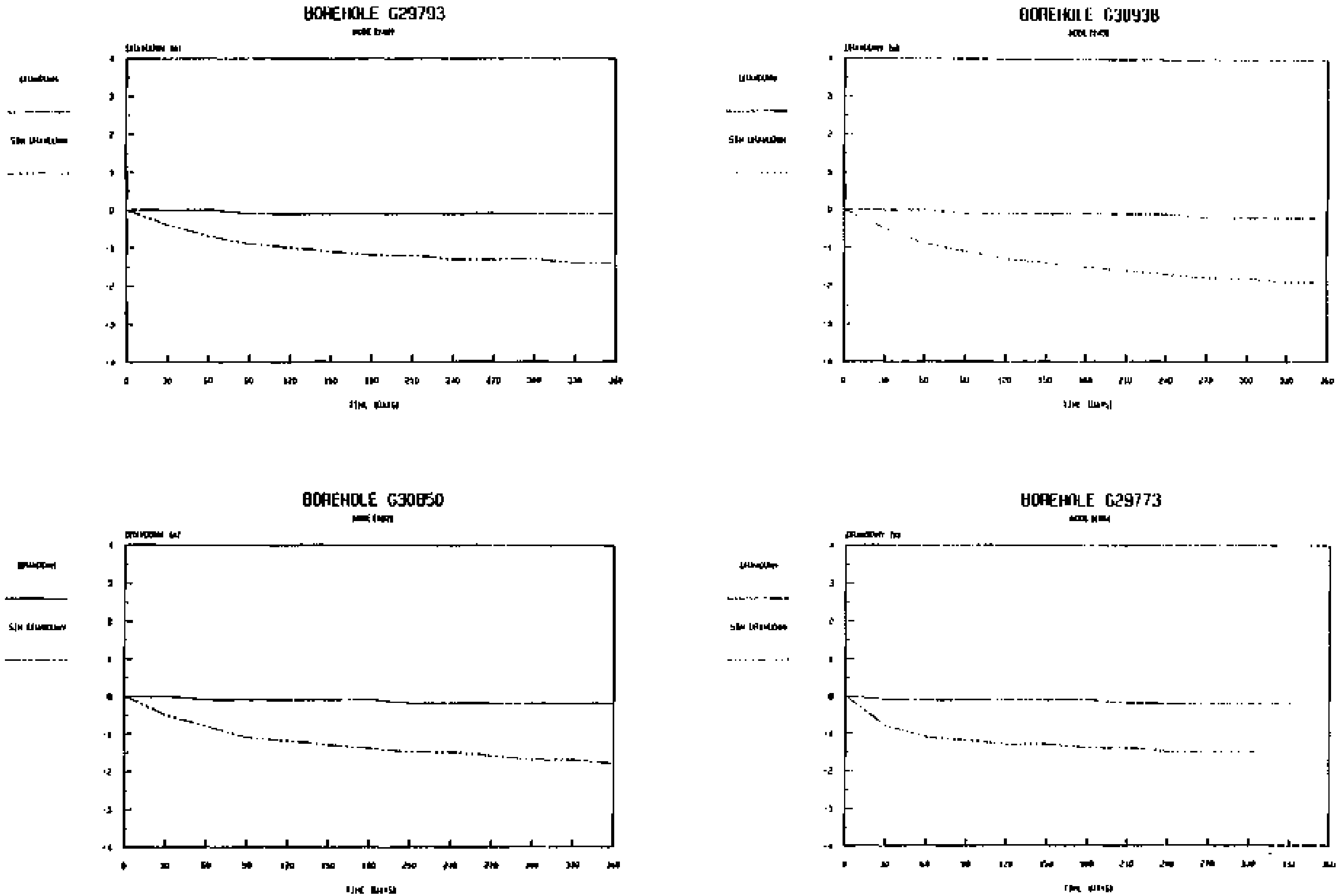

Figure 5.14. Reaction of the model compared to the observed reaction of the ground-water system at selected observation boreholes (Group 3).

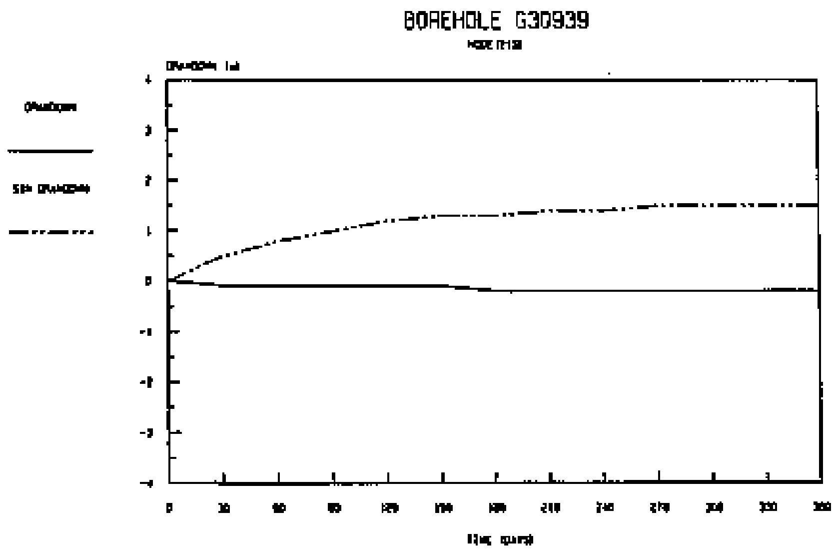

Figure 5.14. (Continued).

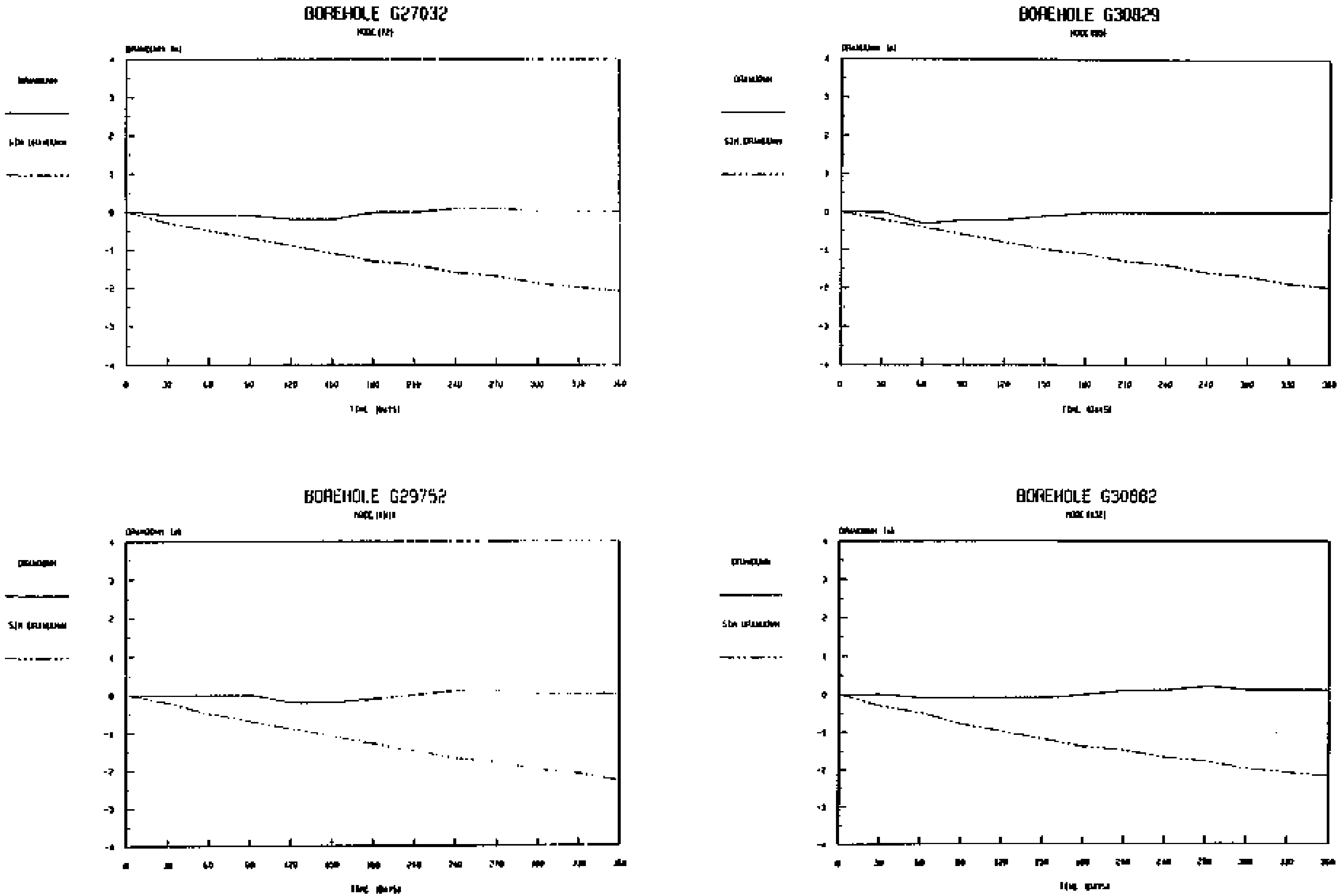

Figure 5.15. Reaction of the model compared to the observed reaction of the ground-water system at selected observation boreholes (Group 4).

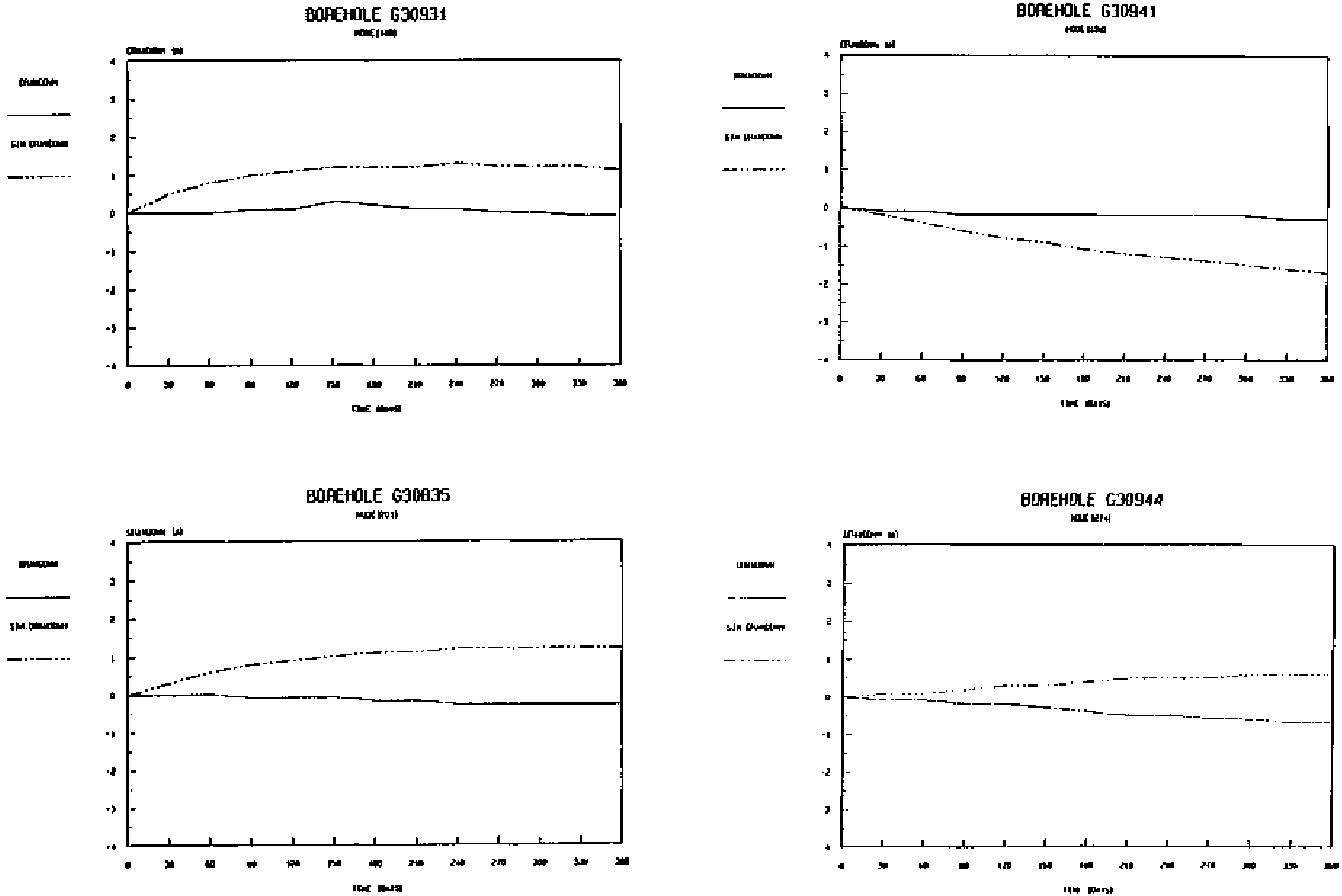

Figure 5.15. (Continued).

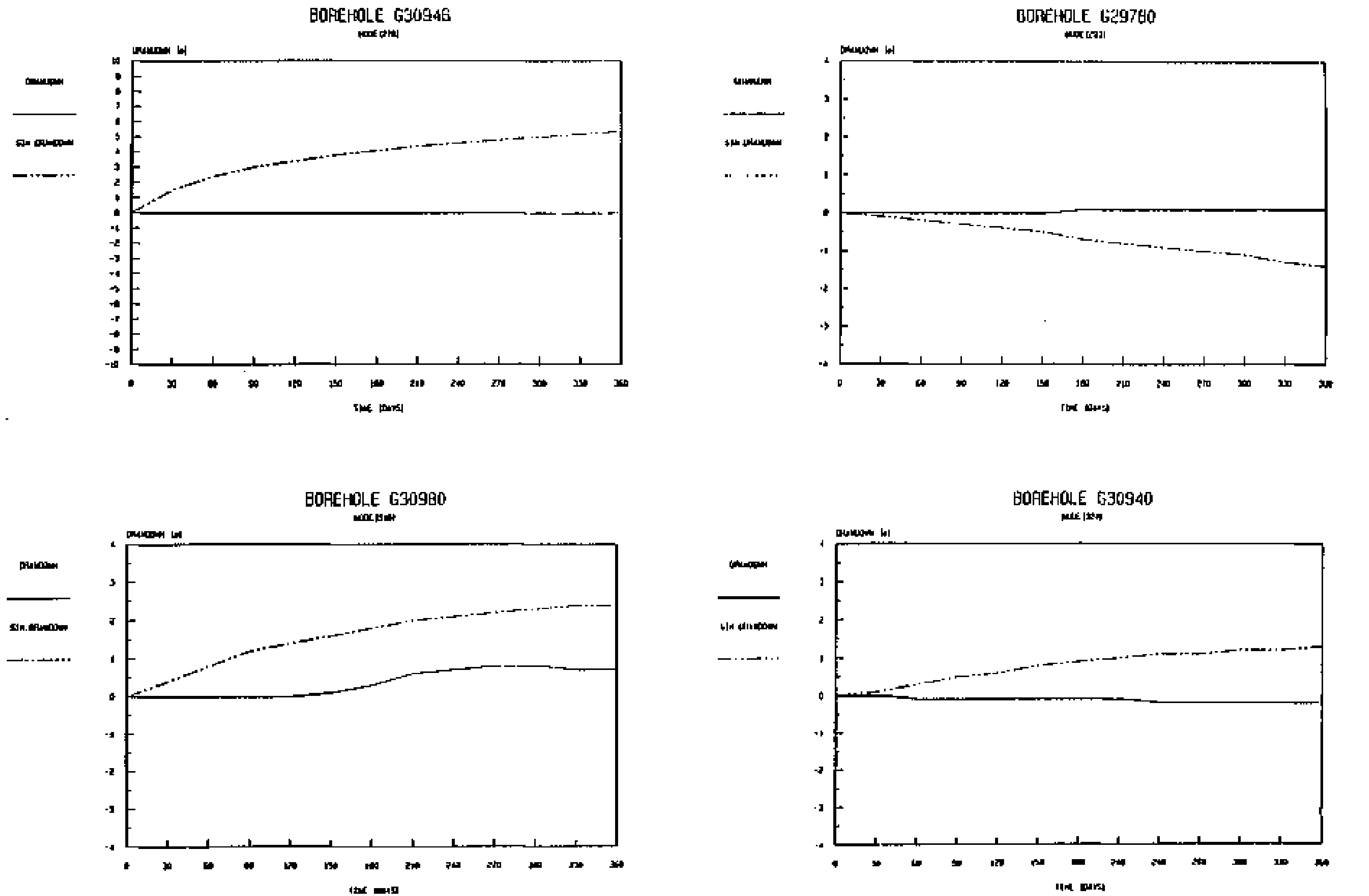

Figure 5.15. (Continued).

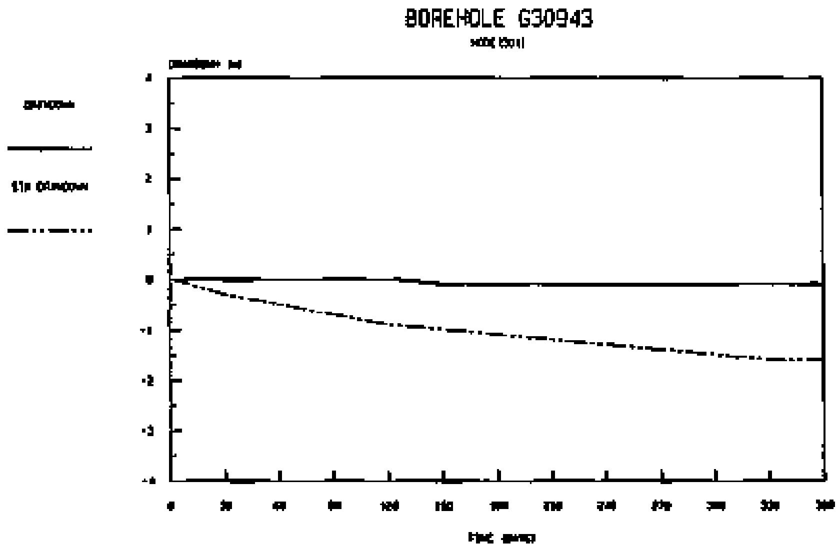

Figure 5.15. (Continued).

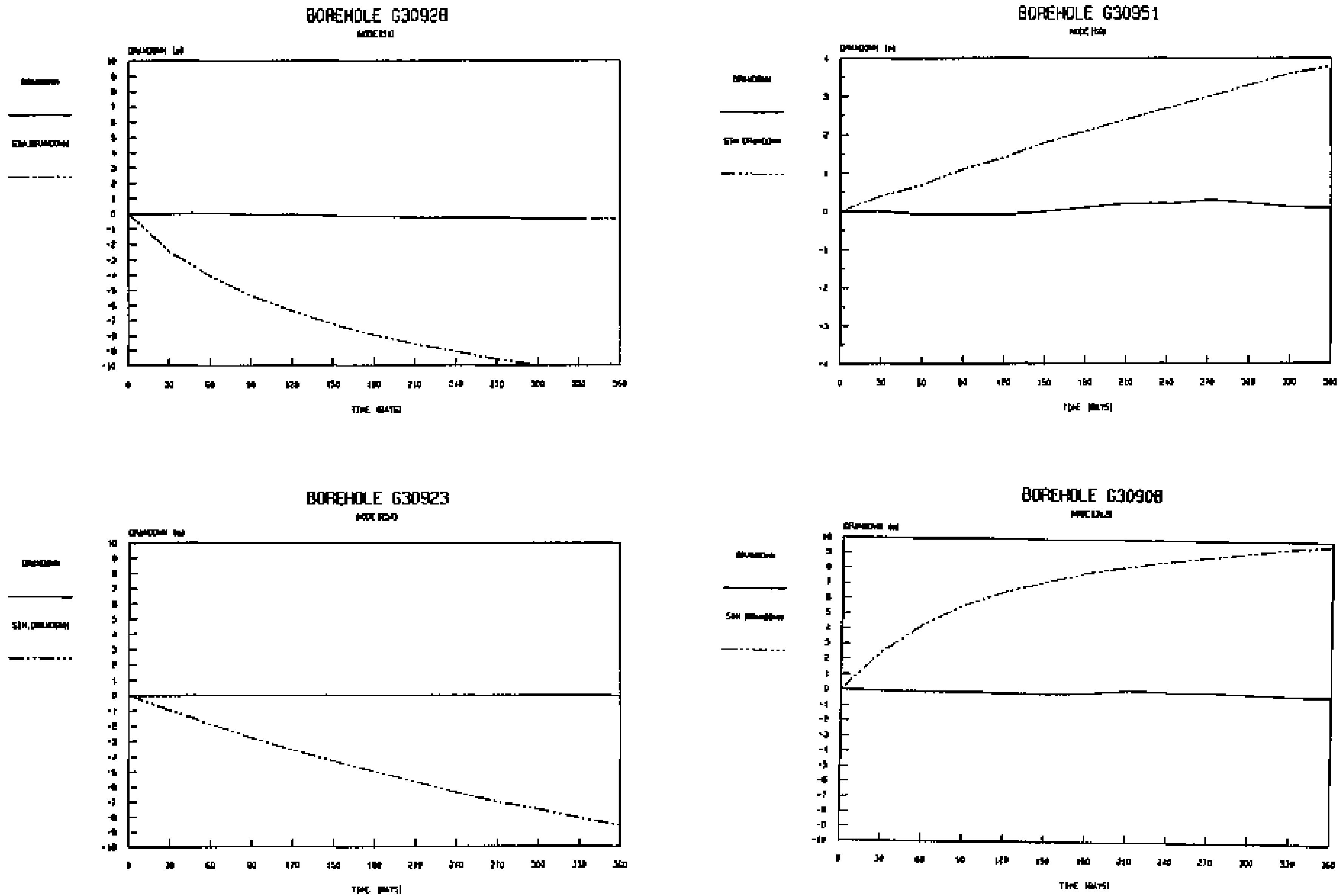

Figure 5.16. Reaction of the model compared to the observed reaction of the ground-water system at selected observation boreholes (Group 5).

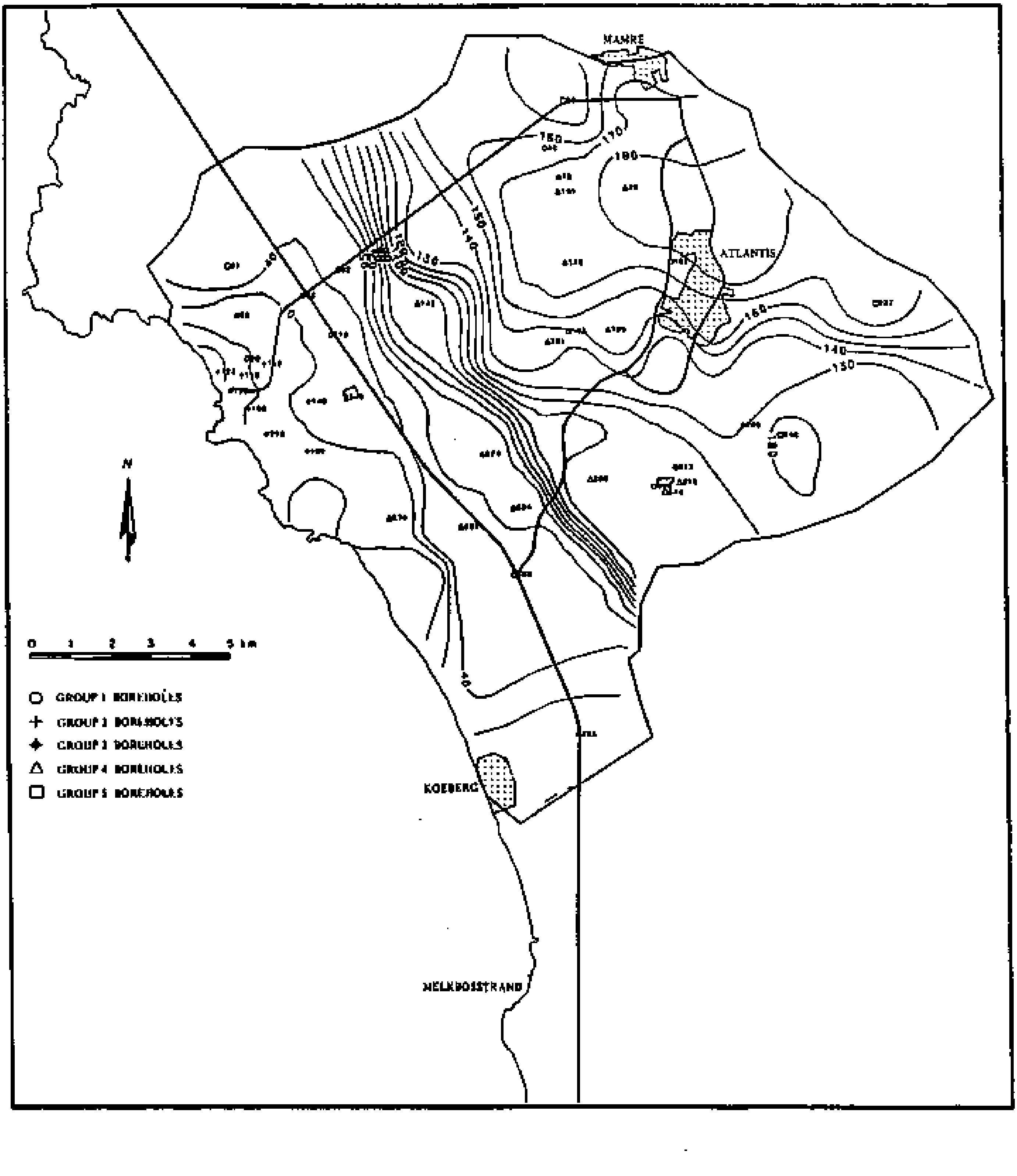

Figure 5.17. Localities of the selected observation boreholes used for comparison of the reaction of the model with the reaction of the observed ground-water system. The number at every location is the node number of the finite element mesh representing the observation borehole.

present model, may not be appropriate in these areas. That this can be the case, was shown in a trial run of the model in which the Dirichlet conditions on parts of the boundary in the vicinity of boreholes G30928 and G30923 (nodes 31 and 257) were replaced by constant inflow, and in the vicinity of boreholes G30951 and G30908 (nodes 69 and 312) by constant outflow boundary conditions. However, as information in these areas is almost non-existent and because the final result depends critically on the assumed properties of the aquifer, the results obtained from the trial run, are not worth reporting here. This illustrates the fact that the effectiveness of a numerical model is almost completely determined by the accuracy of the available physical information regarding the system. It is, therefore, suggested that more work should be done in these areas with special attention given to the following aspects:

- (i) Sand thickness.
- (ii) Water-level elevations.
- (iii) Hydraulic parameters.

5.5.3 THE PERIOD JANUARY 1979 - JANUARY 1982

The final test in the calibration of any numerical model is to ascertain whether it is able to simulate water-levels for periods not used in the calibration. The model developed in the previous section was consequently also used to simulate the water-levels for the period January 1979 - January 1982. The available field data indicates that, notwithstanding increased pumping rates, the water-levels changed very little over the three year period. Hence, if the model is still able to simulate the observed water-levels (taking the previous discussed deviations into account), it can be accepted as being calibrated.

The only difference between the input to the model for this period and that used in the calibration, is the pumping rates given in Table 5.3. The model was then run for a three year period. The results are illustrated by

TABLE 5.3. MONTHLY PUMPING RATES FOR EXISTING PRODUCTION BOREHOLES IN THE ATLANTIS AQUIFER FOR THE PERIOD JANUARY 1979 - DECEMBER 1981

BOREHOLE		SPRING	G29794	G30999	G29757	G30865	G30991	G30972	G30971	G30981	G30965	G30966	G30969	G30926	G29749	G29782	G29800
NODE		119	86	87	88	116	151	302	329	327	326	351	354	200	230	287	260
1979	J	2662.0	122.0	.0	92.0	184.0	.0	.0	.0	.0	.0	.0	.0	.0	.0	.0	.0
	F	2232.0	13.0	.0	335.0	380.0	.0	.0	.0	.0	.0	.0	.0	.0	.0	.0	.0
	M	2483.0	308.0	.0	.0	261.0	.0	.0	.0	.0	.0	.0	.0	.0	.0	.0	.0
	A	2362.0	113.0	.0	89.0	126.0	.0	.0	.0	.0	.0	.0	.0	.0	.0	.0	.0
	M	2068.0	.0	.0	.0	.0	0	.0	.0	.0	.0	.0	.0	.0	.0	.0	.0
	J	1530.0	16.0	.0	5.0	15.0	.0	.0	.0	.0	.0	.0	.0	.0	.0	.0	.0
	J	1443.0	24.0	.0	9.0	7.0	.0	.0	.0	.0	.0	.0	.0	.0	.0	.0	.0
	A	729.0	415.0	.0	280.0	465.0	.0	.0	.0	.0	.0	.0	.0	.0	.0	.0	.0
	S	1460.0	398.0	.0	417.0	146.0	.0	.0	.0	.0	.0	.0	.0	.0	.0	.0	.0
	O	907.0	787.0	.0	517.0	794.0	.0	.0	.0	.0	.0	.0	.0	.0	.0	.0	.0
	N	1757.0	860.0	.0	385.0	614.0	.0	.0	.0	.0	.0	.0	.0	.0	.0	.0	.0
	D	2271.0	792.0	.0	631.0	869.0	.0	.0	.0	.0	.0	.0	.0	.0	178.0	.0	728.0
1980	J	2001.0	932.0	.0	515.0	798.0	.0	.0	.0	.0	.0	.0	.0	.0	.0	.0	520.0
	F	2479.0	448.0	.0	688.0	808.0	.0	.0	.0	.0	.0	.0	.0	.0	.0	.0	530.0
	M	2408.0	681.0	.0	440.0	669.0	.0	.0	.0	.0	.0	.0	.0	.0	469.0	.0	130.0
	A	1518.0	531.0	.0	290.0	437.0	.0	.0	.0	.0	.0	.0	.0	.0	.0	.0	66.0
	M	1401.0	374.0	.0	208.0	314.0	.0	.0	.0	.0	.0	.0	.0	.0	135.0	.0	10.0
	J	1394.0	332.0	.0	185.0	276.0	.0	.0	.0	.0	.0	.0	.0	.0	47.0	.0	.0
	J	2337.0	.0	.0	.0	.0	.0	.0	.0	.0	.0	.0	.0	.0	52.0	.0	135.0
	A	2268.0	56.0	.0	31.0	47.0	.0	.0	.0	.0	.0	.0	.0	.0	2.0	.0	.0
	S	2229.0	192.0	.0	106.0	161.0	.0	.0	.0	.0	.0	.0	.0	.0	88.0	.0	93.0
	O	1391.0	728.0	417.0	342.0	521.0	347.0	.0	.0	.0	.0	.0	.0	.0	91.0	.0	72.0
	N	2509.0	564.0	446.0	263.0	38.0	305.0	.0	.0	.0	.0	.0	.0	.0	.0	.0	.0
	D	1716.0	612.0	536.0	275.0	311.0	370.0	.0	.0	.0	.0	.0	.0	.0	210.0	.0	322.0
1981	J	2210.0	787.0	675.0	117.0	696.0	471.0	.0	.0	.0	.0	.0	.0	.0	.0	.0	301.0
	F	2567.0	834.0	699.0	370.0	720.0	497.0	.0	.0	.0	.0	.0	.0	.0	.0	.0	339.0
	M	2676.0	921.0	758.0	355.0	788.0	553.0	.0	.0	.0	.0	.0	.0	.0	98.0	.0	283.0
	A	2367.0	598.0	485.0	104.0	507.0	247.0	.0	.0	.0	.0	.0	.0	.0	232.0	.0	243.0
	M	2610.0	461.0	376.0	.0	385.0	112.0	.0	.0	.0	.0	.0	.0	.0	53.0	.0	61.0
	J	2523.0	266.0	219.0	.0	222.0	.0	.0	.0	.0	.0	.0	.0	.0	43.0	.0	62.0
	J	2504.0	167.0	136.0	.0	139.0	.0	.0	.0	.0	.0	.0	.0	.0	.0	.0	.0
	A	2662.0	101.0	84.0	.0	85.0	.0	.0	.0	.0	.0	.0	.0	.0	6.0	.0	6.0
	S	2701.0	190.0	159.0	.0	161.0	.0	.0	.0	.0	.0	.0	.0	.0	.0	.0	.0
	O	2650.0	624.0	552.0	268.0	550.0	114.0	.0	.0	.0	.0	.0	.0	.0	224.0	.0	276.0
	N	1765.0	1244.0	1111.0	908.0	952.0	652.0	.0	.0	.0	.0	.0	.0	.0	401.0	.0	464.0
	D	1559.0	1183.0	1030.0	866.0	878.0	705.0	.0	.0	.0	.0	.0	.0	.0	387.0	.0	528.0

PUMPING RATES ARE GIVEN IN m^3/day FOR A 30 DAY MONTH making use of two selected boreholes from each of the five groups, defined during the discussion of the results of the one year simulation period. These graphs are shown in Figures 5.18 - 5.22.

In general the behaviour of the simulated water-levels is in accordance with what could be expected, except perhaps the behaviour of the simulated water-levels for the first group of boreholes. When studying the graphs in Figure 5.18, it is evident that the simulated heads for the last 360 days of the simulation period, are somewhat lower than the observed heads for the same period. A possible explanation for this behaviour may be found in the fact that no recharge to the system was specified in the model; an aspect that will receive more attention in the following chapter.

The form of the graphs in the second group (Figure 5.19) tends to support the belief that the strange behaviour of the model at these locations is caused by erroneous initial head values. The second graph in Figure 5.19 (borehole G30936) shows that, except for the first 30 days of the simulation, the behaviour of the simulated heads is identical to that of the observed heads, for the whole of the three year period.

All that can be said regarding the last three groups of graphs (Figures 5.20 - 5.22), is that the simulated water-levels seem to stabilize towards the end of the three year simulation period. That this is indeed the case, can be seen from the contour map of the simulated water-levels for January 1982 (Figure 5.23). When comparing this map with the contour map of the simulated water-levels for January 1980, it is clear that no large changes in the water-level distribution have occurred. Unfortunately a contour map depicting observed water-levels for January 1982, could not be compiled, due to the fact that only 53 observations were available for January 1982, whereas 93 values were used for the construction of the contour maps used during the calibration procedure.

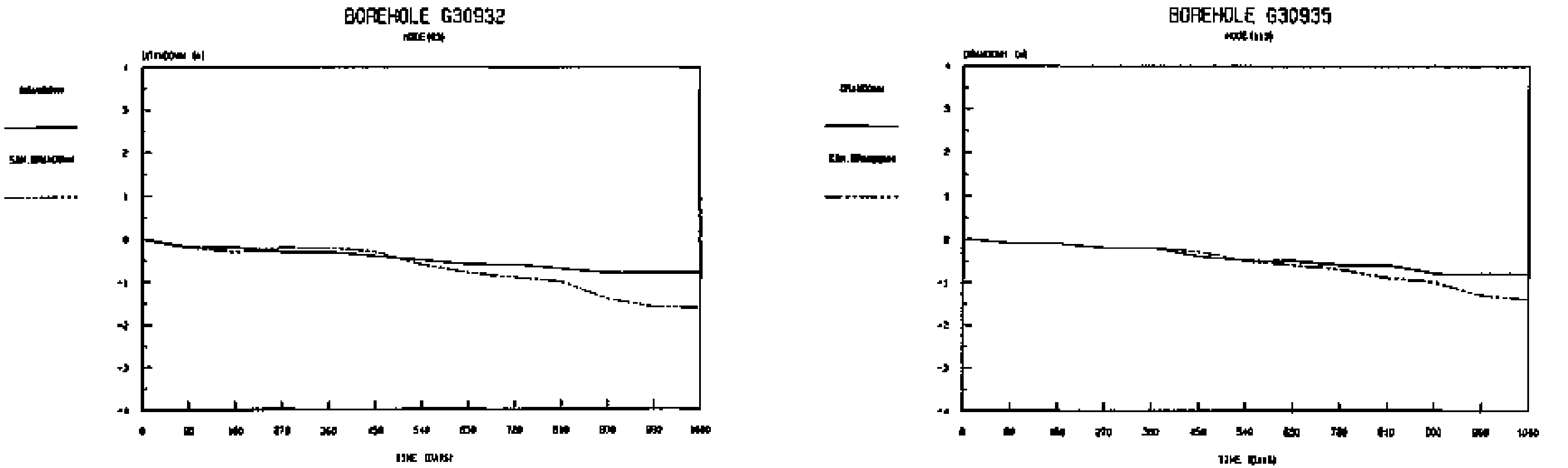

Figure 5.18. Reaction of the model compared to the observed reaction of the ground-water system - three-year period (Group 1).

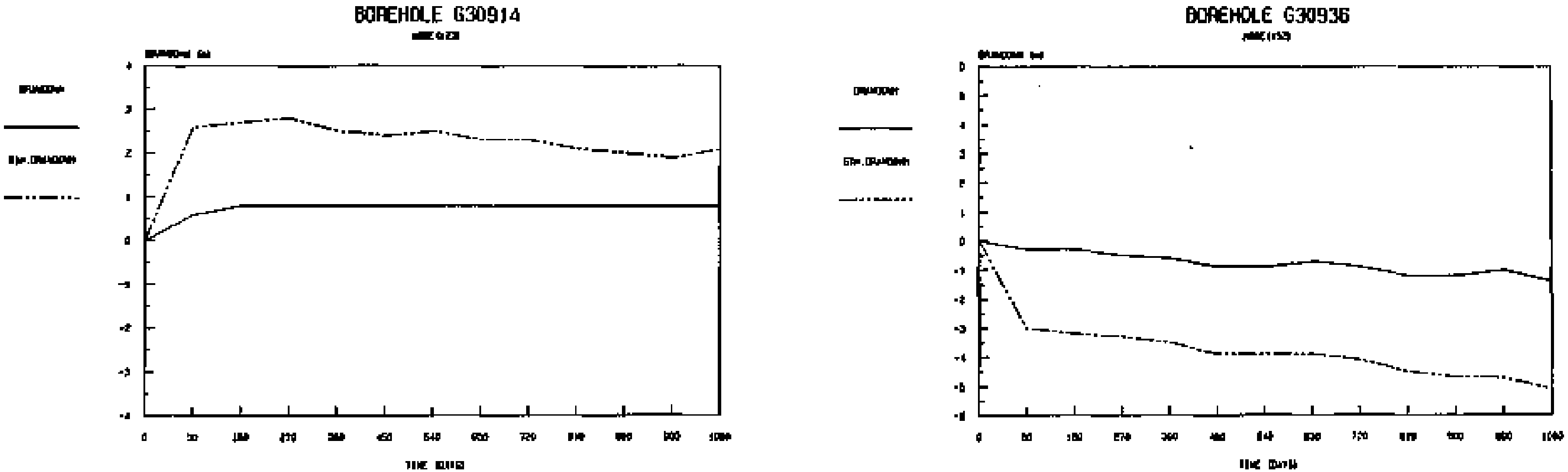

Figure 5.19. Reaction of the model compared to the observed reaction of the ground-water system - three-year period (Group 2).

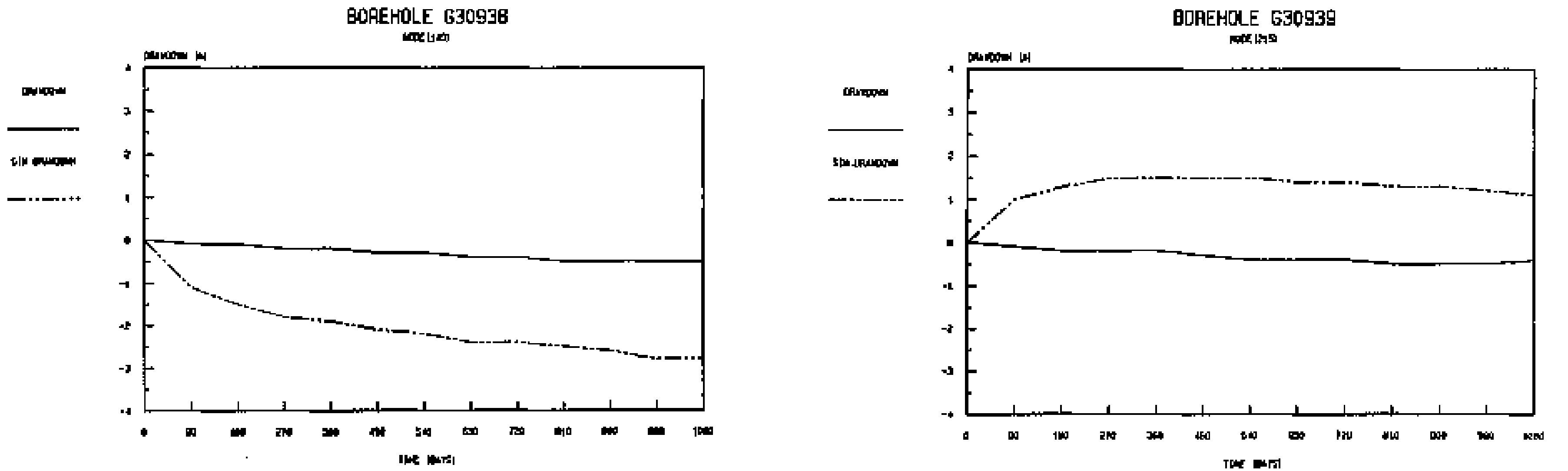

Figure 5.20. Reaction of the model compared to the observed reaction of the ground-water system - three-year period (Group 3).

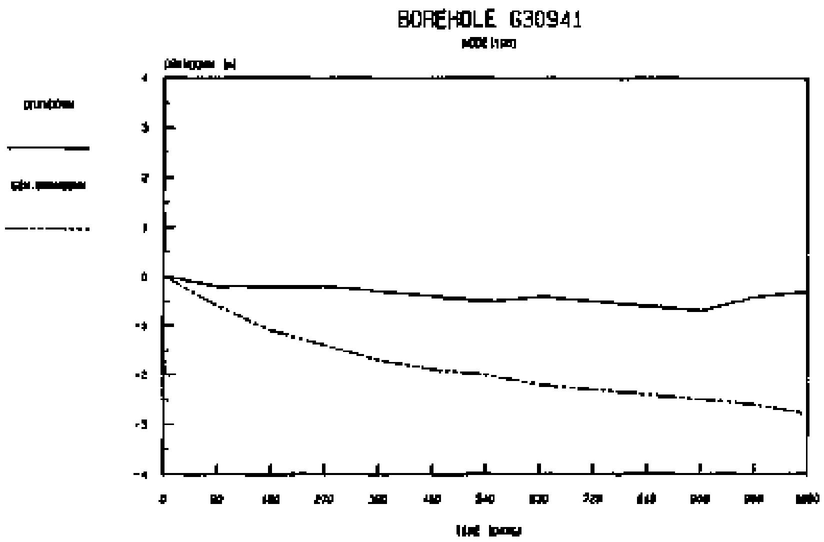

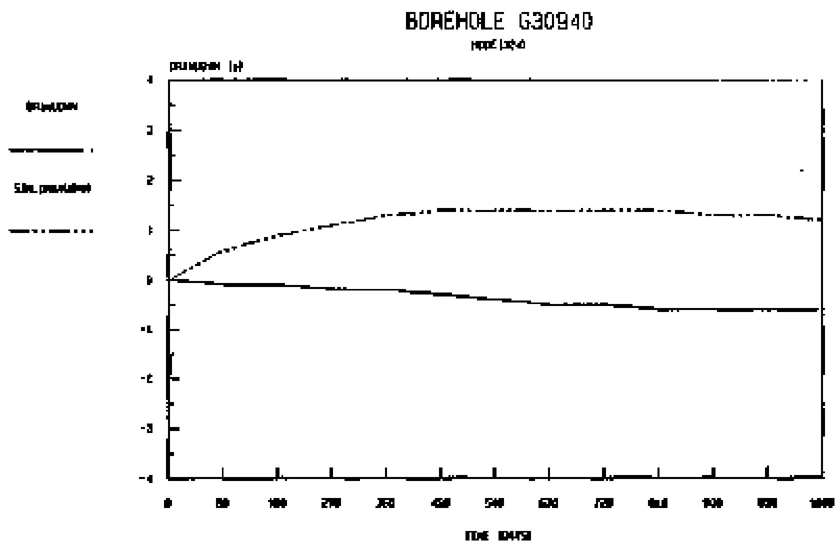

Figure 5.21. Reaction of the model compared to the observed reaction of the ground-water system - three-year period (Group 4).

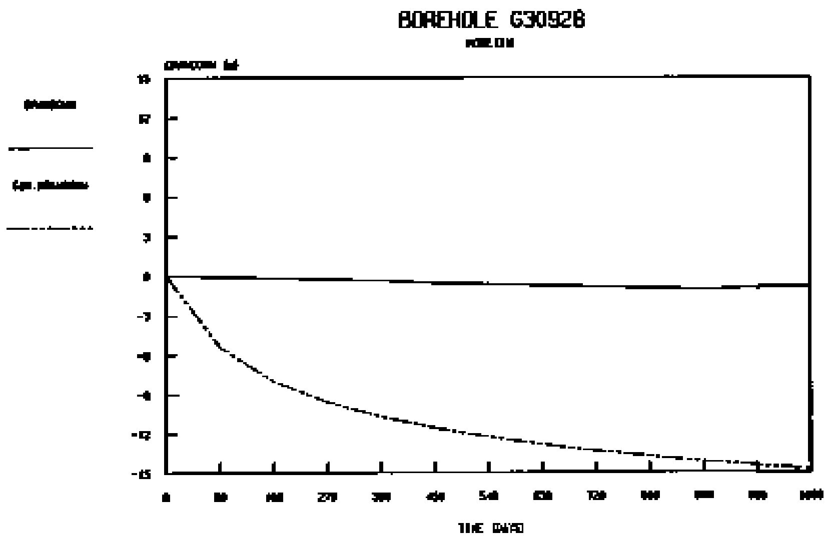

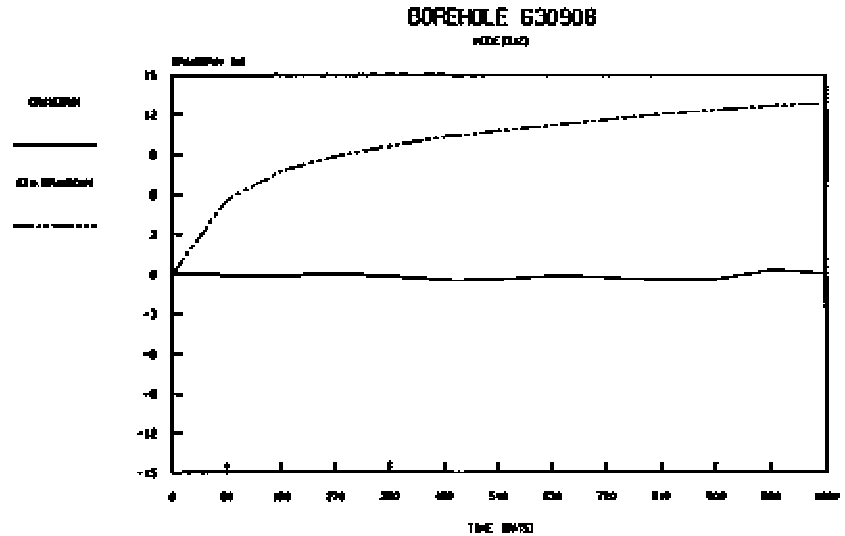

Figure 5.22. Reaction of the model compared to the observed reaction of the ground-water system - three-year period (Group 5).

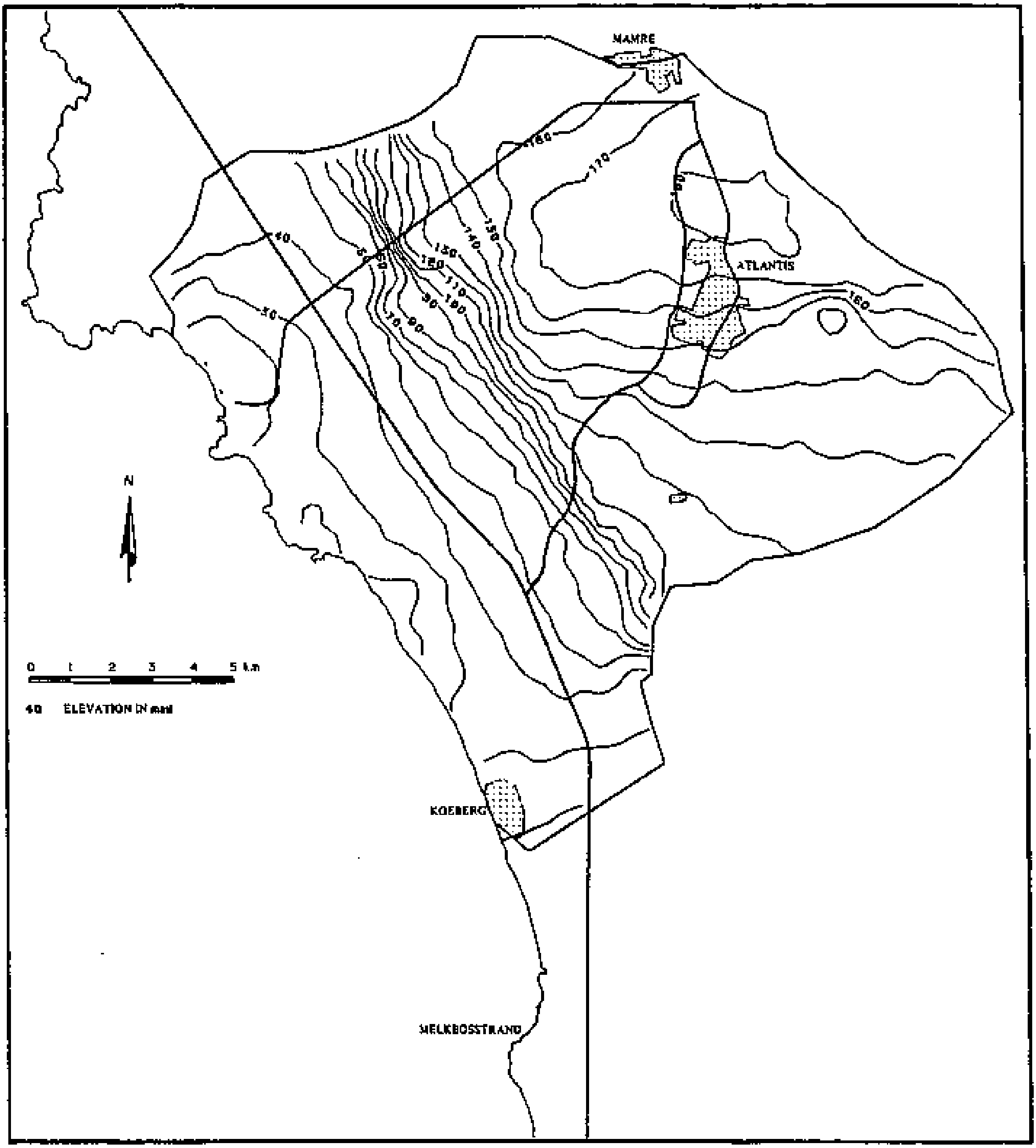

Figure 5.23. Simulated water-level distribution for January 1982.

In conclusion, it can be said that the calibration of the numerical model was as successful as could be expected with the available data. One important aspect that came to light, was that the calibration period of one year might not be long enough for the optimal calibration of the model. This is entirely due to the fact that almost no changes in the water-levels occurred during that period.

CHAPTER 6

APPLICATION OF THE NUMERICAL MODEL

6.1 GENERAL

Due to a lack of information in various parts of the Atlantis aquifer, the present model cannot be considered fit for management purposes. This does not imply, however, that it cannot be used to some advantage in studying the general behaviour of the Atlantis aquifer. As outlined in Chapter 1, two questions that are of particular importance are:

(i) How long will the existing ground-water supply last, given a certain demand?

(ii) How should the existing production fields be expanded to ensure the optimum use of the available ground water?

The volume of water in the aquifer has already been calculated in Chapter 4. Although such a calculation provides an estimate of how long the available water may last, the following must be kept in mind. The dewatering capacity of a single production borehole is limited in areal extent and for that matter, so is the dewatering capacity of an entire production field. It is, therefore, important to see how the ground-water system will react when large quantities of water are abstracted at the Silwerstroom and Witzand production fields. This immediately raises a second question, namely optimization of the expansion of the existing production fields. However, the positions for the additional production boreholes in the Atlantis aquifer have already been agreed upon by the parties concerned and, therefore, it would from the practical point of view, be senseless to determine theoretical positions for these boreholes by means of the numerical model. It would be more interesting to evaluate the potential of these additional production boreholes by means of the model. This is certainly a slight change of emphasis concerning the initial aim of this study, but one that can be reversed if required by the analysis.

6.2 PROPOSED EXPANSION OF THE PRODUCTION FIELDS

6.2.1 WITZAND PRODUCTION FIELD

The information received from the consulting engineers for the Divisional Council of the Cape, Liebenberg and Stander, indicates that a total abstraction rate of 7,7 x 10^6 m^3 per annum, is foreseen in the Witzand production field. The water is to be abstracted from 19 production boreholes comprising the 6 existing and 13 additional production boreholes. To achieve the projected rate, these boreholes will have to be pumped at a continuous rate of 14 litres/second for a 22 hour day.

The positions of the 6 existing and the 13 additional production boreholes are shown in Figure 6.1 and their coordinates given in Table 6.1.

Due to the fact that the proposed locations of the additional boreholes (B1-B13) became available only after the numerical model had already been constructed, they could not be implemented in the finite element mesh. What was done was to distribute the total abstraction required among the finite element nodes in the immediate vicinity of the Witzand production field. These nodes, the boreholes allocated to them and the abstraction rate at each node, is given in Table 6.2.

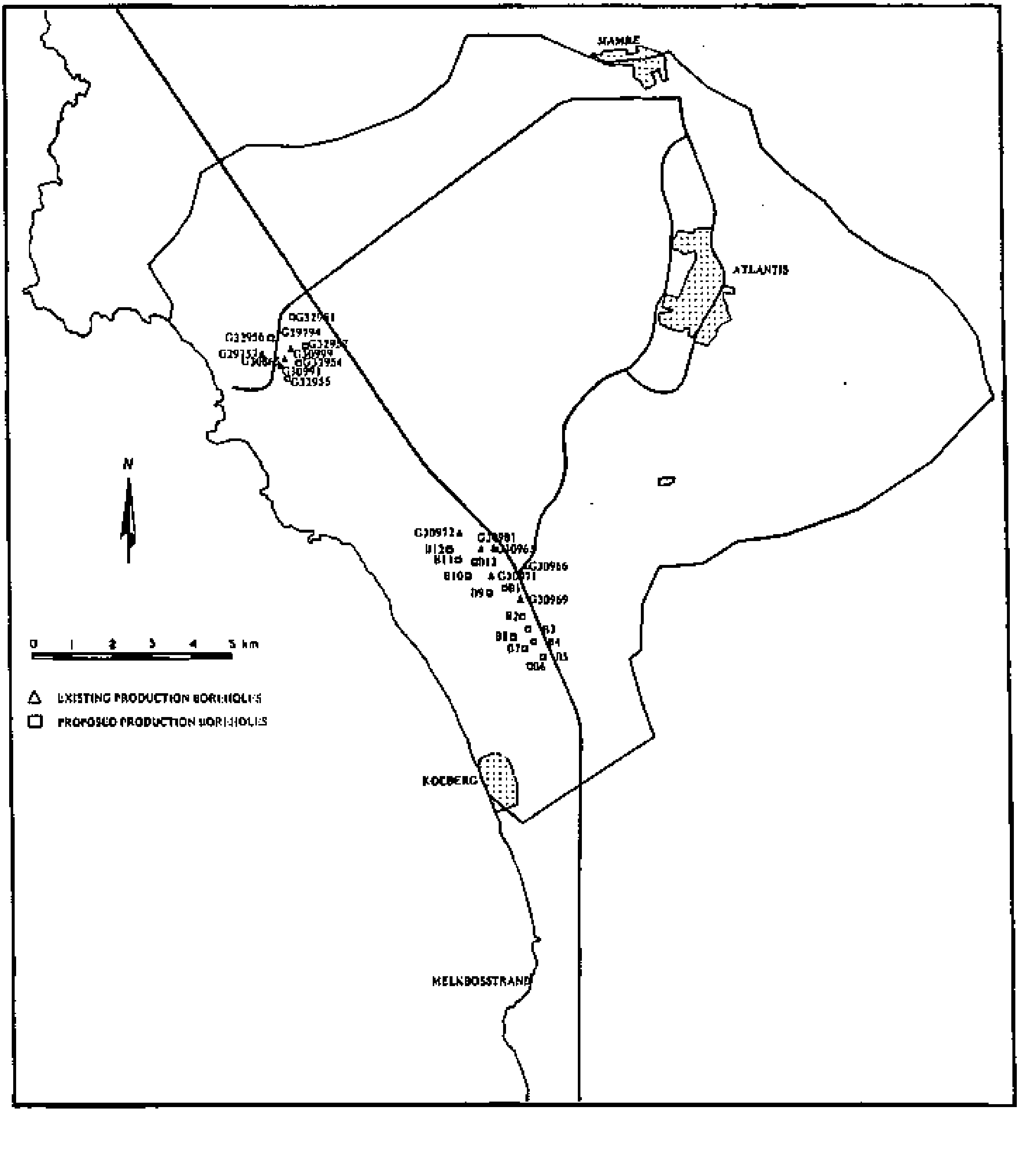

Figure 6.1. Positions of the 11 existing and 18 proposed production boreholes in the Silwerstroom and Witzand production fields.

TABLE 6.1. COORDINATES OF THE 6 EXISTING AND 13 ADDITIONAL PRODUCTION BOREHOLES IN THE WITZAND PRODUCTION FIELD

Borehole	Y (+ 0,00) Lo 19	X (3 700 000,00)
G30965	+ 52 552,00	+ 21 706,00
G30966	+ 51 779,00	+ 22 153,00
G30969	+ 51 890,00	+ 22 995,00
G30971	+ 52 629,00	+ 22 405,00
G30972	+ 53 403,00	+ 21 331,00
G30981	+ 52 870,00	+ 21 734,00
B1	+ 52 301,00	+ 22 724,00
B2	+ 51 855,00	+ 23 439,00
B3	+ 51 697,00	+ 23 756,00
B4	+ 51 560,00	+ 24 081,00
B5	+ 51 328,00	+ 24 463,00
B6	+ 51 664,00	+ 24 704,00
B7	+ 51 795,00	+ 24 248,00
B8	+ 52 080,00	+ 23 975,00
B9	+ 52 682,00	+ 22 849,00
B10	+ 53 209,00	+ 22 423,00
B11	+ 53 455,00	+ 22 019,00
B12	+ 53 667,00	+ 21 767,00
B13	+ 53 044,00	+ 22 067,00

TABLE 6.2. PROJECTED ABSTRACTION RATES AND ALLOCATED NODES FOR THE ADDITIONAL AND EXISTING BOREHOLES IN THE WITZAND PRODUCTION FIELD

Node	*Borehole*	*Abstraction (m^3/day)*
302	G30972	1 125,73
303	B11; B12	2 251,46
326	G30965	1 125,73
327	G30981; B13	2 251,46
329	G30971; B9	2 251,46
330	B10	1 125,73
351	G30966	1 125,73
354	G30969; B1; B2	3 377,19
369	B3; B4	2 251,46
370	B7; B8	2 251,46
378	B5	1 125,73
379	B6	1 125,73
	TOTAL	21 388,87

6.2.2 SILWERSTROOM PRODUCTION FIELD

The maximum potential yield of the Silwerstroom production field is of the order of 4,12 x 10^6 m^3 per annum (Bredenkamp and Vandoolaeghe, 1982). According to these authors, only 5 additional boreholes will be able to maintain a yield exceeding 5 litres/second. To incorporate this abstraction rate in the present model, the maximum potential yield was divided equally among the 5 existing and 5 additional production boreholes, as well as the Silwerstroom spring. Their exact locations are given in Table 6.3 and Figure 6.1.

TABLE 6.3. COORDINATES OF THE 5 EXISTING AND

5 ADDITIONAL PRODUCTION BOREHOLES IN THE

SILWERSTROOM PRODUCTION FIELD

Borehole	Y (+ 0,00) Lo 19	X (+ 3 700 000,00)
G29757	+ 58 312,00	+ 16 848,00
G29794	+ 57 890,00	+ 16 253,00
G30865	+ 57 741,00	+ 16 972,00
G30991	+ 57 857,00	+ 17 146,00
G30999	+ 57 600,00	+ 16 697,00
G32951	+ 58 101,00	+ 16 444,00
G32952	+ 57 399,00	+ 17 060,00
G32954	+ 57 233,00	+ 16 628,00
G32955	+ 57 691,00	+ 17 469,00
G32956	+ 57 558,00	+ 15 892,00

The exact positions of the additional boreholes could, as in the case of the Witzand field, not be included in the finite element mesh, but were distributed among the finite element nodes in their immediate vicinity as shown in Table 6.4.

TABLE 6.4. PROJECTED ABSTRACTION RATES AND ALLOCATED NODES FOR THE ADDITIONAL AND EXISTING BOREHOLES IN THE SILWERSTROOM PRODUCTION FIELD

Node	*Borehole*	*Abstraction (m^3/day)*
83	G32956	1 040,40
86	G29794; G32951	2 080,80
87	G30999	1 040,40
88	G29757	1 040,40
114	G32954	1 040,40
115	G32952	1 040,40
116	G30865	1 040,40
119	Spring	1 040,40
150	G32955	1 040,40
151	G30991	1 040,40
	TOTAL	11 444,40

6.3 NUMERICAL EVALUATION OF THE PROPOSED EXPANSION SCHEME

6.3.1 GENERAL

The evaluation of the proposed production fields is hampered by at least two factors:

(i) at what time should the evaluation start, and

(ii) what is the rate of recharge to the system.

Since the water-levels in the aquifer remained almost constant during the period January 1979 - January 1982 (see Chapter 5), it was decided to use once again the January 1979 water-levels as initial heads.

To investigate the effect of recharge on the system, three simulations were carried out. In the first simulation recharge was completely neglected.

6.3.2 SIMULATION WITHOUT RECHARGE

The simulated water-level elevations without recharge after 12, 24 and 36 months, are shown in Figures 6.2, 6.3 and 6.4 respectively.

It is evident from these maps that with the exception of the production fields, the general configuration of the water-level distribution of the Atlantis aquifer has not been influenced to a large extent. However, as could be expected, this behaviour changed drastically near the production fields and drawdowns of up to 10 metres were observed after 36 months. This is clearly illustrated by the cones of depression that formed around the production fields. Contour maps depicting the cones of depression after 12, 24 and 36 months, are shown in Figures 6.5, 6.6 and 6.7 respectively. Of particular interest is the zero drawdown contour line between the Silwerstroom and Witzand production fields. If these abstraction rates are to be continued for a prolonged period of time, the two fields will certainly interfere. The change in distribution of the zero contour lines to the north of the Silwerstroom production field, also indicates that water of a lower quality (see section 4.9) will be drawn from this region towards the Silwerstroom production field.

One positive conclusion that can be derived from this simulation, is that although the water-levels decreased considerably in the immediate vicinity of the abstraction sites, a positive ground-water gradient is maintained towards

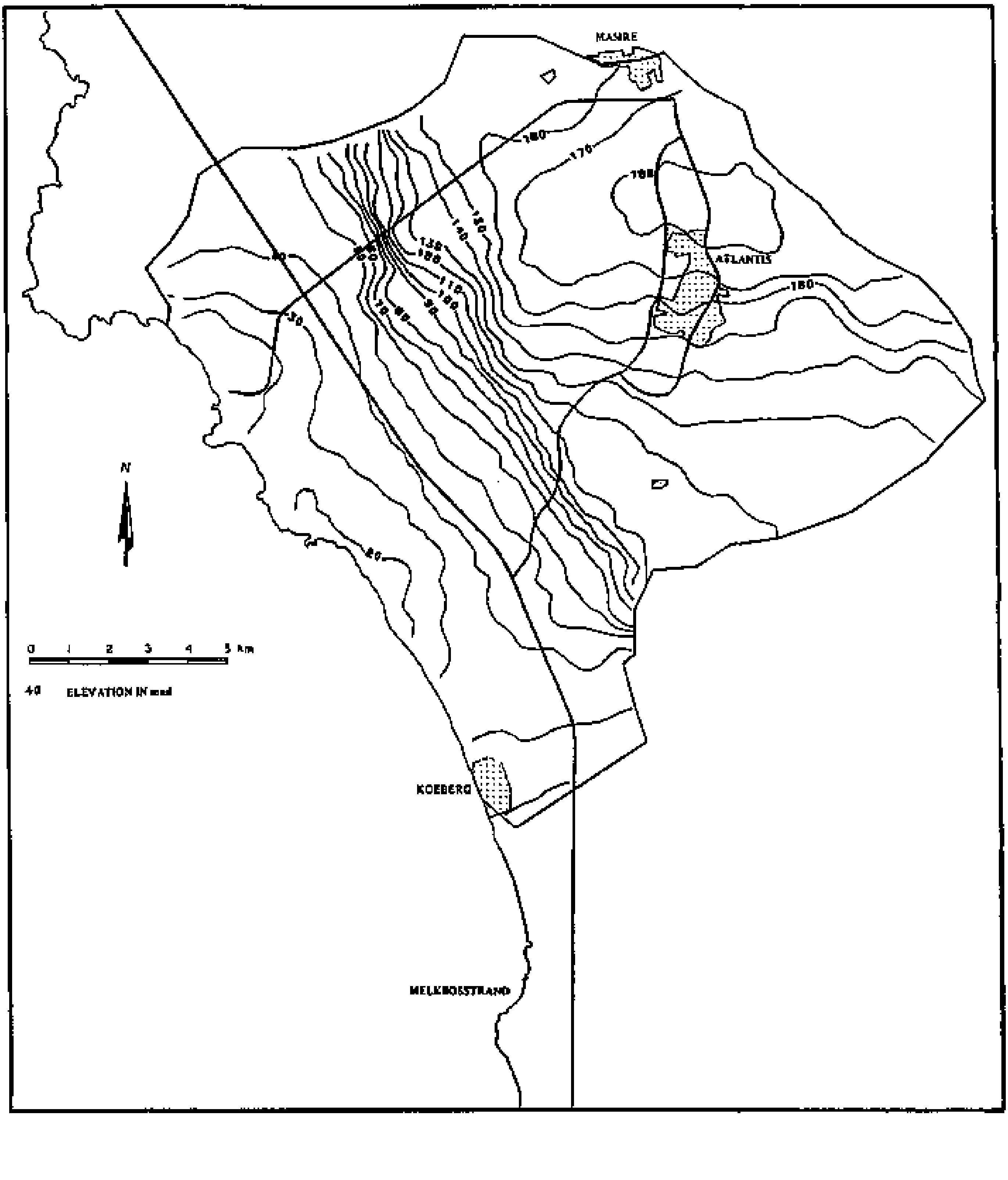

Figure 6.2. Simulated water-levels in the Atlantis aquifer after 12 months with an abstraction rate of 11,82 x 10^6 m^3 per annum.

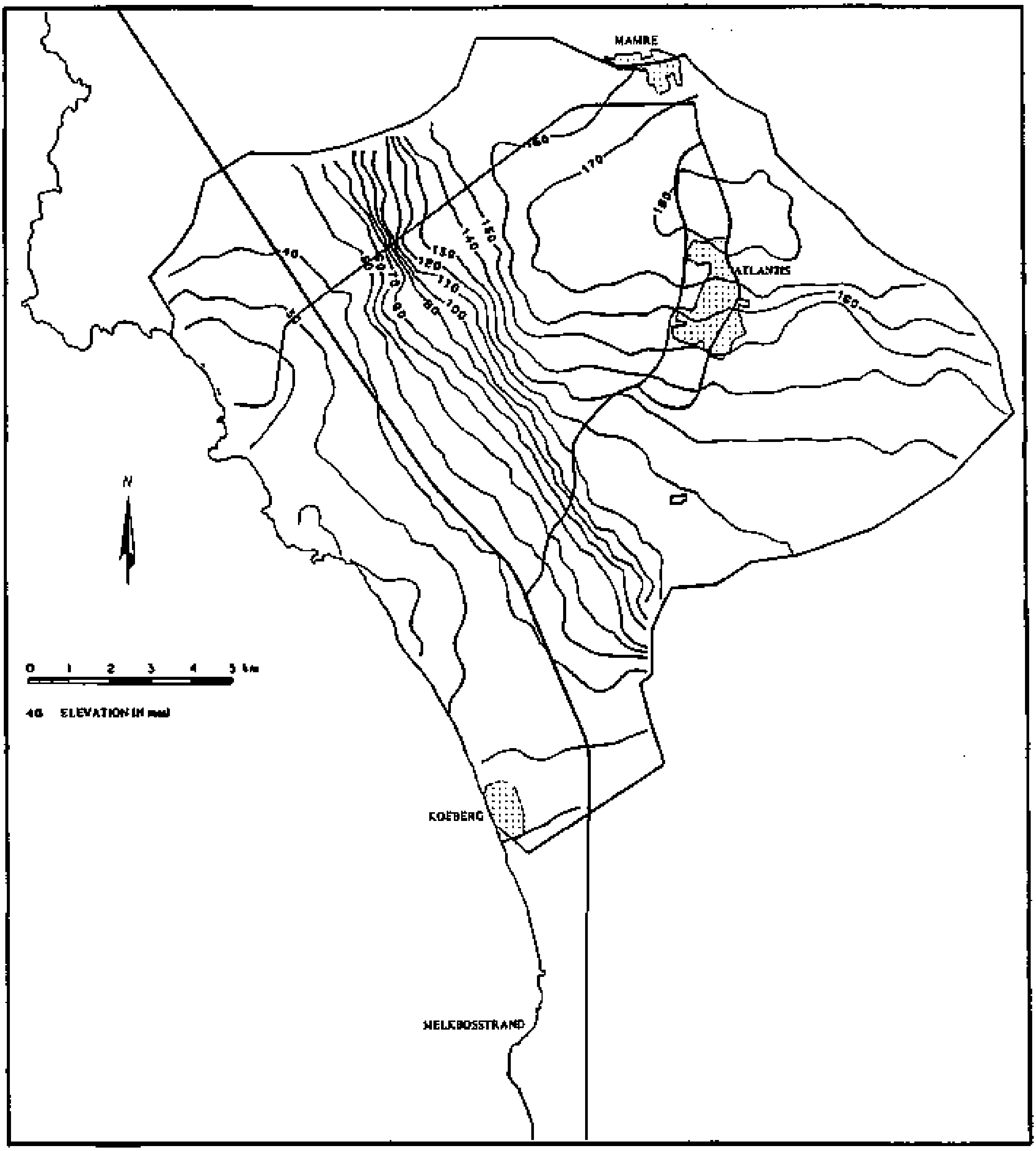

Figure 6.3. Simulated water-levels in the Atlantis aquifer after 24 months with an abstraction rate of 11,82 x 10^6 m^3 per annum.

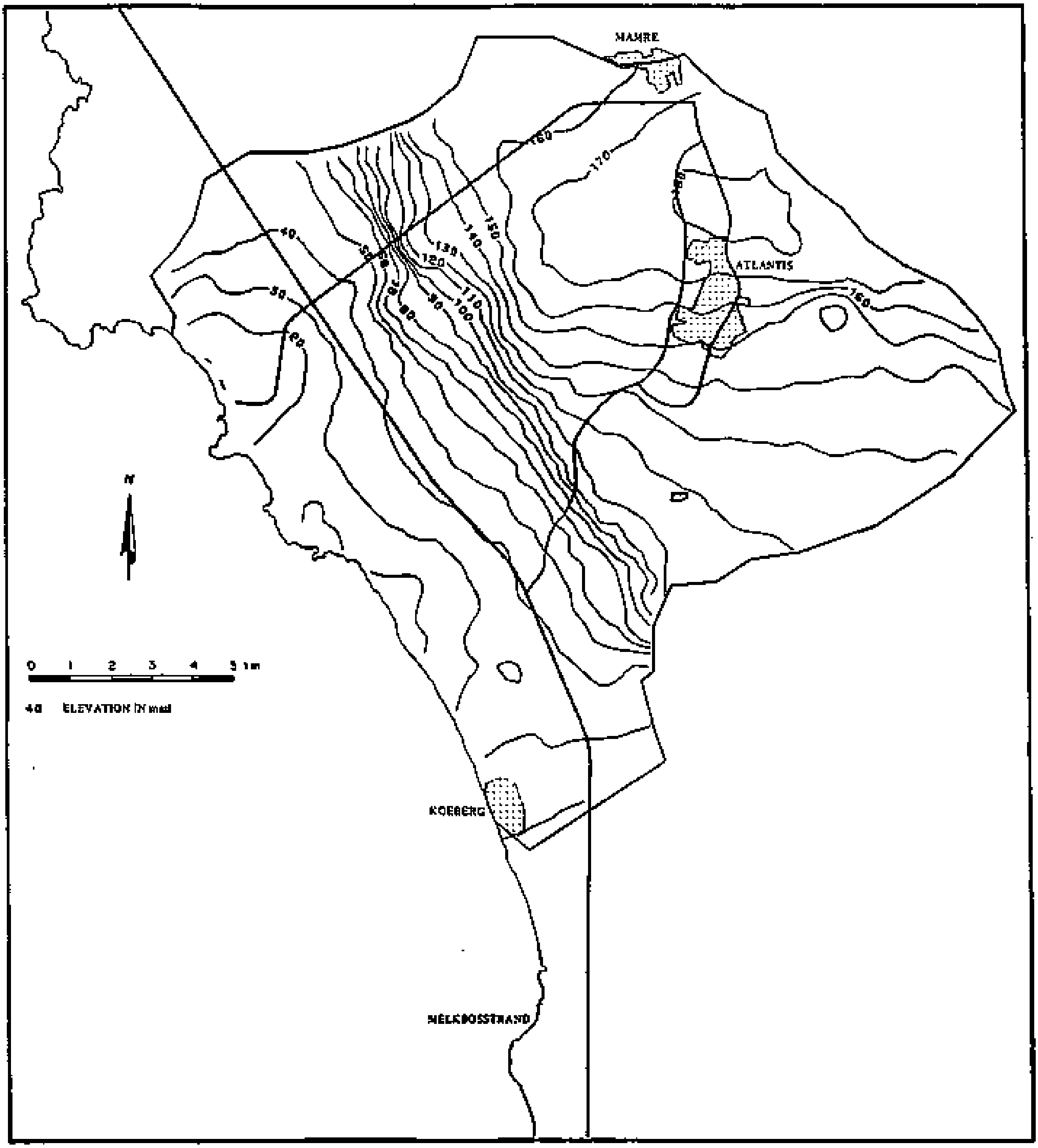

Figure 6.4. Simulated water-levels in the Atlantis aquifer after 36 months with an abstraction rate of 11,82 x 10^6 m^3 per annum.

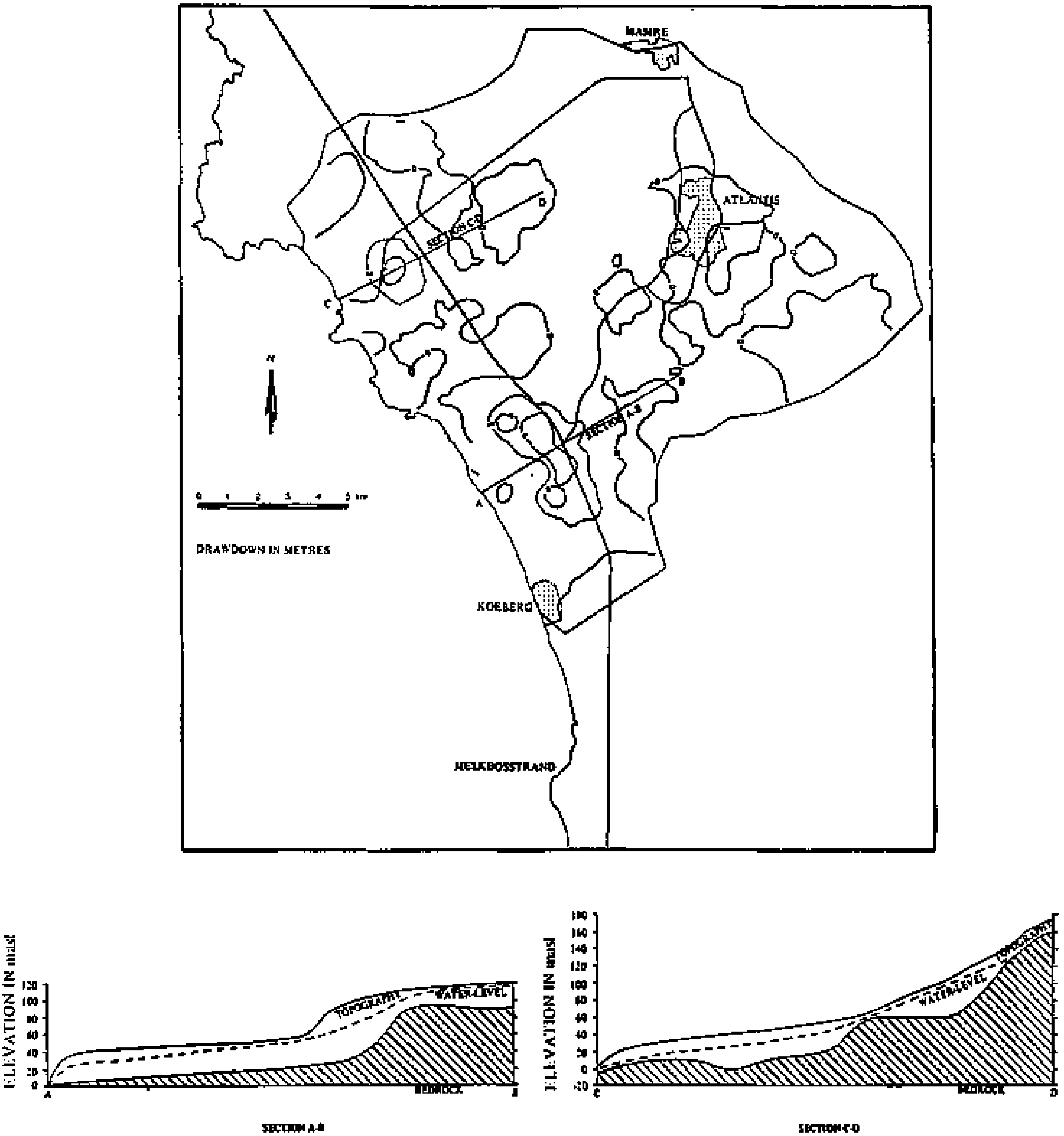

Figure 6.5. Drawdowns in the Atlantis aquifer after a period of 12 months, resulting from an abstraction rate of 11,82 x 10^6 m^3 per annum.

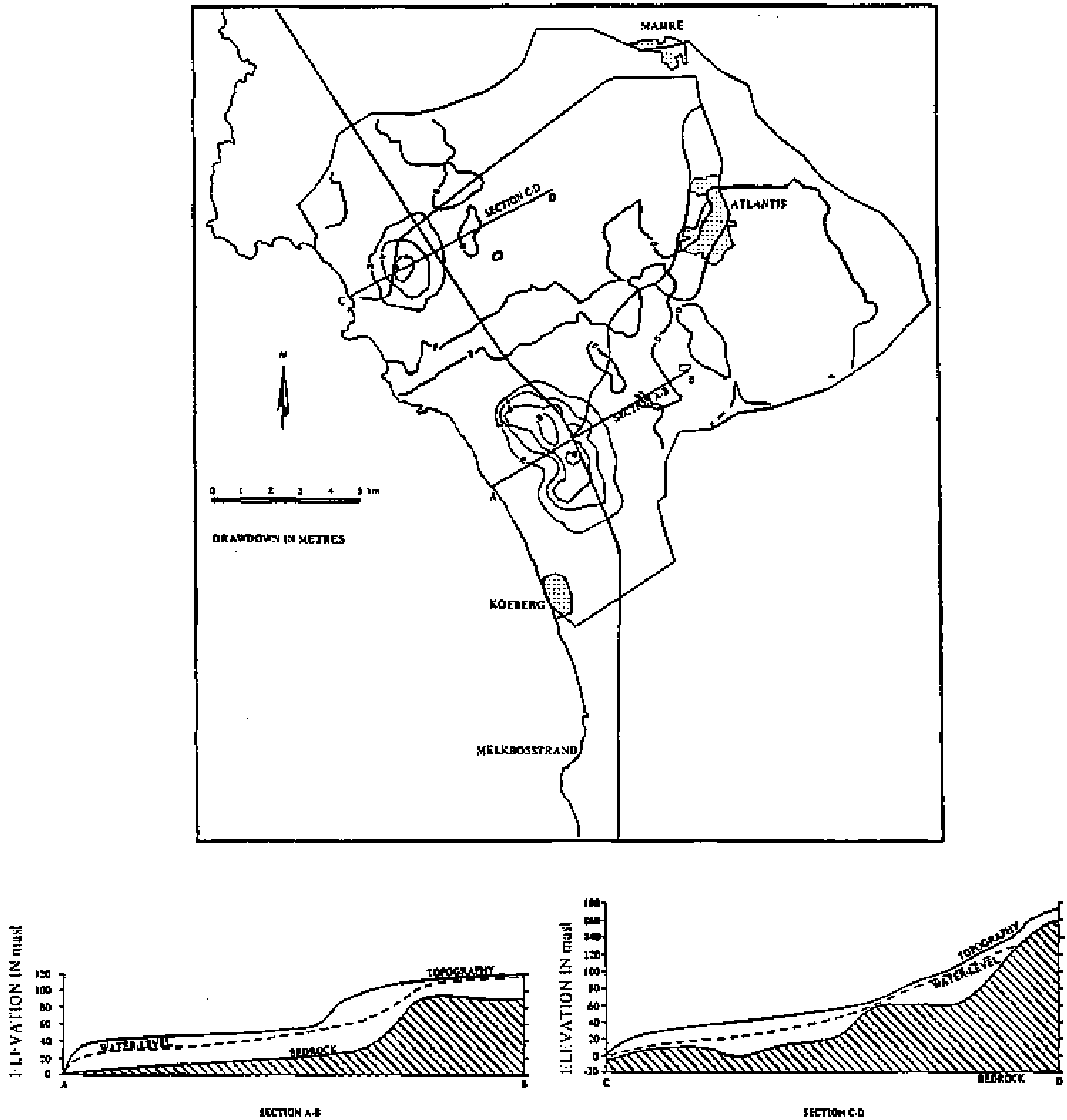

Figure 6.6. Drawdowns in the Atlantis aquifer after a period of 24 months, resulting from an abstraction rate of 11,82 x 10^6 m^3 per annum.

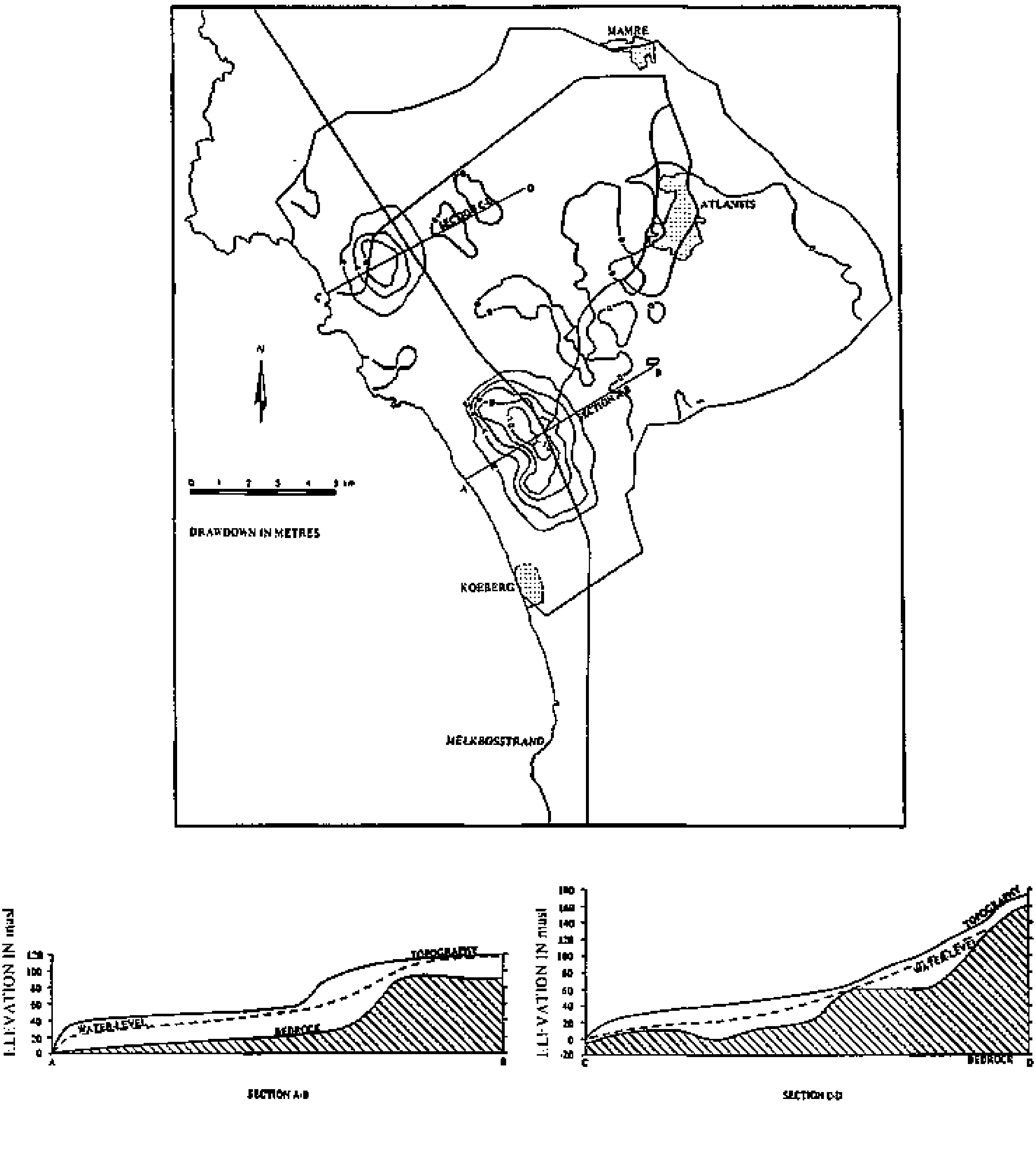

Figure 6.7. Drawdowns in the Atlantis aquifer after a period of 36 months, resulting from an abstraction rate of 11,82 x 10^6 m^3 per annum.

the sea. The possibility of sea-water intrusion thus does not seem to present any problems. A more detailed discussion regarding this aspect will be undertaken in the next chapter.

6.3.3 INFLUENCE OF RECHARGE ON THE PROPOSED ABSTRACTION SCHEME

Recharge can be incorporated into the present numerical model by specifying the rate of infiltration at each node of the finite element mesh. To obtain some idea of the recharge to the system, use was made of the calculations described in sections 4.7 and 4.8. As shown there, the total recharge for the period January 1979 - January 1980 is approximately 6 772 x 10^6 m^3 or 9,59 per cent of the annual rainfall for 1979. This volume of water was divided equally among the 403 nodes of the finite element mesh per unit time and the model ran again for a period of three years with the January 1979 water-levels as initial heads. The water-level distribution maps for the 12, 24 and 36 month periods are shown in Figures 6.8 - 6.10 and the drawdowns in Figures 6.11 - 6.13 respectively.

When comparing the maps in Figures 6.8 - 6.10 with those in Figures 6.2 - 6.4, little or no difference is notable. However, there is a substantial difference in drawdowns between the two simulations, especially in the case of the zero drawdown contour. Nevertheless, the problem areas delineated in the previous section still exist. The two production fields will still interfere and the size of their cones of depression remains almost unaltered.

To investigate the effect of recharge, in particular its rate, more thoroughly, another simulation was carried out assuming that the aquifer can be recharged by 30 per cent of the annual rainfall for 1979. Although the figure of 30 per cent may seem excessive, Bredenkamp and Vandoolaeghe (1982) claimed that in certain areas of the aquifer the figure may be as high as 35 per cent. The January 1979 water-levels were once again used as initial heads. The

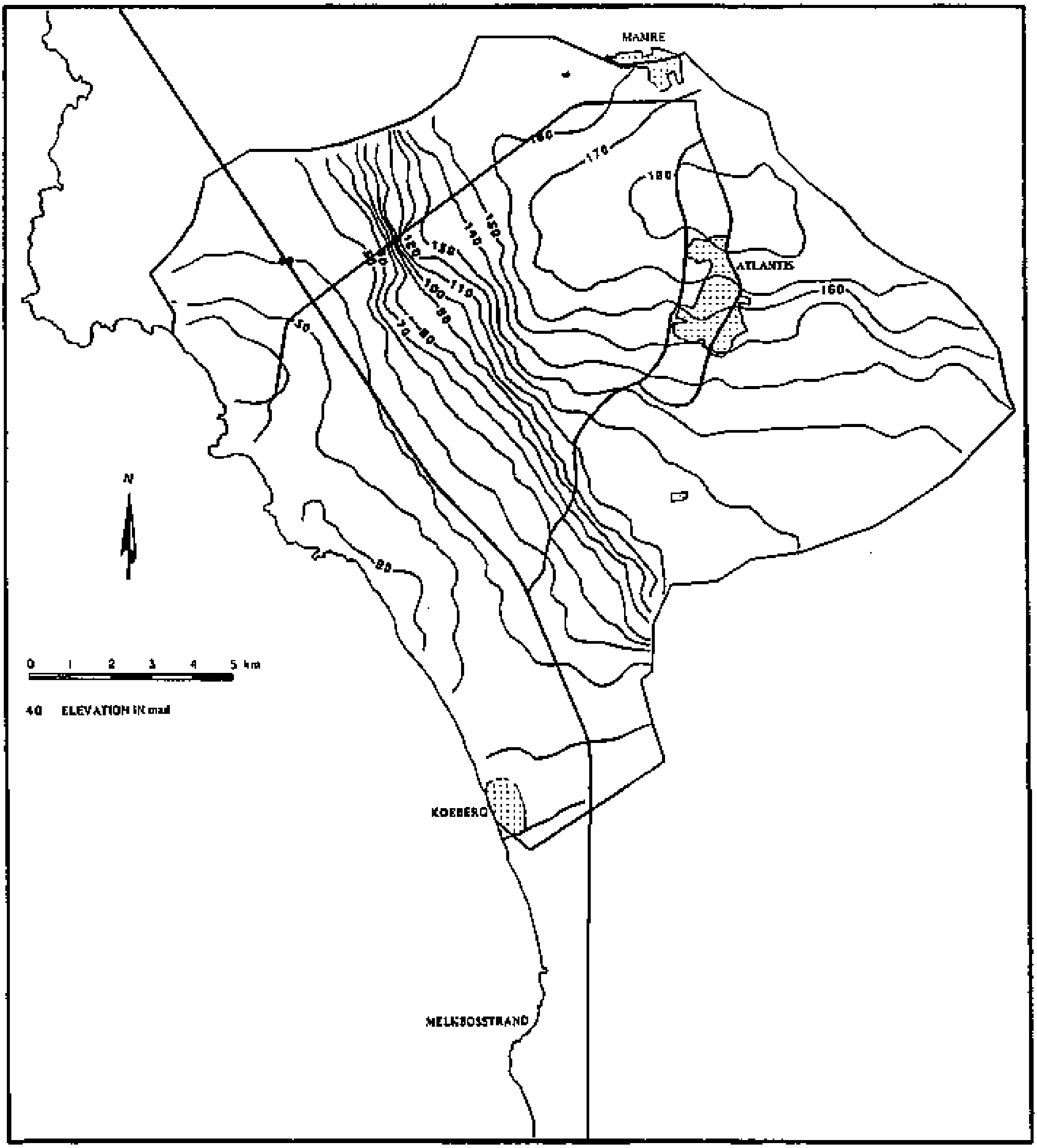

Figure 6.8. Simulated water-levels in the Atlantis aquifer after a period of 12 months, with an abstraction rate of 11,82 x 10^6 m^3 and a recharge rate of 6,772 x 10^6 m^3 per annum.

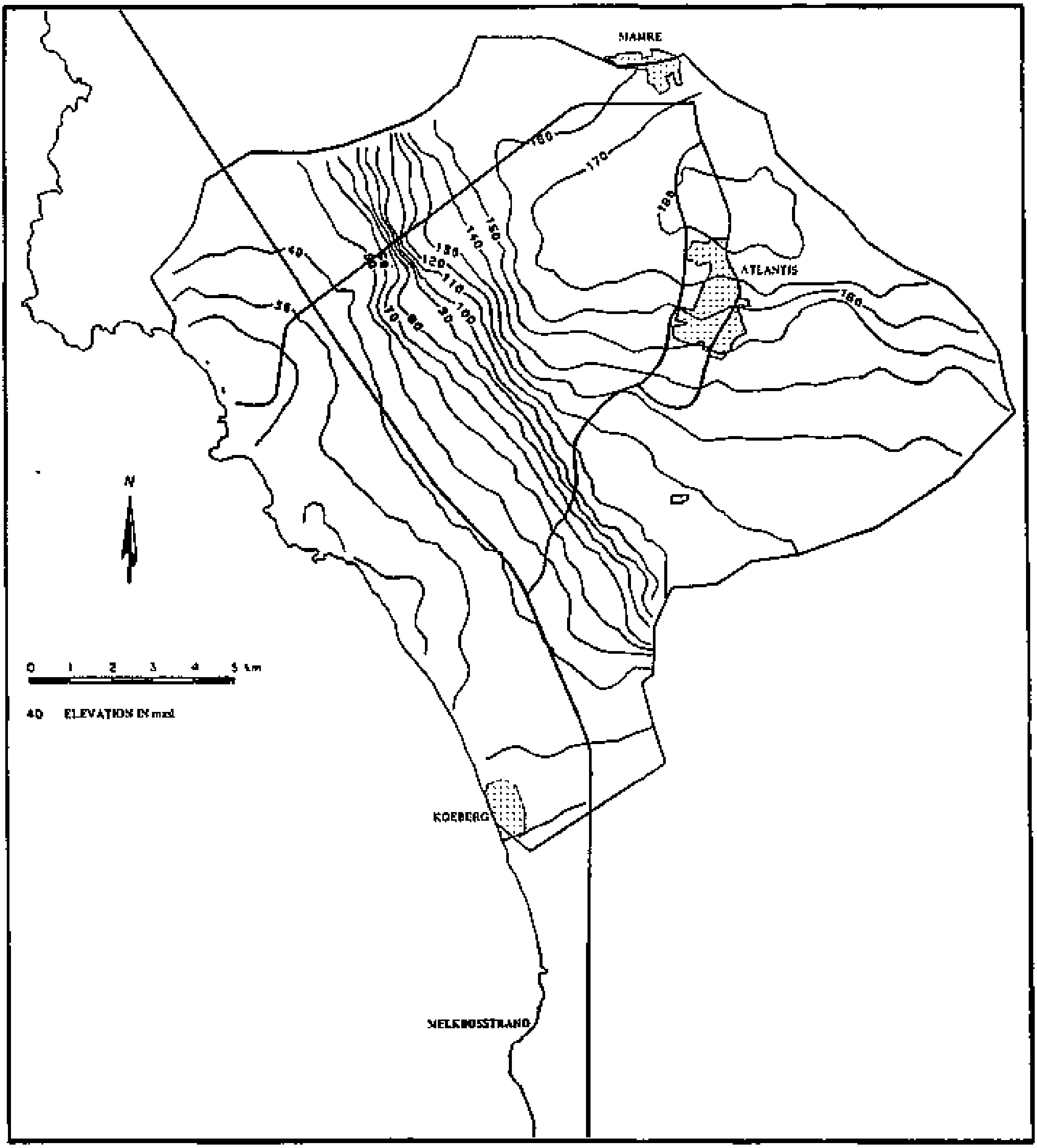

Figure 6.9. Simulated water-levels in the Atlantis aquifer after a period of 24 months, with an abstraction rate of 11,82 x 10^6 m^3 and a recharge rate of 6,772 x 10^6 m^3 per annum.

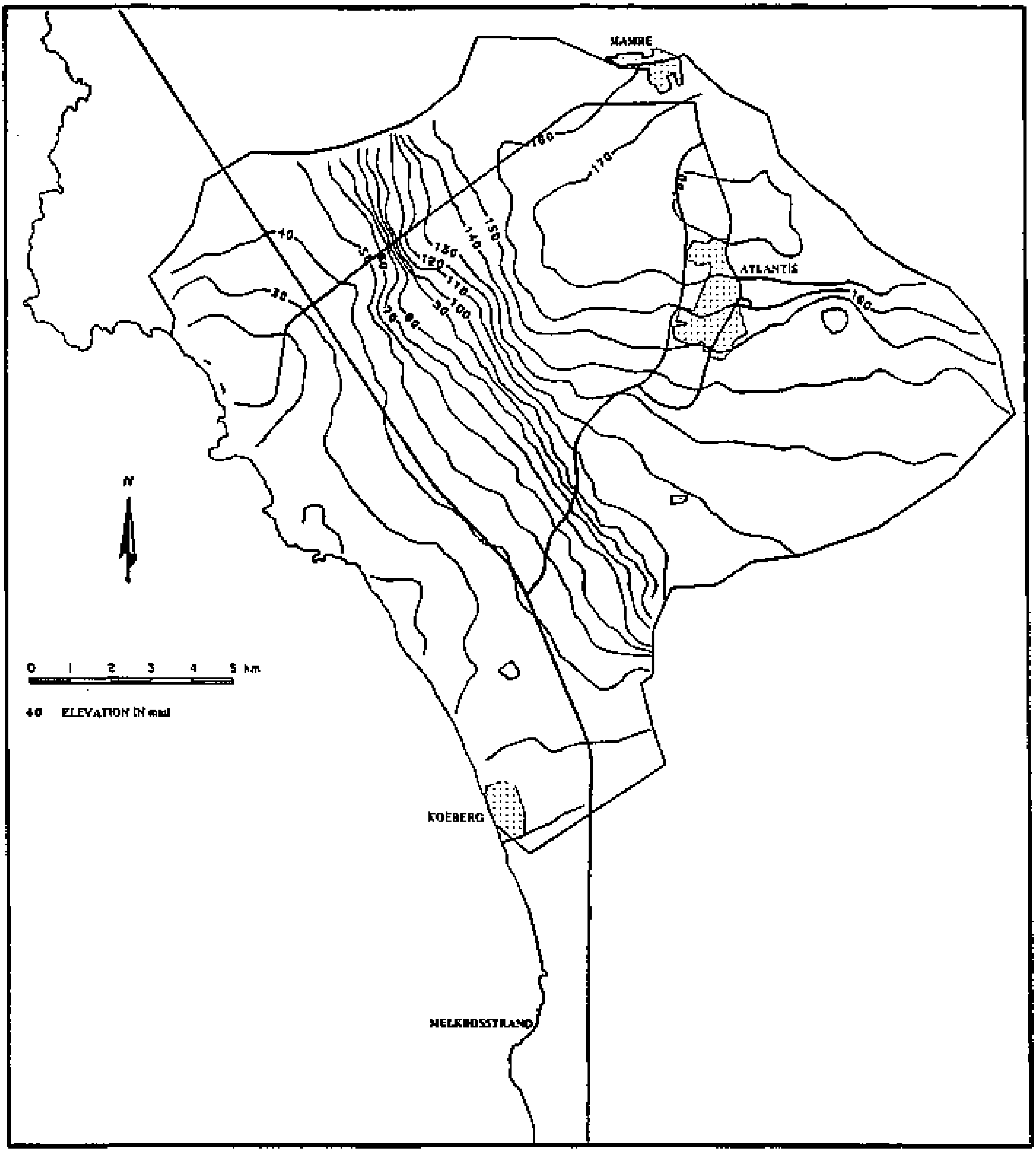

Figure 6.10. Simulated water-levels in the Atlantis aquifer after a period of 36 months, with an abstraction rate of 11,82 x 10^6 m^3 and a recharge rate of 6,772 x 10^6 m^3 per annum.

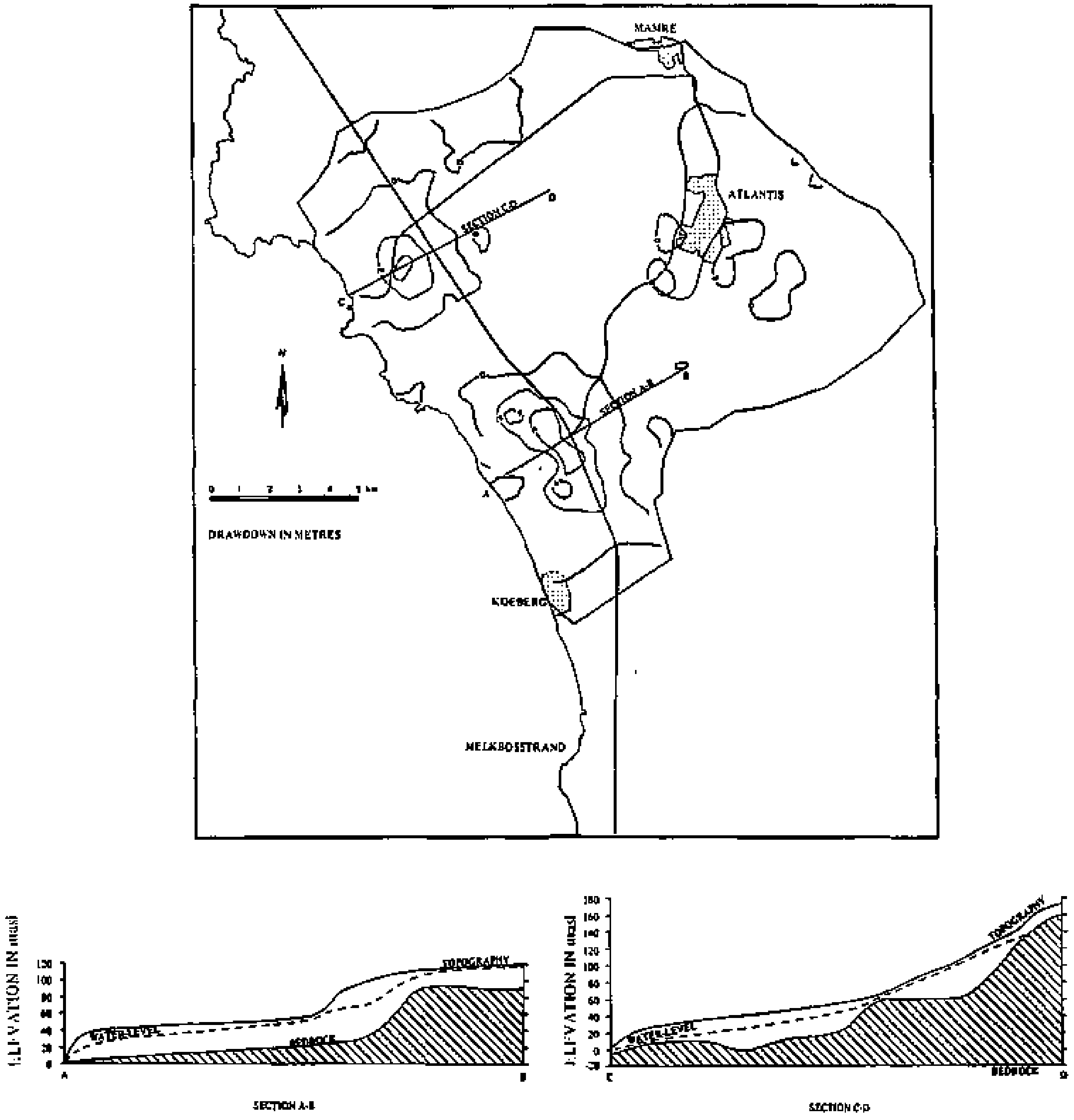

Figure 6.11. Drawdowns in the Atlantis aquifer after a period of 12 months, due to an abstraction rate of 11,82 x 10^6 m^3 and an infiltration rate of 6,772 x 10^6 m^3 per annum.

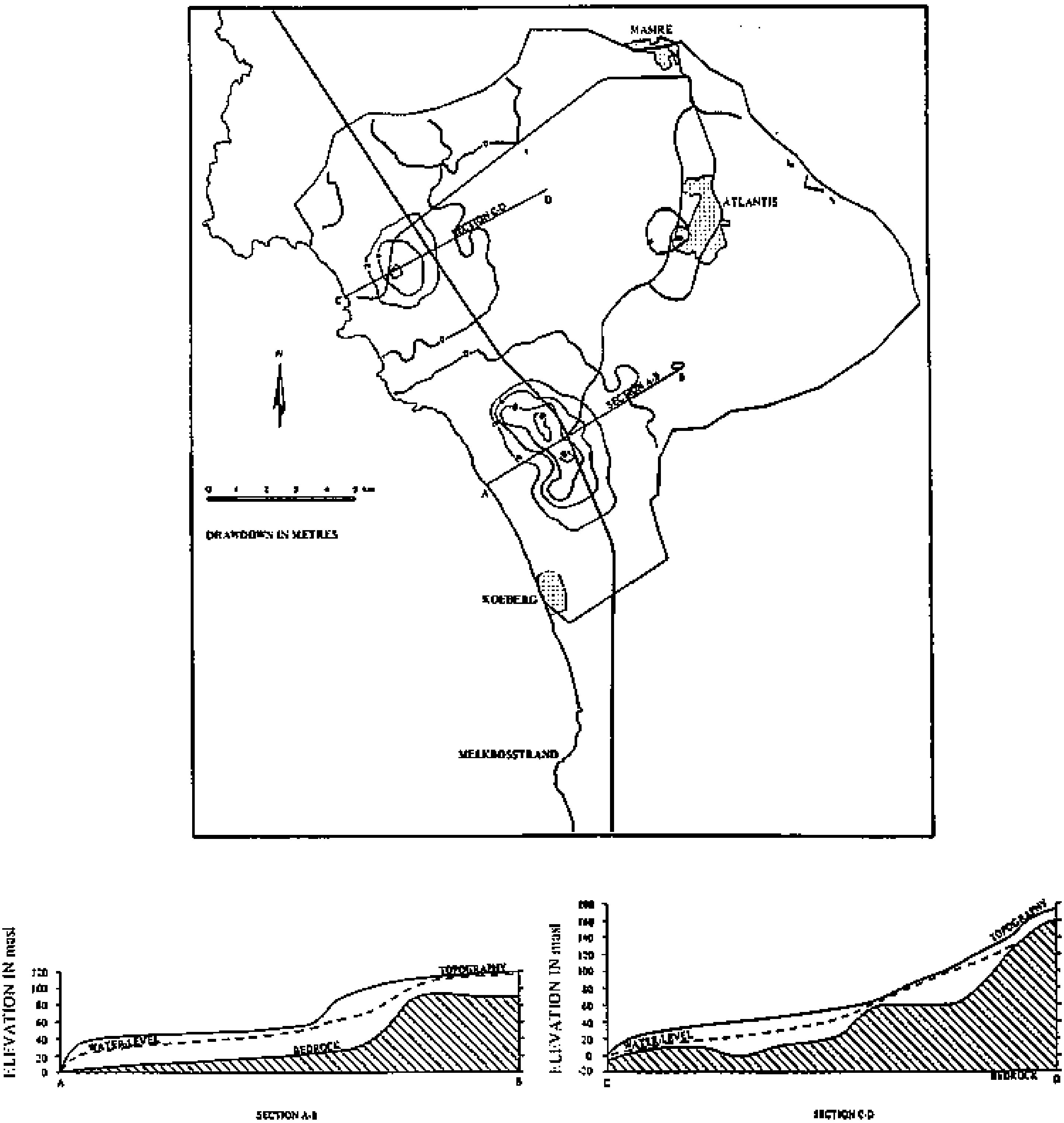

Figure 6.12. Drawdowns in the Atlantis aquifer after a period of 24 months, due to an abstraction rate of 11,82 x 10^6 m^3 and an infiltration rate of 6,772 x 10^6 m^3 per annum.

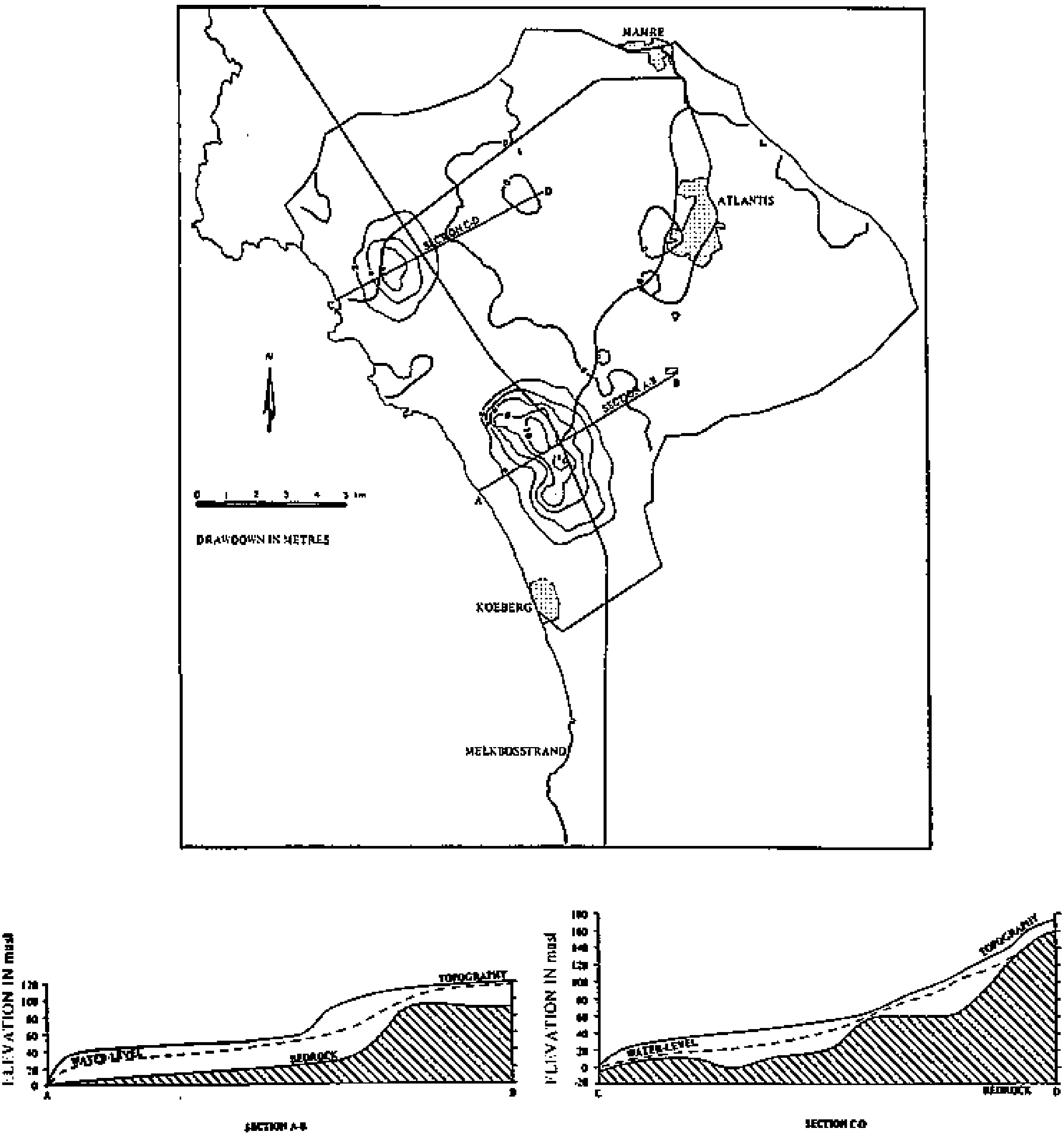

Figure 6.13. Drawdowns in the Atlantis aquifer after a period of 36 months, due to an abstraction rate of 11,82 x 10^6 m^3 and an infiltration rate of 6,772 x 10^6 m^3 per annum.

resulting drawdown cones after 12, 24 and 36 months are shown in Figures 6.14, 6.15 and 6.16 respectively.

As shown by a comparison of Figures 6.11 and 6.14, there is not much difference between the configuration of the cones of depression for the 12 month periods. The only real difference occurs in the Silwerstroom area where the drawdown of 4 metres, observed in Figure 6.11, is now absent. The Silwerstroom area can thus be regarded as the most susceptible to recharge.

After 24 months the influence of the 30 per cent recharge can also be seen in the Witzand area where the biggest drawdowns observed are 6 metres (Figure 6.15), compared to drawdowns of 8 metres observed in the previous simulation (Figure 6.12). The general form of the water-level contours is again not much altered. This also applies to the contours of the 36 month period (Figure 6.16). The higher recharge rate did not prevent the two production fields from interfering with each other.

6.4 CONCLUSION

The main conclusion to be reached from the simulations in section 6.3 is that the proposed additional abstraction of large volumes of ground water from the Silwerstroom and Witzand areas will tend to dewater the lower part of the Atlantis aquifer. Such a dewatering may have serious consequences for the Atlantis aquifer as a future reservoir of water. This is manifested not only in the interference, but perhaps more important is the effect that the dewatering may exercise on the ground-water gradient towards the sea. Reversing this gradient will have grave consequences, particularly in the Silwerstroom area, which as shown in section 4.8, is the most probable area where sea-water intrusion can occur.

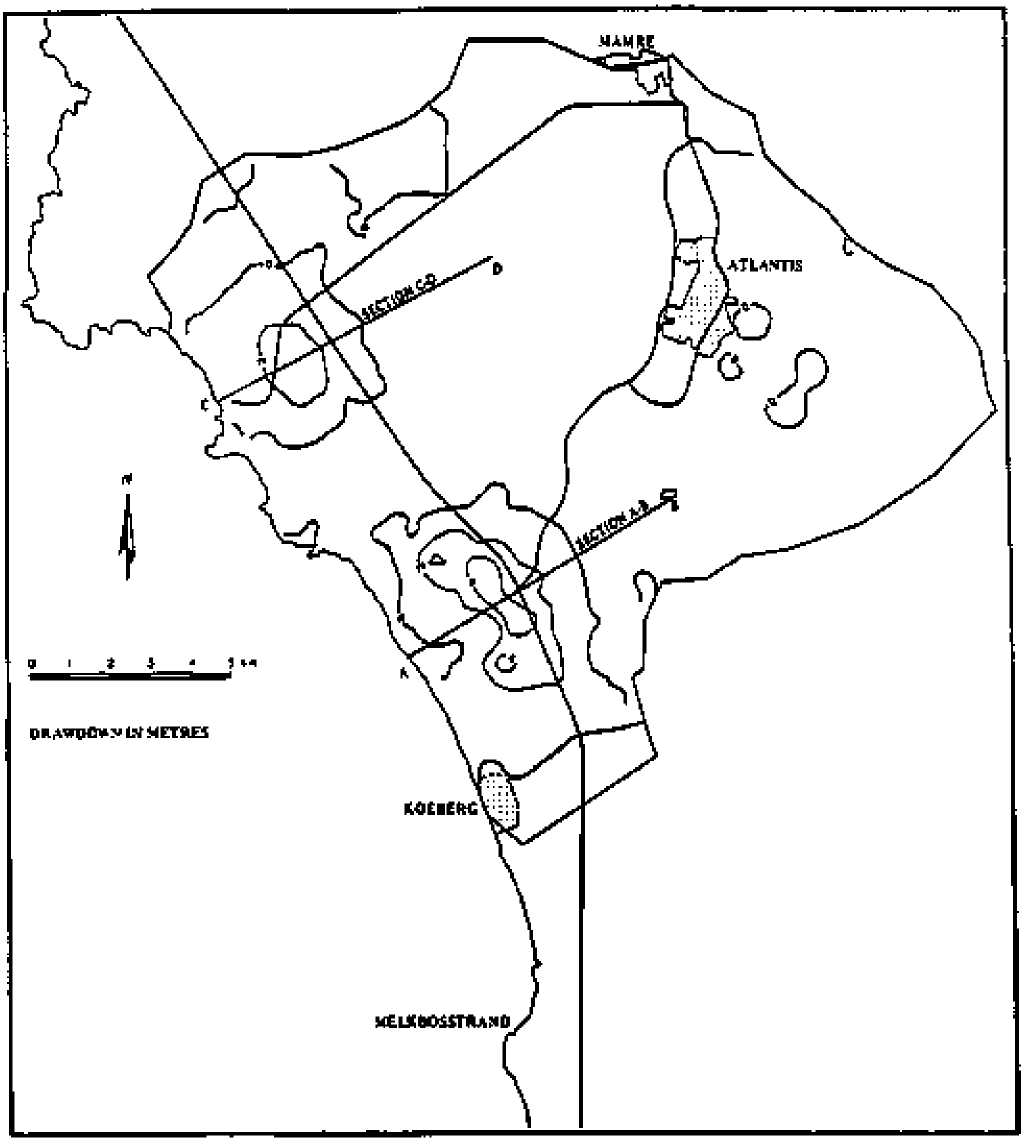

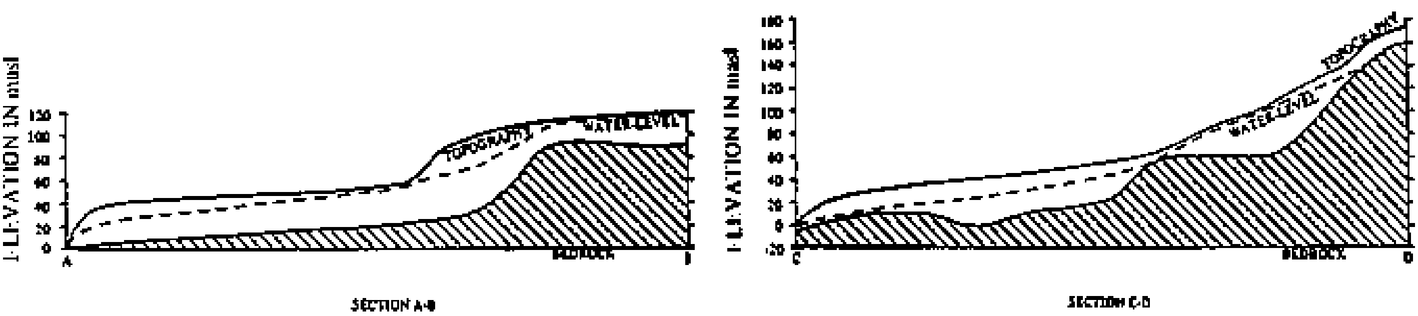

Figure 6.14. Drawdowns in the Atlantis aquifer after a period of 12 months, due to an abstraction rate of 11,82 x 10^6 m^3 and an infiltration rate of 21,185 x 10^6 m^3 per annum.

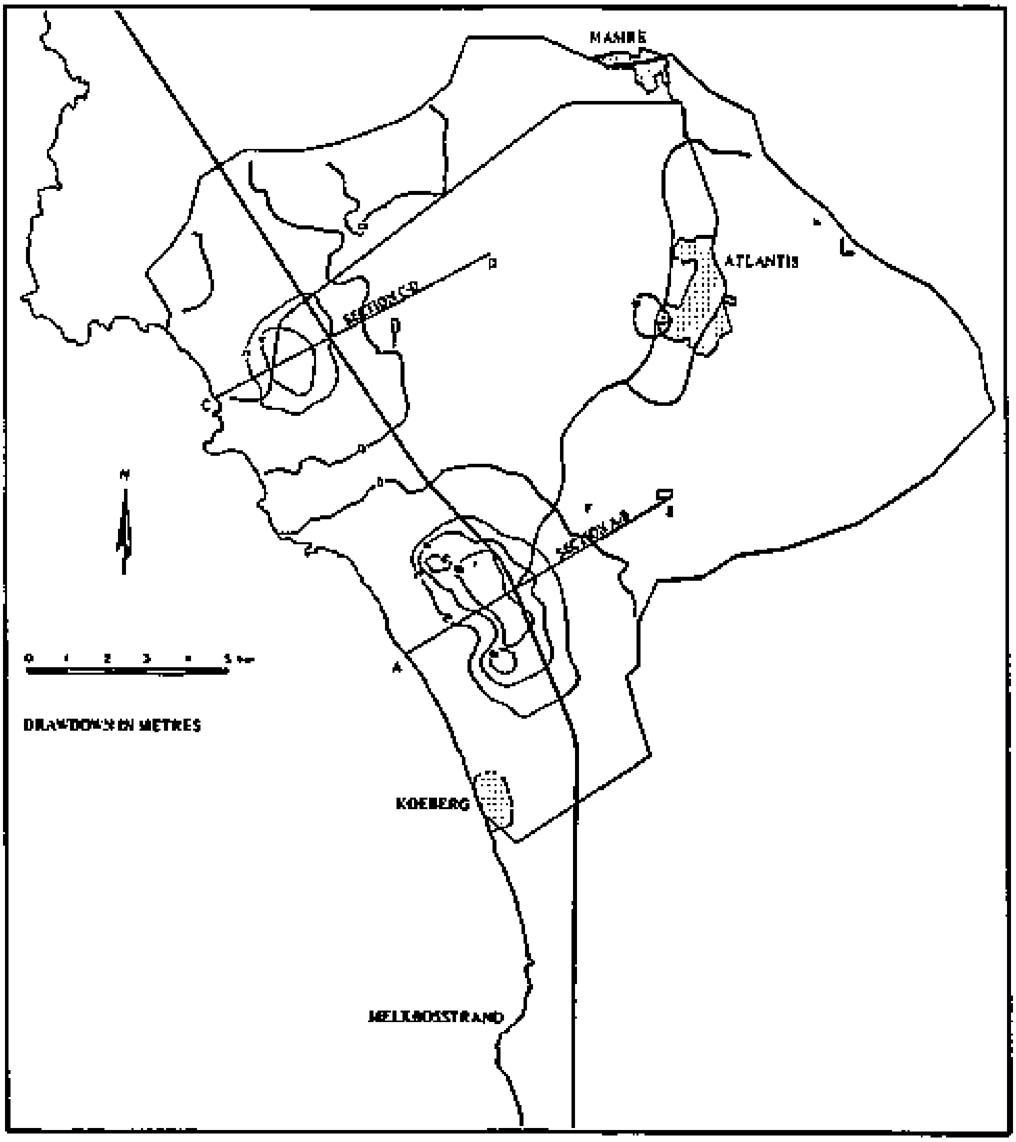

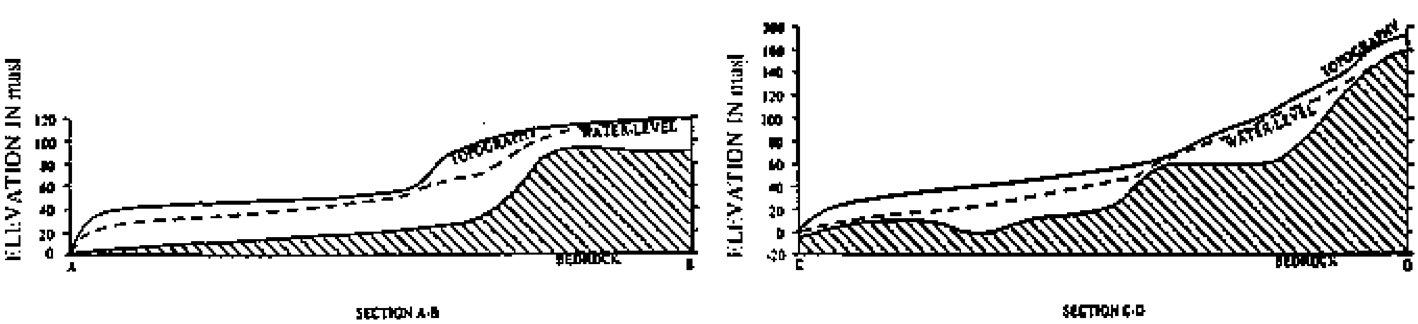

Figure 6.15. Drawdowns in the Atlantis aquifer after a period of 24 months, due to an abstraction rate of 11,82 x 10^6 m^3 and an infiltration rate of 21,185 x 10^6 m^3 per annum.

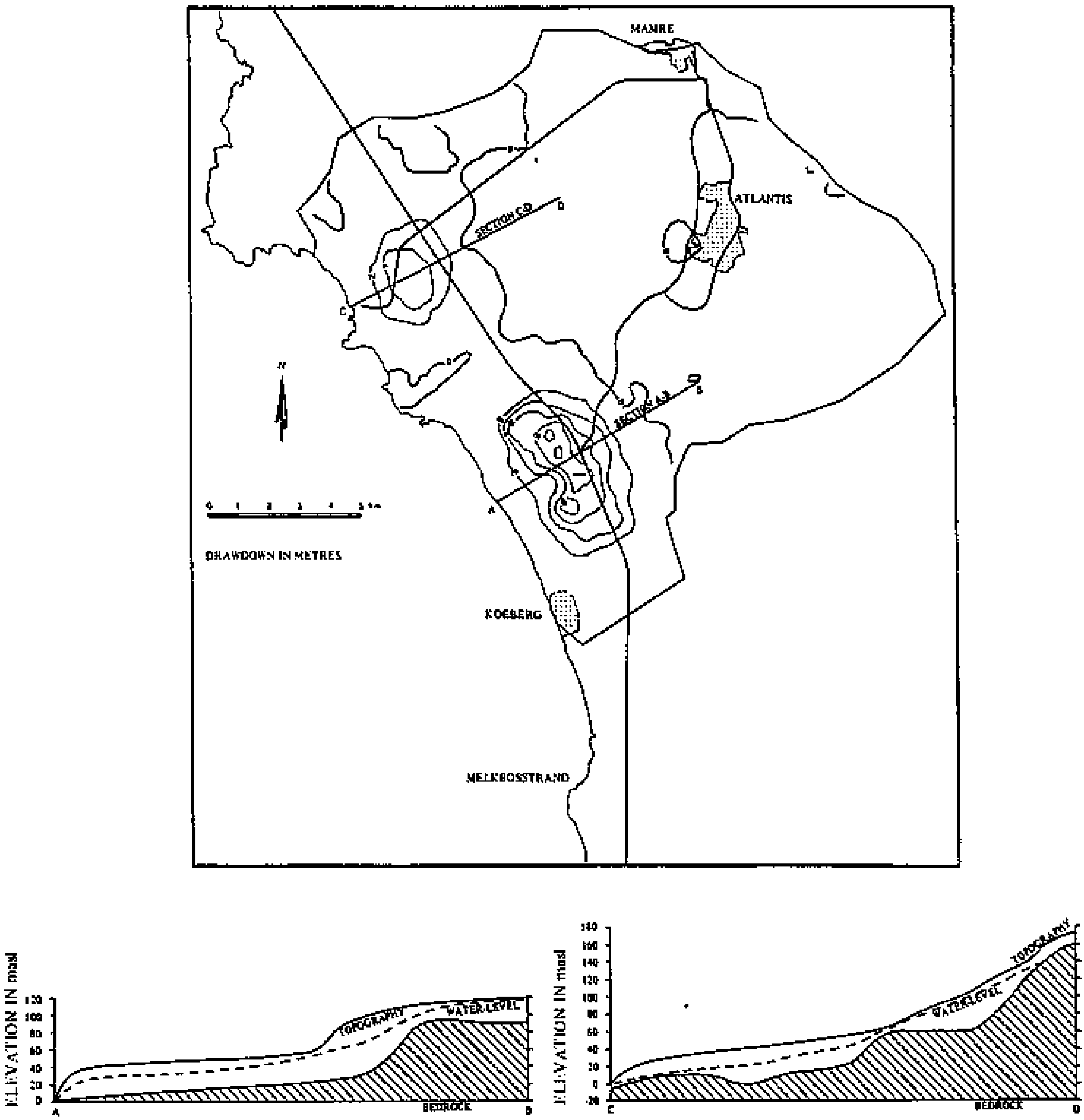

Figure 6.16. Drawdowns in the Atlantis aquifer after a period of 35 months, due to an abstraction rate of 11,82 x 10^6 m^3 and an infiltration rate of 21,185 x 10^6 m^3 per annum.

To prevent intrusion of sea-water in the Silwerstroom area, one of two approaches or a combination of both can be used. The first is to establish new production fields away and more inland from both the Silwerstroom and Witzand fields. The other is to conduct a detailed study of infiltration in the area with particular emphasis on the possibility of recharging the aquifer by injecting partially purified sewage water along the coast-line.

CHAPTER 7

MODELLING SEA-WATER INTRUSION

7.1 GENERAL

The phenomenon of sea-water intrusion, although widely studied in countries abroad, has until recently, not received much attention in South Africa. This can be ascribed to the fact that until the mid 1970's, exploitation of coastal aquifers in South Africa was limited to local abstraction of relative small quantities of ground water from individual boreholes. It was only in the second half of 1970 that the importance of coastal aquifers such as the Cape Flats aquifer and the Atlantis aquifer came to light.

If the assumptions in section 4.8 are correct, the only area of significance where sea-water intrusion may be a problem in the Atlantis aquifer, is in the vicinity of the Silwerstroom spring (see Figure 4.20). The discussion to follow will consequently be restricted to this particular area.

There are two methods that can be utilized to study the possible intrusion of sea-water:

(a) the analytical method and
(b) the numerical method.

The phenomenon of sea-water intrusion is so complicated (Bear, 1970) that a number of simplifying assumptions have to be made in order to derive an analytical approximation. Two of the more serious of these are:

(i) that the ground water at the sea/fresh water interface boundary is at a constant potential, contrary to the fact that it is actually a dynamic system, and

(ii) that there exists an abrupt interface between the sea- and fresh water, while in reality there always exists a transition zone of varying density, separating the two zones.

As these assumptions exclude some of the most important physical features of the real system, it was decided to opt for the numerical approach to analyse the possibility of sea-water intrusion in the Atlantis aquifer.

7.2 NUMERICAL SIMULATION OF SEA-WATER INTRUSION

In view of the complexity of the phenomenon and the lack of suitable data, it was decided to restrict the present investigation to a two-dimensional vertical model, based on the alternating direction collocation approximation (ADC) proposed by Botha and Celia (1981). The computer code was developed by Michael Celia from Princeton University during a short tenure at the Institute for Ground-water Studies in 1982. A complete description of the model can be found in Celia (1984) and, except for a brief summary, will not be repeated here.

The basis of the model is (Celia, 1984; Bear, 1979) the equation of mass conservation which can be expressed in the case of the fluid as

$$D_t(\varepsilon\rho) + \underline{\nabla}\cdot(\varepsilon\rho\underline{v}) = 0 \qquad (7.1)$$

$$\underline{q} = \varepsilon\underline{v} = -\underline{\underline{k}}/\mu\,(\underline{\nabla}p - \rho\underline{g}) \qquad (7.2)$$

and for the solute (salt) as

$$D_t(\varepsilon c) + \underline{\nabla}\cdot(\varepsilon c\underline{v}) - \underline{\nabla}\cdot\underline{J}_s = 0 \qquad (7.3)$$

where

ε	=	void fraction (L^3/L^3)
ρ	=	fluid density (m/L^3)
$\underline{v}$	=	fluid (pore) velocity (L/T)
c	=	concentration of salt (m/L^3)
$\underline{J}_s$	=	diffusive/dispersive flux vector (m/L^2T)
$\underline{\underline{k}}$	=	intrinsic permeability tensor (L^2)
μ	=	dynamic viscosity (m/LT)
p	=	fluid pressure (m/LT^2)
$\underline{g}$	=	acceleration due to gravity (L/T^2)
$\underline{q}$	=	Darcy velocity (specific discharge) (L/T)

By augmenting these equations with appropriate constitutive equations of state such as

$$\rho = \rho(c) = \rho_0 + ac \qquad (7.4)$$

and

$$\underline{J}_s = \varepsilon \underline{\underline{D}} \cdot \underline{\nabla} c \qquad (7.5)$$

where

ρ_0	=	density of zero concentration
a	=	constant
$\underline{\underline{D}}$	=	hydrodynamic dispersion tensor

the final equations utilized in the numerical model can be obtained. They are

$$\rho S_{0p} D_t p + \epsilon D_c \rho D_t c - \underline{\nabla} \cdot [\rho (\underline{\underline{k}}/\mu) \cdot (\underline{\nabla} p - \rho \underline{g})] = 0 \qquad (7.6)$$

$$D_t c + \underline{\nabla} \cdot (c\underline{v}) - \underline{\nabla} \cdot \underline{\underline{D}} \cdot \underline{\nabla} c = 0 \qquad (7.7)$$

$$\rho = \rho_0 + ac \qquad (7.8)$$

Equations (7.6) - (7.8) are solvable only when proper initial and boundary conditions are also given. For initial conditions the initial state of the physical system is used. The only restriction placed on the initial conditions is that they must, in fact, be solutions to the governing equations.

Typical boundary conditions are shown in Figure 7.1. The following should be noted.

(i) The conditions of no flow across the confining layers are time-varying boundary conditions in that $\rho = \rho(c) = \rho(c(t))$. Thus the conditions must be updated as the solution proceeds.

(ii) At the opening to the sea, it is assumed that the dispersion in the porous medium is much greater than the diffusion in the sea, implying that $D_n c = 0$. This follows from equating mass fluxes on either side of the boundary (Botha and Celia, 1981).

(iii) For water-table conditions, no provision is made to accommodate a moving boundary, nor for any but the simplest approximation ($D_y p = - \rho g$) to the non-linear boundary conditions. A constant (in time) pressure could also be input at this boundary.

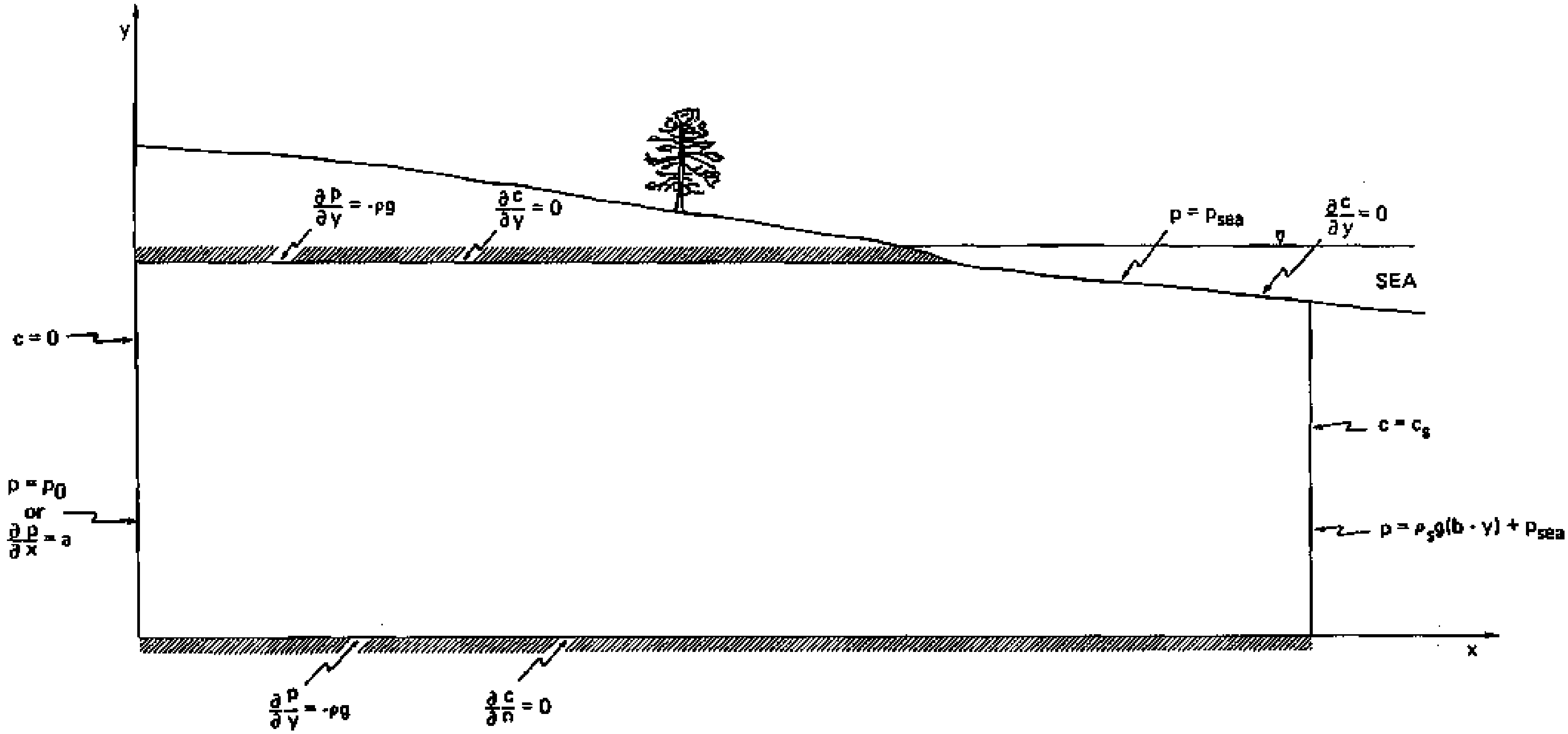

Figure 7.1. *Typical boundary conditions. (p_0 and a are constants. $\partial p/\partial y = -\rho g$ is implied from $q_n = 0$ and b is the thickness of the aquifer).*

7.3 APPLICATION OF THE MODEL

A difficulty frequently encountered in using a two-dimensional vertical model, is the incorporation of production boreholes (Celia, 1984). It was, therefore, decided to try to avoid the necessity of implementing a production borehole by locating a point in the aquifer between the Silwerstroom production field and the coast-line, where the pressure of the ground-water system is relatively stable, regardless of the abstraction of ground water from the Silwerstroom production field. As no evidence could be found in the data available that the abstraction of water from the Silwerstroom production field adversely influenced the flow of the Silwerstroom spring, it was decided to select the spring as landward boundary for the profile to be modelled. This has the further advantage that one can use a constant head boundary condition at the Silwerstroom spring. The seaward boundary selected, consisted of a point 1 000 metres from the coast-line, on the line from the spring that intersects the coast-line perpendicularly. The location of this profile line is shown in Figure 7.2.

The main reason for continuing the profile line 1 000 metres into the sea, is mainly for computational reasons. The high ground-water gradients prevalent in the area, may lead to computational complexity if the seaward boundary is chosen too close to the coast-line.

Another limitation of the present numerical model is the fact that a constant aquifer thickness has to be specified along the entire profile line. This posed a problem in that the aquifer thickness in the vicinity of the Silwerstroom spring is believed to be 18 metres, while only 5 metres at the coast-line. However, it is known (Van Tonder and Botha, 1983) that the danger of seawater intrusion is proportional to the thickness of the aquifer. The assumption of a thickness of 18 metres (the maximum thickness to be encountered in this part of the aquifer) will thus ensure an over-estimate for the distance of intrusion.

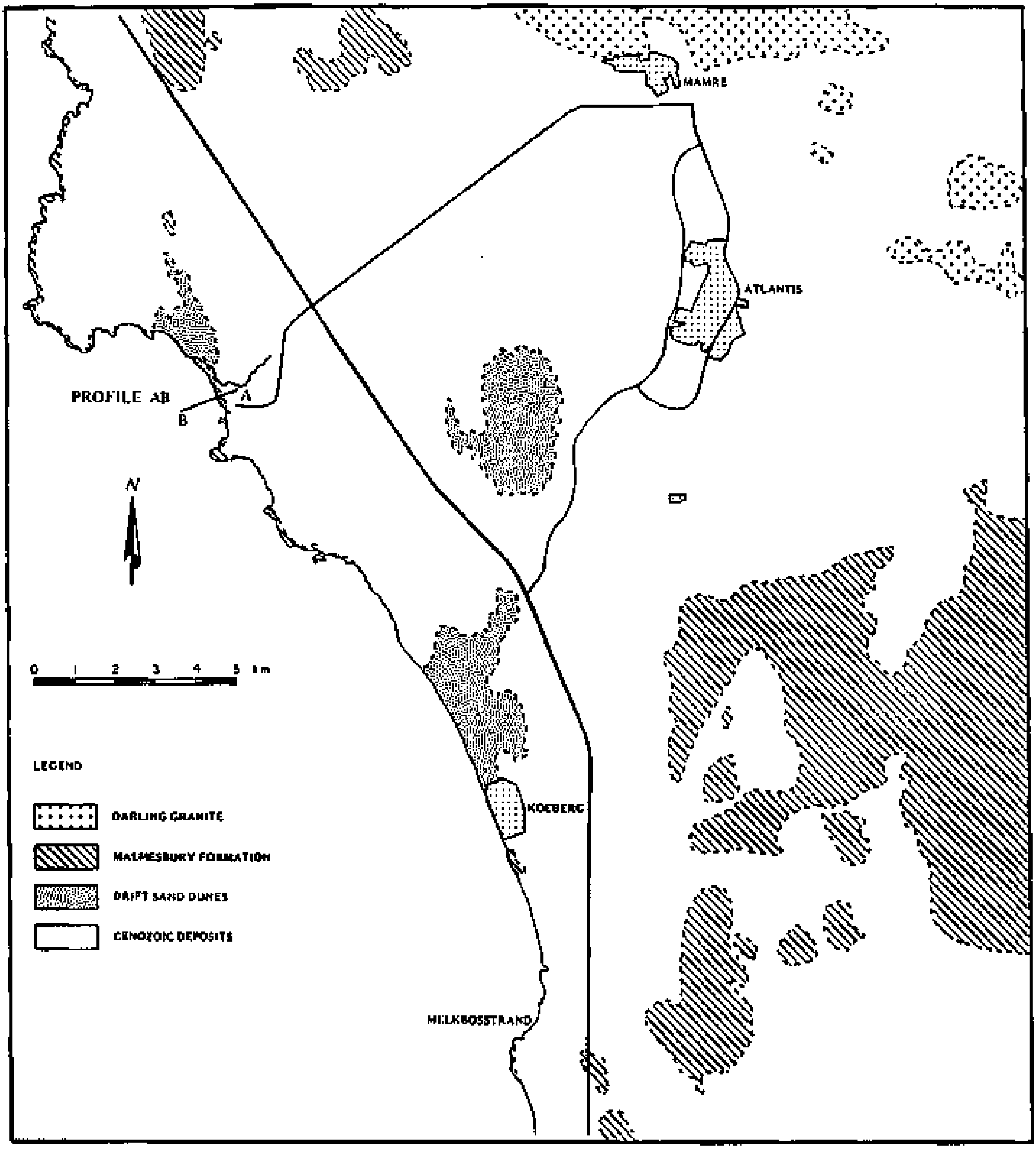

Figure 7.2. Location of profile line AB along which the behaviour of the fresh/sea interface is to be modelled.

The final finite element mesh constructed along the profile line AB, as well as the boundary and initial conditions specified, are shown in Figure 7.3. Since the present position of the sea/fresh water interface is not known, it was decided to represent this as a vertical line on the coast. Although this approach may not be quite correct, it is not expected to have any serious effects on the final results, unless the interface already lies inland. This, however, does not seem to be the case in this instance.

The rest of the parameters used in the model, for example the ground-water gradient and the hydraulic parameters, were chosen so as to agree with those obtained from the calibrated horizontal flow model (section 5.4) and those used in the calculations of the fresh water flux to the sea (section 4.8).

7.4 SEA-WATER INTRUSION SIMULATIONS

Three simulations were carried out to investigate the phenomenon of sea-water intrusion in the Atlantis aquifer. In the first simulation the emphasis was more to get a feeling for the behaviour of the system, rather than to see how it would behave under various stresses. This simulation was consequently conducted with the water-levels observed for January 1979 as initial conditions. The fact that the Silwerstroom spring is still flowing, indicates that there exists a positive head at the spring. A combination of this information with that obtained from the horizontal flow model and the known topographical elevation of the spring, indicates that there should exist a constant head value of 13 metres near the spring. This value was consequently used as boundary value on the landward side of the cross section. On the seaward side a value of zero metres at the coast was used and extrapolated linearly seawards.

Since no information is available on the present position of the sea/fresh water interface, it was decided to use an initial salt distribution with a sharp interface at the coast, i.e. fresh water landwards and salt water seawards.

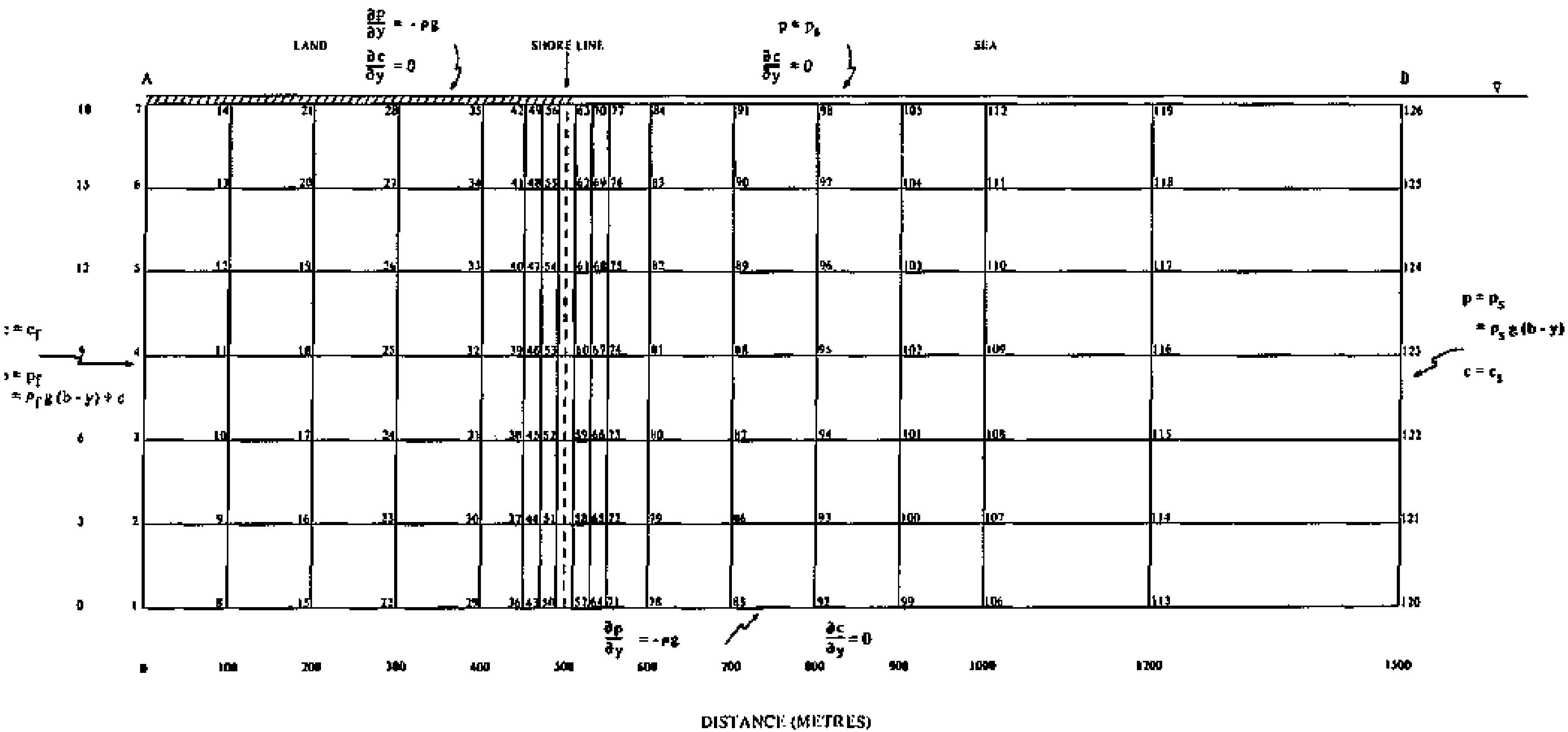

Figure 7.3. Rectangular finite element mesh used for the simulation of the fresh/sea interface. Boundary and initial conditions are also stated.

The second simulation was carried out to see what effect the increased proposed pumping rates may have on the contamination of the aquifer by sea-water. The same initial and boundary conditions as in the first simulation were consequently used, except that the constant head at the spring was (once again in agreement with the horizontal model) now assumed to be only 10 metres.

The third and final simulation was carried out just to show what can happen if the water-level at the Silwerstroom spring is lowered to sea-level.

7.5 DISCUSSION OF THE RESULTS

The phenomenon of sea-water intrusion in a coastal aquifer can best be illustrated by the movement of the various isochlors, i.e. lines of constant salt concentration expressed in such a way that an isochlor of 1 corresponds with sea-water, taken here as water with a total dissolved salt concentration of 35 000 mg/l. In principle, it is thus possible to find isochlors ranging between 0 (fresh water) and 1 in such an aquifer. However, for practical reasons attention is usually paid only to isochlors ranging between 0,01 and 0,9. This procedure will also be followed in the discussion to follow.

The movement of the 0,01; 0,02; 0,1; 0,25; 0,5; 0,75 and 0,9 isochlors observed for simulation 1 over a two-year period at 90 day intervals, is shown graphically in Figures 7.4 - 7.10. It is quite clear that the general behaviour of all the isochlors is more or less the same. There is a rapid movement seawards during the first 90 days, after which they stabilized. This rapid movement during the first 90 days must, however, be ascribed to the initial values used for concentration and not as a physical reality. What is important, is that the isochlors stabilized. This indicates that sea-water intrusion does not present a serious problem as long as the conditions assumed in the model prevail.

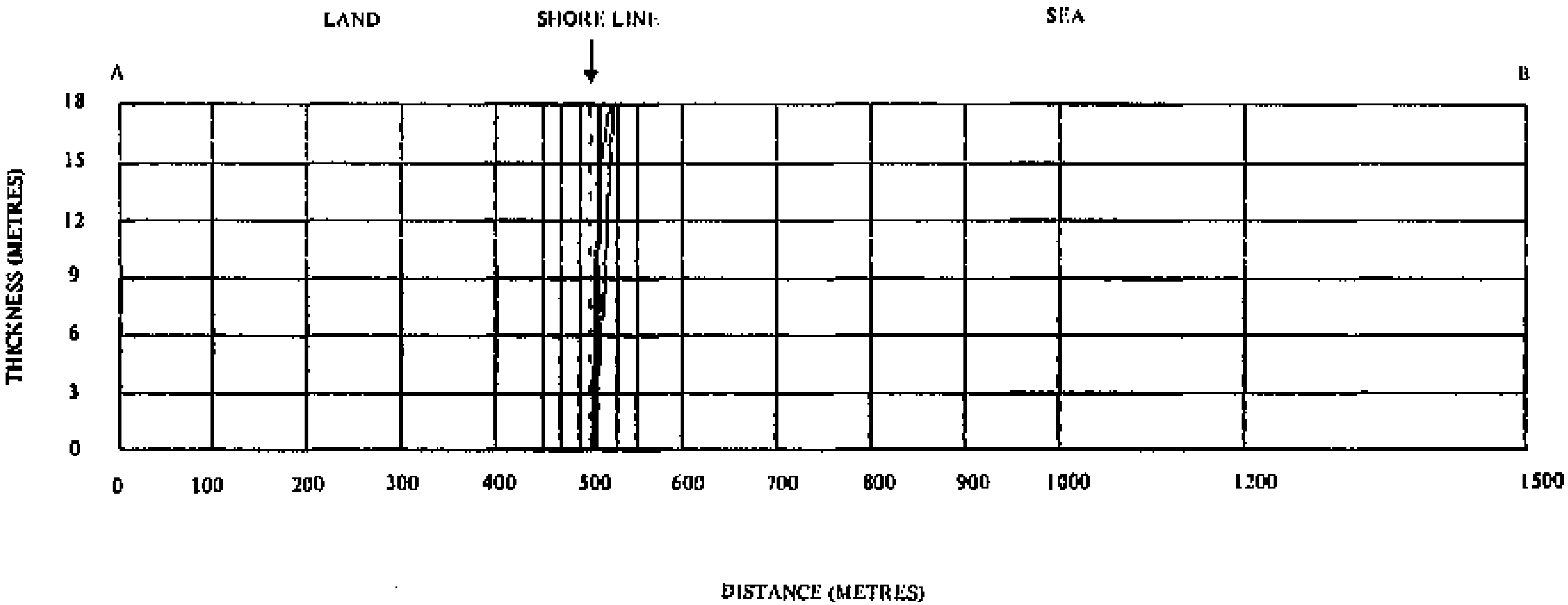

Figure 7.4. Position of the 0,01 isochlor after 3, 6, 9, 12, 15, 18, 21 and 24 months. (Constant head of 13 MASL at A)

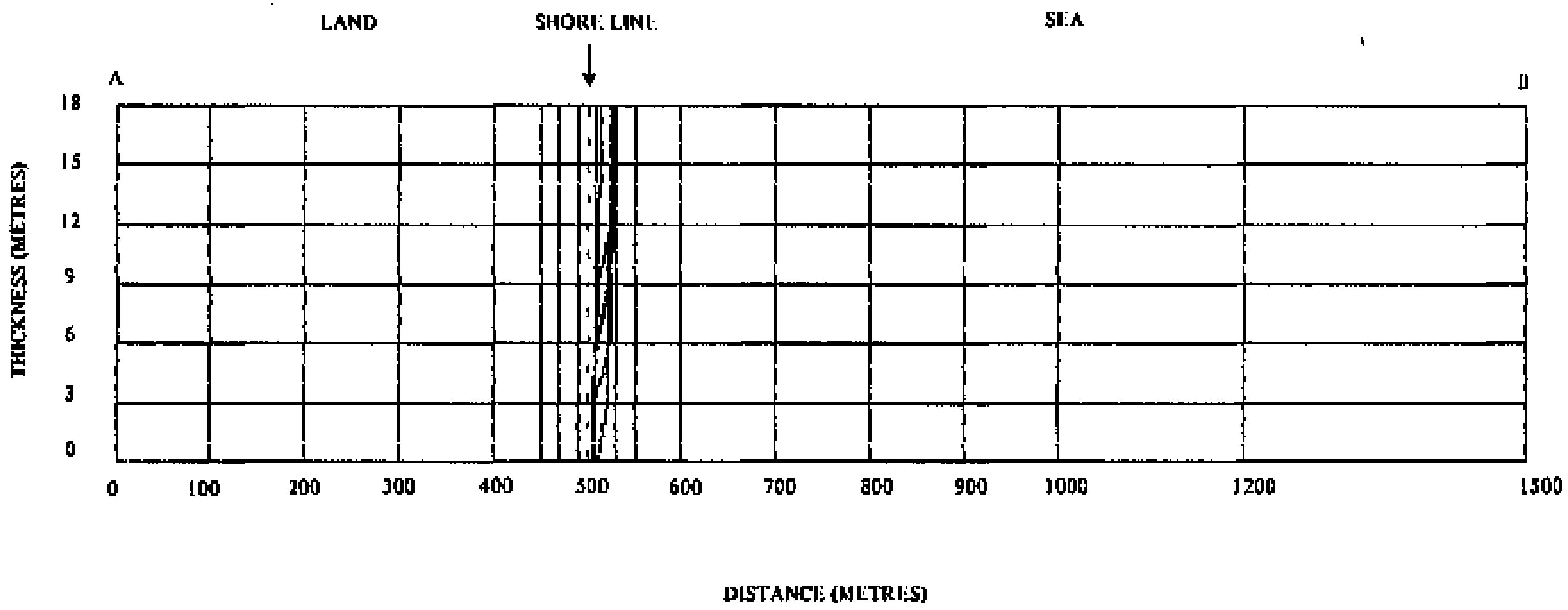

Figure 7.5. Position of the 0.02 isochlor after 3, 6, 9, 12, 15, 18, 21 and 24 months. (Constant head of 13 MASL at A)

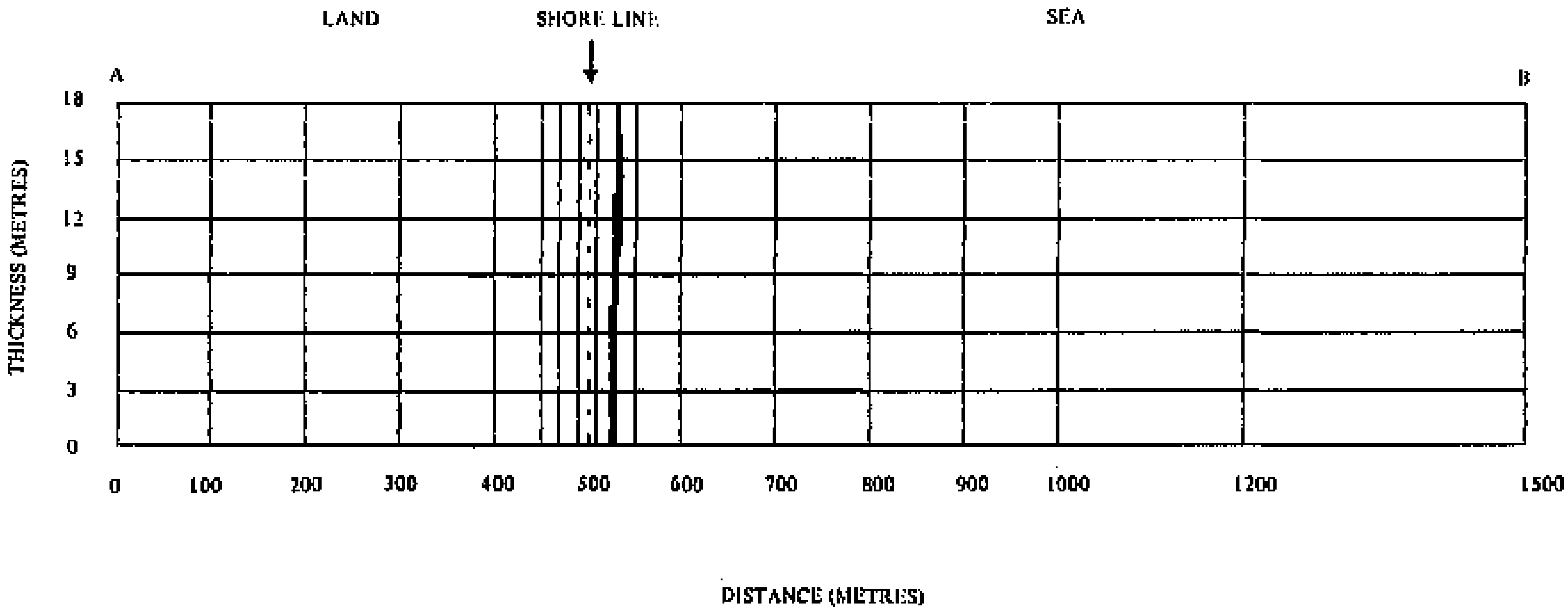

Figure 7.6. *Position of the 0,1 isochlor after 3, 6, 9, 12, 15, 18, 21 and 24 months. (Constant head of 13 MASL at A)*

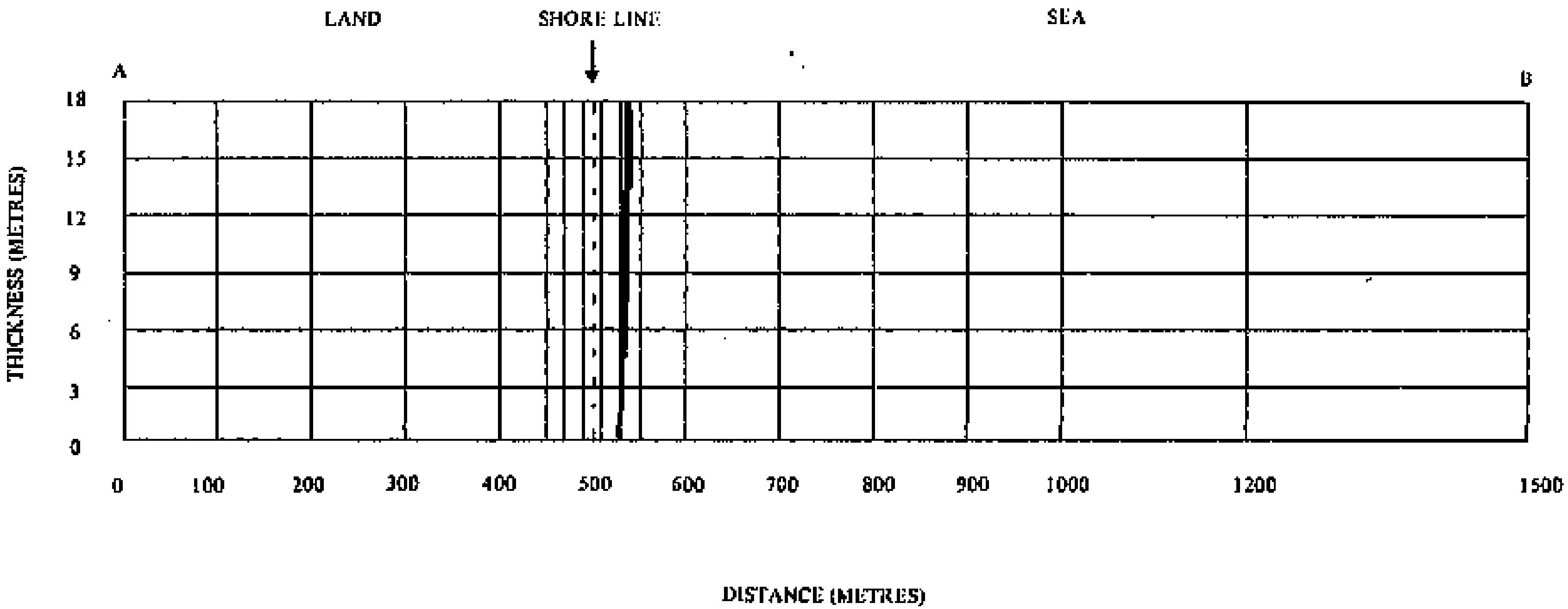

Figure 7.7. Position of the 0,25 isochlor after 3, 6, 9, 12, 15, 18, 21 and 24 months. (Constant head of 13 MASL at A)

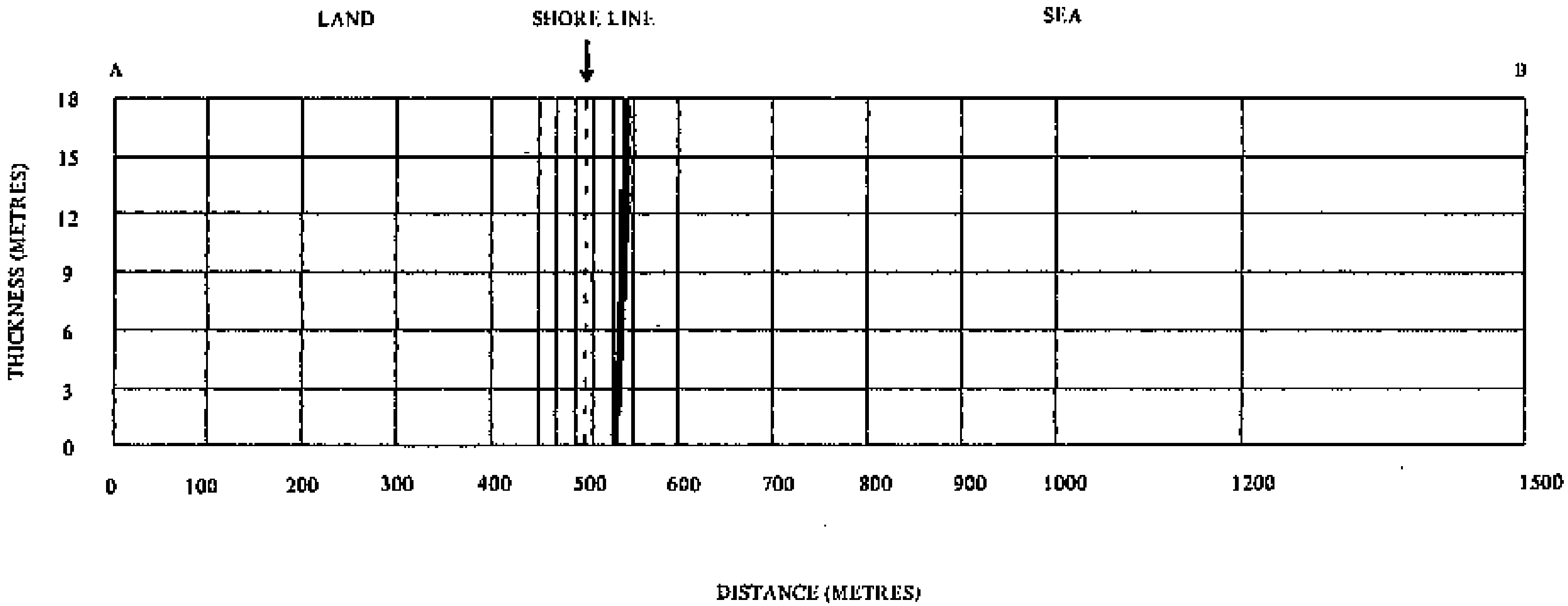

Figure 7.8. Position of the 0,5 isochlor after 3, 6, 9, 12, 15, 18, 21 and 24 months. (Constant head of 13 MASL at A)

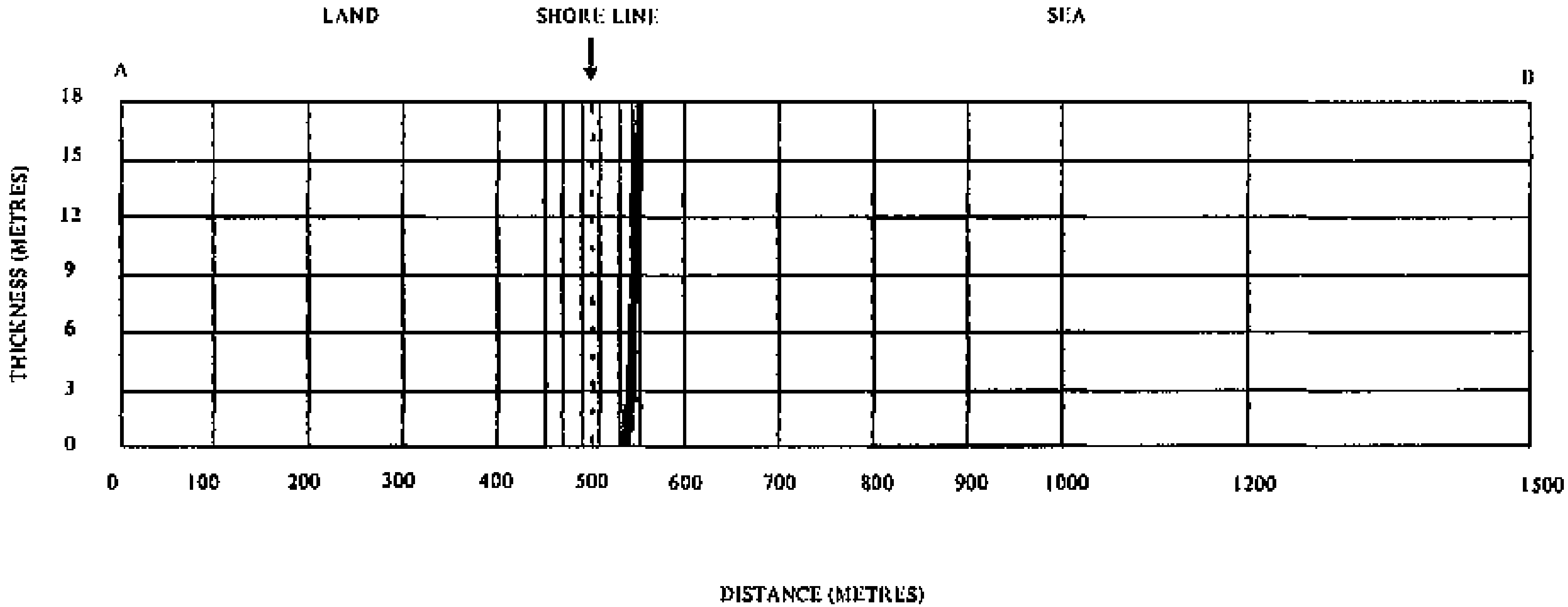

Figure 7.9. Position of the 0,75 isochlor after 3, 6, 9, 12, 15, 18, 21 and 24 months. (Constant head of 13 MASL at A)

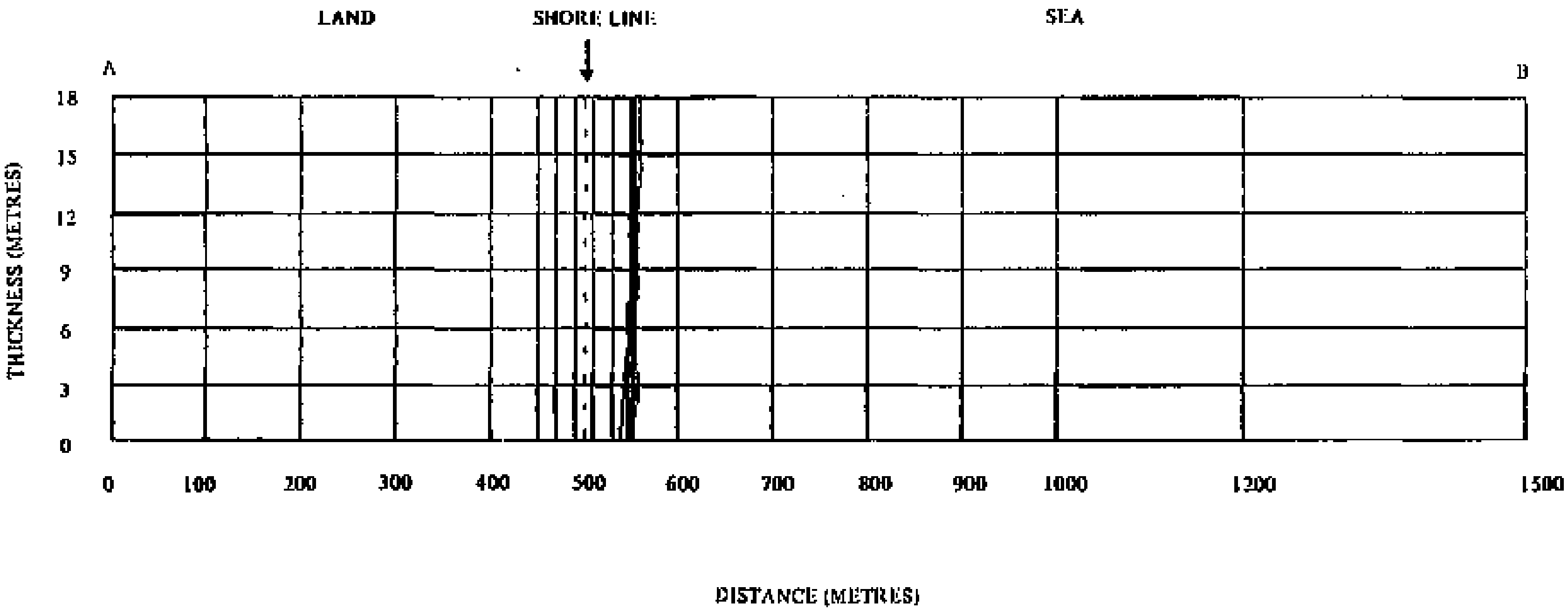

Figure 7.10. Position of the 0,9 isochlor after 3, 6, 9, 12, 15, 18, 21 and 24 months. (Constant head of 13 MASL at A)

A very important feature of sea-water intrusion is the transition or diffusion zone that exists between the fresh- and sea-water. Although the fresh/salt interface is specified as a vertical sharp interface at the coast-line in the initial conditions supplied to the model, the diffusion zone is quickly established by the model. The physical dimensions of this transition zone, taken as the distance between the 0,02 and 0,9 isochlors after 90, 360 and 720 days, is shown in Figures 7.11 - 7.13. From these figures it is evident that the diffusion zone has stabilized at a width of 50 metres to the seaward side of the coast-line. This further strengthens the belief that sea-water intrusion will not be a problem, given the physical circumstances as used in the model.

The results for the second simulation are shown graphically in Figures 7.14 - 7.19. It is evident that although the general behaviour of the system is identical to that of the previous simulation, the isochlors lie slightly closer to the coast-line. This, however, is to be expected, due to the fact that the driving force of the fresh water has been reduced by the lowering of the head at the Silwerstroom spring.

As the total width of the transition zone is still approximately 50 metres (see Figures 7.17 - 7.19), it can be concluded that the projected increased pumping rates will not affect the problem of sea-water intrusion into the Atlantis aquifer adversely.

The third and last simulation was included mainly to show what effect extreme conditions of dewatering may have on the system. This is purely a theoretical exercise, but the results are rather spectacular. As can be seen from Figures 7.20 - 7.22, the isochlors move rapidly inland. Moreover, there is no indication of any stabilization in their respective positions, even after 720 days, which indicates that the intrusion process is still taking place. This is quite discomforting if one notices that the 0,01 isochlor already lies 167 metres inland after 720 days (compared to the distance of 500 metres that the spring is from the coast - see Figure 7.20).

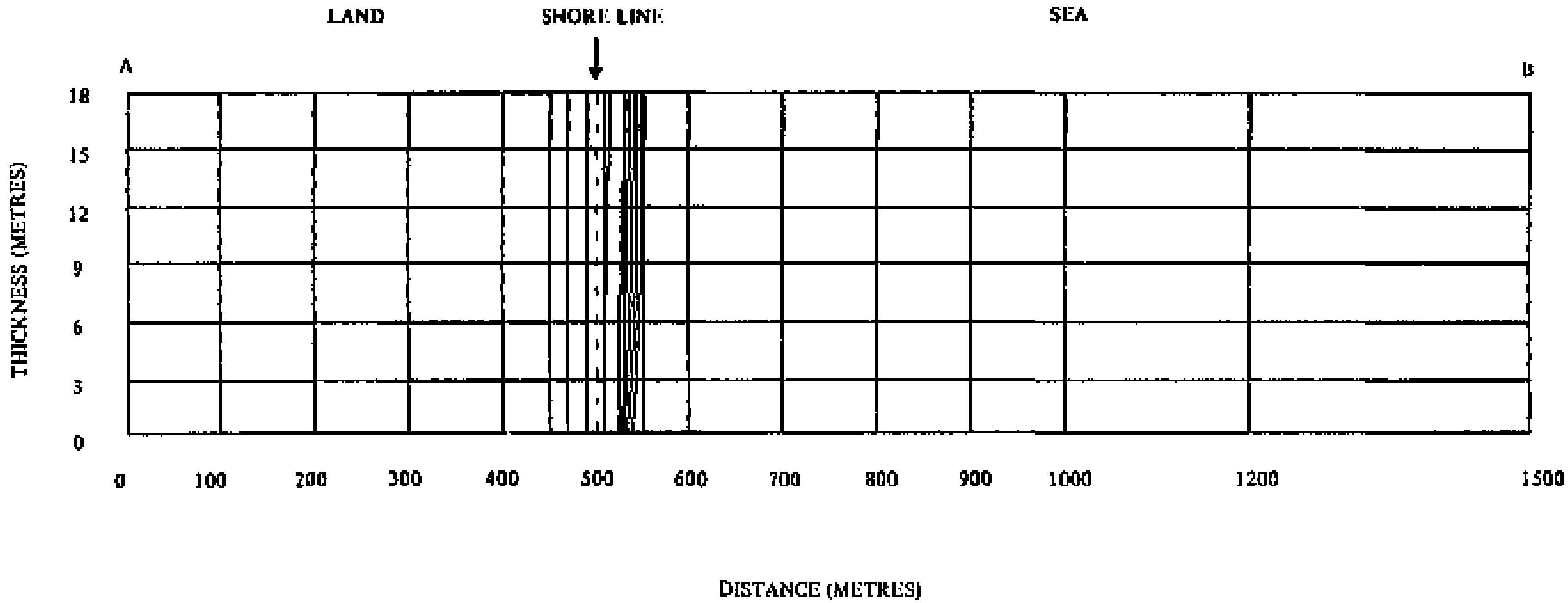

Figure 7.11. Diffusion zone after 90 days. Total width = 50 metres. (Constant head of 13 MASL at A)

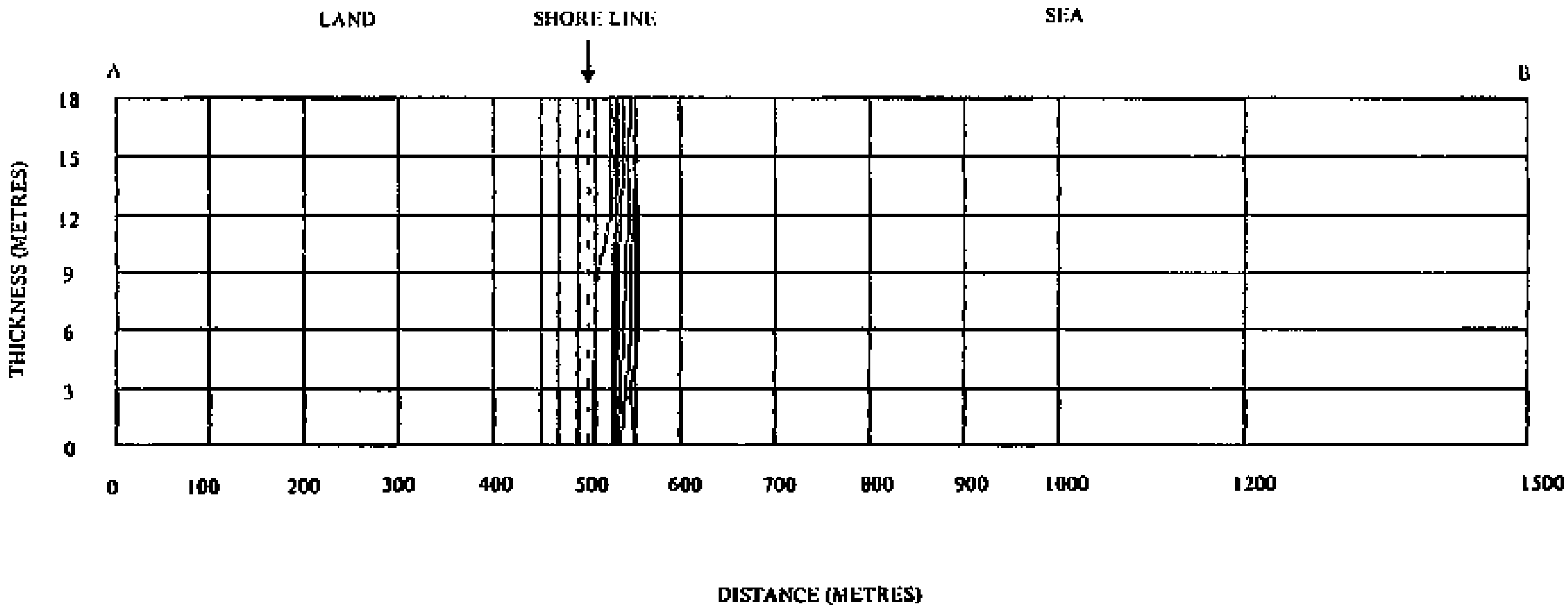

Figure 7.12. Diffusion zone after 360 days. Total width = 50 metres. (Constant head of 13 MASL at A)

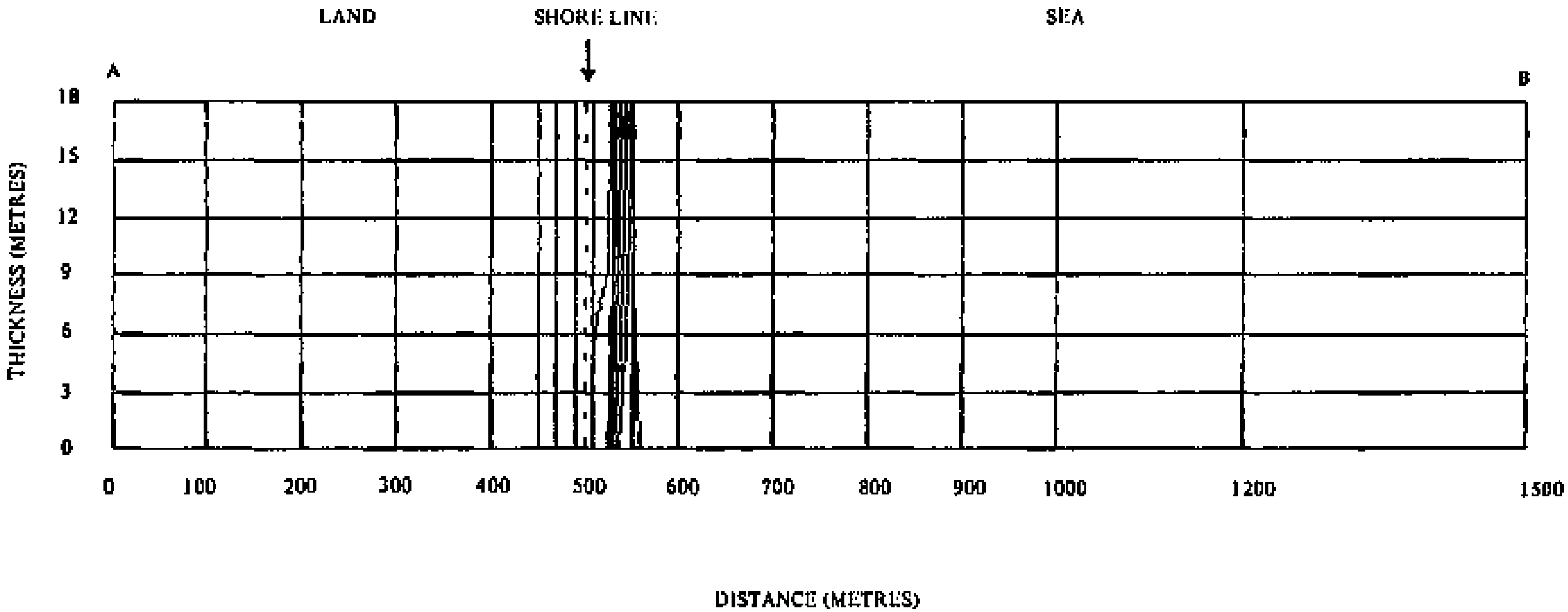

Figure 7.13. Diffusion zone after 720 days. Total width = 50 metres.
(Constant head of 13 MASL at A)

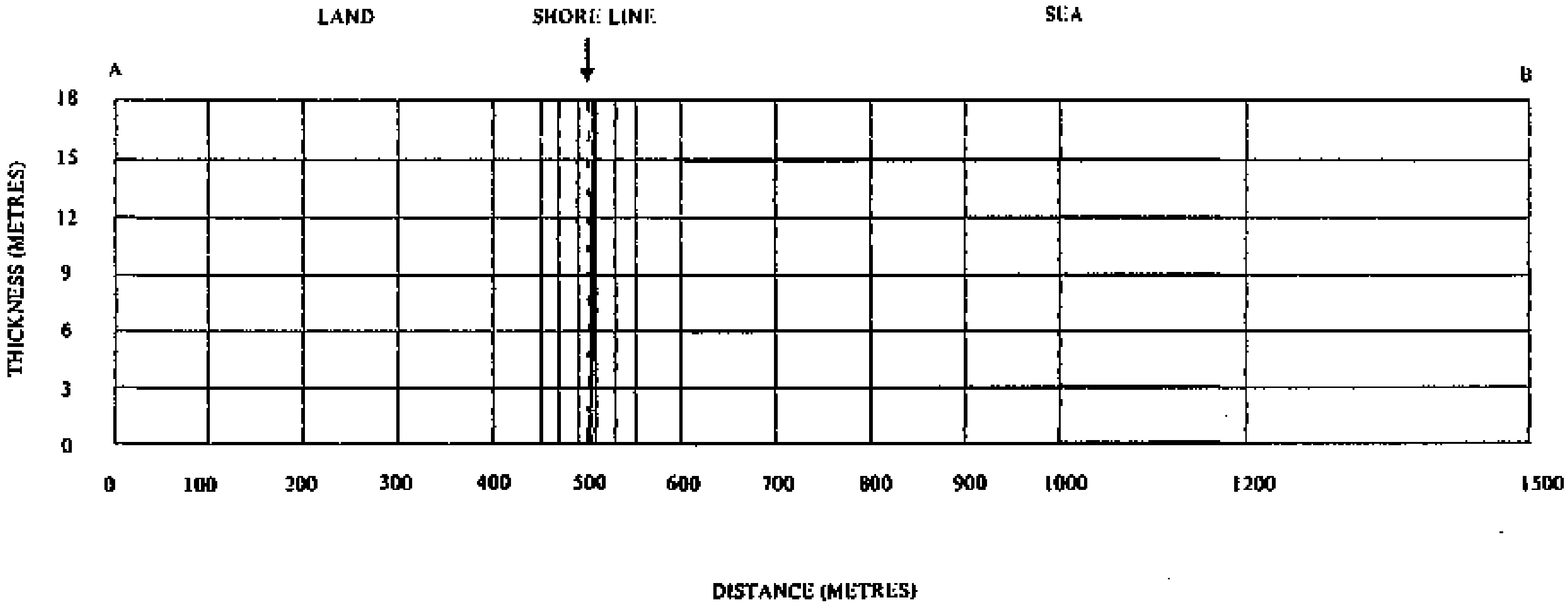

Figure 7.14. Position of the 0.01 isochlor after 3, 6, 9, 12, 15, 18, 21 and 24 months. (Constant head of 10 MASL at A)

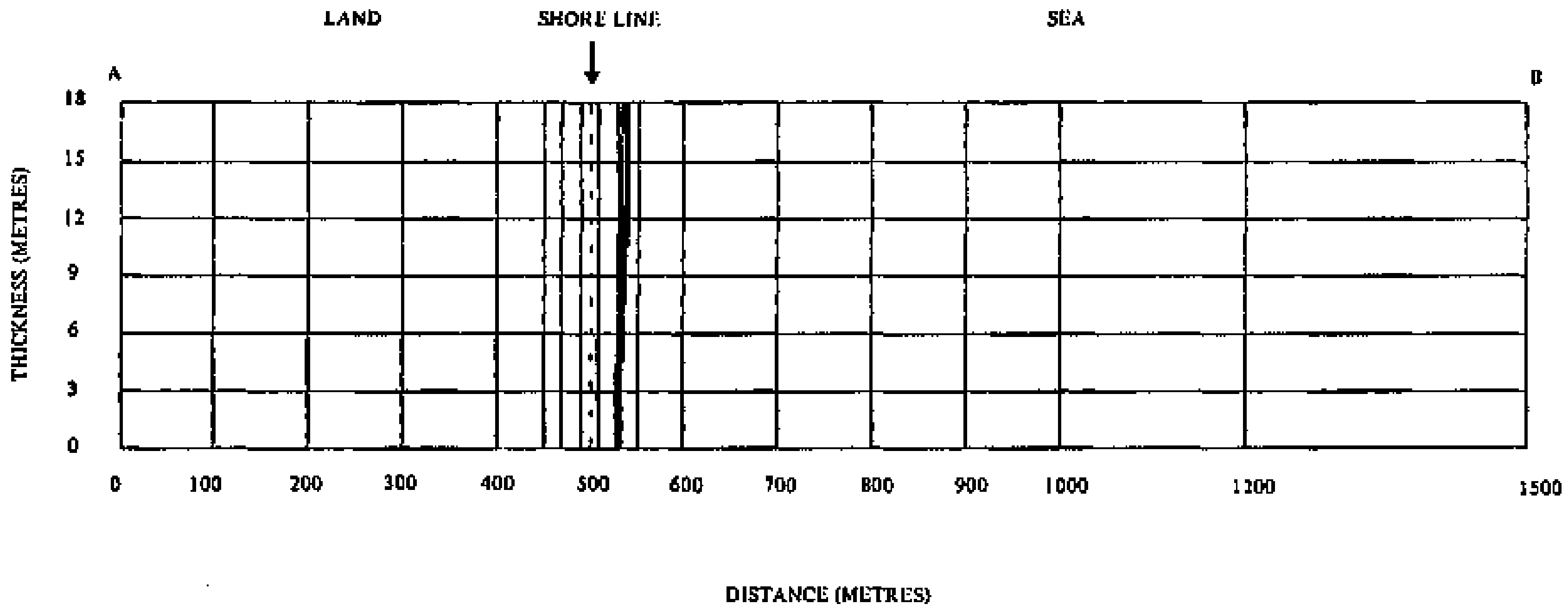

Figure 7.15. Position of the 0,5 isochlor after 3, 6, 9, 12, 15, 18, 21 and 24 months. (Constant head of 10 MASL at A)

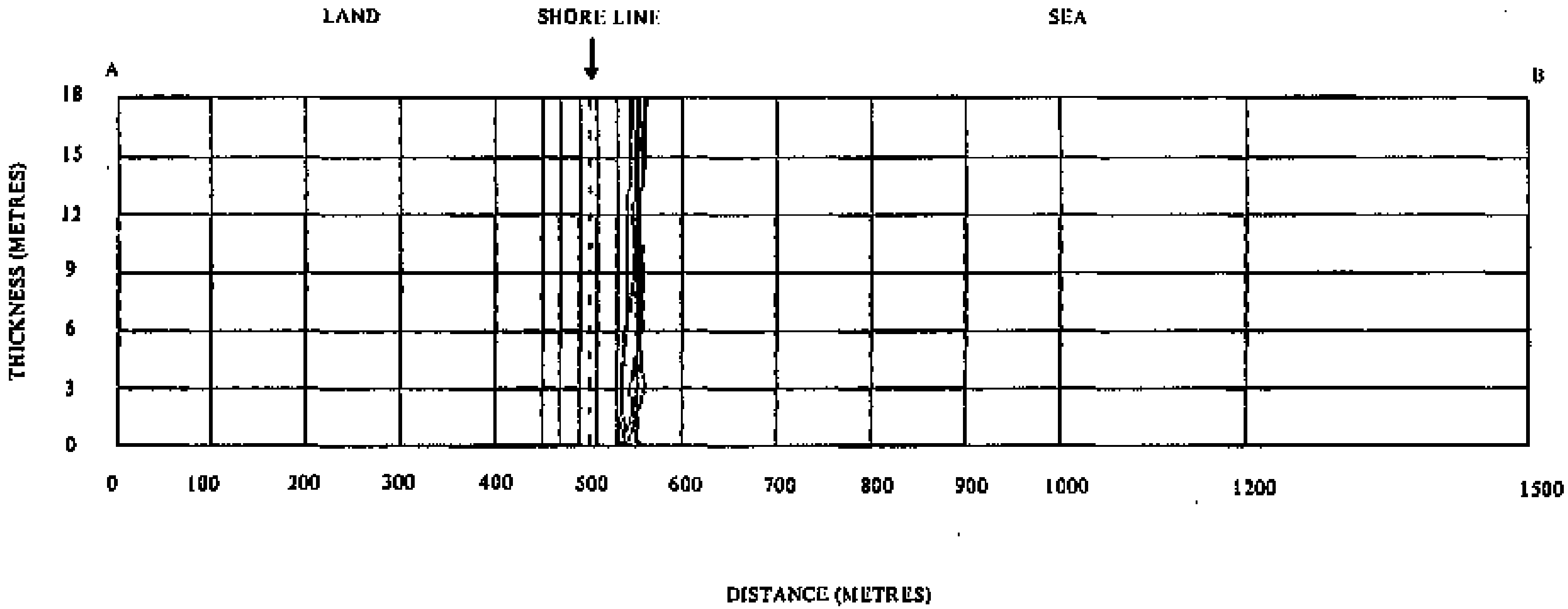

Figure 7.16. Position of the 0,9 isochlor after 3, 6, 9, 12, 15, 18, 21 and 24 months. (Constant head of 10 MASL at A)

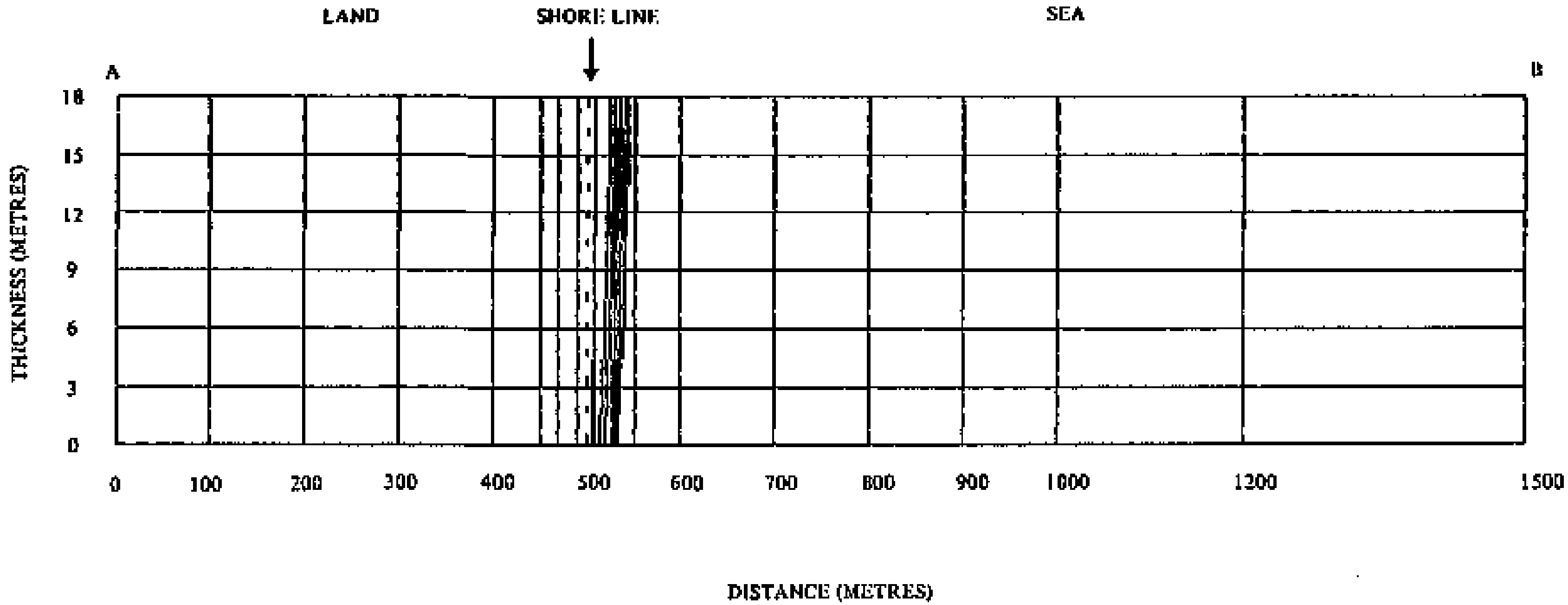

Figure 7.17. Diffusion zone after 90 days. Total width = 50 metres.
(Constant head of 10 MASL at A)

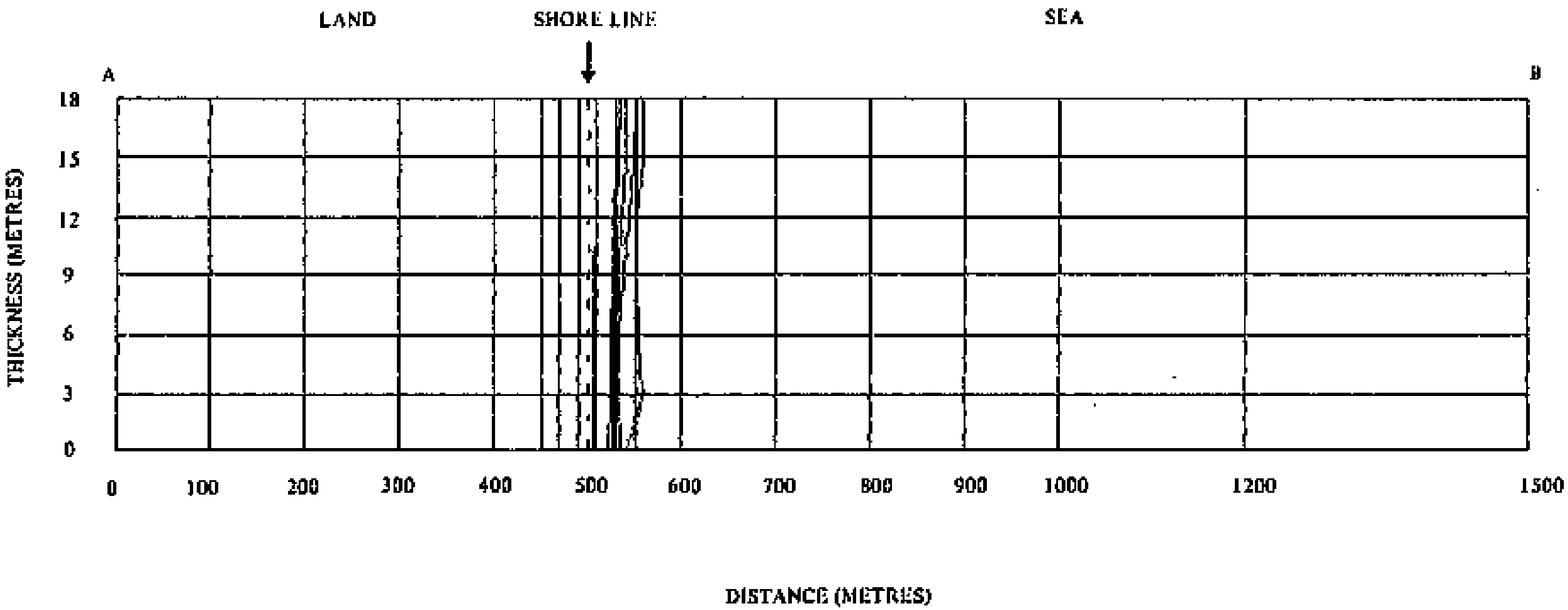

Figure 7.18. Diffusion zone after 360 days. Total width = 50 metres.
(Constant head of 10 MASL at A)

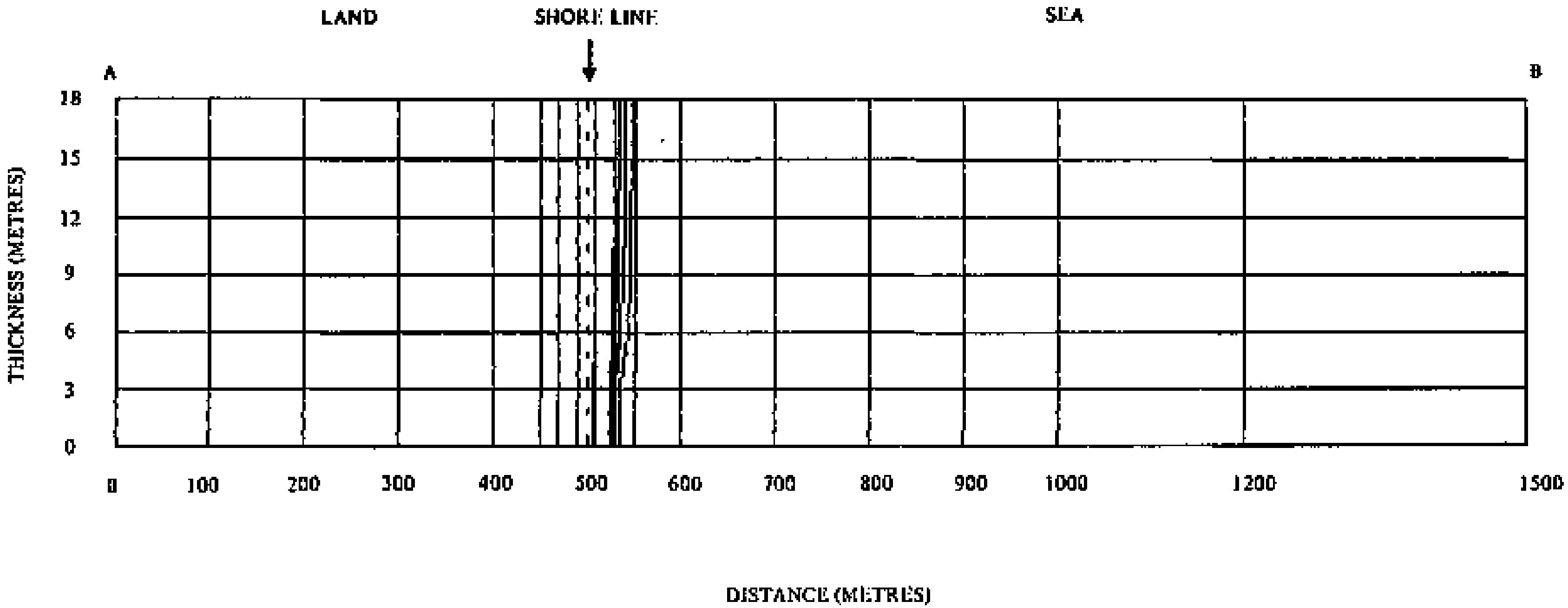

Figure 7.19. Diffusion zone after 720 days. Total width = 50 metres.
(Constant head of 10 MASL at A)

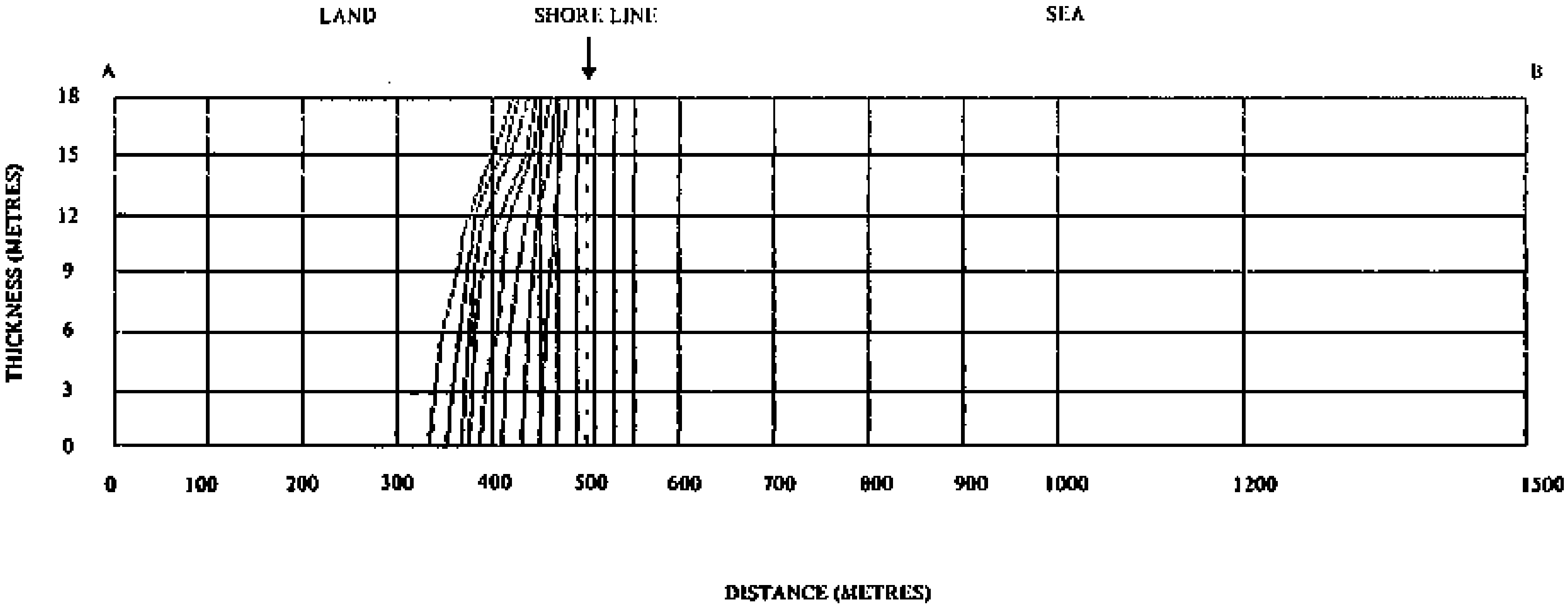

Figure 7.20. Position of the 0,01 isochlor after 3, 6, 9, 12, 15, 18, 21 and 24 months. The 0,01 isochlor lies 167 metres inland after 24 months. (Constant head of 0 MASL at A)

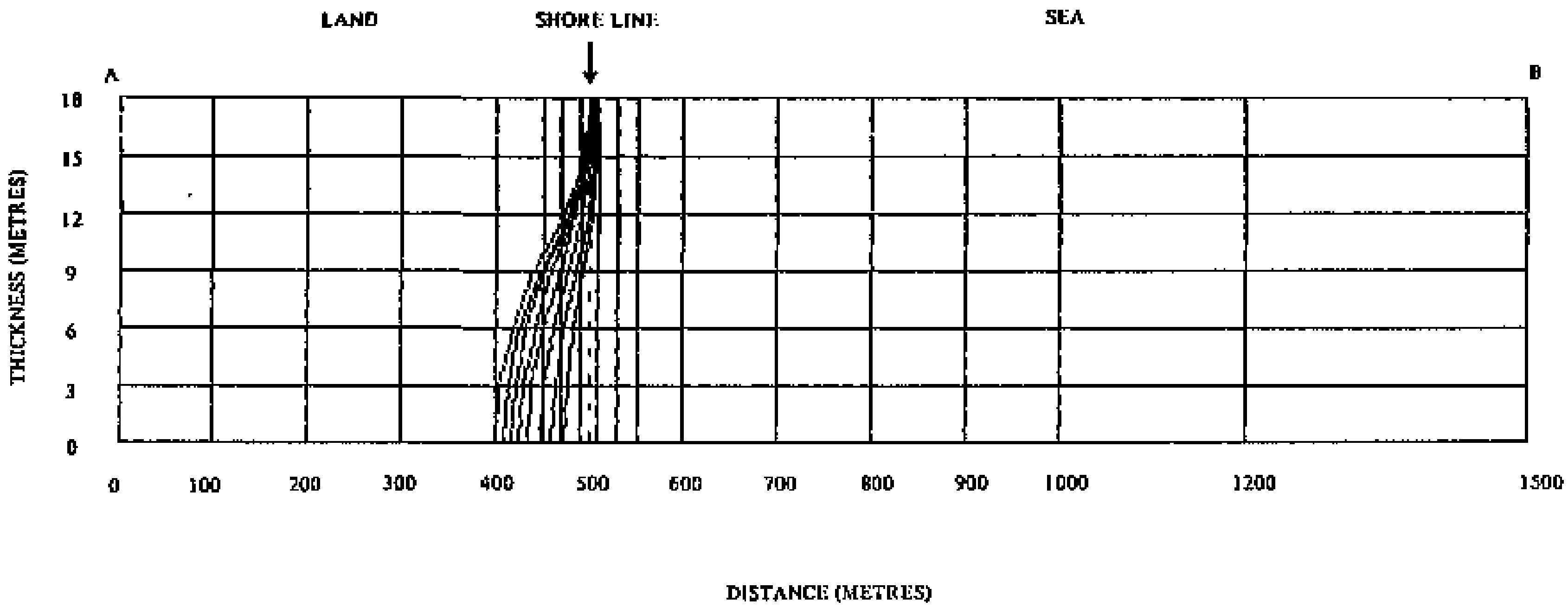

Figure 7.21. Position of the 0,5 isochlor after 3, 6, 9, 12, 15, 18, 21 and 24 months. The 0,5 isochlor lies 100 metres inland after 24 months. (Constant head of 0 MASL at A)

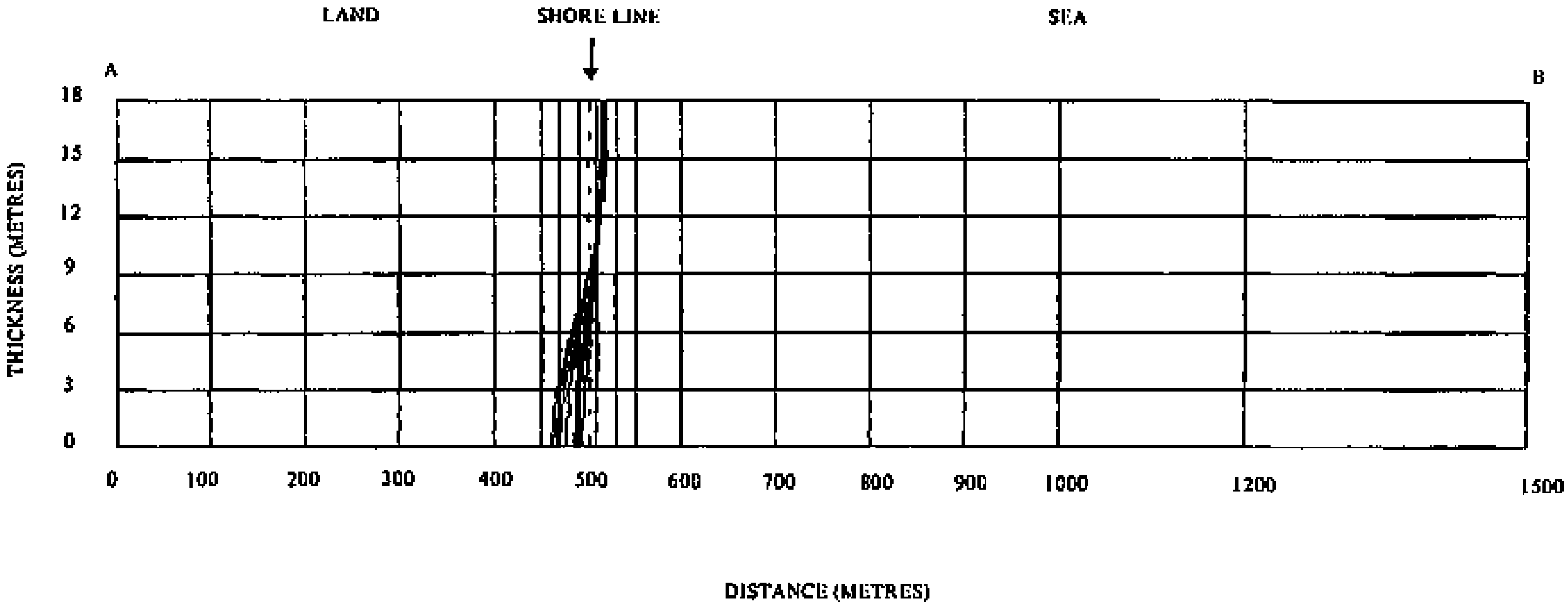

Figure 7.22. Position of the 0,9 isochlor after 3, 6, 9, 12, 15, 18, 21 and 24 months. (Constant head of 0 MASL at A)

The physical dimensions of the transition zone for 90, 360 and 720 days are shown in Figures 7.23 - 7.25. It is interesting to note that the diffusion zone has already spread 60 metres during the first 90 days and reaches a total width of 174 metres after 720 days. There will be grave consequences if this happens.

7.6 CONCLUSIONS

Although the results of the present model indicate that sea-water intrusion does not present a serious hazard for the time being, the results cannot be taken as conclusive. In fact, as shown by the results of the third simulation, a situation of sea-water contamination cannot be ruled out completely. A much more detailed field investigation of the area will have to be carried out before definite answers can be given. In such an investigation attention should in particular be given to:

(i) A detailed study of the permeability of the Malmesburg Formation at the coast and thus the actual thickness of the water-bearing strata in the region.

(ii) The hydraulic conductivity and storativity of the area between the coast and the spring.

(iii) Any possible influence that withdrawal of water may have on the spring flow. (The present data indicates that this is negligible, but the question remains as to what the effect of an increased pumping rate will be).

(iv) An indication of the present position of the fresh/salt interface, if possible.

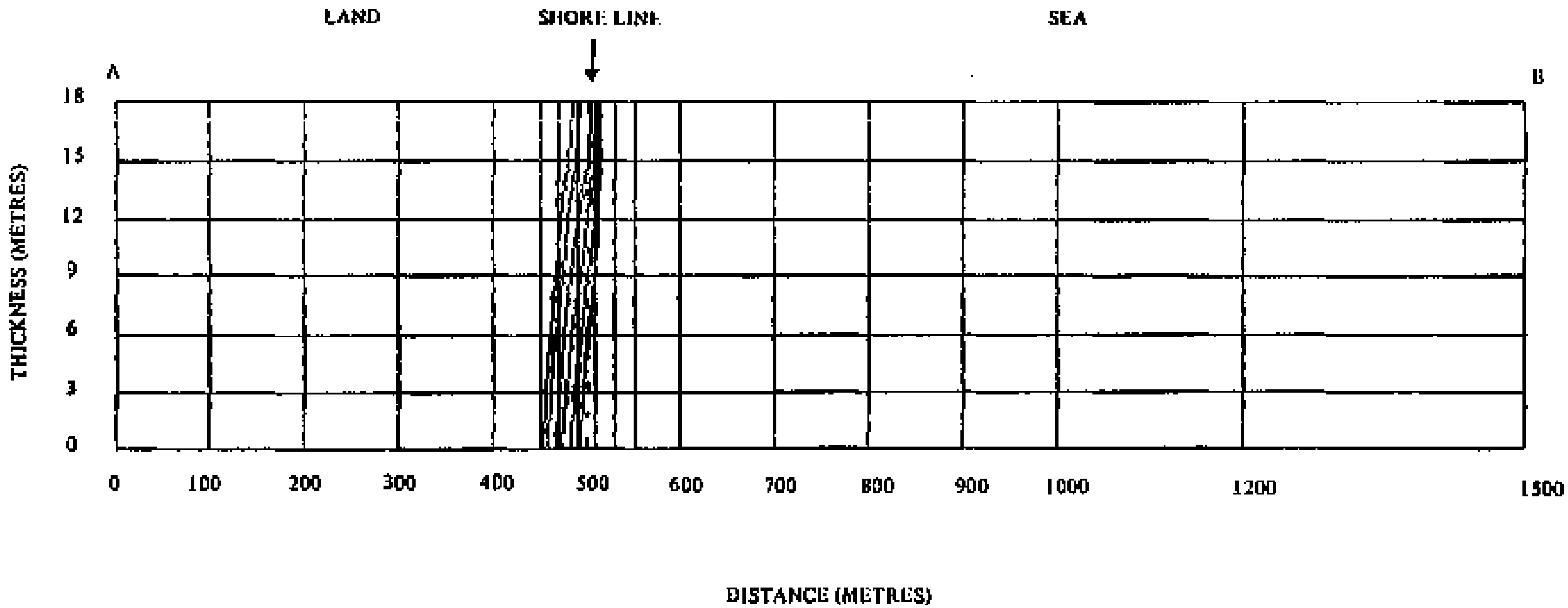

Figure 7.23. Diffusion zone after 90 days. Total width ≈ 60 metres. (Constant head of 0 MASL at A)

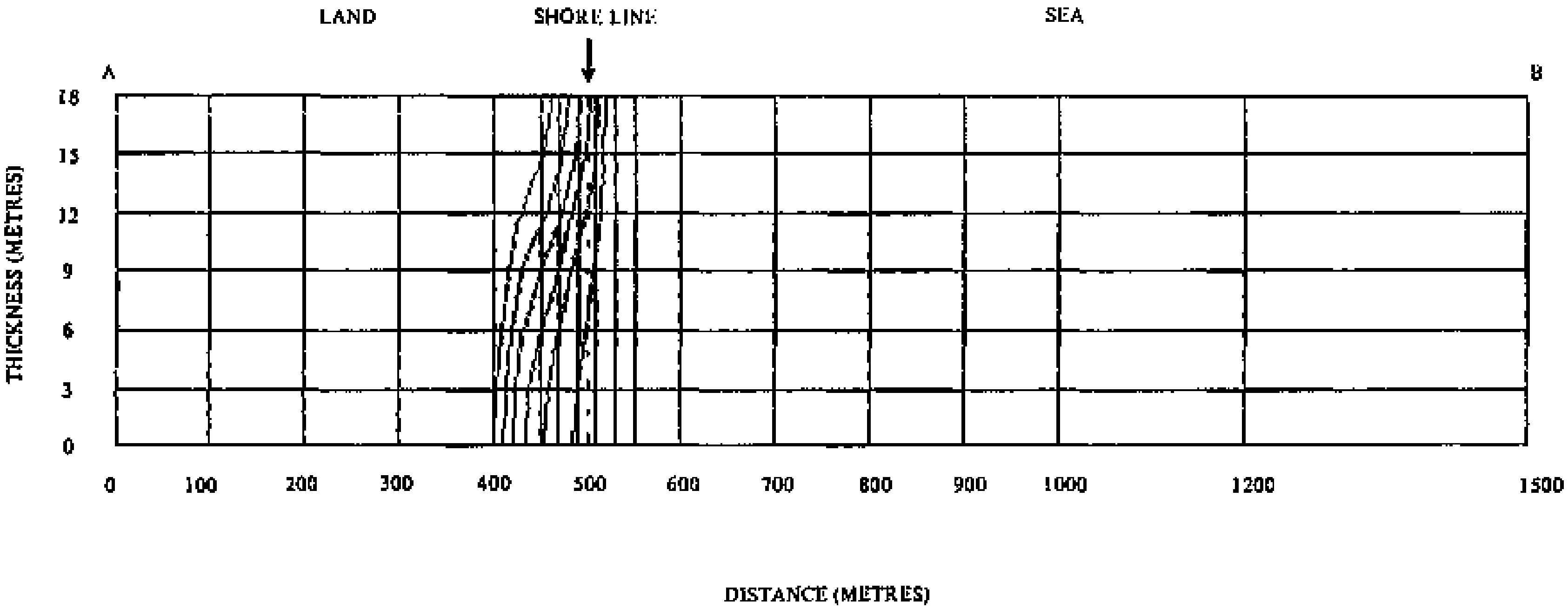

Figure 7.24. Diffusion zone after 360 days. Total width = 118 metres. (Constant head of 0 MASL at A)

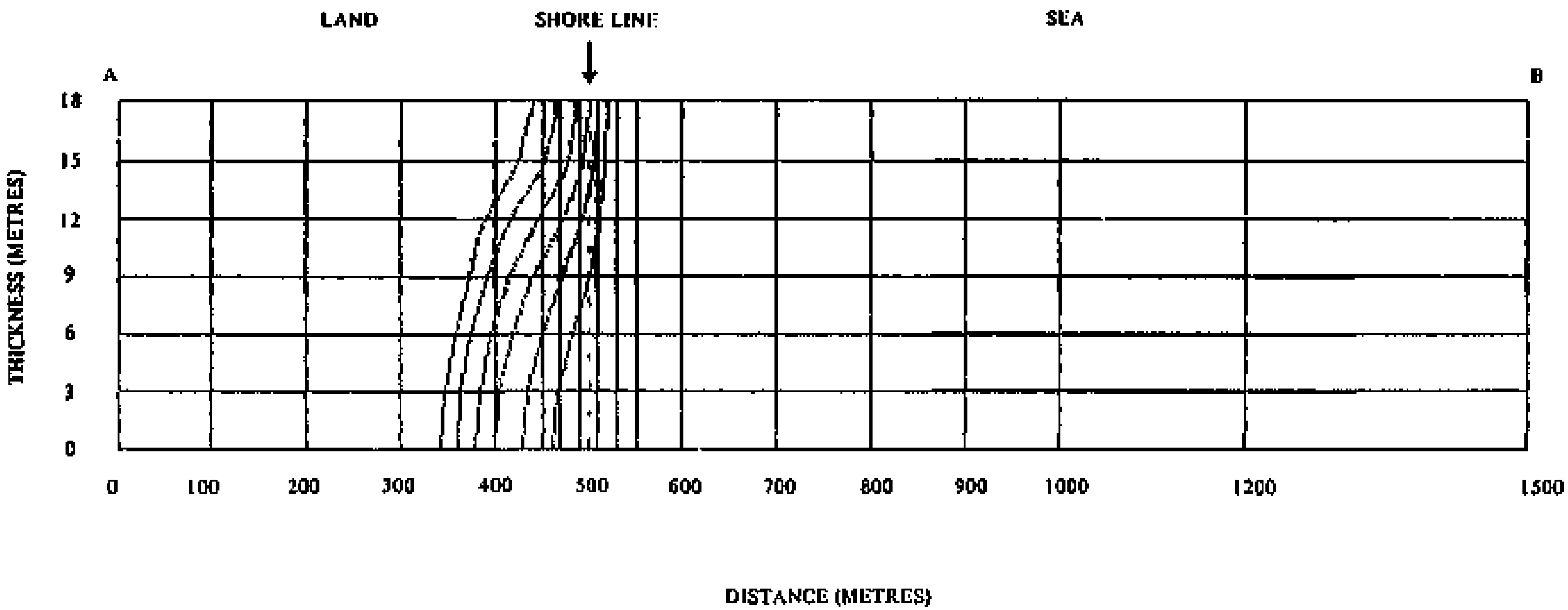

Figure 7.25. Diffusion zone after 720 days. Total width = 174 metres. (Constant head of 0 MASL at A)

REFERENCES

ACOCKS, H.P.J., 1975. Veld types of South Africa. Mem. Bot. Surv. S. Afr., 40, p. 104-106.

BAKKES, G.N. and BOTHA, J.F., 1981. An improved numeric solution for the diffusion equation. Bull. Inst. Ground-water Studies, Bloemfontein, 11, p. 1-25.

BEAR, J., 1979. Hydraulics of groundwater. McGraw-Hill Ltd., New York, 567 p.

BOTHA, J.F. and CELIA, M.A., 1981. Alternating direction approximations for a parabolic partial differential equation. Water Resources Program, Dept. of Civil Engineering, Princeton, Univ., U.S.A.

BOTHA, J.F., WEIDEMAN, J.A.C. and BAKKES, G.N., 1981. The optimal θ-method in numerical analysis. Bull. Inst. Ground-water Studies, Bloemfontein, 11, p. 26-43.

BOTHA, W.J. and BEKKER, J.C., 1977. Interpretation of the gravity survey for the Mamre Groundwater Project of the Department of Water Affairs. Tech. Report, No. 2419, Geol. Surv., S. Afr.

BOTHA, W.J. and THOMPSON, M.W.H., 1977. Geophysical Survey for the Saldanha Groundwater Project of the Department of Water Affairs. Tech. Report, No. 2417, Geol. Surv., S. Afr.

BOWEN, R., 1980. Ground Water. Applied Science Publishers Ltd., London, 227 p.

BREDENKAMP, D.B. and VANDOOLAEGHE, M.A.C., 1982. Die ontginbare grondwaterpotensiaal van die Atlantisgebied. Tech. Report, Gh 3227, Dept. of Environment, S. Afr.

CELIA, M.A., 1984. Density-dependent transport simulation using alternating direction collocation. Bull. Inst. Ground-water Studies, Bloemfontein, 12, p. 1-35.

HAUGHTON, S.H., 1933. The geology of Cape Town and adjoining country. Expl. Sheet 247 (Cape Town), Geol. Surv., S. Afr., p. 1-84.

KOK, T.S., 1977. Die grondwaterpotensiaal van die Atlantisgebied. Tech. Report, Gh 2947, Geol. Surv., S. Afr.

LAURIE, D.P., 1975. Optimal parameter choice in the θ-method for parabolic equations. Special Report, WISK 192, NIMS, CSIR, Pretoria.

LAURIE, D.P., 1977. The numerical treatment of the time variable in parabolic equations. Special Report, WISK 750, NIMS, CSIR, Pretoria.

LYNCH, S.D., 1982. Grondwatermodellering en parameteridentifikasie van die Sishen-akwifeer. Unpublished M.Sc. thesis, UOFS, Bloemfontein, 129 p.

MARINO, M.A. and LUTHIN, J.N., 1982. Seepage and groundwater. Elsevier Scientific Publishing Company, Amsterdam, 489 p.

NOBLE, D.N., 1976. The West Coast survey for groundwater potential - background and scope. Tech. Report, Gh 2936, Geol. Surv., S. Afr.

NOBLE, D.N., 1975/1976. The West Coast survey for groundwater potential. Tech. Report, Geol. Surv., S. Afr.

ODEN, J.T. and REDDY, J.N., 1976. An introduction to the mathematical theory of finite elements. John Wiley and Sons, New York, 429 p.

PINDER, G.F., 1974. Galerkin-finite element models for aquifer simulation. Rep. Water Resources Program, Princeton Univ., USA, 29 p.

PINDER, G.F. and BREDEHOEFT, J.D., 1968. Application of the digital computer for aquifer evaluation. Water Resources Research, 4 (5), p. 1069-1093.

PINDER, G.F. and GRAY, W.G., 1977. Finite element simulation in surface and subsurface hydrology. Academic Press, London, 1st Edition, 295 p.

PRICKETT, T.A. and LONNQUIST, C.G., 1971. Selected digital computer techniques for groundwater resource evaluation. Bulletin 55, Illinois State Water Survey, Urbana.

ROGERS, J., 1980. First report on the Cenozoic sediments between Cape Town and Elands Bay. Tech. Report, 1980-0249, Geol. Surv., S. Afr., p. 16-25.

SMIT, P.J., 1976. Mamre Groundwater Project and proposed sewage disposal works. Tech. Report, Gh 2872, Geol. Surv., S. Afr.

VAN DER MERWE, A.J., 1980. Eksplorasie, ontginning en evaluering van grondwater van die sandafsetting in die Atlantisgebied vir watervoorsiening aan die Atlantisontwikkelingsgebied. Tech. Report, Gh 3187, Dept. of Environment, S. Afr.

VAN DER MERWE, A.J., 1983. Eksplorasie, ontginning en evaluering van grondwater van die sandafsetting in die Atlantisgebied vir watervoorsiening aan die Atlantisontwikkelingsgebied. Unpublished M.Sc. thesis, UOFS, Bloemfontein, 334 p.

VANDOOLAEGHE, M.A.C. and BERTRAM, W.E., 1982. Atlantis grondwatersisteem : herevaluasie van versekerde lewering. Tech. Report, Gh 3222, Dept. of Environment, S. Afr.

VAN TONDER, G.J., 1982. Die toepassing van kriging in geohidrologie. Unpublished Ph.D. thesis, UOFS, Bloemfontein, 178 p.

VAN TONDER, G.J. and BOTHA, J.F., 1983. Modelling water-levels and contaminant transport in the Omaruru Delta. Tech. Report, Inst. Ground-water Studies, Bloemfontein, 171 p.

VEGTER, J.R., NOBLE, D.N. and SMIT, P.J., 1976. Opsporing en evaluasie van grondwater in Weskusgebied. Tech. Report, Gh 2893, Geol. Surv., S. Afr.

VISSER, H.N. and SCHOCH, A.E., 1973. The geology and mineral resources of the Saldanha Bay Area. Mem. Geol. Surv., S. Afr., 63, p. 15-27.

VISSER, H.N. and TOERIEN, D.K., 1971. Die geologie van die gebied tussen Vredendal en Elandsbaai. Expl. Sheets 3118C (Doringbaai) and 3218A (Lambertsbaai), Geol. Surv., S. Afr.

WALTON, W.C., 1970. Groundwater resource evaluation. McGraw-Hill Kogakusha Ltd., Tokyo, 664 p.

WEERBURO, 1972. Klimaat van Suid-Afrika. Part 10, Dept. of Transport, S. Afr.

SUMMARY

The main scope of this investigation is to construct a numerical model describing the physical state of the Atlantis aquifer, using existing information. Although the modelling of ground-water systems in South Africa has been undertaken in the past, it is the first time that a coastal aquifer in the Republic was modelled, using a model based on physical principles.

By utilizing the available information and powerful mathematical techniques, a good flow model for the aquifer was constructed. By using this model, it was possible to predict the behaviour of the aquifer with some success. However, there still exist significant deficiencies in the data, which should be eliminated as far as possible, before an attempt is made to construct a more refined model.

One significant deduction that followed from the present study, is that the proposed expansion of the Silwerstroom and Witzand production fields will dewater the lower part of the Atlantis aquifer. If this proposed expansion is actually implemented, it will be necessary to take all reasonable precautions, including artificial recharge, to prevent a too large drawdown in this area.

Another very important aspect when it comes to coastal aquifers, is the problem of sea-water intrusion. This problem was studied by utilizing a numerical model, describing density-dependent transport in porous media. Although very little information regarding the physical and hydraulic parameters of the profile to be modelled was available, it could nevertheless be shown that given the assumed physical and hydraulic conditions, sea-water intrusion does not, at present, pose a hazard to the aquifer.